



National Library
of Canada

Bibliothèque nationale
du Canada

Canadian Theses Service

Service des thèses canadiennes

Ottawa, Canada
K1A 0N4

NOTICE

The quality of this microform is heavily dependent upon the quality of the original thesis submitted for microfilming. Every effort has been made to ensure the highest quality of reproduction possible.

If pages are missing, contact the university which granted the degree.

Some pages may have indistinct print especially if the original pages were typed with a poor typewriter ribbon or if the university sent us an inferior photocopy.

Reproduction in full or in part of this microform is governed by the Canadian Copyright Act, R.S.C. 1970, c. C-30, and subsequent amendments.

AVIS

La qualité de cette microforme dépend grandement de la qualité de la thèse soumise au microfilmage. Nous avons tout fait pour assurer une qualité supérieure de reproduction.

S'il manque des pages, veuillez communiquer avec l'université qui a conféré le grade.

La qualité d'impression de certaines pages peut laisser à désirer, surtout si les pages originales ont été dactylographiées à l'aide d'un ruban usé ou si l'université nous a fait parvenir une photocopie de qualité inférieure.

La reproduction, même partielle, de cette microforme est soumise à la Loi canadienne sur le droit d'auteur, SRC 1970, c. C-30, et ses amendements subséquents.

UNIVERSITY OF ALBERTA

**The Influence of Fines Content and Specific
Surface Area on Freezing of Sandy Soils**

by

Rafael Sergio Dávila Otazú

A thesis submitted to the Faculty of Graduate Studies and Research in
partial fulfillment of the requirements for the degree of Master of Science

DEPARTMENT OF CIVIL ENGINEERING

Edmonton, Alberta

Spring 1992



National Library
of Canada

Bibliothèque nationale
du Canada

Canadian Theses Service Service des thèses canadiennes

Ottawa, Canada
K1A 0N4

The author has granted an irrevocable non-exclusive licence allowing the National Library of Canada to reproduce, loan, distribute or sell copies of his/her thesis by any means and in any form or format, making this thesis available to interested persons.

The author retains ownership of the copyright in his/her thesis. Neither the thesis nor substantial extracts from it may be printed or otherwise reproduced without his/her permission.

L'auteur a accordé une licence irrévocable et non exclusive permettant à la Bibliothèque nationale du Canada de reproduire, prêter, distribuer ou vendre des copies de sa thèse de quelque manière et sous quelque forme que ce soit pour mettre des exemplaires de cette thèse à la disposition des personnes intéressées.

L'auteur conserve la propriété du droit d'auteur qui protège sa thèse. Ni la thèse ni des extraits substantiels de celle-ci ne doivent être imprimés ou autrement reproduits sans son autorisation.

ISBN 0-315-73137-0

Canada

UNIVERSITY OF ALBERTA

RELEASE FORM

NAME OF AUTHOR: **Rafael Sergio Dávila Otazú**

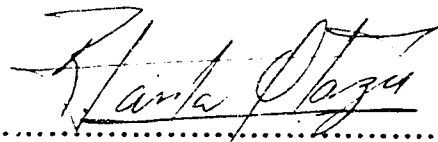
TITLE OF THESIS: **The Influence of Fines Content and Specific
Surface Area on Freezing of Sandy Soils**

DEGREE: **Master of Science**

YEAR THIS DEGREE GRANTED: **Spring 1992**

Permission is hereby granted to the University of Alberta Library to reproduce single copies of this thesis and to lend or sell such copies for private, scholarly or scientific research purposes only.

The author reserves all other publication and other rights in association with the copyright in the thesis, and except as hereinbefore provided neither the thesis nor any substantial portion thereof may be printed or otherwise reproduced in any material form whatever without the author's prior written permission.



.....
PERMANENT ADDRESS:

22 de Agosto, 103/107
Miraflores, Arequipa
Arequipa, Perú

April 22, 1992

UNIVERSITY OF ALBERTA

FACULTY OF GRADUATE STUDIES AND RESEARCH

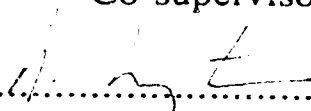
The undersigned certify that they have read, and recommend to the Faculty of Graduate Studies and Research for acceptance, a thesis entitled **The Influence of Fines Content and Specific Surface Area on Freezing of Sandy Soils** submitted by **Rafael Sergio Dávila Otazú** in partial fulfillment of the requirements for the degree of **Master of Science**.



.....
Dr. D C. Sego
Supervisor



.....
Dr. P. K. Robertson
Co-supervisor



.....
Dr. N. R. Morgenstern



.....
Dr. G.S.H. Lock

January 28, 1992

DEDICATION

Durante todos los momentos críticos de mi vida universitaria fue siempre la imagen protectora de mi madre que me confortó. Deseo que su cariño no se pierda en la infinitud del tiempo, y es que con el tiempo es mucho mas facil borrar de la memoria el amor que los rencores. Mismo ella no estando mas en éste austero mundo, brindo por la inmortalidad de su amor a nuestra familia y es por eso que dedico a su memoria éste trabajo de investigación y por su intermedio a las mujeres de mi familia. Pues todas ellas son el espejo de rectitud, perseverancia y cariño en el que se encuentran los cimientos de mi caracter.

Edmonton, 05 de Febrero de 1992

ABSTRACT

Geotechnical engineering has overcome various technical obstacles in order to obtain undisturbed samples of different types of soils. Nevertheless, sampling saturated loose sand at great depths remains the most challenging. Accurate observations of the structure, fabric, void ratio and density of this material require samples in an undisturbed state. Since the soil is disturbed during conventional sampling, the response of the samples to static or dynamic testing may not correspond to that of the *in situ* material. The inability to obtain undisturbed samples of loose sand often results in the use of higher factors of safety during seismic assessments to account for the uncertainty related to the *in situ* behavior. The ground freezing technique has proven to be the most reliable way of obtaining an undisturbed sample of loose sand for liquefaction assessment. A review of the methods used in the past to perform the ground freezing technique is presented. These are compared to a new method which allows for freezing and retrieval of frozen samples from greater depths, as it was successfully carried out at the Duncan Dam in British Columbia.

Characterizing the fines within a cohesionless soil, using the specific surface area, makes it possible to evaluate the use of the ground freezing technique during a particular field sampling program. In order to obtain a truly undisturbed sample, the expansion and disturbance of the soil during freezing has to be avoided. It is demonstrated in this study that the amount and type of the clay mineral have the most influence on whether or not a loose sandy soil is disturbed during the freezing process. A new approach for characterization purposes is proposed to correctly define the boundary between frost heaving and non frost heaving soils. The use of the specific surface area assists in evaluating the frost susceptibility of soils in a better manner compared to other frost susceptibility criteria. The parameters on which the characterization is based also proved to be useful in linking the properties of a soil to the segregation potential.

ACKNOWLEDGEMENT

This thesis is product of the support I have received for the last two years. I am forever indebted to several people and I would like to express my gratitude.

I wish to acknowledge the members of the Geotechnical group of the Civil Engineering Department who advised and guided me through the course of my studies at this University. My supervisors deserve special thanks for their direction, encouragement and patience. Dr. D. Sego and Dr. P. K. Robertson suggested this interesting topic for my study and they were always enthusiastic about the laboratory findings and the importance that this study could have in future research works. More personally, I would like to thank Dr. D. Sego not only for his unconditional trust and comprehension since I arrived to Edmonton, but for his friendship.

I would like to acknowledge the financial assistance by the University of Alberta and the grant from the Department of Energy, Mines and Resources of Canada. Special thanks for the assistance I received from the technicians S. Gamble, C. Hereygers and J. Khajuria, who helped me setting up the testing equipment and characterizing the soils that were used in this study. To G. Cyre for his enthusiasm and optimism in the field program and during our trips to the Duncan Dam.

More than technical support is needed to complete a thesis successfully. My deepest gratitude are extended to my friends here in Edmonton that made my stay more pleasant, for their help with the edition of the present thesis and for their invaluable comments and motivation. To those who I left in Brazil for their continuing support, invaluable friendship and trust in my potential. Finally but more importantly, to the cornerstone of my life: my family, I wish to express my love and respect. Especially for showing me that my education had to be an essential part of my strength.

TABLE OF CONTENTS

Chapter	Page
I. INTRODUCTION	1
1.1 Statement of the Problem	1
1.2 Methodology of Research	3
1.3 Scope and Thesis Organization	3
1.4 Objective of the Study	4
II. THE ARTIFICIALLY FROZEN SOIL	6
2.1 Foreword	6
2.2 General Characteristics of a Frozen Soil	6
2.2.1 The Mineral Particle Interface	7
2.2.2 The Water Interface	8
2.2.3 Ground Ice Classification of Frozen Soils	10
2.3 Undisturbed Sampling in Sands Using Freezing Techniques	10
2.3.1 Historical Review	10
2.3.2 The Use of Ground Freezing for Sampling Purposes	11
2.3.3 The Duncan Dam Experience	15
2.4 Discussion of The <i>In situ</i> Freezing Method	18
III. OUTLINES OF THE FROST HEAVE ANALYSIS	42
3.1 Frost Heave and Frost Susceptibility of Soils	42
3.1.1 Foreword	42
3.1.2 The Konrad and Morgenstern Frost Heave Model	42
3.2 Conditions for an Undisturbed Structure in Sands by <i>In Situ</i> Freezing	46
3.2.1 The Effect of Porewater Migration in Sandy Soils	46
3.2.2 The Effect of Applied Stress	49
3.2.3 The Effect of the Fines Content	52

3.3 Frost Susceptibility Parameters	54
3.3.1 Historical Review	54
3.3.2 Recent Proposed Parameters for Frost Heave Correlations	55
3.3.3 The Importance of the Specific Surface Area in Frost Heave Studies	57
IV. THE UNIAXIAL FREEZING TEST	74
4.1 Apparatus and Auxiliary Equipment Description	74
4.1.1 Foreword	74
4.1.2 The Freezing Cell and Data Acquisition System	74
4.2 Test Procedure	76
4.2.1 Foreword	76
4.2.2 Laboratory Simulation	77
4.2.3 Laboratory Procedures	79
4.2.3.1 The Modified Slurry Deposition Method	79
4.2.3.2 Sample Preparation	79
4.2.3.3 Sealing of the Mixing Cylinder and Mixing Process	80
4.2.3.4 Placement of Mixing Cylinder into Freezing Apparatus	81
4.2.3.5 Assembling the Freezing Cell	82
V. UNIAXIAL FREEZING TESTS RESULTS AND ANALYSIS	97
5.1 Foreword	97
5.2 Laboratory Testing Program	97
5.2.1 Description of Soils Used in this Study	97
5.2.2 Organization of the Laboratory Results	98
5.2.3 Boundary Conditions	99
5.3 Uniaxial Freezing Tests Results	101
5.3.1 Freezing Test Results and Analysis of	

Soil Mixtures with Non-Plastic Fines	101
5.3.2 Freezing Test Results and Analysis of Soil Mixtures with Plastic Fines	104
5.4 Characterization of the Test Soils Based on the Specific Surface Area	107
5.4.1 Re-analysis of the Laboratory Data	107
5.4.2 Background in the Surface Area Parameters	112
5.4.3 The Fines Mineralogy Ratio	114
5.4.4 The Surface Area Index	117
5.5 Laboratory Results Analysis Based on the Surface Area Parameters	119
VI. SURFACE AREA CRITERIA APPLIED TO SEGREGATION POTENTIAL	137
6.1 Introduction	137
6.1.1 Foreword	137
6.1.2 Background on Correlations to the Segregation Potential	137
6.2 The Surface Area Related to Frost Heave Behavior	138
6.2.1 The Segregation Potential Determination	138
6.2.2 Relationship Between Specific Surface Area and the Liquid Limit	140
6.2.3 Frost Heave Behavior with Respect to the Liquid Limit	145
6.3. Consequences	148
VII. CLOSURE	162
7.1 Summary	162
7.2 Conclusions	162
6.3 Recommendations	163
BIBLIOGRAPHY	165
APPENDIX A	175
APPENDIX B	178

APPENDIX C	181
APPENDIX D	210
APPENDIX E	224
APPENDIX F	227

LIST OF TABLES

Table	Page
02-01 - Methods of Sampling by In-situ Freezing in Sands	22
02-02 - Methods of Sampling by In-situ Freezing in Sandy Gravels	22
02-03 - Field Conditions and Physical Properties of In-situ Frozen Sand Samples	23
02-04 - Field Conditions and Physical Properties of In-situ Frozen Gravel Samples	23
02-05.- Distances from the Freezing Pipes to the Sampling and RTD Boreholes	24
03-01.- Influence of Clay Minerals in Frost Heave. After Lambe <i>et al.</i> (1958).	64
03-02.- Compilation of Available Data in Frost Heave	70
05-01.- Sands Characterization	126
05-02a.- Fines Characterization. Atterberg Limits, Specific Gravity and Activity	126
05-02b.- Fines Characterization. Clay Mineralogy, Surface Area Characterization and Specific Surface Area Parameters.	126
05-03.- Table of Uniaxial Freezing Tests Performed During the Laboratory Program	131
05-04.- Summary of the Soil Constitution of the Samples Tested by UFT	132
06-01.- Summary of the Soil Characteristics and Segregation Potential of the Uniaxial Freezing Tests	152
06-02.- Compilation of Available Data including Specific Surface Area and Liquid Limit	155
E-01.- Void Ratio Determination for Non-clay Mineral Mixtures	225

E-02.-	Void Ratio and Final Freezing Front Determination	226
--------	---	-----

LIST OF FIGURES

Figure		Page
02-01.-	The Pötsch Refrigeration Method	25
02-02.-	The Pötsch Refrigeration Method Adapted for Brine Coolant	26
02-03.-	In-Situ Freezing and Sampling Method After Yoshimi <i>et al.</i> (1984)	27
02-04.-	In-Situ Freezing and Sampling Method After Hatanaka <i>et al.</i> (1985)	28
02-05.-	In-Situ Freezing and Sampling Method After Yoshimi <i>et al.</i> (1989)	29
02-06.-	Plan View of the Site at Duncan Dam and Location of the Freezing Pipe, Sample and Temperature Boreholes	30
02-07.-	Soil Profile at the Duncan Dam Freezing Location	31
02-08.-	In-Situ Freezing and Sampling Method After Sego <i>et al.</i> (1991)	32
02-09.-	Layout of the Freezing System at the Duncan Dam	33
02-10.-	Liquid Nitrogen Volume Consumption	34
02-11.-	Rate of Consumption per Hour	34
02-12.-	Temperature Profile Adjacent to the Freezing Pipes	35
02-13.-	Temperature Profile of the Multiple RTD Probe	35
02-14.-	Frost Front Advance in the Duncan Dam using Sanger and Sayles Method	36
02-15.-	Range of Particle Size for Application of the Ground Freezing Sampling Methods	37
03-01.-	The Konrad and Morgenstern Model for a Frost Susceptible Soil	61

03-02.-	The Mechanism of Ice Lens Formation After Konrad and Morgenstern (1980)	62
03-03.-	Region of Study Considering Segregation Potential in Different Plastic Soils	63
03-04.-	Variation of Frost Heave for Sand-fines Mixtures, Part A After Linell and Kaplar (1959)	65
03-05.-	Variation of Frost Heave for Sand-fines Mixtures, Part B After Linell and Kaplar (1959)	66
03-06.-	Effect of Clay Minerals on Frost Susceptibility of McNamara Sand. After Lambe <i>et al.</i> (1969)	67
03-07.-	Effect of Non-clay Minerals (Carbonates). After Lambe <i>et al.</i> (1969)	67
03-08.-	Effect on Non-clay Minerals (Non-carbonates) After Lambe <i>et al.</i> (1969)	68
03-09.-	Variation of the Segregation Potential with the Increase of Fines Content	68
03-10.-	Variation of the Segregation Potential with the Increase of Clay Size Fraction.	69
03-11.-	Variation of the Segregation Potential with the Increase of the Fines Factor	69
04-01.-	Cutaway View (AA') of the Freezing Cell	84
04-02.-	Top Cutaway View of the Freezing Cell	85
04-03.-	Position of the Resistance Temperature Devices on the Freezing Cells Walls	86
04-04.-	Schematic Layout of the Freezing Cell and Data Logging Equipment Set-up	87
04-05.-	Schematic Procedure of Sample Preparation, Part A	88
04-06.-	Schematic Procedure of Sample Preparation, Part B	122
05-01.-	Grain Size Distribution of Duncan 0 Sand	122

05-02.-	Grain Size Distribution of Duncan 2 Sand	122
05-03.-	Grain Size Distribution of Duncan 1 Fines	123
05-04.-	Grain Size Distribution of Silica Flume Fines	123
05-05.-	Grain Size Distribution of Devon Silt Fines	124
05-06.-	Grain Size Distribution of Illite Fines	124
05-07.-	Grain Size Distribution of Athabasca Clay Fines	125
05-08.-	Grain Size Distribution of Kaolinite Fines	125
05-09.-	Mineralogy of the Duncan 1 Fines and Silica Flume Fines by Percentage	127
05-10.-	Mineralogy of the Devon Silt Fines and Illite Fines by Percentage	128
05-11.-	Mineralogy of the Athabasca Clay Fines and Kaolinite Fines by Percentage	129
05-12.-	Mineralogy of the Bentonite Fines by Percentage	130
05-13.-	Water Expulsion Duncan Sand Series	133
05-14.-	Water Expulsion Silica Flume Series	133
05-15.-	Water Expulsion/Intake Devon Silt Series	134
05-16.-	Water Expulsion/Intake Illite Series	134
05-17.-	Water Expulsion/Intake Kaolinite Series	135
05-18.-	Liquid Limit of the Fines Fraction vs. Fines Activity Parameter	135
05-19.-	Fines Factor vs. Fines Activity Parameter	136
05-31.-	Boundary for Frost Behavior Based on the Surface Area Parameters	136
06-01.-	Derivative Curve for the Water Intake Velocity from the Kaolinite 1st Battery	153

06-02.-	Derivative Curve for the Water Intake Velocity from the Devon Silt and Illite 1st Battery	154
06-03.-	Calculated and Theoretical Values for ξ	156
06-04.-	Surface Area Index vs. Liquid Limit Comparison from Different Sources	156
06-05.-	Regression Analysis for Data in Figure 06-04	157
06-06.-	Surface Area Index vs. Liquid Limit Factor. Comparison from Different Sources	157
06-07.-	Regression Analysis for Data in Figure 06-06	158
06-08.-	Surface Area Index vs. Liquid Limit Factor Modified Data after Rieke and Vinson (1982)	158
06-09.-	The Liquid Limit Factor vs. Percent Heave Compiled Data from Different Sources	159
06-10.-	The Liquid Limit Factor vs. Avg. Heave Rate Data Compiled from Different Sources	159
06-11.-	The Liquid Limit Factor vs. Segregation Potential. Data Compiled from Different Sources	160
06-12.-	Proposed Curve Fitting for the Data in Figure 06-11	160
06-13.-	Graphical Determination of Coefficients a and b	161
C-01.-	UFT 14. Specimen D005	182
C-02.-	UFT 26. Specimen D006	183
C-03.-	UFT 22. Specimen LT01D0	184
C-04.-	UFT 25. Specimen LT02D0	185
C-05.-	UFT 38. Specimen D1100	186
C-06.-	UFT 17. Specimen D202	187
C-07.-	UFT 19. Specimen D2CS20	188
C-08.-	UFT 20. Specimen D2CS30	189

C-09.-	UFT 32. Specimen D2DS05	190
C-10.-	UFT 33. Specimen D2DS10	191
C-11.-	UFT 35. Specimen D2DS20	192
C-12.-	UFT 41. Specimen D2IL05	193
C-13.-	UFT 39. Specimen D2IL10	194
C-14.-	UFT 37. Specimen D2IL20	195
C-15.-	UFT 42. Specimen D2IL102	196
C-16.-	UFT 43. Specimen D2IL202	197
C-17.-	UFT 28. Specimen D2KL05	198
C-18.-	UFT 30. Specimen D2KL10	199
C-19.-	UFT 27. Specimen D2KL20	200
C-20.-	UFT 44. Specimen D2KL052	201
C-21.-	UFT 34. Specimen MSKL20	202
C-22.-	UFT 40. Specimen MSIL10	203
C-23.-	UFT 23. Specimen TS0101	204
C-24.-	UFT 24. Specimen TS0102	205
C-25.-	Porepressures Series D0, D1 and D2	206
C-26.-	Porepressure Series DS	207
C-27.-	Porepressure Series IL	208
C-28.-	Porepressure Series KL	209
D-01.-	X-ray Diffractogram of the Duncan 1 Fines	211
D-02.-	X-ray Diffractogram Curve. Duncan 1 Fines Mineral Distribution	212
D-03.-	X-ray Diffractogram Curve. Silica Flume Fines	

	Mineral Distribution	213
D-04.-	X-ray Diffractogram of the Devon Silt Fines	214
D-05.-	X-ray Diffractogram Curve. Devon Silt Fines Mineral Distribution	215
D-06.-	X-ray Diffractogram of the Illite Fines	216
D-07.-	X-ray Diffractogram Curve. Illite Fines Mineral Distribution	217
D-08.-	X-ray Diffractogram of the Athabasca Clay Fines	218
D-09.-	X-ray Diffractogram Curve. Athabasca Clay Fines Mineral Distribution	219
D-10.-	X-ray Diffractogram of the Kaolinite Fines	220
D-11.-	X-ray Diffractogram Curve. Kaolinite Fines Mineral Distribution	221
D-12.-	X-ray Diffractogram of the Bentonite Fines	222
D-13.-	X-ray Diffractogram Curve. Bentonite Fines Mineral Distribution	223

LIST OF PLATES

Plate		Page
02-01.-	Panoramic view of the toe and campsite at the Duncan Dam.	38
02-02.-	Installation of the sliding stabilization rings on the first section of the freezing pipe.	38
02-03.-	View of the second section of the freezing pipe with the Brass coupler attached.	39
02-04.-	View of the freezing system submitted to liquid nitrogen circulation.	40
02-05.-	Close-up of FP1, sampling boreholes and RTD1.	40
02-06.-	CRREL barrel at surface. Removal of drill cutting prior to removal of core.	41
04-01.-	Lateral view of the freezing cell without part of the PVC jacket.	90
04-02.-	Top view of the bottom of the freezing cell.	91
04-03.-	View of the freezing cell and the hanger system.	92
04-04.-	Preparation of samples using the Modified Slurry Deposition Method.	93
04-05.-	View of the freezing cell prepared to receive the sample.	94
04-06.-	View of the mixing cylinder before retrieval.	95
04-07.-	View of the freezing cell ready to receive the temperature gradient.	96
F-01.-	Placement of the jetting pipe and pushing of the first section in FP1.	228
F-02.-	Soldering the 2" copper tubes of the second section of the freezing system.	228
F-03.-	Close-up of the valves distribution.	229

F-04.-	Close-up of FP1 submitted to liquid nitrogen distribution.	229
F-05.-	RTD with attached cable inside the 0.5" PVC tube.	230
F-06.-	Preparation of S1 for sampling and view of surface piping of the freezing system.	230
F-07.-	Retrieved sample of undisturbed Duncan Sand.	231
F-08.-	View of the demodulator for System 01 and System 02 with their RTD signal conditioner boxes.	231
F-09.-	View of the burettes to measure the water expulsion or water intake.	232
F-10.-	View of the data acquisition system.	232

LIST OF PLATES

Plate		Page
02-01.-	Panoramic view of the toe and campsite at the Duncan Dam.	38
02-02.-	Installation of the sliding stabilization rings on the first section of the freezing pipe.	38
02-03.-	View of the second section of the freezing pipe with the Brass coupler attached.	39
02-04.-	View of the freezing system submitted to liquid nitrogen circulation.	40
02-05.-	Close-up of FP1, sampling boreholes and RTD1.	40
02-06.-	CRREL barrel at surface. Removal of drill cutting prior to removal of core.	41
04-01.-	Lateral view of the freezing cell without part of the PVC jacket.	90
04-02.-	Top view of the bottom of the freezing cell.	91
04-03.-	View of the freezing cell and the hanger system.	92
04-04.-	Preparation of sample using the Modified Slurry Deposition Method.	93
04-05.-	View of the freezing cell prepared to receive the sample.	94
04-06.-	View of the mixing cylinder before retrieval.	95
04-07.-	View of the freezing cell ready to receive the temperature gradient.	96
F-01.-	Placement of the jetting pipe and pushing of the first section in FP1.	228
F-02.-	Soldering the 2" copper tubes of the second section of the freezing system.	228
F-03.-	Close-up of the valves distribution.	229

F-04.-	Close-up of FP1 submitted to liquid nitrogen distribution.	229
F-05.-	RTD with attached cable inside the 0.5" PVC tube.	230
F-06.-	Preparation of S1 for sampling and view of surface piping of the freezing system.	230
F-07.-	Retrieved sample of undisturbed Duncan Sand.	231
F-08.-	View of the demodulator for System 01 and System 02 with their RTD signal conditioner boxes.	231
F-09.-	View of the burettes to measure the water expulsion or water intake.	232
F-10.-	View of the data acquisition system.	232

ABBREVIATIONS

Ap	Amphibole
Ca	Calcium
Ch	Chlorite
Dm	Dolomite
Fd	Feldspar
Gt	Garnet
Il	Illite
Ka	Kaolinite
Li	Limonite
Mi	Mica
Mg	Magnesite
Mt	Montmorillonite
Qz	Quartz
Tp	Topaz

I. INTRODUCTION

1.1 Statement of the Problem

Liquefaction assessment of sands and gravel deposits has been a concern for researchers since the earthquakes of 1935 in the Ganges River Valley, India; and of 1964, both in Niigata, Japan and in Anchorage, Alaska. Most of the ground movements have their epicenter in seismic areas within the Pacific rim and the mountainous areas of the Caucasuses and Asia. Due to the frequency and magnitude that these seismic events happen to occur, the potential for liquefaction of soils along with the damage which results is no longer considered a remote possibility. Recent examples of the damage that liquefaction causes, due to sudden earth movements, are illustrated by failure of foundations, bridge abutments and submerged slopes triggered by the San Fernando Valley and Costa Rica earthquakes. The concerns of the international community are reflected by the more demanding building code standards, put in place to prevent the loss of human lives and to minimize the damage caused by these events. In order to have an accurate evaluation of the behavior of saturated loose cohesionless soils under dynamic loading, the retrieval of high quality undisturbed samples is of particular importance.

The present state of the art in assessment of liquefaction on soils confirms that the fines content should be noted in evaluating the resistance to cyclic loading of a deposit (Seed *et. al.*, 1984). The judgement of Seed *et. al.* (op. cit.) indicate that the samples with significant fines content are more resistant to liquefaction than clean sands having the same SPT (N_1)₆₀ value. Liao (1985) using regressive methods confirmed that there is a statistically significant effect of fines on liquefaction of soils. Kuerbis and Vaid (1989) proved using artificially prepared samples that the resistance to liquefaction can remain unchanged provided that the fines content is essentially non-plastic. The Chinese criteria for liquefaction evaluation (Taiping *et. al.*, 1984) reflects the influence of the fines content of sands expressed in terms of percent clay sizes. Hence, it may be probable that the resistance to cyclic loading is not only dependent on the amount of fines but on the soil mineralogy and fabric; therefore, obtaining undisturbed samples becomes even more important in order to study the effects of the fines.

Sampling of cohesionless materials causes void ratio changes inside the sampling tube (compaction in loose sediments and dilation in denser sands), disruption of stratigraphy, and loss of fines during retrieval of the samples. This is especially true when the task has to be performed below the ground water table. Difficulties associated with the sampling of undisturbed saturated sands have led to the development of indirect methods in

which sand properties (strength, deformation characteristics, density, etc.) are related to parameters derived from penetration tests. Many of the existing empirical correlations between penetration resistance and sand density were obtained from tests in large calibration chambers (Schmertmann, 1978). Validation of these empirical correlations in the field, however, requires an independent measurement of the *in situ* density. Furthermore, preserving the actual state of packing, fabric, cementation, and fines is essential since these factors control the sand behavior during both static and dynamic loading. Yoshimi *et al.* (1989) clearly stated that *it is quite difficult, if not impossible, to detect possible signs of the cyclic mobility behavior of medium dense to dense sands in the field during earthquakes.*

Singh *et al.* (1982) examined the process of artificial freezing of soils and concluded that the best way to freeze sands in order to maintain their *in situ* state is by unidirectional freezing, with unimpeded drainage and under *in situ* confining stress. Attempts to freeze the soil before sampling have been recorded in the literature since the work of Langer (1939), but it was not until 1977 that more extensive research was carried out (Yoshimi *et al.*, 1977, 1978). Yoshimi *et al.* (1977) demonstrated that high quality undisturbed samples of saturated sands are obtainable by using ground freezing. Since then several methods of freezing and sampling have been reported in which circulation of a coolant such as a mixture of ethanol and crushed ice, liquid nitrogen or brine (liquid calcium chloride) inside a pipe resulted in radial freezing of the ground. The ground freezing as reported in the literature is expensive because it requires large diameter coring devices and heavy equipment to overcore the frozen soil and to withdraw the samples. Nevertheless, *in situ* freezing has become an attractive method of sampling, especially when liquefaction due to earthquake and ground motions needs to be analyzed. Oh-oka (1991) emphasizes that undisturbed sampling of sand has increased; particularly where important structures are designed to withstand unusually strong earthquakes which may affect even dense sand and gravel; or when unusual cohesionless soil is involved which may behave differently from ordinary sands.

Several factors affect soil while it is going through the process of freezing and clearly this is related to the frost heave susceptibility of the soil. Yoshimi *et al.* (1978) pointed out that neither the coefficient of permeability nor the gradation alone account for the expansion during freezing. Indeed, they attempted to determine the freezing behavior of the sands with an increase in fines content and concluded that for saturated sands the expansion due to freezing increased proportionally to the percent fines. The present study has concentrated on the quantity as well as the type of the fines and how these affect soil during the freezing process.

1.2 Methodology of Research

In order to evaluate the usefulness of the ground freezing technique the boundary between soils affected by the freezing and those not affected must be evaluated. To obtain this boundary at which the structure of the soil is not disturbed by the freezing process, this research was broken down into the following steps:

- 1) Determine a sample preparation method such that the fundamental material characteristics of the soil sample tested in the laboratory are representative of the *in situ* soils.
- 2) Follow a test procedure which can measure the frost susceptibility of the soil using a comprehensive frost heave theory.
- 3) Evaluate in a systematic manner the quantity and type of the fines mixed with a sand sampled by the *in situ* freezing process, in order to observe the behavior of the sand under different grain size gradation conditions.
- 4) Develop a link between frost heave and non frost heave results with a parameter which is dependent on the characteristics of the fines contained within the soil.

1.3 Scope and Thesis Organization

The study is presented in seven chapters. Chapter II is a brief introduction to the characteristics of a frozen soil, followed by a description of the methods used to obtain artificially frozen soil samples. The newest developments of the ground freezing technique are compared with the method developed at the University of Alberta. This technique is described as it was applied at the Duncan Dam in British Columbia. The characteristics of the soils retrieved by using different freezing methods and the characteristics of the soil retrieved at the Duncan Dam are also compared.

In Chapter III a search for a frost heave model is presented which would include the main factors affecting the heaving process for the purpose of this study. The Konrad and Morgenstern model (1980) was chosen not only because of its simplicity but because of the availability of useful data from previous studies for comparison purposes. Conditions for an undisturbed structure in sands by *in situ* freezing are analyzed, exploring available data from the literature. This chapter discusses the effects of different factors such as the pore water migration in sandy soils, the stress applied, the effect of the fines content and their interaction with the Konrad and Morgenstern model.

Chapter IV describes the apparatus and auxiliary equipment used in the laboratory program. Since one of the main purposes of this study is to reproduce potentially liquefiable material, the preparation of the samples using the Modified Slurry Deposition

Method (Kuerbis, 1989) is presented. The description of the whole test mechanism and the variations in procedures is compared to those of former researchers using the same apparatus and methodology.

In Chapter V the uniaxial freezing test results and analysis of the results are presented. The soils used in the study are fully characterized, including use of X-ray diffractograms for all the fines present in the sand-fines mixtures. The role of the specific surface area, the liquid limit and the activity of the fines are fully explored in order to introduce a characterization of the soils based on the specific surface area. This characterization defines a boundary between frost heave and non-frost heave regions providing a confidence margin for design and is based on the amount and type of fines mineral.

Chapter VI provides an analysis of the surface area parameters proposed in Chapter V with respect to the frost heave Segregation Potential parameter explored in Chapter III. Based on a phenomenological model, Chapter V provides the basics for the establishment of a frost heave behavior of soils with the Surface Area Index as the representative of the soil's basic characteristics. Since the results from the laboratory program are too scarce to represent a wide range of soils, an indirect comparison is performed with the use of the liquid limit of the fines fraction as a parallel to the specific surface area. Available data from the literature is used to back up a probable time dependent model.

Finally, Chapter VII presents the conclusions from the overall field testing and laboratory programs. Recommendations for future studies and application methodology of the ground freezing technique are presented. The experimental work demonstrates that the amount and type of clay mineral are the most influential parameters in the freezing process of sandy soils.

1.4 Objective of the Study

Sampling saturated loose sand is difficult since accurate observations of the structure, fabric, void ratio and density of the material require an undisturbed state. A new method for the ground freezing technique allowing sampling of a loose sand at greater depths was successfully applied at the Duncan Dam in British Columbia. The suction and expansion of the interstitial water during freezing is the obstacle to obtaining an undisturbed sample. The aim of this research is to establish a confidence area for design in which the ground freezing technique can be efficiently applied to assist in the retrieval of undisturbed sandy soil samples by analyzing the effect of the colloidal activity and the specific surface area of its fines fraction. The identification of both of these parameters in a given

cohesionless material will make it possible to determine the efficacy of performing *in situ* ground freezing to obtain undisturbed samples.

II. THE ARTIFICIALLY FROZEN SOIL

2.1 Foreword

Since this study is directed to the use of artificial ground freezing, it is appropriate to provide a brief theoretical background of the general characteristics of a frozen soil. Specifically how a cohesionless soil appears to behave when frozen from a macroscopic perspective will be discussed. Ladanyi and Sayles (1979) have pointed out that our understanding of the mechanical properties, and constitutive relationships developed for permafrost can also be used for artificially frozen ground. However, important differences between permafrost and artificial frozen ground must be recognized. In permafrost the temperature below the active layer is warmer than -15°C . Except for polygonal soil where ice wedges exist, the ground ice is dominated by ice lenses which are parallel to the ground surface. In contrast, the temperature of artificially frozen ground is characterized by steep temperature gradients with temperatures as low as liquid nitrogen temperatures near the freezing elements, and varying to 0°C at the advancing freezing front or edge of the frozen zone (Sayles, 1988). Since the orientation of the ice lenses is usually controlled by the direction of the freezing, the lenses which form are generally parallel to the freezing elements. However, ice inclusions nearly parallel to the freezing direction have been reported (Radd and Wolfe, 1978).

2.2 General Characteristics of a Frozen Soil

Soils consist of assemblies of single mineral particles or grains, and the voids between these grains are filled with water or gas, or a mixture of both. Classical mechanics of dry particulate bodies such as the skeleton of the soil is the mechanics of the single-phase particle system as the communication of air with the atmosphere is neglected. In this case there are no interactions between the skeleton and the pore fluid, but even air-dried sand actually contains a small amount of moisture. However, the mechanics of fully saturated soils; that is, for the most part free, unbound, hydraulically continuous (Ting *et al.*, 1983), and without gas content is the mechanics of a two-phase system. Traditionally the mechanics of soils considers the three-phase system where the pores contain vapor and gases, in addition to water. Nevertheless, frozen ground mechanics deals with an even more complex system of particles. Frozen ground is at least a four-phase system which contains, solid mineral particles, viscoplastic ice inclusions (cementing and interlaying ice), water in the bound and liquid states, and gaseous components (vapors and gases)

(Anderson and Morgenstern, 1973). All of these constituents are related to each other in ways that depend both on the properties of the individual phases and on the levels of external disturbances (Tsytovich, 1973).

2.2.1 The Mineral Particle Interface

The solid mineral particles of frozen soils exert an essential influence on the properties of the soils, which depend not only on the sizes and shapes of the mineral particles, but also on the physicochemical nature of their surfaces. This particular nature is determined chiefly by the minerals of the particles and the cations that are absorbed on their surfaces (Tsytovich, 1973). Frozen soils are classified in the same way as an unfrozen soil, but they are strongly influenced by the shape of the mineral particle. The freezing point depression of the unfrozen water, the electric breakdown of the water molecules, and the changes in the structure of the double layer around the soil particles, the change in the dielectric constant of water, and in the thermal properties of the various substances present in soil, are also some of the physicochemical influences on mineral particles during the freezing process (Jumikis, 1966). Thus, frozen soil behaves in a complex manner which cannot be fully described using methods and theory associated with unfrozen soils.

The shape of the mineral particles strongly affects the properties of frozen soils. The magnitude of the local forces transmitted to the frozen soil from an external load depends on the shape of the solid grains. With the passage of time, the contact area increases and the forces at the contacts decrease, as a result of time dependent deformation of the ice between the particles. However, the appearance of substantial pressures between mineral particles and ice at points of contact, no doubt has its effects on the properties of frozen soils, and in particular on the unfrozen water content. The flow of ice between the particles affects the structural matrix of the soils and increases friction between the particles, which results in the frozen soil having a resistance which changes with time (Tsytovich, 1973).

The size of the mineral particles also influences the properties of frozen soils, mainly with respect to physicochemical surface effects. These surface effects depend on the particle specific surface area, which in turn, depends on the mineralogical composition of the soils. For example, the particles of kaolin clay have a specific surface area of $10 \text{ m}^2/\text{g}$, while those of montmorillonite clay have areas ranging up to $800 \text{ m}^2/\text{g}$. For a given particle shape the ratio of the surface to volume is inversely proportional to some effective particle diameter (Mitchell, 1976). Some minerals such as the quartz or the feldspar interact poorly with pore water in contrast with montmorillonite or attapulgite which are much more active (Tsytovich, 1973). As a first approximation, which is valid

warmer than -5°C , failing as it approaches the 0°C , the specific surface area may be used to represent the combined effects of soil texture and of the matrix geometry of frozen soils on unfrozen moisture content (Anderson *et al.*, 1978).

The part played by the mineral component of soils is governed by the enormous energy of the chemical bonds between the surfaces of the mineral particles and the medium surrounding them, such as with the pore water and interstitial ice. When a soil is cooled to or below 0°C , it will tend to cause the pore water to crystallize. The exact temperature at which this can occur depends on pressure, mineralogical composition, exchangeable cations and solute content. Pore water may remain liquid to perhaps -3°C and then it starts freezing. As it does, it releases $3.347 \times 10^8 \text{ Jm}^{-3}$ of latent heat of fusion. This causes the temperature to rise to about 0°C and remain there until the rate of heat extraction from the material can no longer be counteracted by the rate of release of latent heat. At this point, the temperature of the soil will start to drop. The freezing forces then progressively exceed the capillary forces so that some of the more loosely held capillary water also changes into ice (Harris, 1986).

2.2.2 The Water Interface

Ice becomes an inevitable component of a frozen soil. Unlike solid particles, it represents a monomineralic cryohydrate rock with highly unique physicommechanical properties. Frozen soils may also contain other cryohydrate minerals (minerals that exist only at sub-zero temperatures), such as sodium carbonate (Na_2CO_3 , $T_f = -2.1^{\circ}\text{C}$), and magnesium chloride (MgCl_2 , $T_f = -3.9^{\circ}\text{C}$). All solid modifications of water are called ice, irrespective of their crystalline or amorphous state. Ice is defined as any of the solid states of pure water. Water also exists in solid forms that are not usually referred to as ice. Normally water tends to crystallize as ice I. It finds expression in the myriad forms and shapes of snow, ice crystals and frost figures. Ice I exists at ordinary pressures and at ordinary temperatures (at least about -100°C). Other forms of ice known to exist at higher pressures are ice II, III and IV to VIII. Ice I turns into ice II, which is heavier than water, as its temperature is lowered and the pressure is raised to 2200 atm, and then to ice III at a pressure of 2236 atm and temperatures of -34 to -64°C . Vainberg stated that these transitions involve sharp changes in volume and the absorption of tremendous amount of heat (Tsytovich, 1973).

Ice I or I_h because of its hexagonal crystalline system, is the most important component of frozen soils. Its highly peculiar properties are responsible in large measure for the mechanical properties of the frozen soils. It has a maximum viscoplastic

deformation in the direction perpendicular to the principal optical axis, while rheological properties in the parallel direction are so weak that brittle fracture occurs right after elastic deformation. At the same time, ice always has viscoplastic strains (flow strains) under load, even at low stress levels. Appropriate experiments show that viscosity can vary through a factor of 100 and more, depending on the direction of the forces (Tsytovich, 1973). Tsytovich (op. cit.) also cites Vainberg's conclusions, quoting that *ice exhibits elastic properties only under instantaneous loads, and its elastic limit is so low that the range of pure elastic strain is of no practical importance.*

Upon lowering the temperature, the mobility of the hydrogen atoms decreases and the ice acquires a more organized denser and stronger structure. Savelyev points out that at -78°C , the crystal lattice of ice enters a stable state (Tsytovich, 1973), and at temperatures below -70°C , it changes from hexagonal to the cubic system. With rising temperature, the activation energy of its molecules increases. This accelerates the regrouping with weaker intermolecular bonds, leading to a decrease in the strength of the ice. It follows that under natural conditions, when there are always variations of thermodynamic conditions (temperature, pressure, etc.), the properties of ice (structure, viscosity, etc.) may undergo considerable variation. These changes result in the instability of the properties of both the ice and the frozen soils in response to any change in natural conditions. It is also noted that at the particle surface electromolecular bonds of ice are considerably stronger than the molecular bonds of free water, so that free water is absorbed by the surface of the ice (Tsytovich, op. cit.).

Therefore, with the formation of new interfaces, there is an increase in the resistance of the soil to deformation as ice forms in the voids. From the thermodynamic point of view there are three independent variables which influence the non mineral components of the soils: temperature, volume and pressure. Since the soil is saturated the vapor phase is neglected in order to simplify the system, and the pore space is filled with the remaining unfrozen water w_u and the ice w_i . The total water content is the summation of both (Tsytovich, 1973; Anderson *et al.*, 1978; Johnston *et al.*, 1981). The existence and study of the unfrozen water has been described by both Tsytovich and by Anderson and Morgenstern in 1973. Unfrozen water is invariably present in any particulate frozen soil, at least down to -70°C . It is concentrated in extremely narrow chinks, capillaries, and contact points between mineral grains. The quantity of unfrozen water is not constant, but varies with variation of external factors. However, the migration of unfrozen water is an extremely slow process (Tsytovich, op. cit.).

In summary, all the individual components (mineral particles, ice, unfrozen and strongly bounded water, vapor and gases), each with their specific properties, interact in

frozen soils in ways that are determined primarily by the force fields of the mineral particle surface and the ice with water in various states. The strength of interaction depends on the specific surface area and physicochemical nature of the solid soil components and the composition of their exchange cations, as well as external disturbances (Tsyтовich, 1973).

2.2.3 Ground Ice Classification of Frozen Soils

Three basic types of frozen soil texture are distinguished. This classification is dependent on the severity of the temperature gradient and boundary conditions and is based on the type and distribution of the ice within the soil. Frozen soil can have massive, layered or reticulate structures (Tsyтовich, 1973; Johnston *et al.*, 1981). A massive or fused structure is characterized by the predominant presence and uniform distribution of pore ice and by a relative low value of total ice content. Soils with layered or laminar structure contain segregated ice, have a high total ice content, and the ice lenses are well oriented being normally perpendicular to the direction of the freezing direction. In soils with reticulate or cellular structure, ice generally forms a random net. Generally, the above characteristics apply to frozen soil whether the frozen soil is found in nature or as a result of artificial ground freezing.

2.3 Undisturbed Sampling in Sands Using Freezing Techniques

2.3.1 Historical Review

Several attempts had been reported by researchers throughout the world to obtain undisturbed samples of saturated sands by means of freezing. Jumikis (1966) reports that the idea of solidifying soils by freezing began in 1852 with the construction of a mine shaft in Auzin in northern France; when because of the low temperatures, a natural layer of ice formed around the shaft. Artificial soil freezing was first used by Siebe Gorman and Co. in 1862 in Wales, for stabilizing walls of mining shafts in loose, water-logged soils (Lightfoot, 1886). The freezing method was first introduced in the Ruhr region of Germany in 1880 by Pötsch. In the Pötsch method of artificial soil freezing (Figure 02-01), boreholes are made at 0.9 to 1.0 m intervals around the outer perimeter of the designed shaft, through water-logged soil down to impermeable strata. Freezing pipes, closed at the bottom, are inserted into the holes, and smaller pipes, called pressure pipes, are introduced almost to the bottom of the freezing pipes. Through the pressure pipes, chilled brine (liquid calcium chloride) is pumped into the freezing pipes. As shown in Figure 02-02 the

brine circulates up to the freezing pipes, carrying with it the heat adsorbed from the freezing soil by the mantle surface in contact with the soil. The warmed brine is returned to the refrigeration plant, cooled, and returned again in continuous circulation to the freezer pipes (Heise and Herbst, 1923).

From 1884 to 1886, the soil freezing method was used in the construction of a pedestrian tunnel at Stockholm, Sweden. A tunnel 25 m long was dug by freezing coarse gravel, sand and clay. In 1906, during the construction of a section of the Metropolitan, the subway system of Paris, a tunnel under the Seine was partly constructed through artificially frozen soil. The section is 1,902 m long, running from Place du Chatelet to Place St. Michel, under the Ile de la Cité and both arms of the Seine (De Loverdo, 1910). Artificial freezing of soil was applied from 1931 to 1933 to the River Sceldt tunnel in Antwerp, Belgium. In Moscow the method of artificial soil freezing was applied to subway construction from 1933 to 1946. The method was first attempted in America in 1888 with unsuccessful results in the construction of a mining shaft in Louisiana for the National Sulphur Co. (R. E., 1955). Since then several soil freezing jobs have been successfully completed (Smith, 1962).

2.3.2 The Use of Ground Freezing for Sampling Purposes

Ground freezing has been used for a long period of time as a soil stabilization method for underground excavations. However, the first attempts to obtain samples of undisturbed soil by *in situ* freezing were made by the U.S. Corps of Engineering in sampling at Fort Peck Dam (Hvorslev, 1949). Core samples of frozen sands were obtained after the ground had been frozen by circulating a freezing mixture through seven pipes driven in a circle and by retrieving the sample from the centre of the frozen shaft by coring. The quality of the samples was described as excellent on the basis of visual inspection and photographs of the cut frozen samples. Formation of ice lenses was observed in samples containing shale and clay, but not in samples of clean sands and gravels.

Freezing of the bottom of the samples to prevent the loss of a saturated sand sample during retrieval, was also used by the U.S. Corps of Engineering (Fahlquist, 1941). Singh *et al.* (1982) cites works in France by Langer (1939) and Kollbrunner and Langer (1939) in Germany showing the use of freezing techniques for partial solidification of loose and very uniform fine sand and silt before sampling. Freezing was accomplished by pumping a mixture of alcohol and dry ice through a series of pipes driven into the ground and advanced a short distance ahead of the drilling device. The use of liquid nitrogen for sampling is reported by Balla *et al.* (1971) where sand pushed into a sampler was frozen *in*

situ by applying the coolant above the sampler at the bottom of the borehole. Ishihara and Silver (1977) and Silver *et al.* (1976) stabilized samples of sand while they were being transported from the field to laboratory spraying liquid nitrogen over the tube. In 1973 Yoshimi and Hatanaka (Yoshimi *et al.*, 1978) attempted the same procedure as Hvorslev did in 1949 with the difference that the method was performed using liquid nitrogen as the coolant of the system.

Yoshimi *et al.* (op. cit.) proposed a method of soil sampling by freezing and demonstrated that it was an effective technique to obtain high quality undisturbed samples of clean, saturated sands. Since then, several methods using the ground freezing have been used in different ground conditions. Da Roit *et al.* (1981a) analyzed Yoshimi's work and tried to achieve a direct measurement of the intergranular movement during the freezing and thawing process, from the displacement of a lead-shot network within the soil mass, as observed by radiographic techniques. Only one test was carried out but it led them to the conclusion that dilation was well inside the elastic range at the end of the freezing phase. They also attempted an improved freezing technique *in situ* using liquid nitrogen and were successful in retrieving a sample 310 cm in length and 55 cm diameter which was pulled out by a crane (Da Roit *et al.*, 1981b). The procedure was carried out by drilling a borehole without circulating water, a 76 mm in diameter tube was installed open ended in order to minimize any excess pore water pressure in the borehole. After installation the tube was plugged with an inner 17 mm diameter freezing pipe positioned inside it. The coolant used was liquid nitrogen, which was later circulated in an open system.

Yoshimi *et al.* (1984) successfully retrieved *in situ* frozen samples. The samples were judged to be acceptable based on the observation that the sand appeared to preserve its structure during freezing and that the testing of the liquefaction potential based on the laboratory cyclic data appeared to be consistent with estimated field behavior during the 1964 Niigata earthquake. The procedure of sampling followed by Yoshimi *et al.* (op. cit.) (Figure 02-03) at a site with a stratigraphy dominated by a very clean, dense, uniform, fine sand with little variation in SPT N-value, was performed by drilling a 75 mm diameter hole to a depth of 10 m with a rotary drilling machine using bentonite mud. A steel pipe 73 mm in diameter and 6 mm in wall thickness was placed in the hole with the lower end open. After sealing the borehole and removing the drilling fluid, a copper freezing pipe 15.9 mm in outer diameter was installed and liquid nitrogen circulated through the annular space between the two pipes. The frozen sample was retrieved by lowering a steel casing using a boring machine to reduce the friction between the frozen soil and surrounding soil. The frozen block of sample was then lifted by gripping the freezing pipe and lifting the frozen column of soil to the surface with a crane.

In order to minimize the costs of the technique (Yoshimi *et al.*, 1985; Hatanaka *et al.*, 1985) (Figure 02-04), a different method was performed in a soil called Shirasu primarily composed of volcanic sand. A 420 mm hole was drilled until the top of the sampling zone with a boring machine and a steel casing 406 mm in diameter installed, therefore limiting the freezing process to a predetermined region. A 55 mm hole was then drilled in the centre of the borehole, and a steel pipe fixed to a PVC rod was introduced into the hole until the targeted depth was reached. The top of the steel pipe was screwed to another one 73 mm in diameter and covered with glass wool for thermal insulation. Another steel pipe 42.7 mm diameter was placed inside the 73 mm pipe for additional thermal insulation. The way in which the copper pipe was placed, the liquid nitrogen circulated and the frozen sample retrieved is basically the same as described by Yoshimi *et al.* (1984). The same method was successfully used to obtain undisturbed Shirasu samples from a depth of 23.3 to 25.7 m below the ground surface at another site.

One of the last attempts to recover sand by freezing methods was in 1986 (Yoshimi *et al.*, 1989) at a site designated as Meike in Niigata, Japan (Figure 02-05). They mention as well other experience at a site called Showa Bridge in the same region but no data concerning to the samples is published. At the Meike site a borehole 1 m in diameter was drilled to a depth of 5 m with a TBM-70 type rotary machine. A 813 mm in diameter steel casing was placed to prevent the collapse of the hole. Using a cement mortar base with a hole in the centre as a guide, a 76 mm hole was drilled. The method used is nearly the same as described by Yoshimi *et al.* (1984) except for the fact that chilled brine was used as coolant which was continuously circulated for 3 weeks. The temperature of the brine was at -28°C at the moment of entering into the freezing pipe and at -26°C when coming out. The quality of the samples was judged to be good based on the fact that the small strain shear moduli measured in the laboratory were consistent with those measured in the field. At Showa Bridge the coolant used was liquid nitrogen, but the procedure was the same as that followed at the Meike site.

Successful attempts to obtain undisturbed samples of pure gravel (Goto *et al.*, 1987) and interlaying gravel with sandy material (Hatanaka *et al.*, 1988) have also been achieved. Due to the inherent difficulties of freezing gravels new techniques had to be added to the main freezing method. Goto *et al.* (op. cit.) introduced steel refrigeration pipes of 10 cm diameter and 9.5 m length insulated for the upper 5.5 m, in boreholes spaced 1 m apart. The freezing pipes were positioned in a trapezoidal layout. In this case, the material was frozen by circulating brine using a small conventional refrigeration unit. The freezing was fully completed with the brine at -30°C after 4 weeks. In order to sample a layer of unsaturated gravel located within the upper ground water table, water was

injected through the prebored boreholes during the freezing phase. All the frozen gravel samples (300 mm in diameter, 600 mm in height) were obtained by coring with a double tube core barrel with diamond teeth, rotated by a DH-4 boring machine at different locations, at about 50 cm away from the refrigeration pipes. The author has a concern with the application of this methodology since the samples obtained within that region might be disturbed. The water expelled from the frozen zone to the non frozen zone starts to accumulate in the sampling region mainly because of the advance of several freezing fronts towards the same point at the same time. Consequently, depending on the amount and type of fines, a frost heave process might be triggered due to impeded drainage of pore water.

Hatanaka *et al.* (op. cit.) reported their experience with Tokyo gravel where a single freezing pipe was installed. The installation was achieved by predrilling a 120 cm borehole to the desired depth, at about 18.5 m below the ground surface, and then installing guide pipes fixed by two steel plates at both ends in order to determine the locations of the freezing pipe. A 73 mm steel tube was installed in the 76 mm guide pipe to a depth of 21 m. A PVC pipe was installed within the 73 mm pipe for heat insulation purposes and a steel tube, 21.7 mm in diameter and 3.5 mm thick, was placed in the PVC pipe. Liquid nitrogen was circulated for about 160 hours between the annular space of both pipes and a total of 40 tons were consumed. The diameter of the frozen column was estimated from the monitored temperatures provided by the thermocouples placed in a PVC rod attached at the end of the 73 mm steel pipe. The sampling of the frozen soil from the undisturbed area was carried out by lowering the double-tube core barrel with diamond teeth and then rotating it with a DH-4 type boring machine using chilled mud to about -10°C. The size of the recovered sample was about 300 cm in diameter and 80 to 90 cm long. From this a 60 cm long specimen was prepared for testing.

A better observation of the differences between the methods of sampling using ground freezing in sands and sandy gravels is presented in Table 02-01 and Table 02-02 respectively. The ground conditions and the physical properties of the undisturbed soil samples retrieved by the methods compared in Table 02-01 and Table 02-02 are presented in Table 02-03 and Table 02-04. These tables include features and data on the method used and the soil retrieved from the Duncan Dam site, as well. Probably the main difference between the material sampled at the Duncan Dam and the materials sampled by the Japanese researchers is the amount of fines. At a first glance, the Duncan Dam soil, due to the high amount of fines, probably would be classified as potentially frost susceptible. This is one of the main points that this study will try to evaluate. In fact, even though this material possesses a high proportion of fines, the probability of frost heave occurring during ground freezing is negligible.

2.3.3 The Duncan Dam Experience

What was probably the first application of ground freezing to obtain undisturbed samples in Canada is presented in this section. The sampling operations were carried out during the summer of 1990 (Sego *et al.*, 1990; Robertson *et al.* 1991). The site was located at the toe of the Duncan Dam situated in the Columbia basin in the Province of British Columbia. A site plan showing freeze pipe and sample boreholes is shown in Figure 02-06 and Plate 02-01. The soil profile, the SPT -N value throughout the layer and the depths of the soil samples recovered are shown in Figure 02-07. The steel freezing pipes were installed as illustrated in the layout in Figure 02-08.

Prior to the installation of the refrigeration system, a total of eight open ended 15.3 cm diameter casings were driven through the first 10 m of the thick gravel stabilizing berm placed during the construction of the dam. The 10 m depth was selected to ensure that the uniform sand layer which began at a depth of 12 m would not be disturbed by the process of driving the steel casings. The boreholes were named as FP1 and FP2 for Freezing Pipes No. 1 and No. 2, respectively; and S1 to S6 for Sampling Boreholes No. 1 to No. 6 (Figure 02-06). The sampling boreholes were therefore preselected and located an average distance of about 50 cm from their centres to the centre of the freezing boreholes. The exact distances from the freezing pipes to the sampling boreholes are shown in Table 02-05. The sampling zone was defined to be between 12 and 18 m below the ground surface at FP1 and between 16 and 20 m at FP2.

Due to the depth of the sampling zone, the freezing pipes consisted of two different metal sections connected by a brass coupler. The first section of the freezing pipe consisted of a steel pipe of 5.1 cm diameter and 7 m length, attached to a special hardened steel cutter shoe. Figure 02-08a shows the cutter at the tip of the first section of the freezing pipe. This section of the freezing pipe was stabilized and centered within the upper steel casing using sliding stabilization rings which were evenly spaced along the pipe section using interconnected ropes (Plate 02-02). As the freezing pipe advanced into the soil the rings stopped at the bottom of the surface casing for later retrieval using the interconnected ropes. The pipe was advanced until a depth of 18 m below the ground level so that only 1 m of the first section of the freezing pipe was left above the bottom of the 15.3 cm diameter casing. This length was left in order to improve the connection using the brass coupler attached at the bottom of the second section.

To minimize disturbance to the soil adjacent to the freeze pipe, the freezing pipes were self-bored into the soil using an internal jetting pipe. As can be observed in Plate D-01 the jetting pipe (Figure 02-08a) was kept between 10 to 20 cm above the advancing

cutter shoe to reduce the potential for disturbance of the soil which surrounded the freeze pipe. In Plate 02-03 the second section is shown, it consisted of a 3.8 cm diameter copper pipe and the brass coupler attached at its bottom. This piece was machined in such a way that it would prevent water entering into the freezing pipe, with the aid of a silicone seal. The second section was then coupled to the first one as shown in Figure 02-08b. The second section consisted of 5 m copper pipes which were soldered where needed (Plate D-02) to achieve the desired length. The next step (Figure 02-08c) was the installation of a 1.3 cm diameter copper pipe inside the 5.1 cm diameter freezing pipe. Both the 1.3 cm diameter and the 3.8 cm diameter copper pipes, were left for connection with the refrigeration system.

The FP2 was installed using the same procedure followed in FP1, with the only difference that the upper 15.3 cm diameter casing was advanced to 16 m. The first section of the freezing pipe was advanced to 21 m below the ground surface using the same procedure as in FP1. This provided 2 m of pipe above the bottom of the casing to couple the second section of the freezing pipe and 1 m at the bottom for a seal composed of bentonite pellets to provide an impermeable seal. Another 1.3 cm diameter copper pipe was also installed inside the 5.1 cm diameter freezing pipe and connected to the freezing system. Bentonite seals were placed at the end of the 15.3 cm diameter steel casings to define the boundaries of the sampling zone, prevent heat loss during circulation of the liquid nitrogen and provide an impermeable seal. After the seals became impermeable the water in the casings was removed by flushing with air and the space was back-filled with vermiculite insulation. FP2 presented leakage problems probably at the depth of the brass coupler connection. Due to this fact the bentonite seal had to be flushed out from the hole by injecting water into the hole. The procedure was completed prior to circulation of liquid nitrogen.

The layout of the refrigeration system can be observed in Figure 02-09 and the piping can be observed in Plate 02-04. The freezing system consisted of 1.3 cm diameter copper tubing, heavily insulated with Styrofoam and glass wool to prevent heat loss, and it was connected to the liquid nitrogen tanker. The system was arranged in such a way that both freezing pipes could be independent of each other, so that either one or both of them could receive the liquid nitrogen. A third option of circulation was also arranged to allow either pipe to receive the cold gas previously vented in the other pipe. The liquid nitrogen was pumped into the 1.3 cm copper pipe and circulated between the annular space of the 1.3 cm and the 5.1 cm in diameter pipes. However, the phase change occurred within this annular space, and the resultant gas was vented to atmosphere or recirculated. Figure 02-10 shows the nitrogen usage versus time through the project yielding a rate of nitrogen

consumption averaged about 180 L/h (4230 L/day). It can be observed in Plate D-05 that a pressure valve was installed at the top of the freezing pipes. With the aid of this device the vaporized liquid nitrogen pressure could be controlled, but it was more useful to allow the gas to be vented to the atmosphere without allowing a back pressure in the pipe.

In order to obtain a continuous reading of the advance of the freezing front, Resistance Temperature Detectors (RTD) described in section 4.1.2 were installed at about 0.5 m and 1.0 m away from the freezing pipes. These devices allowed determination of the radial advance of the freezing front at any moment with good accuracy and reliability. The locations of the temperature monitoring boreholes are shown in Figure 02-06 and the distances at the ground surface between the pipes are presented in Table 02-05. The RTDs were placed at the top of the sampling zone in 1.3 cm diameter plastic tubes (Plate D-05) which were, in turn, lowered in boreholes drilled without use of a casing. A deviation from this usage occurred between 240 and 280 hours as observed in Figure 02-10 and Figure 02-11, and is related to changes in the advance of the temperature as recorded by RTD 1 associated with FP1 and by RTD 6 associated with FP2. The monitored ground temperatures at both freezing pipes by RTD 1, RTD 2, RTD 5 and RTD 6 can be observed in Figure 02-12. The sampling boreholes and RTD 1 associated to FP1 can be observed in Plate 02-05.

The initial ground temperature recorded at RTD 1, 50 cm away from FP1 and at a depth of 11.5 m below the ground surface was +8.2°C which was 4°C warmer than the temperature used during the design. The initial ground temperature recorded at RTD 6, 60 cm away from the FP2 and at a depth of 13.4 m below the ground surface, was about +7.5°C. The difference between the temperatures shows the existence of a temperature gradient of 0.37°C/m between 11.5 and 13.4 m below the surface, therefore indicating the existence of a flow of heat downwards at the sample location. In both pipes, after the liquid nitrogen started to circulate, the temperature decreased rapidly but then the rate of freezing gradually decreased. The ground temperature recorded by RTD6 decreased at a much lower rate than that recorded by RTD1 where 0°C was achieved after 260 h. To investigate this slower rate of heat extraction a deeper temperature probe was installed at location S3 by drilling a borehole to a depth of 16 m below the ground surface, after 240 h of freezing. Borehole S3 was chosen due to the position of its bottom, which was tilted away from the frozen column. The ground temperature profile was better determined by using the multiple RTD probe in which a total of four RTDs were installed at 13, 14, 15 and 16 m of depth and at about 77 cm from FP1. The recorded temperatures can be observed in Figure 02-13, where the vertical temperature gradient illustrates clearly the vertical heat flow at the sampling zone, at FP1. The steady decrease in temperature versus

time shows the advance of the freezing front.

After 12.5 days of continuous circulation of liquid nitrogen, and based on the temperature readings, it was decided to core in the borehole S1. The adopted methodology of coring was to make use of the CRREL core barrel originally designed for permafrost soils sampling (Plate 02-06). The barrel was modified on site to install core catchers between the cutting foot and the cutting shoe to enhance the recovery, by preventing the bottom portion of the core from breaking and falling back down the hole. The bentonite plug which had previously been installed at the top of the sample boreholes was cored even though it was not frozen. At a depth of 13.2 m below the ground level the barrel sampled a uniform grey frozen sand. The frozen sand was easily drilled with the tungsten carbide tips inserted in the cutting shoe and a total of 10 individual cores were recovered, giving a total core length of 3.4 m of the 3.5 m drilled. Although the temperature readings showed that the frozen column did not achieve the desired diameter in the FP2, it was decided to core in borehole S6. The retrieval of frozen core from this sampling borehole was unsuccessful.

A decision to retrieve as much frozen sample as possible was made, so attention was turned to FP1, where the chances of finding frozen material were greater. Because the sampling borehole S2 was considered too far away from the frozen column, the decision to drill a new borehole was made. This new borehole, designated as S7 was drilled adjacent to the S1 casing. Due to the urgency with which the drilling process was carried on, as the refrigeration system had stopped working, the borehole was found after the drilling process was completed to be tilted slightly outwards from the frozen column. Nevertheless, once the casing was set and the coarse material cleaned from it, the CRREL core barrel was mounted and the coring phase started. The top of the frozen column was found about 12.2 m below the ground surface and continuous coring produced a total length core of 4.0 m from 4.3 m drilled. During the sampling in S7, water seeped in between the bottom of the casing and the frozen column causing a small thermal disturbance during the drilling and sample recovery operation. In both cases, S1 and S7, the core was of very good to excellent quality. The recovered samples were appropriately wrapped in plastic, damp paper towels and aluminum foil so that sublimation would be prevented. After this, the samples were also wrapped in bubble plastic and placed in PVC tubes which were sealed in order to prevent damage during transportation.

2.4 Discussion of The *In Situ* Freezing Method

Taking into consideration the experiences for *in situ* freezing of sands and gravels, described in sections 2.3.2 and 2.3.3, it is observed that since Yoshimi *et al.* (1977)

introduced this technique to obtain undisturbed samples of saturated sands the procedure has gone through several improvements. The retrieval of a sample at a desired depth and even under different overburden conditions, as well as the ability to sample coarser material, are the main advances in the technique. The most common method to determine both the time to freeze the soil as well as the energy which must be extracted from the ground is the method by Sanger and Sayles (1978). The frost front advance was recalculated with the various ground temperatures encountered at the field (Figure 02-14). Figure 02-15 describes the range of soil particle size at which this technique can be applied. Tables 02-01 and 02-03 compare the different conditions and techniques with which artificially frozen sands were retrieved.

In order to obtain samples by *in situ* freezing while achieving negligible volume change and therefore, an undisturbed condition; the obtained soil sample has to meet two main conditions: unimpeded drainage and adequate confining pressure. Thus, if a large enough sample is obtained under such conditions by *in situ* freezing, and if the zone of sampling is at a sufficient distant from a possible zone of disturbance caused by the drilling, the sample may be considered to be of high quality. That is, the structure of the soil *in situ* is preserved. Singh *et al.* (1982) stated that the method of unidirectional freezing of sands appears to provide an effective means of preserving the structure of a sand. *Such a method, when adopted for in situ freezing and then coupled with a suitable coring procedure, would, therefore, appear to provide a suitable means for recovering undisturbed samples of much higher quality than can be achieved with current practice.* Yoshimi *et al.* (1977, 1978, 1984) found a third condition to ensure that the pore water freezes without an increase in soil volume, by allowing the excess water to flow out from the freezing front. This third condition is controlled by the amount of fines within the soil, and is therefore fundamental in the success of the sampling technique. This condition, from the author's perspective, should not only include the quantity but also the type of fines within the soil. Indeed, Hoshino (1977) reports that the *in situ* density may be underestimated; that is, the structure of the soil is disturbed if fines content exceeds a certain limit value. This statement is important primarily because of the type of fines which the soil contains rather than its quantity, and the present study will try to evaluate the importance of the type of fines.

Yoshimi *et al.* (1978) completed a fairly extensive research, studying different aspects of the problems affecting the disturbance in cohesionless soils. The equipment used in their study (Yoshimi *et al.*, 1978, 1984) resembled an oedometer, except that thermal insulation was provided around the container, so that the specimen would freeze in an upward direction only. The apparatus itself was roughly similar in design to that

described in section 4.1.2. The steel bottom plate was submerged in a mixture of ethanol and crushed dry ice, therefore the freezing front developed upwards but the apparatus was not attached to a hanger system. This test attempts a simulation of the sampling procedure by the freezing technique proposed by Yoshimi *et al.* (1978). The tests performed on three different sands studied the effect of surcharge pressures, coolant temperature, relative density, soil type and fines content, as well as the freezing and thawing process. Their results showed that freezing and thawing had negligible effects on the strength and deformation characteristics of sands. Yoshimi *et al.* (op. cit.) concluded that radial freezing in the field would not cause significant change in the *in situ* stresses in the sand and therefore, the method of soil sampling by freezing is an effective technique to obtain high quality undisturbed samples of *clean* saturated sands.

Yoshimi *et al.* (1978) state that *the expansion due to freezing increases with an increase in density or a decrease in the coefficient of permeability. It appears, therefore, that the expansion is more influenced by the rate at which pore water is expelled than by the quantity of pore water.* The fact that a coolant temperature of -20°C resulted in small expansion due to freezing suggests that conventional refrigeration methods using brine may be effective in field applications. Their research was less detailed related to the surcharge and fines content than it was on the density aspect. Nevertheless, results are presented in which the trend of three different sands is to decrease their expansion (inhibiting frost heave) as the surcharge increases. Therefore stress plays an important role in impeding the soil of expanding in volume when submitted to a cold temperature.

Yoshimi *et al.* (op. cit.) published as well results provided by the behavior of artificially prepared Tonegawa sand-fines mixtures tested under a coolant temperature of -66°C and submitted to a total stress of 33 kPa. The trend shown by the mixtures of this sand with different amounts of a fine grained soil (which was not specified) is to increase the expansion due to freezing as the amount of fines content increases in the soil. The author has his concerns with respect to the conclusions drawn by the results based on this part of Yoshimi's research. Doubts exist around the description of the equipment, testing procedures and preparation of the specimens. Primarily, the boundary conditions imposed to the specimens were not well established. The samples were tested under a variable temperature gradient since only one side of the sample was under a constant temperature. It is now known (Konrad and Morgenstern, 1980), that soils submitted to a temperature gradient with one side under sub-zero temperature will be much more influenced by the fluctuations on the warm side than on the cold side. Secondly, exists the probability that the tests were conducted in a closed system; thus, no drainage was provided, therefore the migration of water may have been inhibited. This condition could led to an expansion of

the interstitial water within the specimen and therefore specimens which were not supposed to undergo frost heave may have experienced this behavior.

The method that Yoshimi *et al.* (op. cit.) used for the preparation of their specimens and the short period of time that the samples were tested are other issues concerning the reproducibility of the test. In summary, a reasonable doubt is established with respect to the methodology under which the specimens were tested. The present study will try to establish reasonable boundary conditions and limits on the possible variables to avoid confusions with the results. The conditions which a sandy soil must meet for its structure to remain undisturbed are discussed separately in Chapter III, defining what is an unimpeded drainage condition, and explaining the effect of surcharge on soil and why it is believed that the type and quantity of fines influences the behavior of soils subjected to negative temperature boundary conditions.

Methods of Sampling by In-situ Freezing in Sands

Table 02-01

Site	Source	Sampling Date	Coolant	Method of Sample Recovery	Maximum Sample Diameter (cm)	Depth of Sample Recovered (m)	Depth of Sample Tested (m)	Designation
Niigata Station	Yoshimi et al, 1984	Aug, 1982	Liquid Nitrogen	Coring	50.0	7.0 - 10.0		A
Kawoyima City	Hatanaka et al, 1985		Liquid Nitrogen	Pull	57.0	1.4 - 7.0	9.3 - 9.6	B
Kawoyima City	Hatanaka et al, 1985		Liquid Nitrogen	Coring	34.0	8.0 - 10.6	5.4 - 5.7	C
Kawoyima City	Hatanaka et al, 1985		Liquid Nitrogen	Coring	34.0	23.3 - 25.7		
Showa Bridge	Yoshimi et al, 1989	Mar, 1983	Liquid Nitrogen	Pull with water jet	40.0	7.0 - 10.7		D
Meike	Yoshimi et al, 1989	Jan, 1986	Chilled Brine	Coring	57.0	5.9 - 9.3		E
Duncan Dam	Sego et al, 1992	Jul, 1990	Liquid Nitrogen	Coring	10.8	13.2 - 16.6		F1
Duncan Dam	Sego et al, 1992	Jul, 1990	Liquid Nitrogen	Coring	10.8	12.2 - 16.2		F2

Methods of Sampling by In-situ Freezing in Sandy Gravels

Table 02-02

Site	Source	Sampling Date	Coolant	Method of Sample Recovery	Maximum Sample Diameter (cm)	Depth of Sample Recovered (m)	Sample Size (d*h) (cm)	Designation
Chiba Prefecture	Goto et al, 1987		Chilled Brine	Coring	30.0	6.0 - 9.0	30 * 60	A
Tokyo Station	Hatanaka et al, 1988		Liquid Nitrogen	Coring	30.2	18.5 - 21.0	30 * 60	B

Table 02-03 Field Conditions and Physical Properties of In-situ Frozen Sand Samples

Sample Designation	A	B	C	D	E	F1	F2
N-value	32.00			18.00	24.00		
Effective vertical stress (kg/cm ²)	1.08			1.00	0.90		
N1-value	30.00			18.00	26.00		
Specific Gravity	2.68 - 2.76	2.43 - 2.45	2.42 - 2.58	2.70	2.72	2.74	2.74
Maximum Dry Density (g/cm ³)	1.51 - 1.53	1.21 - 1.27	0.96 - 1.08	1.61	1.62	1.64	1.64
Minimum Dry Density (g/cm ³)	1.21 - 1.22	0.88 - 0.92	0.70 - 0.79	1.27	1.27	1.12	1.12
50% Diameter, D ₅₀ (mm)	0.28 - 0.30	0.38 - 0.51	0.28 - 0.43	0.30	0.23	0.13	0.13
10% Diameter, D ₁₀ (mm)	0.16 - 0.19	0.05 - 0.07	0.024 - 0.065	0.20	0.15	0.023 - 0.032	0.023 - 0.032
Uniformity Coefficient, U _c	1.70 - 1.90	11.60 - 13.80	8.20 - 15.3	1.60	1.70	4.06 - 5.65	4.06 - 5.65
Fines Content (%)	0.00	11.10 - 14.40	11.10 - 17.40	0.20	0.30	21.80	21.80
Mean Dry Density (g/cm ³)	1.47			1.47	1.55		
Mean Relative Density Dr(%)	87.00	63.00	77.00	64.00	84.00		
Elastic Shear Modulus, Gr (kg/cm ²)	800.00			600.00	740.00		

Table 02-04 Field Conditions and Physical Properties of In-situ Frozen Gravel Samples

Sample Designation	A	B
N-value	50.00	50.00
Gravel Content (%)	50 - 60	60 - 80
Maximum Dry Density (g/cm ³)	1.96	2.14 - 2.25
Minimum Dry Density (g/cm ³)	1.65	1.85 - 1.92
50% Diameter, D ₅₀ (mm)		5.6 - 11.8
10% Diameter, D ₁₀ (mm)		0.046 - 0.740
Uniformity Coefficient, U _c	10.00	60 - 122
Fines Content (%)		6.0 - 11.8

Table 02-05 Distances from the Freezing Pipes to the Sampling and RTD Boreholes.

Freezing Pipe	Borehole	Distance (m)
FP1	S1	0.57
FP1	S2	0.51
FP1	S3	0.44
FP1	RTD1	0.42
FP1	RTD2	0.99
FP2	S4	0.48
FP2	S5	0.54
FP2	S6	0.45
FP2	RTD5	0.92
FP2	RTD6	0.55

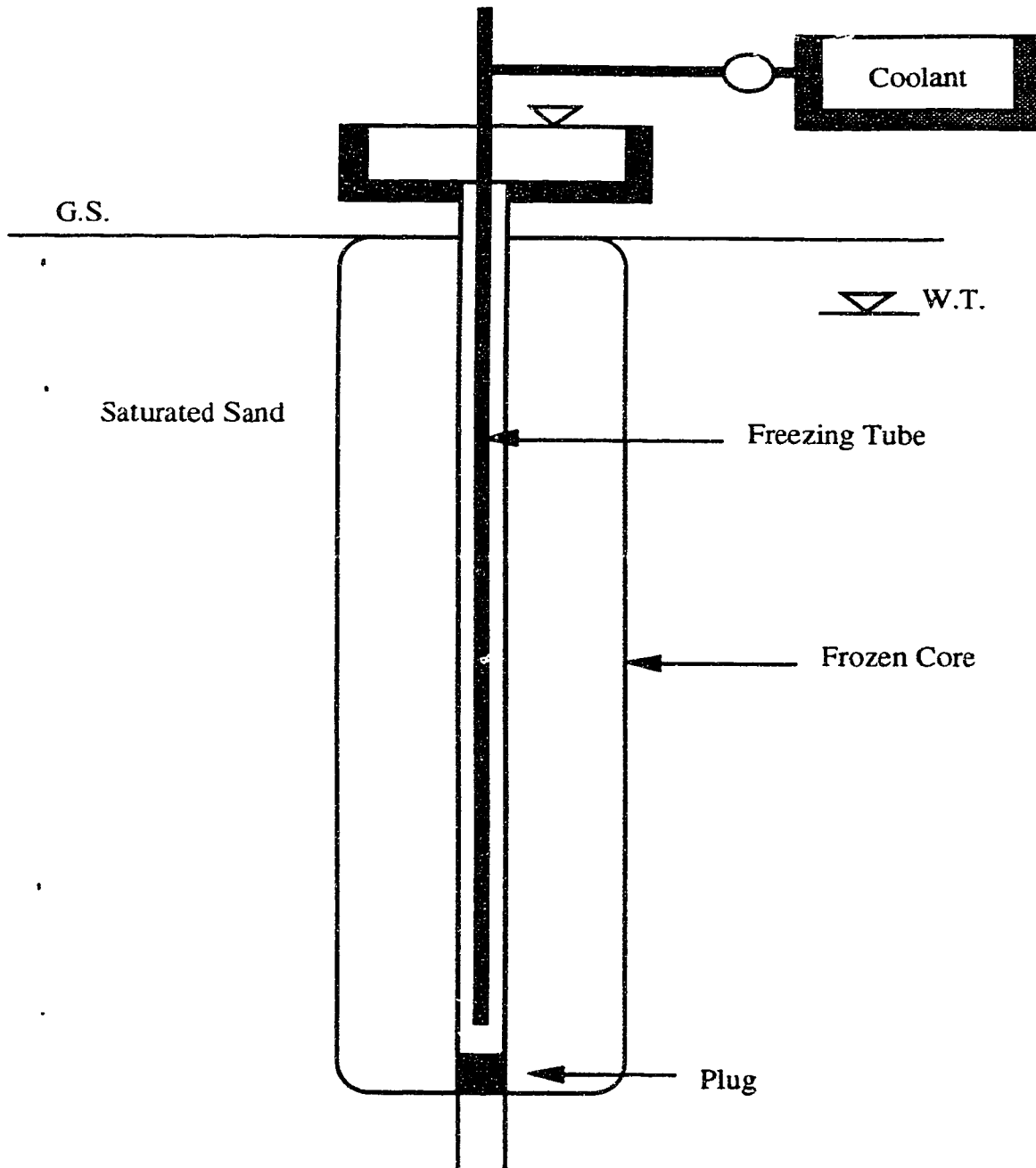


Figure 02-01.- The Pötsch Refrigeration Method

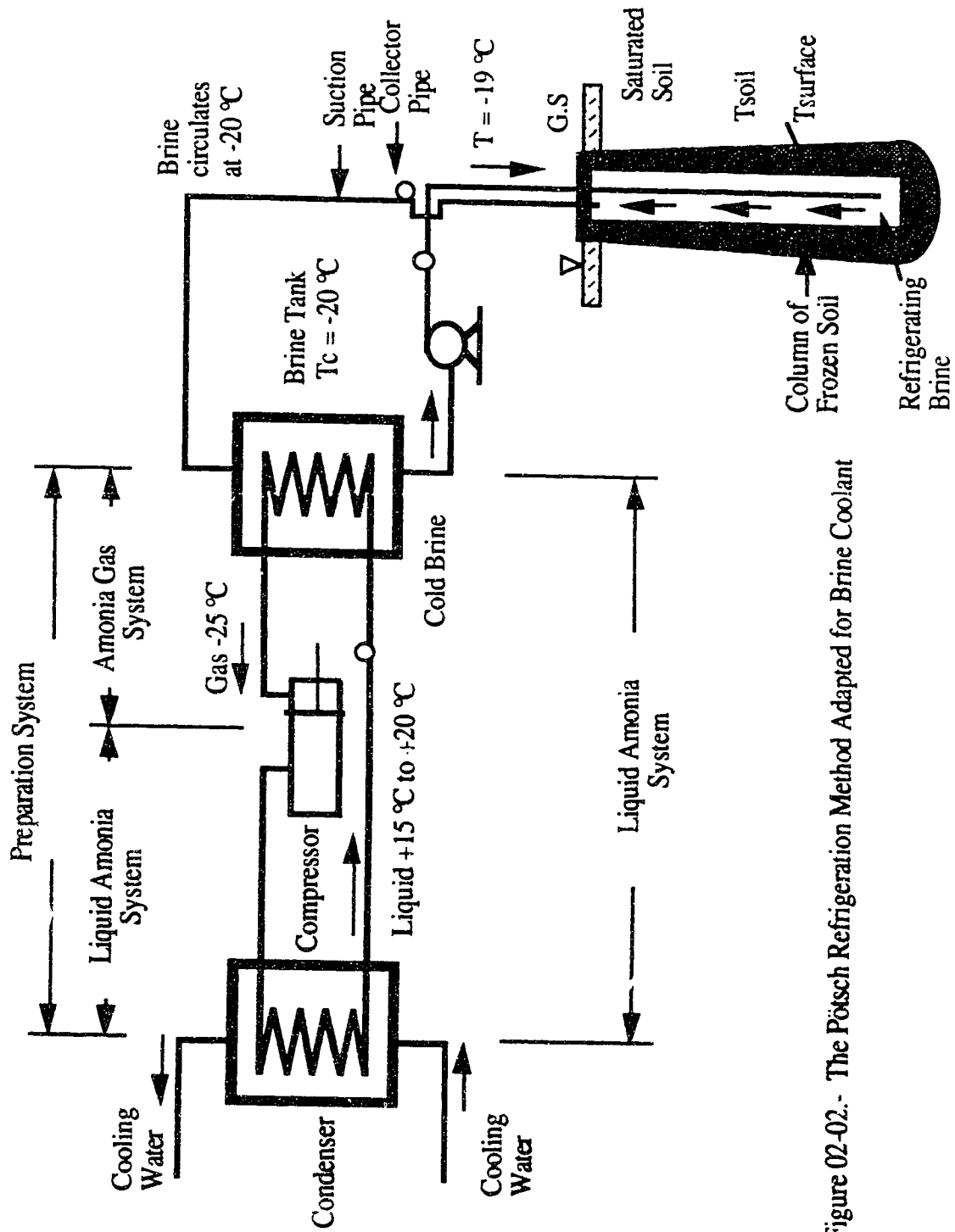


Figure 02-02.- The Pötsch Refrigeration Method Adapted for Brine Coolant

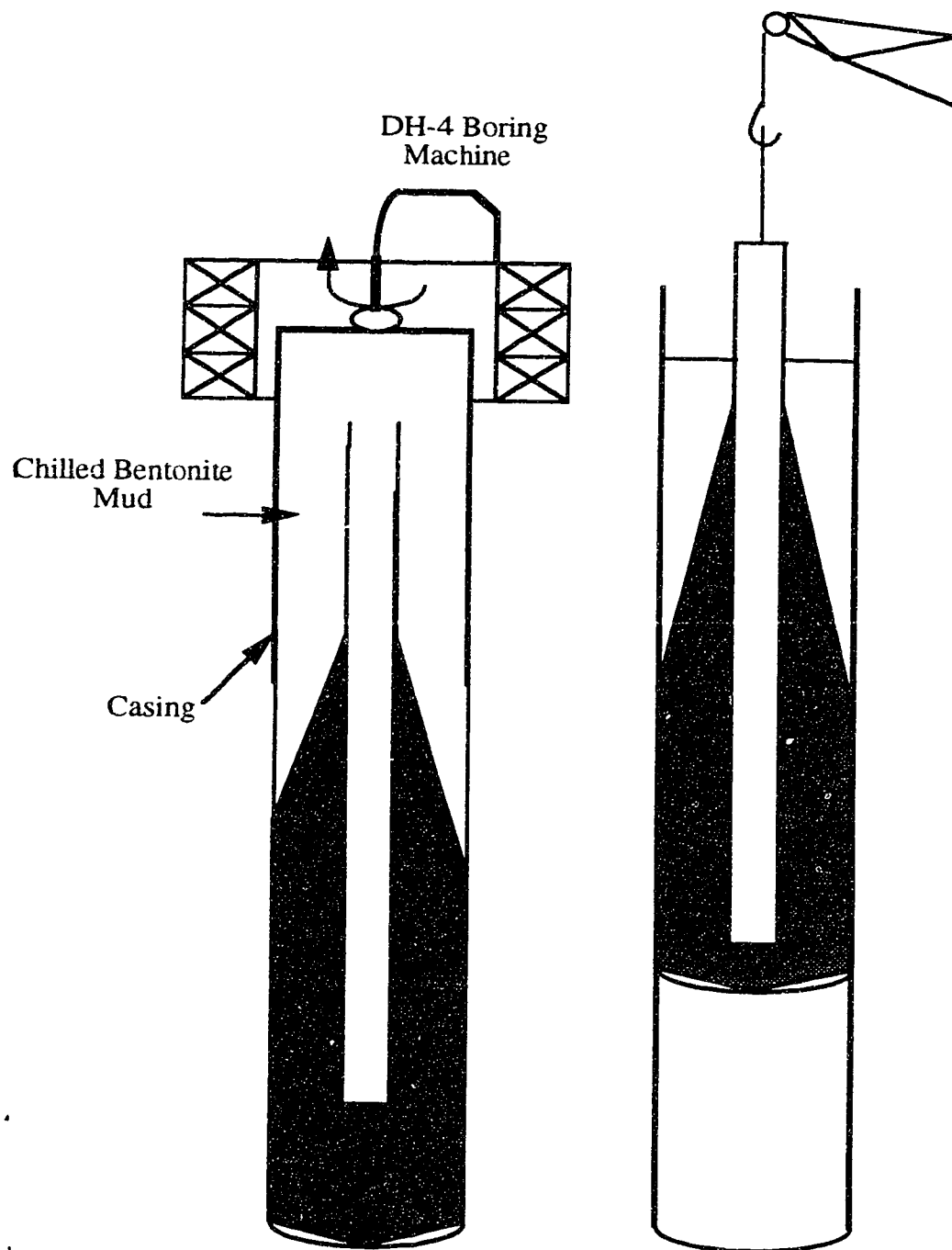


Figure 02-03.- In-Situ Freezing and Sampling Method
After Yoshimi *et al.* (1984)

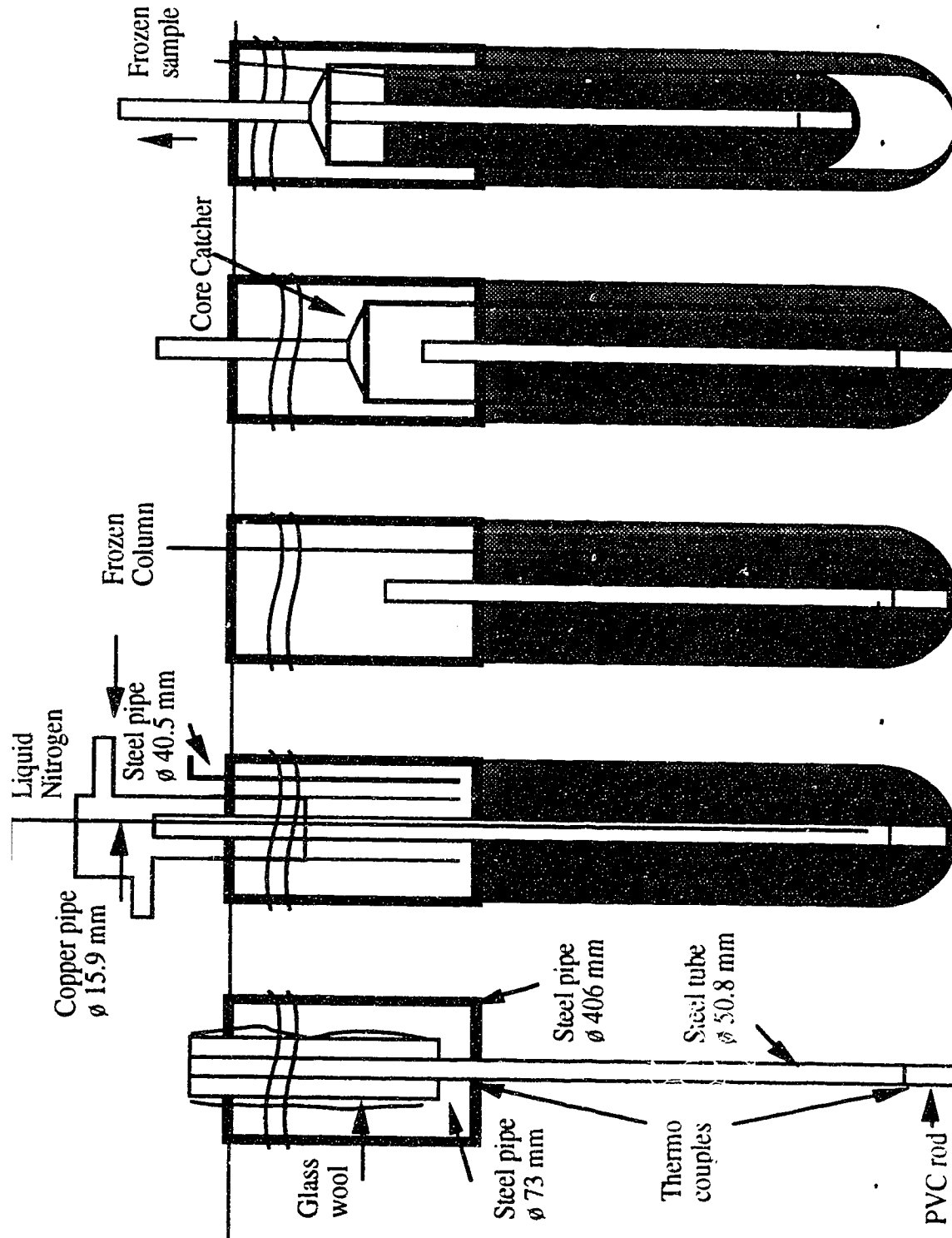


Figure 02-04.- In-Situ Freezing and Sampling Method. After Hatanaka *et al* (1985)

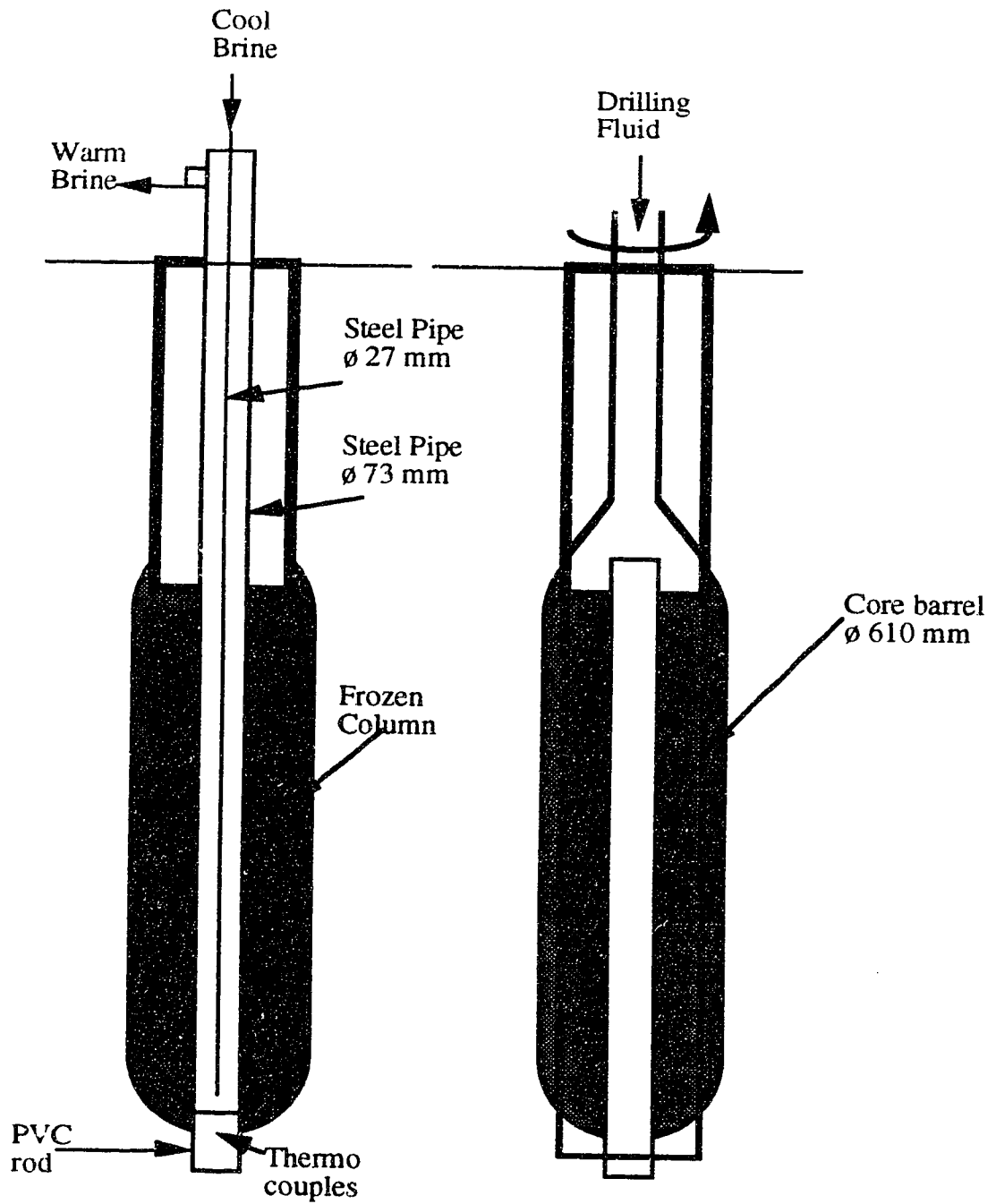


Figure 02-05.- In-Situ Freezing and Sampling method. After Yoshimi *et al.* (1989)

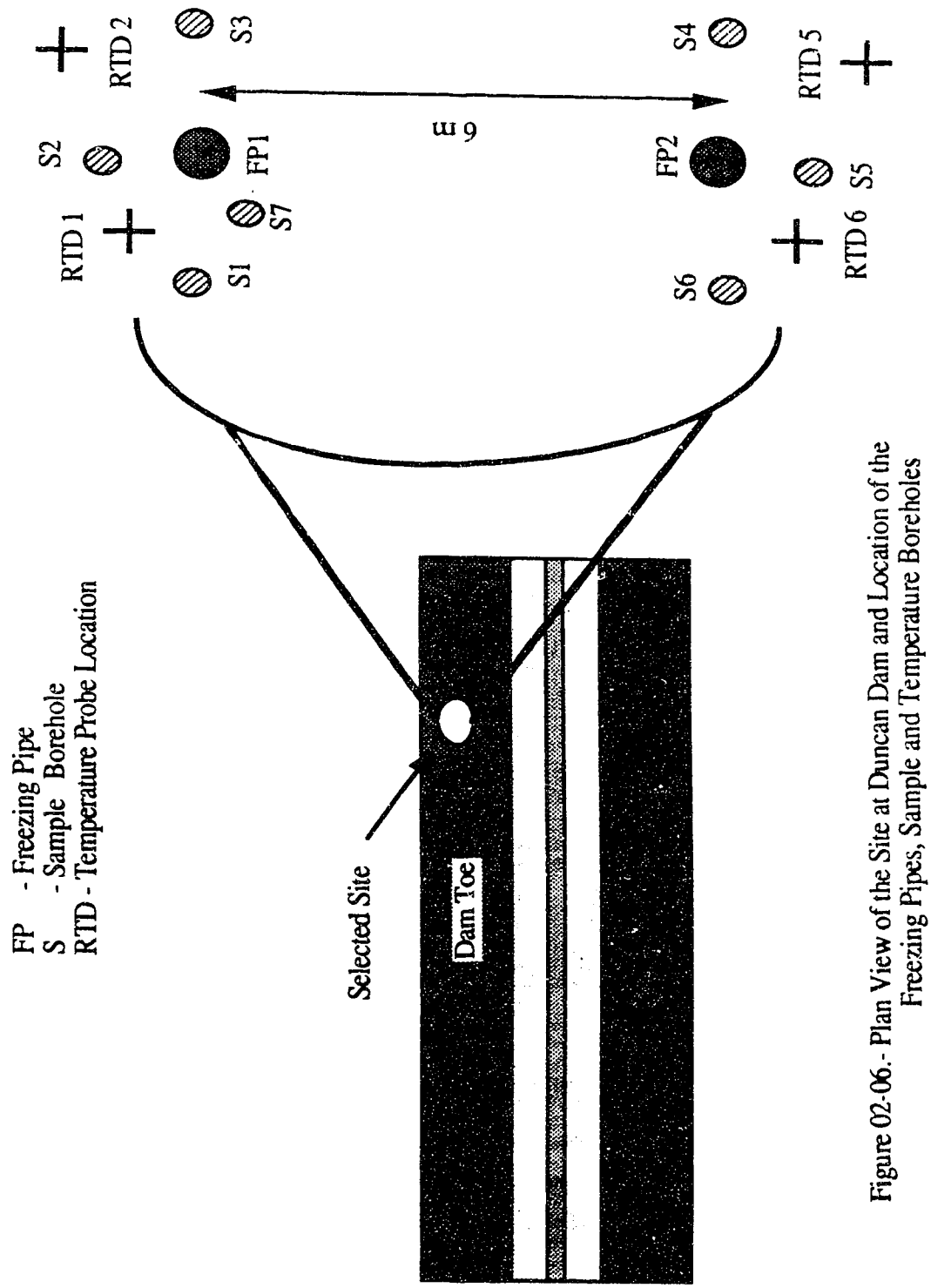


Figure 02-06.- Plan View of the Site at Duncan Dam and Location of the Freezing Pipes, Sample and Temperature Boreholes

ELEVATION (m)		DEPTH (m)		PROFILE		DESCRIPTION		SAMPLE TYPE		SAMPLE NO.		SAMPLE RECOVERY %		TEST RESULTS						WATER CONTENT OF No. 4 FRACTION						PLASTICITY AND LIQUID LIMITS						PENETRATION RESISTANCE						REMARKS																																																																																																																																																																																																																																																																																																																																																																																																																																																																																																																																																																																																																																																																																																																																																																																																																																																																																																																																																																																																																																																																																																																																																																																																																																																																																																																																																																																																																																																																																																																																																																																																																																																																																																																																																																																																																																																																																																																																																																																																																																																																																																																																																																																																																																																																																																																																																																																									

Figure 02-07.- Soil Profile at the Duncan Dam Freezing Location

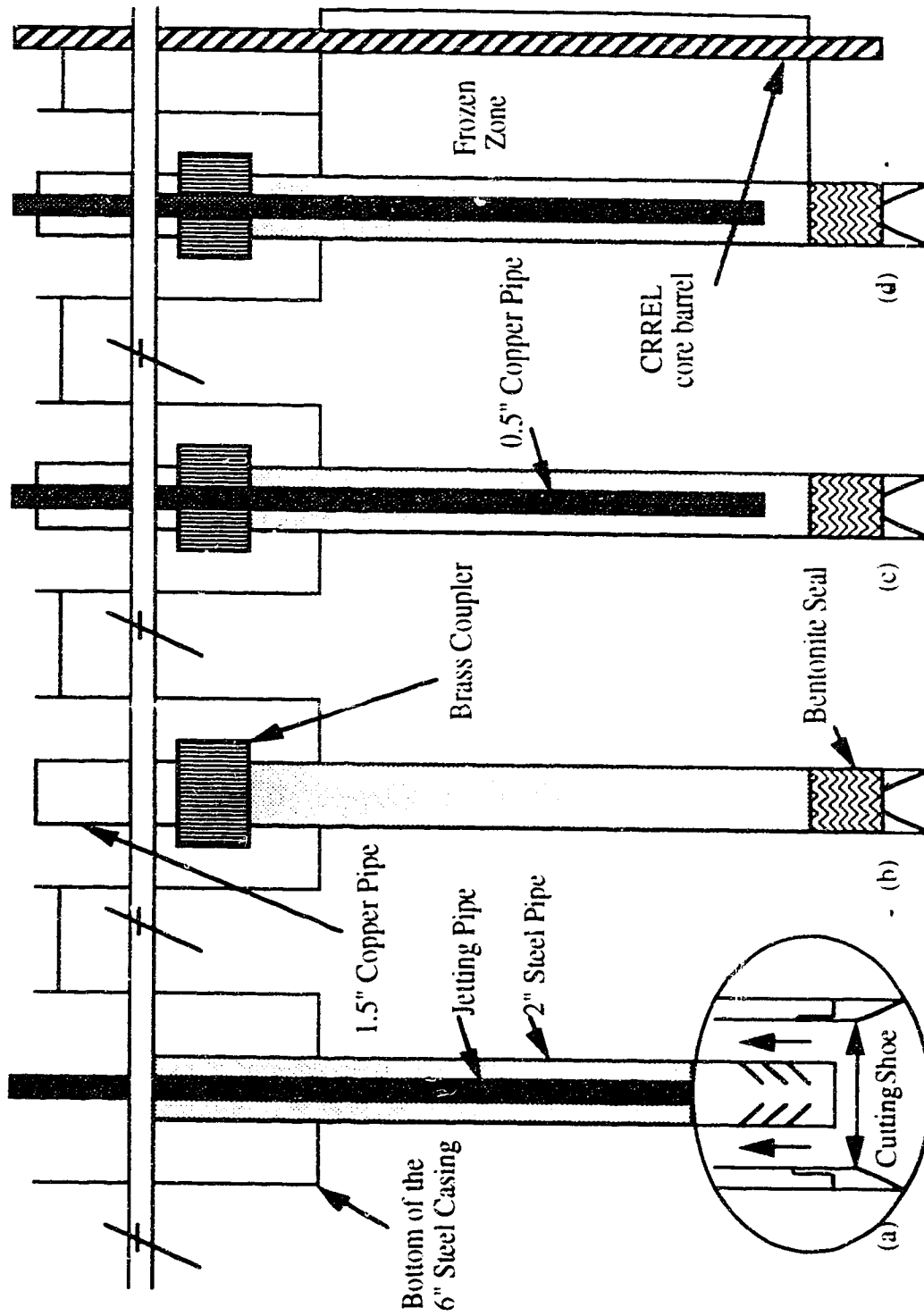


Figure 02-08.- In-Situ Freezing and Sampling Method. After Sego *et al.* (1991)

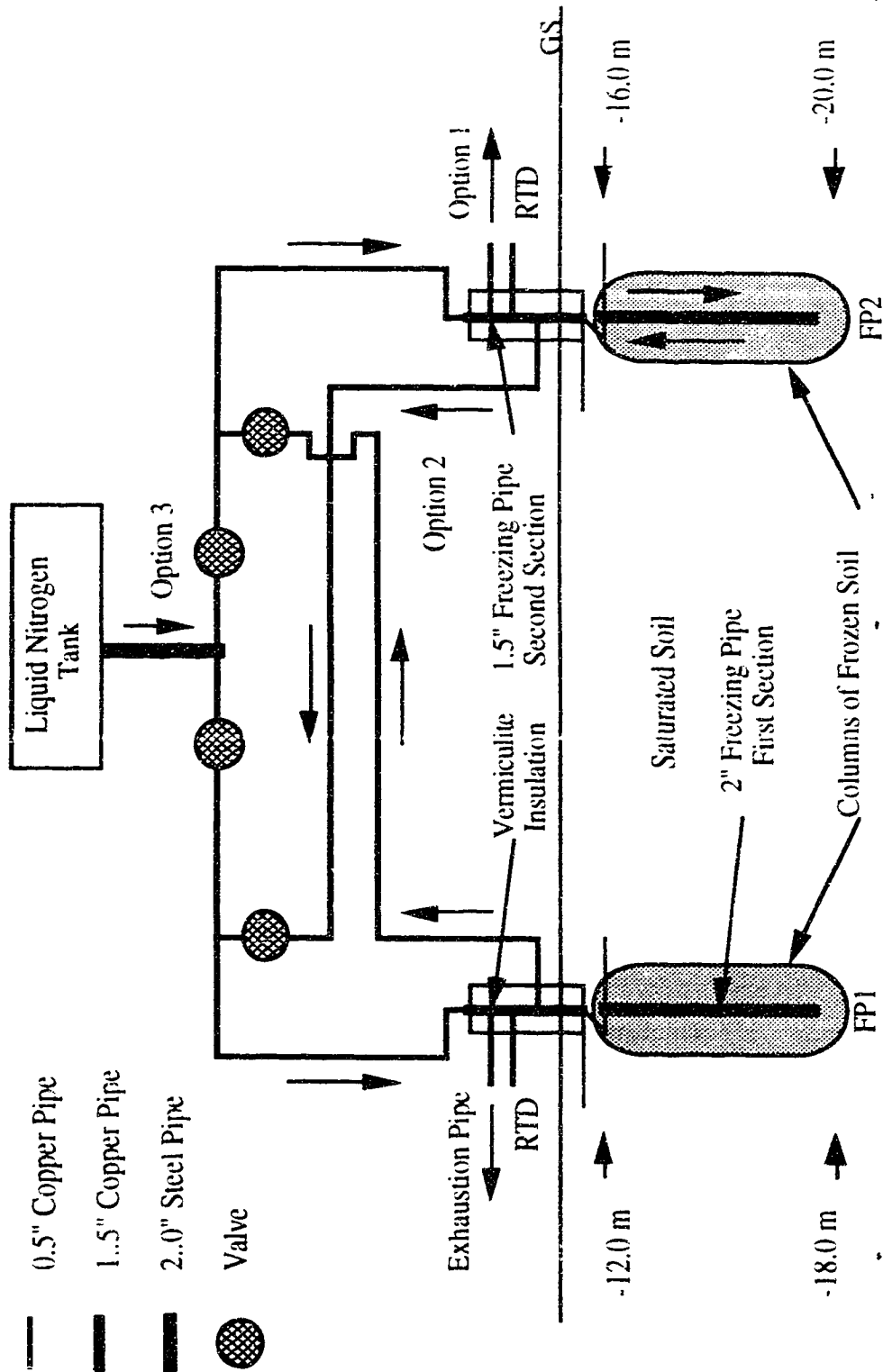


Figure 02-09.- Layout of the Freezing System at the Duncan Dam

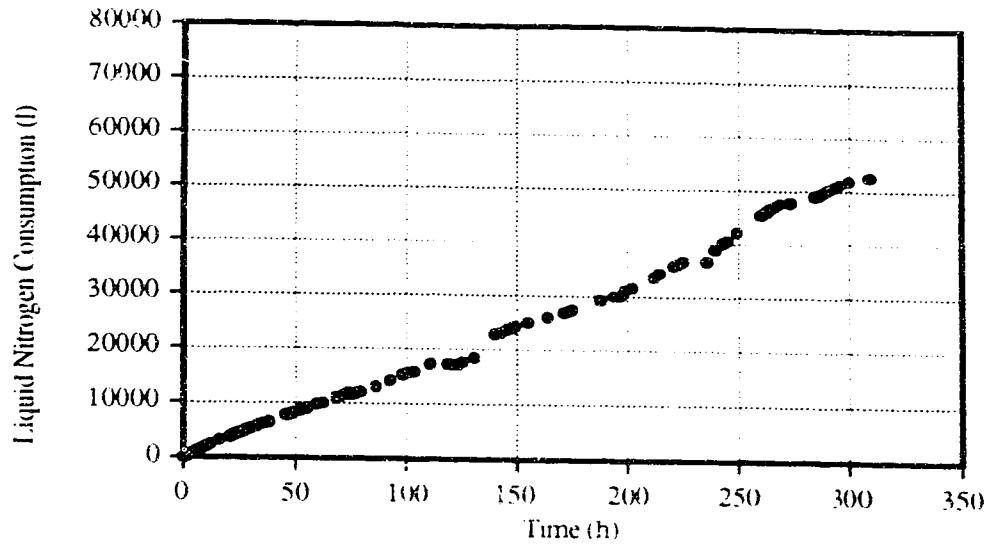


Figure 02-10.- Liquid Nitrogen Volume Consumption

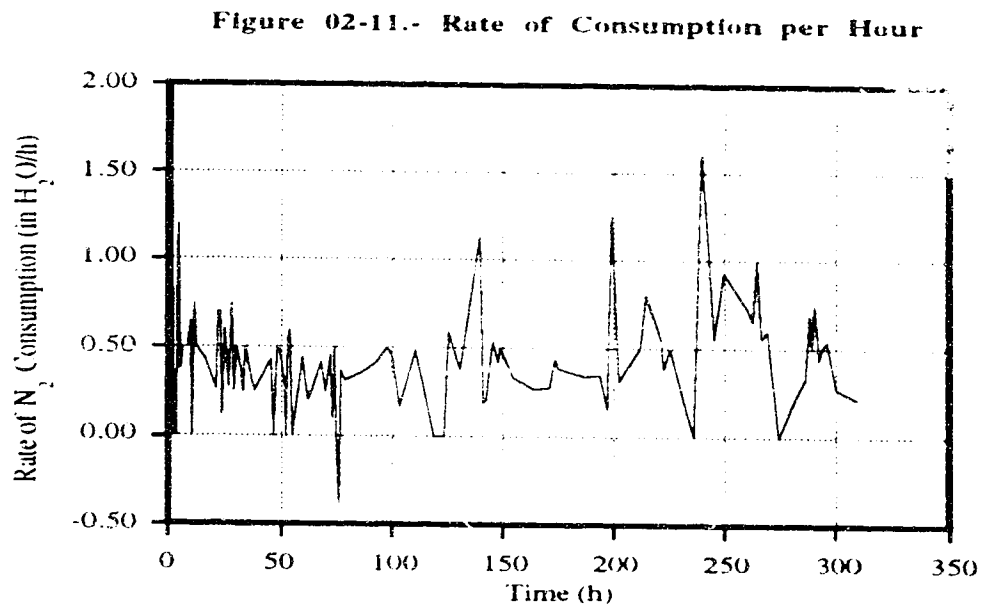


Figure 02-11.- Rate of Consumption per Hour

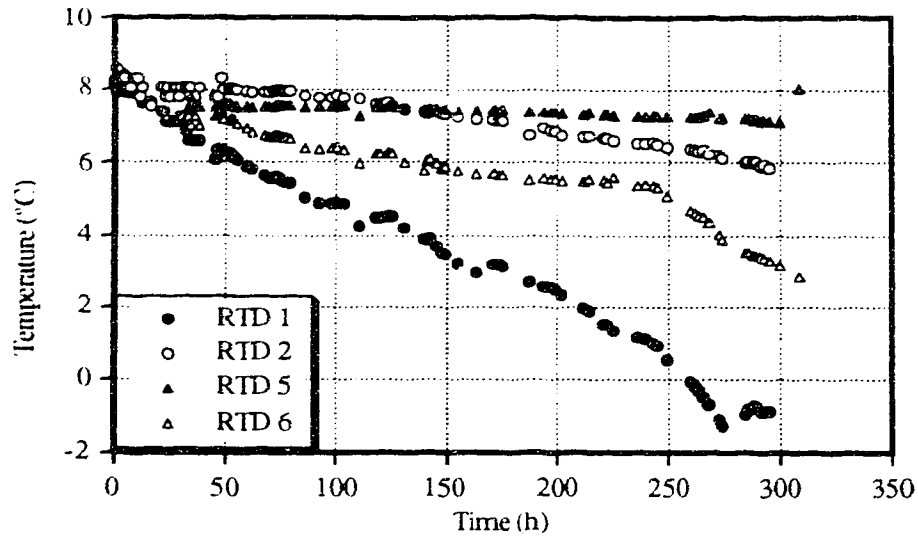


Figure 02-12.- Temperature Profile Adjacent to the Freezing Pipes

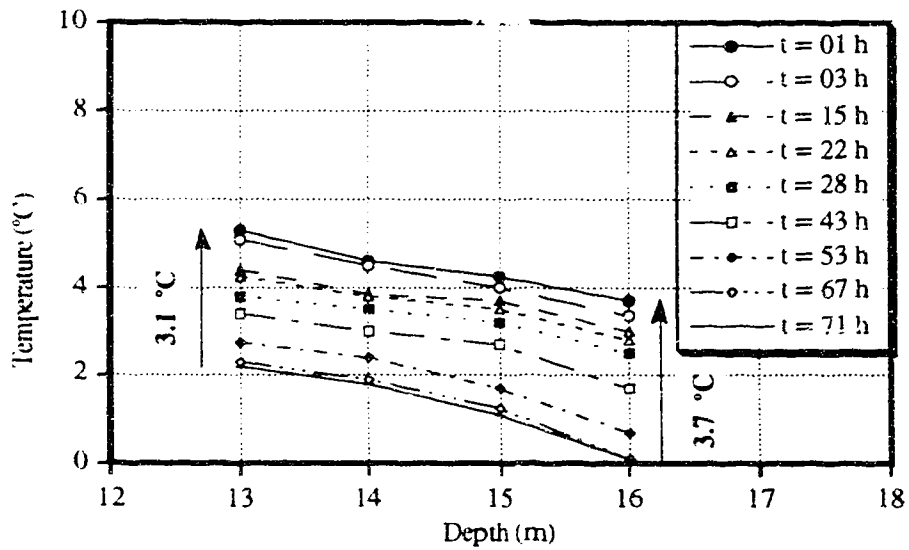


Figure 02-13.- Temperature Profile of the Multiple RTD Probe

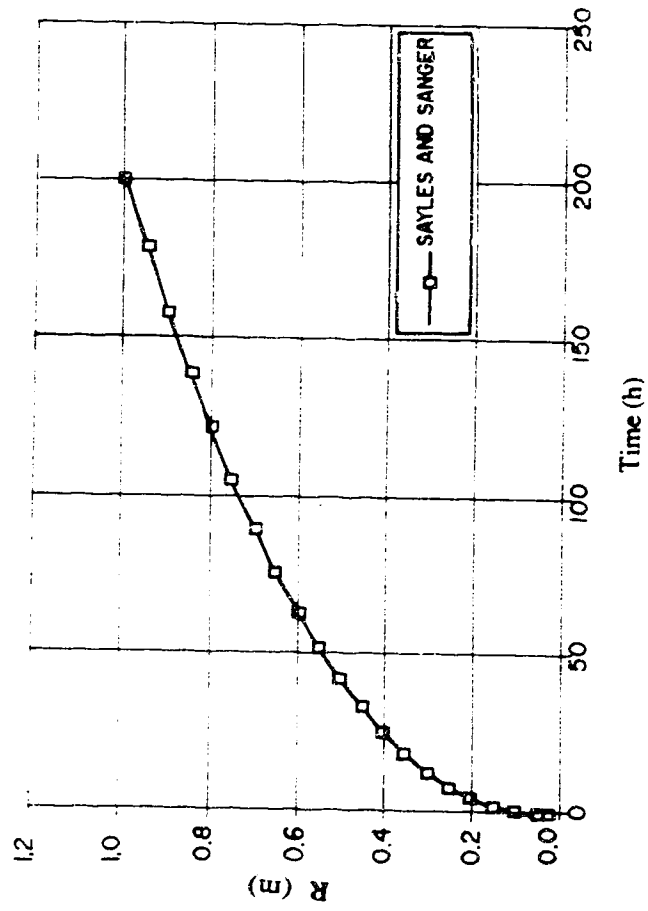


Figure 02-14.- Frost Front Advance in the Duncan Dam
using Sanger and Sayles Method

K m/s	Soil Types			Soil Condition	
	Groups	Kinds	Average Particle size (Less than)	Application of Frost Heave Criteria Particle Size Range	
10 ⁻⁹	Colloids	Fine Coarse	0.1μ 0.8μ		Frost Heave Criteria
10 ⁻⁸	Cohesive Fines	Clay			
10 ⁻⁷		Silty Clay	2μ		
10 ⁻⁶	Particled Fines	Loess	5μ		
10 ⁻⁵					
10 ⁻⁴		Silt	0.02 mm		
10 ⁻³	Sand	Fine Medium Coarse	0.10 0.20 1.00		
10 ⁻²					
10 ⁻¹					
1	Gravel	Fine Medium Coarse	5.00 15.00 30.00		
10					
>10					High Velocity of Water



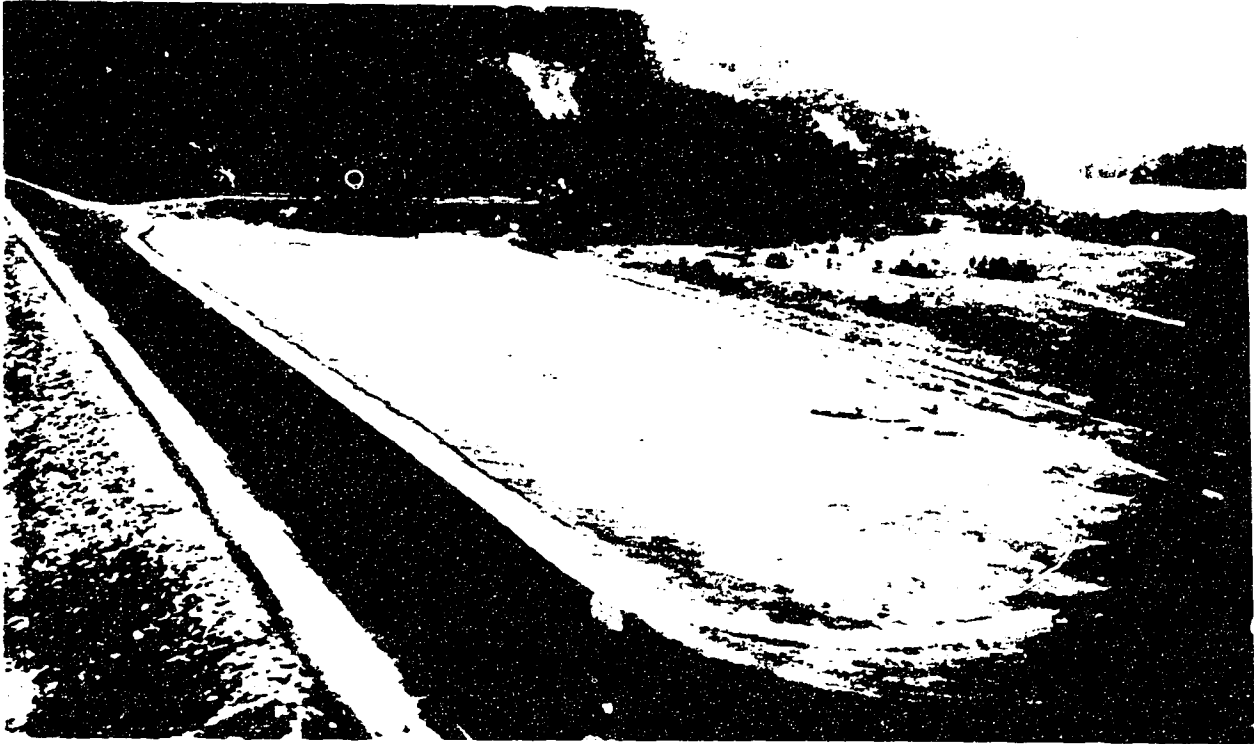
-  Interval for Liquefiable Soil
 Interval for Artificial Freezing

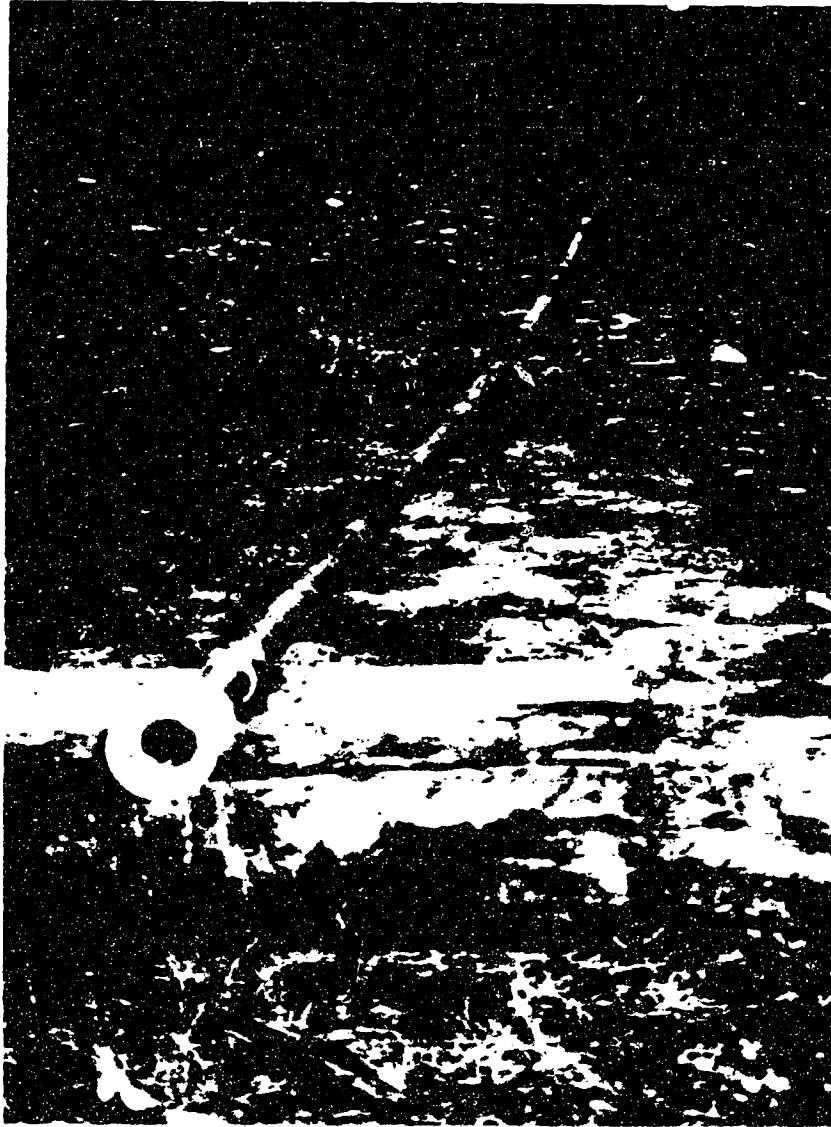
Figure 02-15.- Range of Particle Size for Ground Freezing Sampling Methods



02-01.- Panoramic view of the toe and campsite at the Duncan Dam.

02-02.- Installation of the sliding stabilization rings on the first section of the freezing pipe.



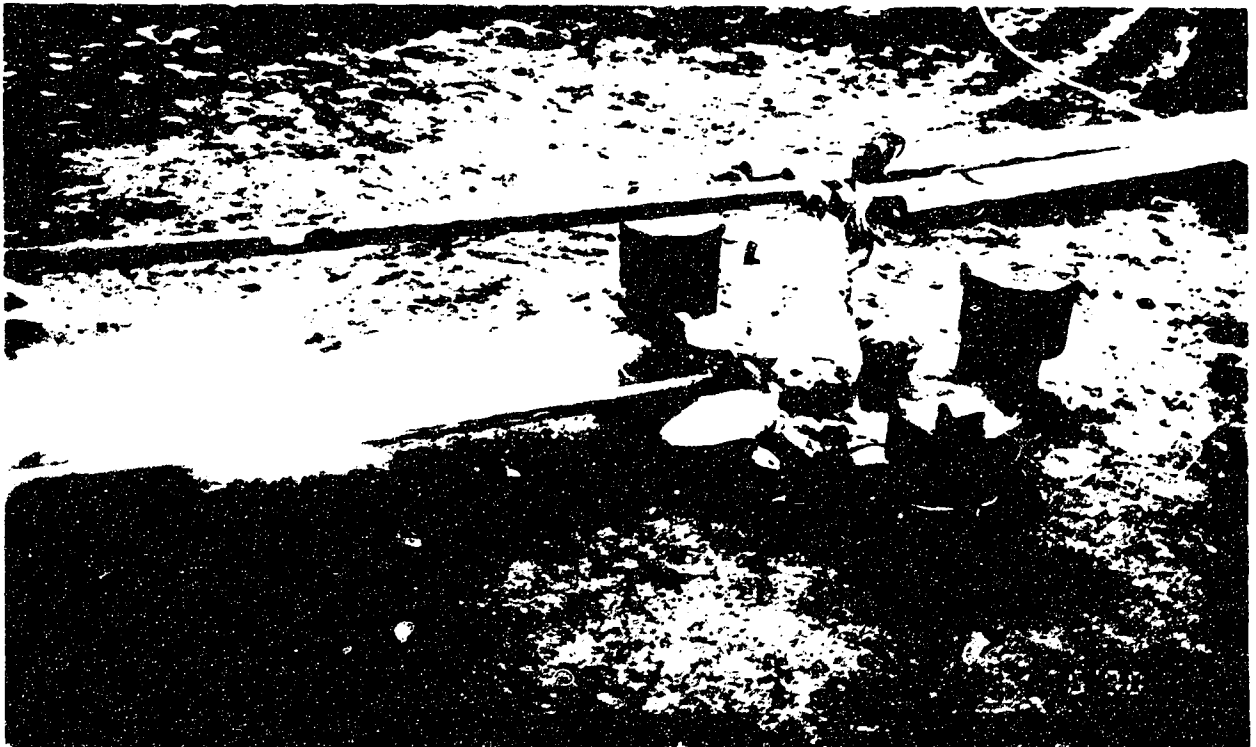


02-03.- View of the second section of the freezing pipe with the Brass coupler attached.



02-04.- View of the freezing system submitted to liquid nitrogen circulation.

02-05.- Close-up of FP1, sampling boreholes and RTD1.





02-06.- CRREL barrel at surface. Removal of drill cutting prior to removal of core.

III. OUTLINES OF THE FROST HEAVE ANALYSIS

3.1 Frost Heave and Frost Susceptibility of Soils

3.1.1 Foreword

Frost heave and the major parameters affecting the soils subjected to freezing temperatures have been a matter of profound study. Several models have been proposed to fully explain the behavior of soils subjected to freezing. Current frost heave models, like the ones proposed by Takagi (1980), Gilpin (1980), O'Neill and Miller (1985) and Horigushi (1987), use assumptions which have yet to be proven in the laboratory or field. As Akagawa (1988) points out, the assumptions made in the frost heave theories discussed before, relate to the *frozen fringe* because the phenomena which occurs in this zone drives the entire frost heaving process. Some of the major recent advances in frost heave testing were developed by Akagawa (op.cit.) to better observe the process and to confirm the assumptions about the frozen fringe. Making use of an X-ray radiography associated with image processing techniques, he was able to observe some of the mechanisms that develop within the frozen fringe with relative success. Akagawa (1988) concluded that expansion occurs over a relatively wide layer during the initial stage of freezing. He also concluded that the width of this layer and the expansion rate decrease with time and finally that between the frost front and the expanding layer, exists a consolidating layer, which indicates the probability of an unsaturated state in this zone. The model proposed by Konrad and Morgenstern (1980) is the theory that is more applicable for the purpose of the present study. Their model is used because it is a practical engineering theory which incorporates the main process in the frozen fringe and allows the prediction of the magnitude of frost heave (Nixon, 1982; Konrad and Morgenstern, 1984; Collins, 1986; Horne, 1987). An excellent review of the potential use of this model in sandy soils is given by Rieke and Vinson (1982) and Horne (1987) applies this model for frost heave predictions with the help of a computer program.

3.1.2 The Konrad and Morgenstern Frost Heave Model

Konrad and Morgenstern (op. cit.) presented a model of frost heave that includes the effects of soil permeability, the segregational freezing temperature, the temperature gradient through the frozen fringe, suction at the freezing front, rate of cooling, and the applied pressure. The model has been used to successfully analyze both laboratory and field freezing experiments (Konrad, 1980; Konrad and Morgenstern, 1982b, 1983; Nixon,

1987, Jessberger and Jagow, 1989). This model uses parameters to predict heave that are more easily determined in the laboratory than parameters used in other models.

Questions were raised about the ability of this theory and the Segregation Potential parameter to model transient freezing conditions, as outlined by Konrad and Morgenstern (1981). Especially after Konrad (1987, 1988, 1989) and Svec (1989) presented data of extremely well controlled conditions using the ramping technique, first introduced by Myrick *et al.* (1982) and developed later by Penner and Eldred (1985). They concluded that the Segregation Potential is not a unique value for a given soil but varies depending on the rate of cooling which takes place in the frozen fringe. Problems with the use of the model to describe transient freezing tests are also pointed out by Van Gassen and Sego (1989). Some of the main criticisms have to do with the lack of explanation by the theory of pore water expulsion that is observed during the initial part of a frost heave test. It is also generally agreed that the heave rate is sensitive to the suction at the advancing freezing front and to the rate of cooling over a range of cooling rates applied in the laboratory. Nevertheless, the *in situ* cooling rate or the *in situ* suction at the freezing front do not significantly affect the *in situ* rates of heave. In any case, this theory continues to be used since no other one has been developed which is better from the practical engineering point of view.

Since this model will be used, it is appropriate to present the background and the formulation of the model. The derivation of the model is discussed extensively by Konrad and Morgenstern (1980, 1981, 1982a, 1982b), Collins (1986) and Horne (1987), but a brief summary of the derivation of the model is presented in Appendix A. Konrad and Morgenstern (1980), following the secondary heave model, considered a potentially frost susceptible soil as a system in which, at a certain point, the flow to an ice-water interface is impeded from the unfrozen soil by a zone of low permeability: the frozen fringe. Their derivation is based on two equations: the Clausius-Clapeyron and Darcy's law. The Clausius-Clapeyron equation describes the suction created at the ice-water interface at the bottom of an ice lens to the temperature. Darcy's law relates velocity of water through the frozen fringe to the average permeability through the frozen fringe and its hydraulic gradient.

The Konrad and Morgenstern model for a frost susceptible soil consists of frozen soil, an ice lens, a frozen fringe and unfrozen soil as observed in Figure 03-01. Between the unfrozen soil located behind the 0°C isotherm, which is termed the frost front and the final ice lens is the *frozen fringe*. The soil in this zone is only partially frozen and some unfrozen water remains as adsorbed films on the surfaces of the fine grained particles. It is considered that water migration to the ice lens occurs through a layered medium composed

of a saturated unfrozen soil and the frozen fringe. The water moving under the influence of the temperature gradient is best characterized by suction at the segregation-freezing front, and by permeability within the frozen fringe. The suction and the permeability are both pressure and temperature dependent.

The mechanism of ice lens formation and the frozen fringe formation is briefly detailed as follows. As a step freezing temperature is imposed on the surface of an unfrozen soil mass a freezing front begins to propagate through the soil. During the first stage, the suction created by the unfrozen water does not have time to draw sufficient water to a given level to form an ice lens owing to the rapid progression of the frost front and the freezing of interstitial water. But, as the advancing freezing front begins to slow down, more water is drawn to the zone of accumulation which is governed by the local permeability of the frozen fringe. Since the temperature of the unfrozen water is rarely equal to zero, there is continuous suction throughout the frozen soil. As the temperature decreases, the unfrozen water content and the permeability decrease.

At a critical temperature referred to as the maximum segregation temperature, T_{sm} , the permeability is sufficiently low to preclude the migration of moisture to the growing ice lens. At this time another ice lens is initiated closer to the frost front where the temperature is more conducive to moisture flow. This temperature at which a new lens is started is referred to as the formation segregation temperature, T_{sf} . Konrad and Morgenstern (1980) demonstrated that at the onset of steady state conditions and the formation of the final ice lens, the average of T_{sf} and T_{sm} , referred to as the segregation temperature, T_s , is constant and is a unique property of a soil. Then, the suction developed at the growing ice lens can be represented by the Clausius-Clapeyron equation

Konrad and Morgenstern (1981) proved that at the time of formation of the final ice lens, the velocity of water migration towards the frost front (v) is proportional to the overall thermal gradient in the frozen fringe, ($\text{grad } T_{ff}$). This statement was based on the validity of the Clausius-Clapeyron equation at the base of the ice lens, combined with the uniqueness of T_s , with an overall permeability (k_{ff}) characterizing the frozen fringe and continuous water flow across the fringe.

$$v = SP * dT_{ff}/dz \quad [3.01]$$

Hence, the water intake velocity is the product of the temperature gradient across the frozen fringe and the Segregation Potential of the soil. The Segregation Potential of the soil is a function of the intrinsic parameters T_s and k_{ff} (the average permeability of the frozen fringe). It is, therefore, a unique soil parameter (Appendix A). Although these

parameters provide a better insight into the physical processes involved during freezing. from a practical point of view they are difficult to measure directly. Since the size of the frozen fringe is relatively small, its temperature gradient is approximated by the measured overall temperature gradient in the unfrozen soil just ahead of the 0°C isotherm, **grad T_u**. Therefore, the experimental determination of **SP** becomes relatively simple to calculate since it is the ratio of two measurable quantities: the water intake rate and the temperature gradient across the active system (i. e. unfrozen soil and frozen fringe) for constant boundary conditions. The Segregation Potential in its simplest form can be expressed as

$$SP = v / \text{grad } T_u \quad [3.02]$$

Since there is no accumulation within the frozen fringe, the velocity of the water can be related to the heave rate as follows:

$$h_s = 1.09 \text{ SP grad } T_u \quad [3.03]$$

Most of the criticism towards this model has to do with the Konrad and Morgenstern (1981) general assumption that effect of the rate of cooling on **SP** is not appreciable. Svec (1989) demonstrated, as pointed out before with the use of the ramping technique, that this is not always the case by presenting differences in the **SP₀** values for the same soil. He considers that the influence of cooling should be analyzed as the combined effect of temperature gradient in the frozen fringe and the frost penetration as two independent variables. Therefore, including both, geometrical and thermal boundary conditions. The rate of cooling is defined as the change in the average temperature of the frozen fringe per unit time. Its value can be approximated by the change of temperature at the 0°C isotherm per unit time from:

$$\frac{\partial T}{\partial t} = \frac{\partial T}{\partial z} \frac{\partial X}{\partial t} \quad [3.04]$$

where **X** is the advance of the frost front (0°C), $\partial T / \partial z$ the temperature gradient and $\partial X / \partial t$ is the rate of advance of the frost front. The mechanics of ice lens formation is shown schematically in Figure 03-02.

Svec (1989) has explained the rate of cooling as follows: at a constant temperature gradient, the rate of frost penetration is directly proportional to the rate of cooling. At low cooling rates, that is at low frost penetration, once the ice lense is established, the rate of heave is also low because the frozen fringe is very thick. The low frost-penetration rate

does not cause the ice lens to form at a new location. As well, the latent heat is able to keep the thermodynamic processes relatively steady. The amount of time required to relocate the ice-segregation site (i.e. start of a new lens) is relatively long. In the middle range of frost-penetration rates, the above process is faster which, in a dynamic sense, allows a thinner freezing fringe to form. Moreover, the segregation temperature decreases with the increase in penetration rate (Konrad, 1988). A thinner fringe accompanied by a lower segregation temperature results in a higher rate of heave. In the high range of frost-penetration rates, the freezing process occurs so quickly that there is not sufficient time to establish significant water flow between ice segregation and the still unfrozen soil. As a result, the heave rate is low.

3.2 Conditions for an Undisturbed Structure in Sands by *In Situ* Freezing

3.2.1 The Effect of Porewater Migration in Sandy Soils

It is a fact that frost action can be controlled or eliminated by controlling water availability. Russian agronomists were the first to study the redistribution of moisture in freezing soils at various time intervals after the onset of freezing, back at the end of the 19th century. However, it was not until specially designed experiments were performed (Sumgin, 1929; Taber, 1929), that it was proved that water migrates towards the freezing front in a freezing soil. Tsytovich (1973) reports that in 1937 Tsytovich and Sumgin conducted experiments in a closed system and noticed that soil freezing is accompanied by the movement of water towards the freezing front. Taber (1930) also proposed that two classes of freezing systems have to be distinguished: closed systems, in which the existing water is redistributed, and open systems, in which there is an influx of water from the outside. This subdivision of freezing soil is generally accepted (McRoberts and Morgenstern, 1975).

A general review of observations of migration of water in different soils by different researchers is given by Tsytovich (1973) and McRoberts and Morgenstern (1975). The movement of water to the freezing front is accomplished by electrostatic and osmotic forces (Scott, 1969), producing what is often called the suction potential of the freezing system (Anderson and Tice, 1971). The dipole effect of freezing water causes reorientation of the adjacent liquid water molecules and the generation of electrical freezing potential which may reach as high as 1200 mV (Parameswaran and McKay, 1983). As Anderson and Tice (1973) pointed out, the existence of a continuous unfrozen water phase that separates ice from the mineral or organic matrix in frozen soils is now generally

accepted (Anderson, 1963; Lovell, 1958; Martynov, 1959; Miller, 1963; Nersesova and Tsytovich, 1963; Williams, 1964).

Questions regarding such things as the mobility of the interfacial unfrozen water under given conditions have been answered, at least in qualitative terms. The unfrozen, interfacial water possesses the properties of a liquid, and water molecules, ions and solutes are freely mobile in this zone (Ducros and Dupont, 1962; Graham et al., 1964; Hecht et al., 1966; Hoekstra and Chamberlain, 1964; Hoekstra, 1965; Cary and Mayland, 1972; Mageau and Lorgenstern, 1980). Although it was once claimed that anomalous ice phases might exist in frozen soil, in all instances so far reported the ice formed is normal, hexagonal ice (Anderson and Hoekstra, 1965). These results imply that water is able to pass through partially frozen soil to freeze on a growing ice lens. The principal factor determining the quantity of water remaining unfrozen in frozen soils is temperature (Nersesova and Tsytovich, 1963). Pressure is a less important, but significant factor: at a given temperature, an increase in pressure, increases the unfrozen water content. Solute concentration exerts an effect roughly equal to that predicted from the freezing point depression (Bouyoucos, 1916).

Tsytovich (1973) discusses the findings of Bozhenova (1940) and Bozhenova and Bakulin (1957), that while the water content of the clays increased in the direction of the freezing front the water content of medium-grained sand decreased. Tsytovich (op. cit.) had emphasized this because it must be established if ice accumulates or if water is squeezed out when sandy soils freeze and, under which conditions this occurs. In saturated free draining sands water does not migrate toward the freezing front but is squeezed out with the result that the void ratio remains the same (variation less than 2%). When no drainage is provided, as when material is frozen from all sides, an increase in porosity of the frozen saturated sand was observed, ranging up to 4% (Tsytovich, 1973).

Another important merit attributed to Tsytovich (1973) is the experimental proof that in fully saturated particulate soils, water migrates in the liquid phase. Khakimov (1957) demonstrated by laboratory experimentation that water migration towards the freezing front decreases with the increasing rates of freezing. If pore water is subjected to a freezing temperature and no drainage is provided, that is, the soil is a closed system according to Taber's definition, its volume expands by about 9%. Hence, the porewater undergoes a volume expansion defined by:

$$\Delta V = k_f n V \quad [3.05]$$

where n is the porosity, V is the total soil volume and the constant $k_f = 0.09$ represents the

fractional increase in volume of water when it undergoes phase change (McRoberts and Morgenstern, 1975).

According to Tsytovich (1973), in the case of fine grained soils, the water pressure that is developed as the ice crystals grow, decay at a short distance from the freezing front due to the high internal resistance to filtration. The crystallization-film mechanism of water migration continues to operate, but the application of surcharge can inhibit this migration. Beskow (1935) also observed this fact and noticed that the heave rate was identical if the difference between the applied stress and the pore water pressure remained constant. The larger the difference between the two stresses the lower was the heave rate. According to Wissa and Martin (1968) this is nothing more than a straight application of the effective stress principle.

The work developed by Linell and Kaplar (1959) and Penner (1959) confirms this position. Volume expansion occurs in these kind of soils even in an open system, due mainly to the growth of ice lenses at the freezing front caused by the ice segregation process forming normal to the direction of the heat flow. Penner and Ueda (1977) showed that although water may be expelled during the initial stage of freezing when the freezing rates are fairly rapid, the flow reverses and water moves to the freezing front after the rate of frost penetration had decreased and then there is a total positive heave rate. Only when the total heave is zero the expulsion of water will not be followed by intake of water.

According to Tsytovich (1973) a general principle of moisture migration in freezing soils is formulated as follows: *the migration of water in freezing moist soils is a process of moisture transport that operates consistently whenever the equilibrium state of the soil's phases is disturbed and external factors change (the presence of temperature, moisture content, pressure, mineral particle surface energy, mobility of molecules in water films, gradients, etc).* From this general concept, it is understood that the process of moisture migration is only possible if the equilibrium state of the phases is disturbed, hence conditions will not be altered if isothermal and homogeneous states are not changed by external disturbances.

Tsytovich (op. cit.) uses this principle to explain the consistently observed migration of water towards the freezing front in fine grained soils. Points with lower vapor pressures, larger soil-skeleton adsorption forces, and larger crystallization forces in the direction of the heat sink will exist and will cause migration of liquid water in this direction. Excess separation of ice will occur only in hydrophylic moistened soils since these soils have water films. A variety of conditions can create a disturbance of the phase equilibrium. Gradients of moisture, temperature, adsorption-film and osmotic pressures and finally of the isobaric potential of mineral particle free energy are the motive forces for

this disturbance.

All of these motive forces had been studied separately but can also be considered as a generalized force and included in a more general equation and written in the form

$$i_{\text{mig}} = k \text{ grad} F \quad [3.06]$$

where i_{mig} is the migration water flux, k is the proportionality coefficient and F is the motive force. It is worthwhile to note that this equation is parametrically the same as the one for Segregation Potential defined in section 3.1.2.

Some conclusions can be drawn from the observed water migration processes. In general, the freezing of soils under any condition is accompanied by a change in energy of the moisture from its initial value. An increase in moisture takes place during the freezing of fine grained soils. A decrease in moisture takes place during the freezing of saturated sands. The moisture can increase during the freezing of sands, if the initial moisture content is lower than the total water capacity (unsaturated soils). Khakimov (1957) proposed a model to determine the preservation of the natural structure of saturated sands during freezing. A brief summary of his derivation is presented in Appendix B since it is considered that this derivation should mark an starting point for future developments in the area. Khakimov (op. cit.), also observes that the freezing of sands is accompanied by a decrease of their moisture content because:

a) The quantity of bound water in sands is very small; even in fine grained sands the maximum molecular moisture capacity does not exceed 0.3% (Lebedev, 1936).

Numerous experiments have proved that practically all the water in sands freezes at about 0°C. Nersesova's experiments (1950, 1951) have shown that in sand having a maximum molecular moisture capacity of 0.5%, about 97% of all the water freezes at a temperature between -0.5 and -0.6, while in loam only about 40% of the water freezes at that temperature, and clay does not freeze at all. It follows that in saturated frozen sand the pores are filled with ice formed at about 0°C, and that no conditions exist for the motion of liquid water; therefore no suction pressure will develop during the freezing of sands in an open system.

b) The pressure developed, as a result of the expansion during the transformation of water into ice squeezes out a part of the water into the unfrozen zone. This is made easy by the high permeability of the sands.

3.2.2 The Effect of Applied Stress

Studies on the effect of externally applied pressure on the amount of frost heave have been carried out by Beskow (1935), Arvidson (1973), Takashi et al., (1974), Aitken (1974), Hill and Morgenstern (1977), Penner and Ueda, (1977), Konrad and Morgenstern (1982b). Tsytovich (1973) presented an experimental proof that external pressure strongly increases the unfrozen water content in frozen soils. This effect is larger the greater the pressure applied to the soil as it freezes, indicating therefore that the phase change and hence the expansion can be minimized if freezing is accomplished under high confining pressure. Studies (Arvidson and Morgenstern, 1974; McRoberts and Morgenstern, 1975) confirm that the migration of water to the freezing front decreases with the increase in surcharge. Even though the application of load can reduce the rate of heave significantly, it appears that the rate of heave is always a finite quantity. Relatively high confining stresses (about 1000 kPa) are required to stop heaving even in coarse material (Johnston et al., 1981).

Penner and Ueda (1977) stated that it is not possible to independently control the frost heaving process by loading the soil in contradiction of what was called the *shut-off pressure* (Arvidson and Morgenstern, 1974). This term was later defined by McRoberts and Nixon (1975) as the effective stress at the frost front which will cause neither flow of water into or away from the freezing front. Controlled tests (Penner and Ueda, 1977) allowing the sample to be tested for a long period of time proved that the so called shut-off pressure is greater than that originally proposed by Hill and Morgenstern (1977). Hence, it is a matter of time for a soil specimen tested under different stress levels to develop water suction, and therefore start heaving. Penner and Ueda (op. cit.) observed that when there is a positive total heave during a uniaxial freezing test, although water may be expelled from the sample initially, the water flow reverses from expulsion to intake, unless the experiment is terminated early. They concluded that only when the the expulsion of water is not followed by water intake that the heave rate is zero, hence no frost heave behavior develops.

Yoshimi *et al.* (1978) showed that the trend of three different sands is to decrease the expansion as the surcharge is increased. Yoshimi et al (op. cit.) attempted to develop a relationship between expansive strain due to freezing and applied surcharge for the Tonegawa sand by a hyperbolic expression:

$$\epsilon = \frac{\epsilon_0}{1 + \alpha p} \quad [3.07]$$

where ϵ is the expansive strain due to freezing, ϵ_0 is the initial expansive strain, p is the

surcharge and α is a constant. It is worth noting that this relationship is only valid for a soil made up of sand and cannot be compared to the behavior of clays. Furthermore, as detailed in section 2.4 the author has his concerns with the results presented due to the conditions in which the specimens were tested.

As pointed out in the previous paragraphs, the effect of the applied stress plays an important role on the frost heave behavior of a soil. This phenomenon can be explained, as well, using the Konrad and Morgenstern frost heave model (Konrad, 1980; Konrad and Morgenstern, 1982b). The suction at the base of the ice lens is a function of both the temperature and the pressure at this location. Increasing the overburden pressure decreases the suction potential at the base of the ice lens. Increasing pressures also results in increasing amounts of unfrozen water within the frozen fringe, since the radius of the ice-water interface (i.e. the thickness of the water film) increases with increasing pressures (Williams, 1976). This leads to a colder segregation freezing temperature, thus increasing the thickness of the frozen fringe.

All of these factors contribute to a decrease in the Segregation Potential (Konrad, 1980). Konrad and Morgenstern (1982b) showed that the effect of applied load on the Segregation Potential for a reasonable cooling rate in a freezing soils can be expressed by:

$$SP = a \exp(-bP_e) \quad [3.08]$$

where a and b are soil constants determined from frost heave tests. This equation is better expressed by the following expression (Konrad and Morgenstern, 1983)

$$SP = SP_0 e^{-aP_e} \quad [3.09]$$

where SP_0 corresponds to the Segregation Potential for the formation of the final ice lense under zero applied load and for suction close to the atmospheric pressure, and the parameter a is a constant from tests for various applied pressures, P_e .

The Segregation Potential for various applied pressures can be expressed by using equation 3.09 for many soils ranging from sandy silts to silty clays. Konrad and Morgenstern (op. cit.) presented a survey of frost heave data, as can be observed in Figure 03-03. The survey reveals that the more the clay content of the soil, the higher the applied stress needed to inhibit the soil from heaving. Therefore, the lower the soil's unfrozen water content the more sensitive they are to changes in their Segregation Potential when overburden pressures are increased. This definitively is not the case for soils with higher unfrozen water contents such as clays. In Figure 03-03 is also presented the stress region

to which this study will be directed, which is clearly within the highly variable Segregation Potential region. It can be concluded then that for a small variation in stress on artificially prepared loose saturated sand-fines mixtures, one should expect large variation in the soil's response to freezing.

3.2.3 The Effect of the Fines Content

Grim (1951) analyzed the possible effects of clay mineral composition on frost action in soils. Grim (op. cit.) evaluated the potential of various clay mineral types in developing ice segregation in soils. His first consideration was that the movement of water through the soil is necessary to supply the growing ice crystal, confirming the conclusions of other researchers such as Sumgin (1929) and Tsytovich and Sumgin (1937). His second consideration was that soils consisting of *very colloid-sized clay materials show very little or no segregation of ice on freezing*. Grim stated that clay minerals which adsorb a quantity of water in a definite molecular pattern immobilize the water adjacent to the adsorbing surface, thus reducing the permeability and the ability of the soil to supply water for ice segregation. Regardless of this conclusions, Linell and Kaplar (1959) felt that in Grim's work substantial field or laboratory data of frost heaving characteristics were not included. A somewhat similar concept to that expressed by Grim (op. cit.) is given by Winterkorn (1943) stating that *directly adjacent to the adsorbing soil, solidly adsorbed water is found; the center of the pore space is occupied by ordinary water freezing at about 0°C, and between the ordinary water and the solidly adsorbed water there is a zone of liquid water possessing a melting point down to -22° which serves as a passage way for the conduction of water to freezing centers*. This statement gives the first insight to what was later defined as the *unfrozen water and frozen fringe* (Konrad, 1980; Konrad and Morgenstern, 1980), and the important role that the colloidal particles play in this region.

In order to see the effect of the composition of the fines on the frost susceptibility of soils, Linell and Kaplar (1959) refer to data available from tests conducted at the ACFEL performed using a larger variety of soils, including gravels, sands, silts and clays. The results show that as the silt and clay content of the gravel soils increases, denoted by an increasing percentage of material finer than 2 μm , the average rate of heave also increases. Most of the poorly-graded sandy gravels (GP), as well as the sands classified as SP fall into the negligible or very low frost susceptibility classification. On the other hand, the well graded gravels containing more than 4% finer than the 2 μm material and sands with more than 10% finer than 2 μm , are considered to have a high probability of heaving. The silts and lean clays generally exhibit the highest heave rates. The fat clays (CH) and

organic fat clays (CH-OH) showed markedly smaller rates of heave than most of the silts and lean clays.

Linell and Kaplar (1959) found that the fines from limestone sandy gravel from Chapman Pit were more efficient in producing ice segregation than the fines from East Boston till and New Hampshire silt (Figure 03-04 and Figure 03-05). The composition of the fines can be observed in Table 03-01. This might appear to indicate that the presence of kaolinite had a somewhat greater effect on frost susceptibility. However, as shown in Figure 03-04 and Figure 03-05, the fines from these soils differed in particle size distribution yielding different gradations, and this may have accounted for the differences in ice segregation. Freezing tests were therefore performed on the minus 200 mesh fractions of the soils. The average rate of heave for these fines are presented in Table 03-01. As can be observed, the heave rates were very high and similar.

Linell and Kaplar (op. cit.) concluded then that if there would be any differences in the potential effects of the different mineral compositions upon the tendency for ice segregation at the plane of freezing, they should be countered by other factors such as the difference in permeability. Other interesting results were obtained by them by testing three different soils in which various percentages of relatively pure sodium montmorillonite, ranging from 0.01 to 12% of dry weight of soil were added. The natural gradations of a highly frost-susceptible silt (New Hampshire Silt), a sandy clay (Ft. Belvoir Sandy Clay) and a lean marine clay (Boston Blue clay) were changed. The results show that low treatments (less than 0.05%) increased the frost heave in the silt and lean clay; additions of 1.0 to 2.0% and greater reduced the frost heaving of these soils.

Lambe *et al.* (1969) using a clean cohesionless sand to which various mineral fines were added, demonstrated the significant influence of the composition of the soil fines on frost behavior. The pronounced effect of the nature of the exchangeable ions on the frost-heave-producing ability of montmorillonite fines has also been demonstrated. The clay mineral fines used in these experiments were kaolin (kaolinite, hectorite, pyrophyllite), illite, chlorite and attapulgite. The non-clay minerals used were quartz, labradorite, muscovite, calcite, magnesite, dolomite and limonite. The tests results are shown in Figures 03-06, 03-07 and 03-08. Lambe *et al.* (op. cit.) concluded that:

- a) In most instances, at low concentrations of fines, the clay minerals are higher frost-heave producers than the non-clay minerals. At higher concentrations, the heave producing ability of the clay minerals varies over a very wide range, which brackets the effects produced by the non-clay minerals.
- b) If montmorillonite is the soil fine, the rate of heave can vary over a hundred-fold, depending on the nature of the exchangeable ion.

- c) Sodium as an exchangeable ion gives the lowest heave, while ferric iron gives the highest heave.
- d) Iron montmorillonite, nontronite, attapulgite and possibly kaolinite are minerals of high frost heave producing ability.
- e) The increase of fines concentration can result in a decrease of frost heave rate for the more plastic clays such as montmorillonite (exceptions are iron and lead montmorillonite), illite and hectorite.

The above conclusions reinforce, as Lambe *et al.* (1969) pointed out, that *when a clay mineral is present in a soil in a minor amount, its effect may be quite different than when the percentage of that mineral is high enough so that its properties are predominant. For example, a clay mineral which forms such highly impervious soil that frost heave is negligible if that mineral is predominant, may intensify frost heave or may make significant ice segregation possible in otherwise non-frost-susceptible material, when present in amounts insufficient to make the basic soil impermeable.* This statement may not represent a general rule, since the boundary conditions as well as the fabric of the soil play fundamental roles in frost heave. Nevertheless, it clearly shows that soils tested for a short period and dominant by fine grained particles will behave significantly different than those which are not dominated by clay mineral colloids or which are tested for longer periods of time.

3.3 Frost Susceptibility Parameters

3.3.1 Historical Review

Taber (1929) carried out many experiments with various fine and coarse grained soils as well as soil mixtures. He effectively demonstrated that the fine particle size does influence ice segregation. Observable heaving (i.e., ice segregation) was first observed in the soil fraction containing particles ranging from 50 to 100 μm . Heaving occurred in the soil fraction containing soil grains with diameters ranging from 5 to 2 μm . Casagrande (1932), after years of experience, drew the following conclusion: *Under natural freezing conditions and with sufficient water supply one should expect considerable ice segregation in non-uniform soil containing more than 3% of the grains smaller than 0.02 mm, and in very uniform soils containing more than 10% smaller than 0.02mm. No ice segregation was observed in soils containing, less than 1 percent of grains smaller than 0.02 mm, even if the ground water level was as high as the frost line.* Casagrande (op. cit.) hence succeeded in establishing a practical division between non-frost-susceptible and frost

susceptible soils. However, Dücker (1956) affirms that *it is quite impossible to draw a sharp line between frost susceptible and non frost susceptible soils* arguing that the frost susceptibility of a soil is not determined by its percentage of grain sizes below $2\mu\text{m}$, but by *the mineralogical and chemical composition of the "binding" material*. Dücker (op. cit.) concluded this after a testing program which included different types of fines contained in soils.

In order to verify Casagrande's statement Linell and Kaplar (1959) conducted experiments at the Arctic Construction and Frost Effects Laboratory (ACFEL) with natural and combined soils of various gradations ranging from well-graded sandy gravel to very uniform sand. The standard laboratory tests carried on at ACFEL were performed under severe boundary conditions and unlimited availability of water. The intensity of heaving experienced in the laboratory is not encountered in nature unless conditions are quite extreme. Nevertheless, their results will be briefly described since they were the first serious attempt to correlate amount of clay to the magnitude of frost heave. Three cohesionless soils were combined with the fines (minus #200 mesh material) from a silt, a till and a clay respectively, to observe the effect of different soil fines on frost behavior. Other soils were recombined with their own fines to produce the desired percentages finer than $2\mu\text{m}$. The test results are summarized in Figure 03-04 and Figure 03-05 in plots showing the rate of heave versus percent finer than $2\mu\text{m}$ size.

Linell and Kaplar (op. cit.) concluded that the Casagrande frost susceptibility criterion, based upon the percent of grains finer than 0.02 mm by weight, was admittedly a rough engineering rule-of-thumb but was the best available criterion at that time. They observed that for equal percentages of material finer than $2\mu\text{m}$, relatively large variations in the average rate of heave were recorded. Based only on the grain size distribution, it appears that the finer the grains or the more colloidal sizes contained in the finer soil fraction, the more effective the finer soil fraction is at producing ice segregation. Linell and Kaplar (1959) concluded that the intensity of ice segregation in soils is dependent not only on the percentage of grains finer than $2\mu\text{m}$, but also on the grain size distribution and the physicochemical properties of these fines. This is compatible with Dücker's (1956) findings in which he quotes that *the soil fractions with a high percentage of clay sizes were found in these tests to be more effective than those with a high percentage of silt sizes, in producing ice segregation in soils of borderline frost susceptibility*.

3.3.2 Recent Proposed Parameters for Frost Heave Correlations

Penner (1959) does not accept the idea of an abrupt delineation based on grain size

considerations between frost susceptible and non-frost susceptible soils. Nevertheless, he believes that the maximum moisture suction increases as the grain size decreases, therefore causing the permeability to decrease. This suggests that two main conditions affect the degree to which a given soil can be frost susceptible. These are the degree of moisture suction and the permeability of the soil, which facilitates moisture migration through its matrix as described in section 3.2.1. Silt is the soil that better fits within the boundaries imposed by these previous conditions, that is, with a high degree of suction and sufficient permeability to allow water migration. In fact, in engineering practice, it is commonly observed that silts heave at a much greater rate than clays and so these soils are considered much more troublesome.

A more recent attempt to correlate the amount of fines with frost heave was presented by Rieke *et al.* (1983). They noticed that the Segregation Potential varied as the fines content increases (Figure 03-09) and that it could be correlated with the increasing amount of clay size (Figure 03-10). Furthermore, Rieke *et al.* (op. cit.) proposed that the Segregation Potential (Konrad and Morgenstern, 1981) (section 3.1.2), was inversely proportional to the activity of the fines fraction and directly proportional with the amount of fines in the soil. Thus the Segregation Potential, which defines the ability of a given soil to heave due to sub-zero temperature conditions, could be correlated to the Atterberg Limits and grain size. The proposed relation was called the Fines Factor or R_f .

$$R_f = (\% F)(\% C) / LL_{ff} \quad [3.10]$$

where $\% F$ is the amount of the material under the 75 μm diameter and the $\% C$ is the amount of material that is smaller than 2 μm diameter. LL_{ff} is the liquid limit of the material smaller than 75 μm diameter. This definition of liquid limit differs from the standard definition of liquid limit (ASTM-D-3281), which states that the liquid limit test is performed with the material passing the #40 sieve. Knutsson *et al.* (1985) rearranged this equation assuming that for the same clay mineral the liquid limit of the soil mixture increases linearly with clay content. This more general relationship includes the amount of material under the 0.425 mm and the liquid limit of the soil, as follows.

$$R_f = (\% < 2 \mu m) \times (\% < 74 \mu m) \times 100 / (\% < 400 \mu m) \times LL \quad [3.11]$$

Jessberger and Jagow (1989) applied the relationship proposed by Rieke *et al.* (1983) to different available published data using Knutsson's modified version of the Fines Factor and compared it to the Segregation Potential. Plotted in a logarithmic scale and, as

shown in Figure 03-11 replotted with Rieke's concept, this data shows a trend in which increasing the Fines Factor causes the Segregation Potential to increase until a value of $R_f = 30$ is achieved. For higher R_f values this tendency reverses, and the Segregation Potential decreases with increasing R_f . The soils of about 100% fines or material under the $75\mu\text{m}$ possess the same Segregation Potential of soils with less than 25%. Figure 03-11 includes data from tests using the liquid limit of the soil and not only from the fines fraction as Rieke stated.

Horne (1987), who attempted a similar study, outlines that the data plotted in Figure 03-10 was obtained using different testing procedures, which could result in possible errors such as:

- a) The suction at the frost front cannot be calculated in all cases, and it varies from case to case due to different warm side temperatures and unfrozen soil permeability.
- b) Sample preparation is not consistent for all cases, which results in different soil fabrics.
- c) Experimental errors are present in each case and may be different from study to study.
- d) Soil properties are variable throughout the soil profile in the field tests.
- e) Soil properties are not reported in all cases.

Using the conclusions at which Rieke *et al.* (1983) arrived, Horne (op. cit.) concluded that attempts to correlate the Segregation Potential parameter to soil properties was inaccurate for frost heave prediction purposes. Nevertheless, Jessberger and Jagow's (1989) comparison supports Lambe's statement (1958) that *upon the increase of fines concentration above a certain minimum results in a decrease of frost heave rate for the more plastic clays*. Although this attempt showed that the R_f parameter used for the correlation does not give satisfactory accurate results, it did prove that if a relationship is defined, it must consider the amount of clay mineral in the soil. Horne (1987) proposed another parameter, which he called the Surface Area Factor, that is also based on the clay size fraction to correlate the Segregation Potential with the soil characteristics, but it will be discussed in Chapter VI for demonstration purposes. Concluding, this study will attempt to develop a relationship based on the amount and type of clay mineral, which are believed to be more accurate factors than the clay size and the fines content.

3.3.3 The Importance of the Specific Surface Area in Frost Heave Studies

Nersesova and Tsytoich (1963) clearly pointed out the importance of specific surface area as it relates to the chemical and mineral nature of the soil matrix (section 2.2.1), the nature of the exchangeable cations and the hysteresis in unfrozen water versus temperature (section 2.2.2). Lambe and Whitman (1968) gave a logical explanation for the

interaction between the surface of the particle and its behavior. Every soil particle carries an electrical charge on its surface and therefore ions are attracted to its surface such that the particle achieves overall electrical neutrality. These ions in turn attract dipole molecules of water and in addition, water is attracted directly to the surfaces of soil particles. Once the ions have formed the double layer, the water in it is under an attractive force to the soil particle since this water is attached to the exchangeable ion. The attractive force is dependent on the magnitude of the electrical charge, which in turn is directly related to the particle surface area. The influence of these electrical charges on the behavior of the particle relative to the gravity forces, that is, the weight of the particle, will be directly related to the surface area per mass of particles. Because of this, although forces of attraction and repulsion act between all soil particles, they are more important between fine grained compared to coarse grained particles. The magnitude of the surface area per mass is therefore a good indication of the relative influence of the electrical forces on the behavior of the particle and thus the soils.

Attempts to relate specific surface area to the magnitude of frost heave go back to the work of Linell and Kaplar (1959). They believed that the specific surface area of the fines portion would be related to the heave rates exhibited by both the parent soil and its minus #200 mesh fraction (75 μm). The basis for their thinking was the following logic. The energy needed to draw water to an ice lens and to lift the overlying soil, is made available as a result of supercooling the pore water below its normal freezing temperature. The greater the supercooling, the more energy is made available when the pore water eventually changes phase. The magnitude of supercooling is dependent upon the mean radius of curvature of the ice-water interface. The effective radii is determined by the pore sizes present between the particles of soil. The pore sizes in turn are controlled by the shapes, sizes and size distribution of particles within the soil.

It is at this point that the soil fabric and its associated aspects such as cementation, packing and aging reveals its importance on the process of frost heave. If the particles are of different sizes and shapes such that they pack well between each other, the channels will be smaller than for uniformly sized particles of the same average size. If the range of particle sizes present is large and the smaller particles fill the spaces between the larger ones, the channel sizes formed will be more characteristic of the smaller particles present. Bouyoucos (1917) held that the geometrical arrangement of soil particles, and the manner in which freezing was accomplished was also important. It can be concluded from the above that Linnel and Kaplar (1959) and Bouyoucos (1916), considered the clay content and surface area, but also the arrangement of the particles to have important influences on the frost heave behavior of soils.

As indicated earlier the attraction of water molecules to the particles to achieve overall electrical neutrality is driven by the magnitude of the electric charge deficiency on the particles, which is directly related to its surface area. With this reasoning, one may assume that the amount of unfrozen water depends on the type of dominant colloids present in the soil. On the other hand, it is a fact that the lower the temperature, the lower the unfrozen water content. Tsytoich (1973) states that only extreme temperatures will completely freeze the water in the adsorbed film around the grains within the passive layer. Anderson and Tice (1972) were able to demonstrate that the unfrozen water content of frozen soils depends not only on the temperature but also on the specific surface area of the soil particles. Horigushi and Miller (1983) and Smith and Tice (1988) also attempted to correlate the specific surface area to the unfrozen water content of different soils. However, Anderson and Morgenstern (1973) noted that even though montmorillonite has a higher unfrozen water content than kaolinite, the thickness of the unfrozen water zone is greater in kaolinite. It seems then, that the thickness of the unfrozen zone plays a more fundamental role with respect to the segregation process than does the unfrozen water content.

Smith and Tice (1988) reported a relationship between the apparent dielectric constant K_a and unfrozen water content, based on 25 soils covering a wide range of specific surface areas. Nevertheless, their research was devoted to establish a relationship between the unfrozen water content and the freezing temperature. Verifying the accuracy and comparing results obtained from techniques used to measure unfrozen water content such as the Time Domain Reflectometry (TDR) and the Nuclear Magnetic Resonance (NMR) methods was their second main objective, but no data on the frost susceptibility of the soils was published. Nevertheless it became clear after the research developed by Anderson and Tice (op. cit.) as well as the of Smith and Tice's study (op. cit.) that, in general, the unfrozen water content increases as the specific surface area increases at a given temperature.

Linnel and Kaplar (1959) reported no discernible relationships between specific surface area of a soil and its frost heaving characteristics. Since then, the only more recent study has been developed by Vinson et. al. (1985). Of course, if the frost heave problem is being analyzed, a variety of considerations have to be taken into account. Macroscopic aspects such as geology and stratigraphy, and microscopic aspects such as void ratio, *in situ* localized stress conditions, degree of saturation, and salt content are also part of the frost heave problem. However, the present research is limited to the influence of the type and quantity of the clay minerals on the frost susceptibility of coarse grained soils. Thereby, narrowing the possible variables involved in the frost heave phenomenon and

leaving aside the fabric of the soils, the specific surface area may be advantageous for frost heave predictions and ground freezing design.

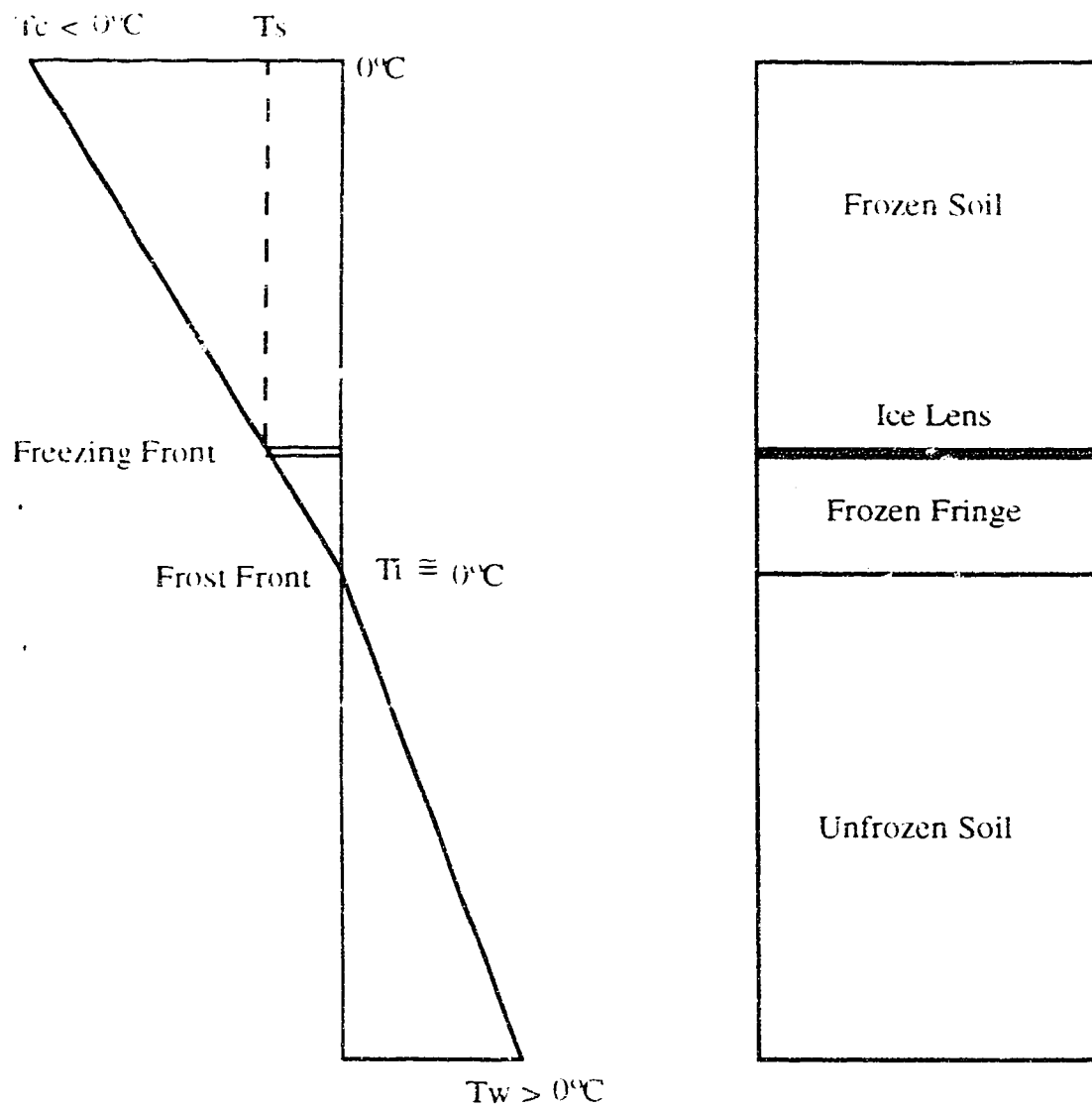
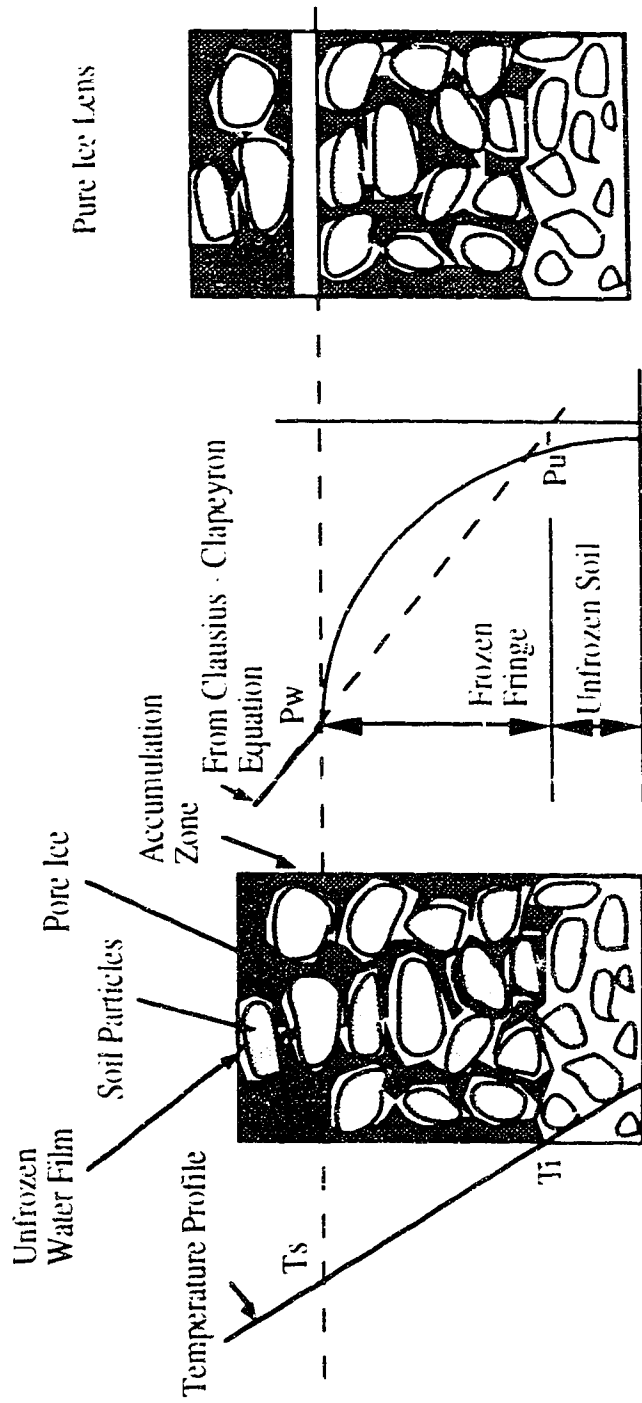


Figure 03-01.- The Konrad and Morgenstern Model
for a Frost Susceptible Soil



Suction Profile Across the Sample

Figure 03-02 - The Mechanism of Ice Lens Formation. After Konrad and Morgenstern (1980)

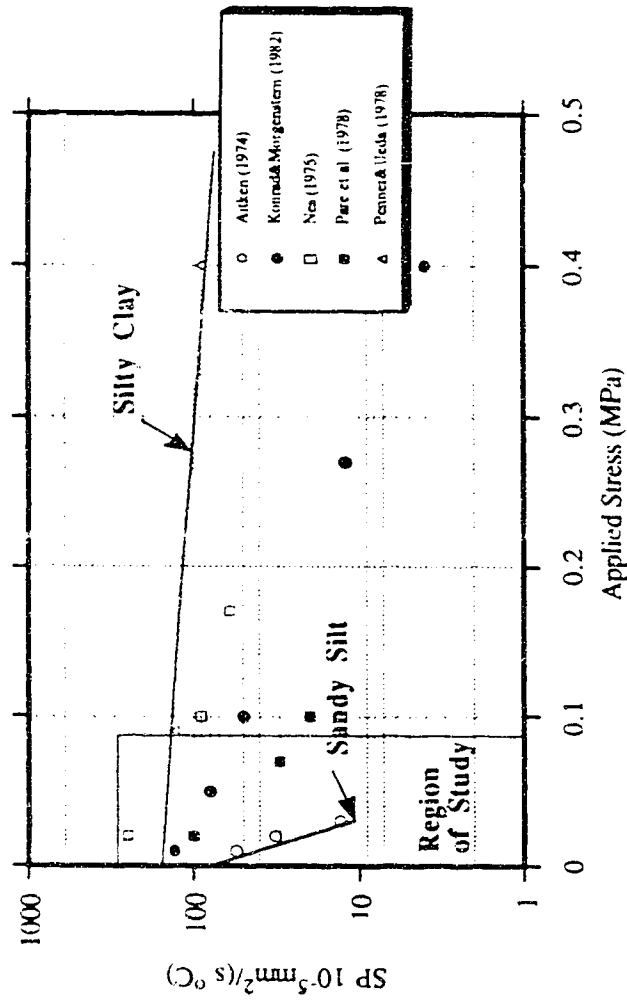


Figure 03-03.- Region of Study Considering Segregation Potential in Different Plastic Soils

Table 03-01 Influence of Clay Minerals in Frost Heave. After Lambe et al. (1958)

Source of Material < 75 μ m	Average Rate of Heave mm/day	Principal Minerals*	Content (%)
Chapman Pit Sandy Gravel	15.5	Ka Il Li Mg	40 20 5 5
East Boston Till	15.0	Ka Il Qz,Fd,Mi,Li	20 20 60
Truax Drumlín Soil	17.5	Il Qz Dm	65 15 20
Peabody Sandy Gravel	17.0	Qz Gt,Tp,Ap	40 60

* See Abbreviations

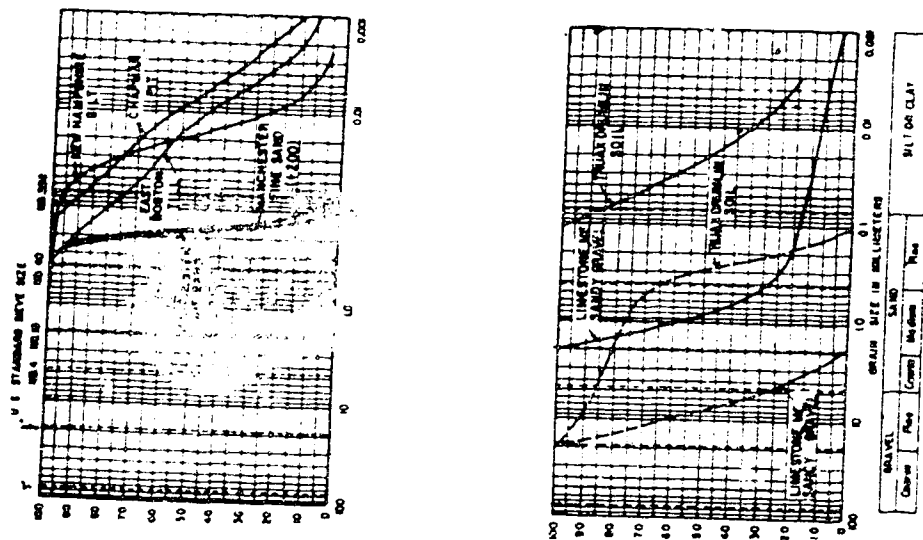
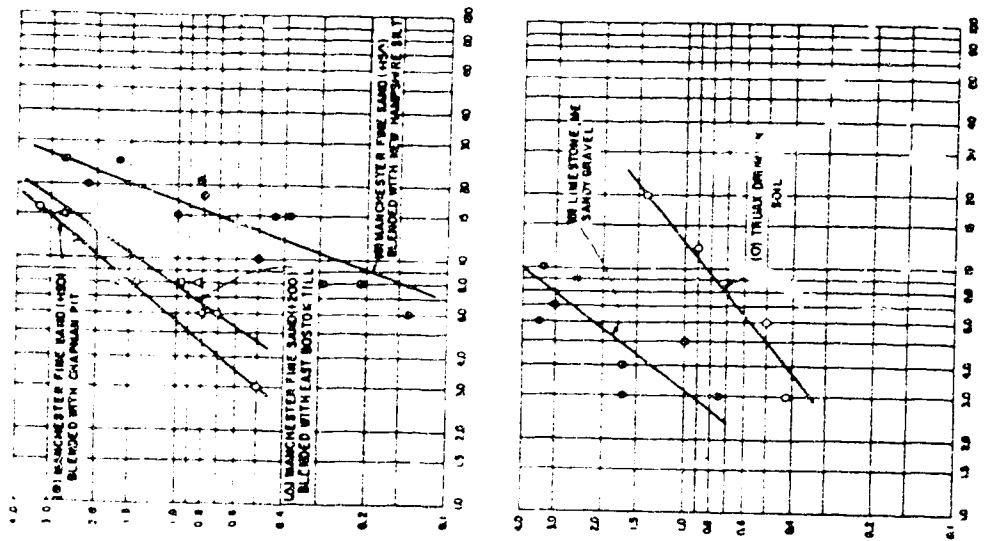


Figure 03-04.- Variation of Frost Heave for Sand-fines Mixtures, Part A
After Lincell and Kaplan (1959)

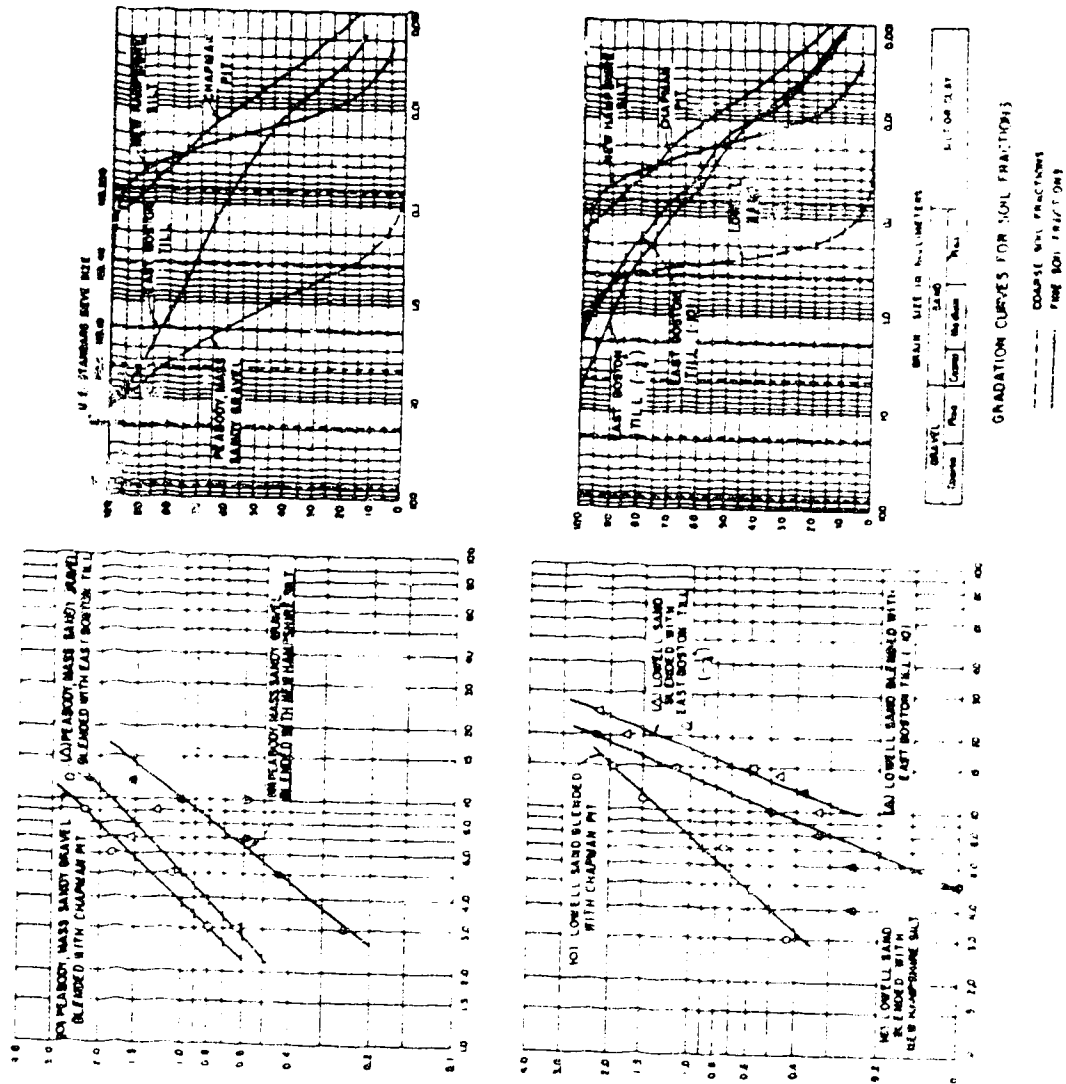


Fig. 03-05.- Variation of Frost Heave for Sand-fines Mixtures, Part B
After Linell and Kaplan (1959)

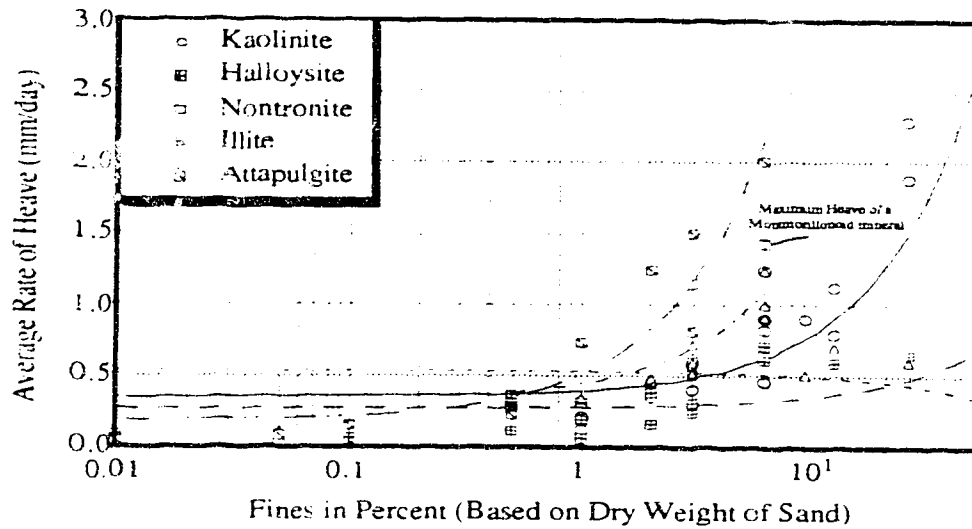


Figure 03-06.- Effect of Clay minerals on Frost Susceptibility of McNamara Sand. After Lambe et al. (1969)

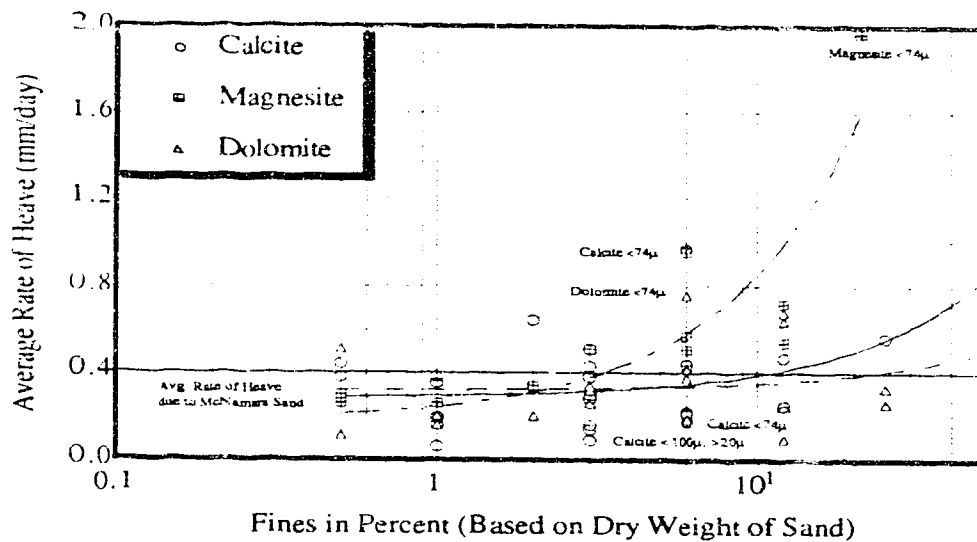


Figure 03-07.- Effect of Non-clay minerals (Carbonates) After Lambe et al. (1969)

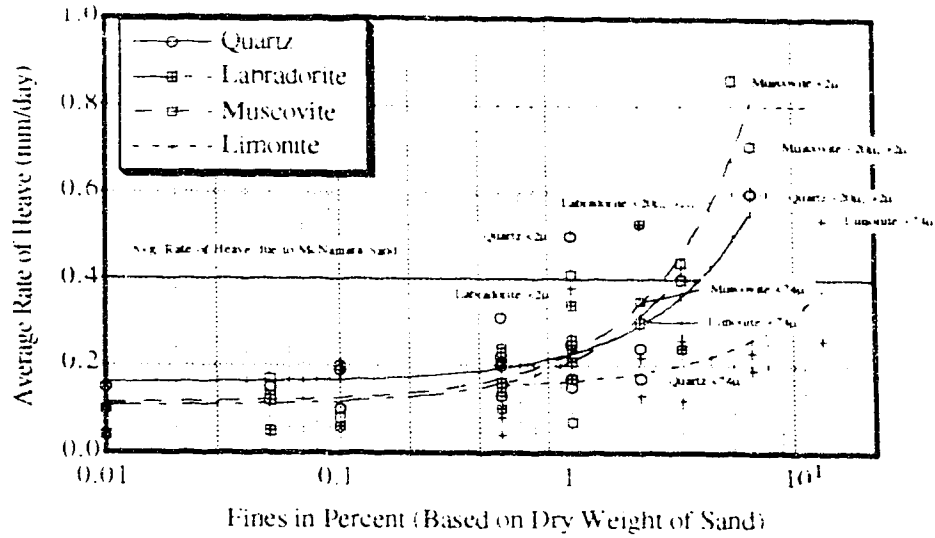


Figure 03-08.- Effect of Non-clay minerals (Non-carbonates)
After Lambe et al.(1969)

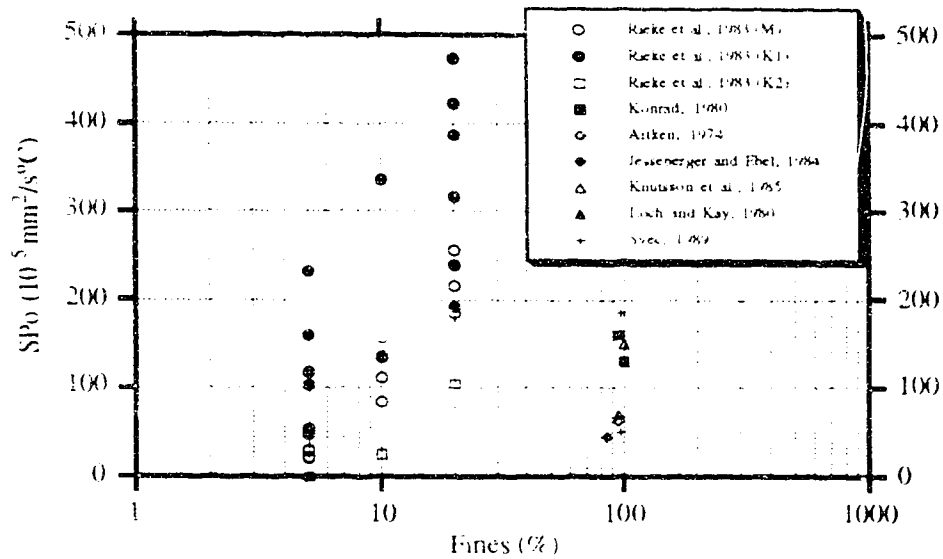


Figure 03-09.- Variation of the Segregation Potential
with the Increase of Fines Content

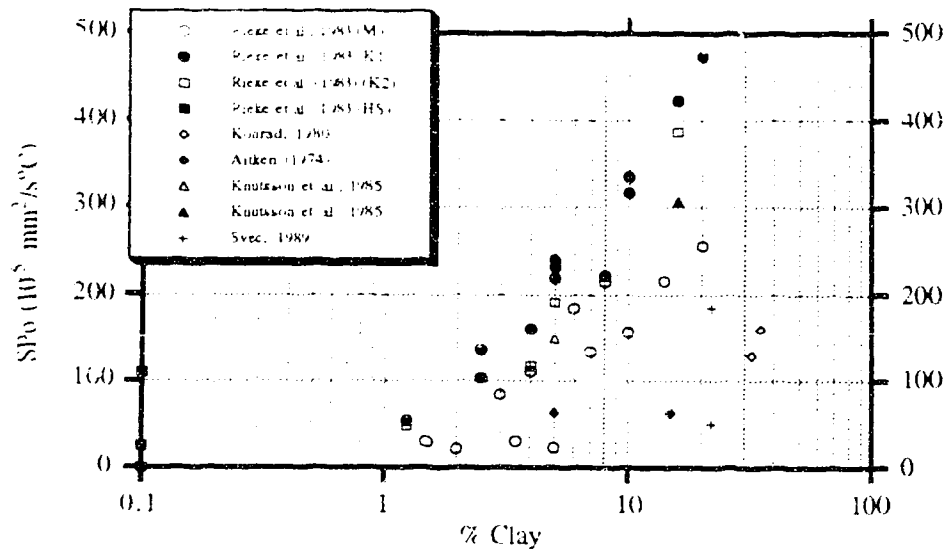
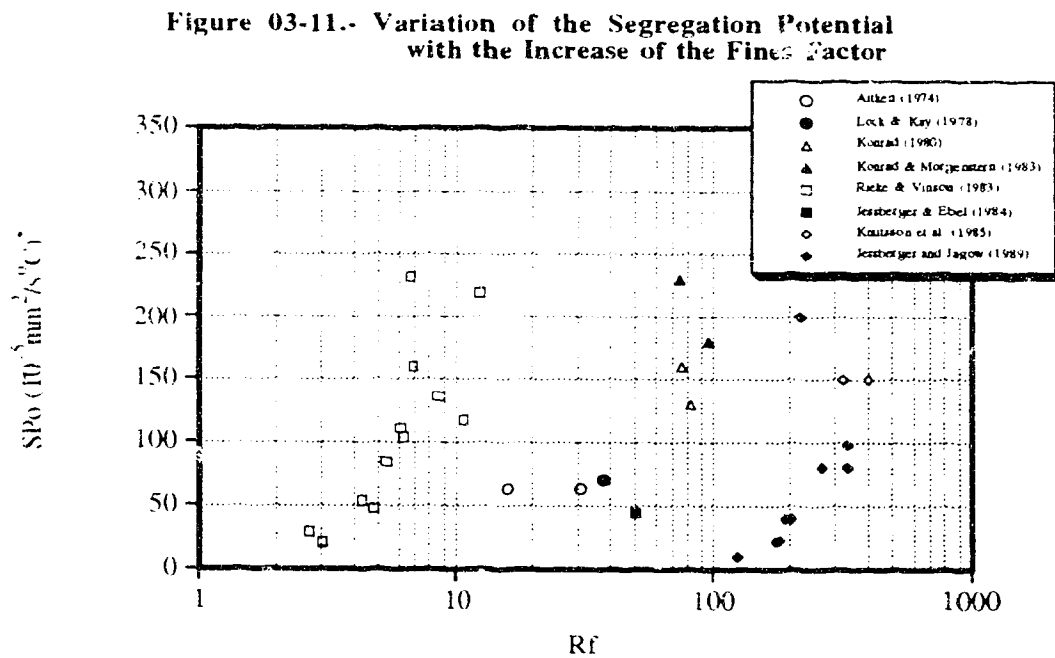


Figure 03-10.- Variation of the Segregation Potential with the Increase of Clay Size Fraction



Source	Soil	Grain Size ≤ 75µm %	Grain Size ≤ 2µm %	Void Ratio e	Atterberg Limits LL, PI	% Heave	Avg. Rate of Heave Total Heave Rate mm/day	Free Heave Parameter S _h 10-5 mm/day	S _h mm/day	RI
Kedzie & Vireman (1982)	Test No.1	20.0	20.0		135.0			286.1	91.4	
	Test No.2	5.0	0.0						5.0	
	Test No.3	5.0	5.0		135.0			22.7	97.4	
	Test No.4	10.0	10.0		135.0			186.5	97.4	
	Test No.5	10.0	0.0					29.3	5.0	
	Test No.6	20.0	0.0					106.4	5.0	
	Test No.7	20.0	6.0		56.0			184.6	32.7	
	Test No.9	10.0	3.0		56.0			84.1	42.7	5.46
	Test No.10	10.0	4.0		66.0			111.2	42.0	6.06
	Test No.11	10.0	7.0		99.0			133.8	69.7	
	Test No.13	5.0	3.5		99.0			30.2	69.7	
	Test No.14	5.0	2.0		66.0			21.2	42.0	3.03
	Test No.15	5.0	1.5		56.0			29.5	32.7	2.68
	Test No.16	5.0	4.0		58.0			160.1	19.7	6.7
	Test No.17	20.0	16.0		58.0			422.9	17.9	
	Test No.18	20.0	10.0		40.0			316.5	6.7	
	Test No.19	20.0	5.0		29.0			219.5	9.6	
	Test No.20	10.0	8.0		58.0			227.1	19.8	
	Test No.21	10.0	2.5		29.0			136.1	9.6	8.62
	Test No.22	5.0	1.3		29.0			54.1	9.6	4.41
	Test No.23	5.0	1.3		26.0			47.8	6.3	4.81
	Test No.24	20.0	5.0		26.0			197.6	6.3	
	Test No.25	20.0	16.0		37.0			387.0	9.0	
	Test No.26	5.0	4.0		47.0			117.6	9.0	10.81
	Test No.27	20.0	8.0		66.0			215.6	42.0	
	Test No.28	20.0	14.0		99.0			215.9	69.7	
	Test No.29	10.0	5.0		40.0			218.9	14.2	12.80
	Test No.30	5.0	2.5		40.0			101.6	14.2	6.25
	Test No.31	5.0	5.0		75.0			231.9	23.4	6.67
	Test No.33	10.0	10.0		55.0			115.1	23.4	
	Test No.34	20.0	20.0		75.0			477.7	23.4	

Source	Soil	Grain Size $< 2 \mu\text{m}$ %	Void Ratio e	Atterberg Limits LL PI	ϵ Heave	Avg. Rate of Heave mm/day	Frost Heave Parameter Total Heave Rate mm/day	Shv. to 5 mm/4%	SI (m ² /g)	wt
Carter and DeJong (1977)	Soil No. 4	63.5	18.5	36.9	16.1		5.5			
							4.2			
							2.6			
							2.2			
							1.2			
							0.6			
							0.3			
							7.6			
	Soil No. 9	67.5	32.5	33.1	10.7		5.3			
							2.4			
Leach & Kay (1978) California Highway Department	New Hampshire Silt No. 10, 11, 12, 13, 14, 15, 16, 17, 18, 19, 20, 21, 22, 23, 24, 25, 26, 27, 28, 29, 30, 31, 32, 33, 34, 35, 36, 37, 38, 39, 40, 41, 42, 43, 44, 45, 46, 47, 48, 49, 50, 51, 52, 53, 54, 55, 56, 57, 58, 59, 60, 61, 62, 63, 64, 65, 66, 67, 68, 69, 70, 71, 72, 73, 74, 75, 76, 77, 78, 79, 80, 81, 82, 83, 84, 85, 86, 87, 88, 89, 90, 91, 92, 93, 94, 95, 96, 97, 98, 99, 100	93.0	10.0	26.5	6.0					
		87.0	18.0	46.1	27.1					
		83.0	33.0	30.0	21.0					
		81.0	33.0	24.0	1.0					
Kornfeld & Morgenstern (1983)	California Silt California Silt California Silt California Silt	87.0	33.0	31.0	13.0					
		88.0	15.0	29.0	7.3					
		100.0	17.0	28.0	6.0					
		100.0	5.0	25.0						
Hesselerger & Hsu (1984) Krusson et al. (1985)	Oregon Silt Oregon Silt Oregon Silt Oregon Silt	100.0	5.0	31						
		100.0	5.0							
		100.0	5.0							
		100.0	5.0							
Vane et al. (1984)	Test No. 1 Test No. 2 Test No. 3 Test No. 4	2.0	1.3							
		4.0	2.5							
		8.0	5.0							
		20.0	12.5							
	Test No. 5 Test No. 6 Test No. 7 Test No. 8	20.0	15.0							
		5.0	4.5							
		8.0	5.0							
		20.0	12.5							
	Test No. 9 Test No. 10 Test No. 11 Test No. 12	20.0	15.0							
		5.0	4.5							
		8.0	5.0							
		20.0	12.5							
	Test No. 13 Test No. 14 Test No. 15 Test No. 16	5.0	4.5							
		8.0	5.0							
		20.0	12.5							
		5.0	4.5							

Source	Soil	Grain Size mm φ	Void Ratio e	Atterberg Limits LL PI	q Heave mm/day	Avg. Rate of Heave mm/day	Frost Heave Parameter mm/day	SP _h mm/day	SI mm/day	R _f
Leschberger and Jazraw (1989)	Lab. No. 1977	100.0	55.0	51.8				400		1.00
	Lab. No. 1978	84.0	42.0	47.6				22.0		176.47
	Lab. No. 2041	81.0	21.0	30.4				80.0		266.45
	Lab. No. 2039	100.0	44.0	54.5				23.0		183.49
	Lab. No. 2029	95.0	60.0	76.0				10.0		125.00
	Lab. No. 2031	82.0	24.0	40.5				40.0		202.42
	Kashan	100.0	55.0	45.5				200.0		219.78
	Kashan	100.0	55.0	45.5				290.0		219.78
	Silt	100.0	18.0	29.9				80.0		113.45
	Silt	100.0	18.0	29.9				98.0		113.45
	Ohara	87.0		71.0	51.0	7.1				
	Nimonshiro	92.0		98.0	55.0	4.8				
	Okamura	76.0		124.0	59.0	19.7				
Murata and Sakurada (1989)	Ishizawa	99.0		92.0	63.0	4.7				
	Utagami(1)	89.0		45.0	35.0	16.1				
	Utagami(2)	50.0		90.0	52.0	29.0				
	Oyaji(1)	85.0		177.0	80.0	31.0				
	Oyaji(2)	100.0		83.0	61.0	20.5				
	Iwayanagi	90.0		69.0	43.0	16.6				
	Tsuruta	95.0		71.0	55.0	11.9				
	Sayagawa	91.0		105.0	43.0	13.3				
	Azugesawa	88.0		65.0	42.0	9.2				
	Namika	34.0		21.0	1.0	10.3				
	Fuzusaki	83.0		68.0	43.0	19.8				
		54.0	22.0					130.570		
Svein (1989)	Fairbanks	94.0		31.0	7.0		14%			
	Siberia (1989)	42.0		19.0	4.0		18%			

IV. THE UNIAXIAL FREEZING TEST

4.1 Apparatus and Auxiliary Equipment Description

4.1.1 Foreword

The experimental apparatus utilized in this research to conduct the uniaxial freezing tests is the Permode or Permafrost Oedometer. This apparatus was originally used to study the properties of thawing permafrost. This device, also called the freezing cell, is an apparatus designed for controlled temperature conditions and one-dimensional freezing of a soil sample. The freezing cell is placed in a cabinet insulated with Styrofoam which in turn is placed in a controlled temperature room maintained at temperatures above the freezing point. Previous experiences with the freezing cell (Konrad, 1980) highlight the importance of the combined effect of the use of the cold room with the freezing cell to help minimize the radial heat flow into the soil specimen.

Although, the cold room is temperature controlled, defrost cycles are necessary to prevent ice build-up on the refrigeration system. Thereby, patterned temperature fluctuations in the cold room environment could be detrimental to the reproducibility of the test, but these fluctuations are attenuated by the insulated cabinet. Nevertheless, in order to observe any significant and unusual temperature fluctuations the cabinet temperature is continuously recorded. Monitoring the cabinet temperature is not only important because of the possibility of radial heat flow, but because of the effect that these variations could have on other temperature sensitive devices such as the porepressure transducer. Therefore the reliability of all the tests carried out during the laboratory program, as well as the correct functions of the equipment were never jeopardized because the temperature conditions were carefully monitored throughout the tests.

4.1.2 The Freezing Cell and Data Acquisition System

Modifications to this apparatus were required to accurately measure the temperature profile of the soil sample during the test. The freezing cell is shown in Figure 04-01, Plate 04-01 and Plate 04-02. The apparatus is basically the same as used by Hill (1977), Mageau (1978) and Konrad (1980). The split cell is a 10 cm in diameter and 17 cm long Teflon lined cylinder (Item 2, Figures 04-01 and 04-02). The outer jacket of the cell (Item 3, Figure 04-01 and 04-02) was machined from thick walled PVC pipe which prevents lateral strain during the application of load and during freezing. The thermal conductivity of the FVC is very low, thereby reducing radial heat gain and resulting in primarily one

dimensional heat flow through the soil sample (Figure 04-02). The freezing cell was placed on a table constructed to provide not only stiffness, but a counterbalanced hanger-weight system as well (Figure 04-04 and Plate 04-03). The stress was applied to the soil sample using the top piston which will be referred to as the top plate (Item 10, Figure 04-01).

The thermal gradient is applied by circulating a coolant through the top piston and the bottom plate (Items 14, 15, in Figure 04-01; Items 6, 7 in Figure 04-02). Aluminum pieces specifically designed for this purpose act as the heat sinks of the system (Items 4, 10 in Figure 04-01). The temperature of the coolant is controlled and maintained constant throughout the experiment by separate HOTPACK 334 temperature baths (Figure 04-04). The high rate of pumping (80 ml/s) minimizes temperature fluctuations. The temperature profile of the soil specimen is monitored during the test by the Resistance Temperature Devices (RTD). The RTDs are installed and sealed in the inner wall of the cells (Item 4, Figure 04-02), thus they could be in contact with the sample during the whole test. The freezing cell is provided with 8 of these devices but only 6 of them were used during the test program. The RTD ports in the external part of the PVC jacket can be observed in Plate 04-07 and their position on the two freezing cells in Figure 04-03.

This temperature sensor is an OMEGAFILM Series F with standard configuration. The platinum RTD element is a thin, flat shaped, ceramic encased, resistance temperature detector offering the advantages of having small dimension (2.3 x 2.0 x 1.0 mm), and providing a rapid, accurate and reliable surface temperature measurement. The temperature rating of the RTD goes from -50 to 600°C with 100 ohm resistance at 0°C. The temperature boundaries, that is, the top and bottom plates, are also controlled using these RTD devices in order to check if the applied temperature gradient is constant at any time. The RTDs is calibrated after every 4 tests by using a cold bath with crushed ice and water at 0°C.

The effectiveness of the seal is achieved by means of O rings placed in grooves in the wall of the top plate and at the wall of the pedestal in the bottom plate. The O rings are effective to pressures up to 103 bars (Item 11, Figure 04-01). Drainage is provided at both the top and bottom plates through sintered zinc porous stones, to permit rapid consolidation of the sample (Item 12, Figure 04-01). At the bottom plate a highly accurate porepressure transducer was installed, connected to one of the ports at the bottom of the sample (Item 8, Figure 04-01). The differential pressure transducer used is a Validyne DP 15 using internal 3-36 plates, which provides for this type of transducer a range of ± 135 kPa and able to withstand extreme pressure overloads of 200% of the range. This device is designed to operate with the Validyne CD15 Sine Wave Carrier Demodulator (Plate D-07),

which provides a DC amplified and demodulated output for the measurement. The porepressure transducer not only identifies the development of excess porepressures due to water expulsion, or suction pressures due to water intake, but also offers an indication of the water migration within the soil specimen.

The other port at the bottom of the sample (Item 9, Figure 04-02) is connected to a burette (Figure 04-04, Plate D-08) to measure the volume of water intake or water expulsion. The system operates on an open system basis, that is. allowing free access of water during the whole period of time that the specimen is tested. The burette is the only device whose data cannot be monitored using an electrical signal and therefore its readings are not recorded by the data acquisition system. On the ram of the piston a horizontal aluminum support is attached (Item 22, Figure 04-01), to which are mounted both, a dial gauge (Item 24, Figure 04-01), to measure the height of the soil sample in order to verify the initial and final void ratio of the sample, and the body of a Linear Variable Differential Transformer (LVDT), Schaevitz 500 HR-DC (Item 23, Figure 04-01). The core of the LVDT rests on PVC jacket of the cell, so that any vertical movement of the piston due to heaving pressures developed during the test is measured by the device and recorded by the data acquisition system.

The electrical signals provided by the RTDs and the porepressure transducer are recorded using the data acquisition system through the signal conditioners (Plate D-07). The signal conditioner is an electronic assemblage which provides a constant voltage source for the datalogger. The data is continuously recorded using the FLUKE 2240B data acquisition system employing a digital voltmeter (Plate D-10). The experimental data is collected, using a time interval of 30 minutes during the whole test period. The FLUKE 2240B is connected to an IBM PC in order to store the data on a 5¹/₄" diskette, which in turn is adapted to a spreadsheet format by a program developed at the University of Alberta. The data is then processed using a commercial program to observe the plots and results. The system layout can be observed in Figure 04-04. Two systems of this kind were prepared to carry out the laboratory program, but the data acquisition was common to both of them.

4.2 Test Procedure

4.2.1 Foreword

One of the purposes of this research is to ensure that the soil specimens are homogeneous and relatively loose. Since samples were required with different amounts of

fines content, a sample preparation technique was needed that would avoid segregation of the fines and coarse particles during sample preparation. For this reason, the water pluviation Slurry Deposition Method described by Kuerbis and Vaid (1989) was used and modified for the purposes of this study. The modified slurry deposition method used during the preparation of 10 cm in diameter soil specimens is described, after a review of the parameters proposed by Kuerbis and Vaid (op. cit.).

As Kuerbis (1989) mentions in his review, samples have been prepared by the water pluviation technique to ensure proper saturation since Lee and Seed (1967) described the procedure. The terminal velocity of sand falling through water is lower than that of sand falling through air. This leads to a lower energy of deposition in water pluviated samples and hence a looser deposit, as long as sedimentation currents are not set up within the water in the deposition mold. As pointed out by Oda (1972), the characteristics of the initial fabric of granular sand are determined not only by the shape of constituting grains but also by the manner in which they are deposited.

The water pluviation technique simulates the deposition of sand through water found in many natural environments and mechanically placed hydraulic fills. Oda *et al.* (1978) concluded that the anisotropic parallel alignment of particles is an important fabric characteristic not only in natural sand deposits but also in artificial sand beds. Oda *et al.* (op. cit.) reported that natural alluvial sands and water pluviated sands have similar fabric characteristics and thus similar stress-strain and strength behavior. The slurry deposition method offers the advantage of easy handling, and being able to prepare homogeneous specimens. Furthermore, the way in which the technique is carried out ensures the reproducibility of similar fabric for the artificially prepared specimens.

4.2.2 Laboratory Simulation

Vaid and Negussy (Kuerbis, 1989) concluded that the water pluviation technique produces uniform samples of poorly-graded sand, but particle size segregation is a problem during water pluviation of well-graded or silty sand. Therefore, this technique can only be used to prepare poorly graded sands. When a well-graded soil is subjected to grain size segregation during pluviation, the segregated soil has a larger average maximum void ratio than that of the unsegregated soil. Since the uniaxial freezing test requires uniform samples to ensure uniform permeability conditions and the same physical properties throughout the sample the water pluviation technique alone is not sufficient. To overcome the problem of segregation the slurry deposition method used was modified for the size of the freezing cell as discussed elsewhere in this chapter.

Kuerbis (1989) compared the ASTM dry maximum and minimum void ratios with the slurry deposition maximum void ratios of silty 20/200 Brenda sand. He noted that the maximum void ratio obtained by air pluviation is much higher, as the silt content is increased, than that obtained by water pluviation. Although the standard ASTM maximum and minimum density tests are not generally considered applicable to soils with greater than 12% fines passing the No.200 sieve, Kuerbis (op. cit.) noted that the observed behavior of a sand is similar to that of a silty sand. This behavior, nevertheless, is valid only until the silt content is about 20% by weight. When the silt fraction exceeds 20% by weight, the silty slurry turns into a thick and viscous medium, decreasing the velocity of the settling sand grains and apparently increasing the maximum sand skeleton void ratio.

There is a large difference in maximum void ratios obtained when the sample is pluviated in the dry and when the pluviation is performed in a saturated state. This might be explained due to the difference in the materials produced by both methods. When silty sand is pluviated through water, the deposition terminal velocity of sand grains is lower than when pluviated by air. Another explanation is provided by the observation, that during the determination of maximum ASTM dry void ratios, electrically charged dry silt particles are repulsed away from the container into which they are being poured. In the saturated state, electrical charges may be somewhat neutralized by the water, enabling the particles to settle into a denser structure in a manner similar to that of coarser grained sand. The difference in maximum void ratios is explained by the fact that when sand is deposited through a silty slurry, the sand fraction settles through the slurry water much faster than the silt fraction due to the difference in the particle size as predicted by Stoke's law.

In his analysis of void ratio Kuerbis (1989) proposes an equation to calculate the sand skeleton void ratio.

$$e_{skl} = \left(\frac{V_t G_s \rho_w}{M - M_f} \right) - 1 \quad [4.01]$$

where V_t is the total volume of the specimen, G_s is the specific gravity, ρ_w is the density of water, M is the total mass of soil solids in the specimen, M_f is the mass of fines in the specimen and e_{skl} is the sand skeleton void ratio.

This equation considers that the mechanical properties of water-pluviated silty sand is controlled by the density of the sand fraction, or sand skeleton void ratio. The increase in the maximum void ratio is not noticeable until the slurry, in which the coarse material is being pluviated, is thick and viscous enough to retard the deposition of the grains. At lower fines content, the sand deposition will behave as it would while being pluviated

through clean water. Kuerbis (op. cit.) concluded that the ASTM maximum and minimum void ratio specifications provide a rather poor basis for the classification of hydraulic fill silty sand behavior.

4.2.3 Laboratory Procedures

4.2.3.1 The Modified Slurry Deposition Method

Kuerbis (1989) describes a method of preparing reconstituted sand samples used in the preparation of 63 mm diameter specimens for cyclic and monotonic triaxial tests. One of the purposes of the present study was to produce the loosest possible sand-fines mixtures. The obtainment of the maximum possible void ratio is imperative in order to simulate a potential liquefiable sand deposit, but it is also important to achieve a non-segregated sample. The slurry deposition method offers the advantages of easy of handling and repeatability. This method leads to homogeneous, or in the worst cases, to poorly segregated specimens. Based on the evaluation of undrained monotonic test responses carried out by Kuerbis (op. cit.), this method also achieves fabric similar to natural fluvial sands. The slurry deposition method was adapted to the conditions required for the experimentation in order to prepare 100 mm diameter specimens to carry out the uniaxial freezing test. The procedure for the modified technique is described in the next sections.

4.2.3.2 Sample Preparation

The sequence of sample preparation is schematically shown in the layout of the procedure in Figure 04-05 and Figure 04-06. Due to the dimensions of the freezing cell, it was determined that the amount of soil to be tested should not exceed 1300 grams. The sand was poured into a 2000 ml flask with water and boiled for 20 minutes in order to de-air it (Figure 04-05a, Plate 04-04). After cooling for about 15 minutes, a vacuum system was applied to the soil (Figure 04-05b) and then manually centrifuged to allow any air trapped at the bottom of the flask to be released. Nearly the same procedure was carried out with the fines fraction to be used in the test (Figure 04-05a, Figure 04-05b). The fines fraction was boiled, cooled and deaired using a 750 ml flask, which was filled with water, equal to approximately 60% of the final sample volume. The mixture of the sand and fines fraction then took place in the mixing cylinder.

The mixing or preparation cylinder is a clear Plexiglass cylindrical tube 25 cm long, 10 cm in diameter and 5 mm thick, with an inner diameter at the bottom to fit the bottom porous stone of the freezing cell. The mixing cylinder is closed at the top by a rubber

stopper and submerged in a glass tank previously filled with water for vacuum purposes (Plate 04-04). The mixing cylinder is filled with a small amount of distilled deaired water until the rubber stopper is completely submerged (Figure 04-05c) and stable at the bottom of the glass tank. Then the fines slurry is poured into the sample mixing cylinder (Figure 04-05c). The fines left in the 750 ml flask are flushed into the mixing cylinder using deaired water. After this operation is completed the mixing cylinder is filled with distilled deaired water. During this period the heaviest particles of the fines portion settle to the bottom of the mixing cylinder.

The sand flask is filled with distilled deaired water and its opening is narrowed with a tapered rubber stopper provided with a glass tube. Figure 04-05d shows how this procedure is carried out during the pluviation of the sand through water from the flask to the mixing cylinder. Thus, this mechanism procedure ensures that the sample is saturated, and maintained saturated during all stages of the the preparation. The pluviation may take from 12 to 24 hours, depending on the type of fines, if allowed to settle by themselves. The slurry fines, which may move up into the sand flask or out of the mixing cylinder during pluviation, are retained and weighed when dry to adjust the weight of the fines retained within the sand sample.

4.2.3.3 Sealing of the Mixing Cylinder and Mixing Process

After the sand is completely transferred from the flask to the mixing cylinder, the mixing cylinder is sealed in the following way (Figure 04-05e). The boiled and deaired syntered zinc porous stone is placed in its groove upon the open end of the mixing cylinder within the water bath, maintaining saturation of the porous disk within the water bath. The porous disk becomes at this stage the bottom plate of the sample, but when placed over the freezing apparatus pedestal the porous disk reassumes its normal function. A metal disk, 10 cm diameter and 2 mm thick is then placed upon the porous stone and a piece of rubber membrane is adapted around the cylinder and over the metal disk. The rubber membrane is covered with vacuum grease, because the membrane tends to slide out from the cylinder. The system is, therefore, completely sealed and saturated.

The mixing cylinder is then withdrawn from the glass tank and a firm pressure is maintained at both ends of the tube. The slurry within the mixing cylinder is then mixed with the sand by vigorously rotating the mixing cylinder upside down and laterally (Figure 04-06a). The process of mixing can be observed through the plastic tube and, if the fines sludge is of different color, the uniformity of the specimen could be visually verified. Each mixing movement involving a rotation of the mixing cylinder and takes about 10 minutes.

The soil is allowed to settle for 5 minutes and then it is mixed again with a rotational. A better mixing and bonding between the sand and the fines, develops during the first sedimentation and is helped by the rotational movement. The sample is then ready to be placed in the freezing apparatus.

4.2.3.4 Placement of Mixing Cylinder into Freezing Apparatus

The insulation cabinet in which the freezing cell is placed is shown in Plate 04-05. During the sample preparation stage, the freezing apparatus is assembled using a dummy aluminum sample. This aluminum dummy sample is 10 cm in height and is 10 cm in diameter, (a constant volume of 785.4 cm³). This solid is used as a reference to assist in determining the dry density of the sample with the help of a 50 mm displacement dial gauge (accuracy of a $\frac{1}{100}$ mm). The dry density in turn assists in determining the initial and final void ratio of the specimen. The zero reading for vertical displacement of the dial gauge is set at the 15 mm mark. Then the apparatus is carefully dismantled, first removing the top plate and then disassembling the split PVC cylinder.

Once the PVC split cell is disassembled, the aluminum part of the bottom plate, the sides of the pedestal and the O rings are covered with vacuum grease. The burette is filled with deaired water, as is its plastic tubing, which is linked to the volume change port in the bottom plate. Once the bottom plate pedestal is filled with water, the first burette reading is taken and recorded. The porepressure transducer, described in section 4.1.2, is opened to atmospheric pressure. Using a 5 cc syringe the porepressure transducer is bled using deaired water so that no air bubbles are trapped in the plastic tubing. After this process is completed, the port in the porepressure transducer is closed. At this point, the two valves in the bottom plate are left open until the experiment is finished. Next to this, the porepressure transducer reading is set to zero by making use of the sine wave carrier demodulator. After this operation, the porepressure developed in the base of the sample is recorded during the test at an interval of 30 minutes. The bottom plate is then ready to receive the mixing cylinder as shown in Plate 04-05.

The sides of the PVC jacket are covered with vacuum grease, that is, over the PVC jacket split sides and on the bottom, which has contact with the bottom plate. The inner part of the cell is covered with a lubricant to help avoid wall friction, that may develop during the freezing test. A low permeable filter paper is placed on the pedestal, the piece of rubber membrane and the metal disk are removed (Figure 04.-06b). The mixing cylinder is then sat over the pedestal of the freezing cell, ensuring that the void for the porous stone is completely filled with deaired water. This operation is the most difficult in the procedure,

due to the fact that every extra movement must be avoided to prevent densification of the specimen. No variation of the water level is registered in the burette, but the porepressure readings show that negative porepressures are developing, confirming that the system is under vacuum. The vacuum system facilitates the remainder of the procedure, because it is possible to work for a period of time assembling the freezing cell without fear that the sample leaks and falls apart.

4.2.3.5 Assembling the Freezing Cell

The PVC jacket is assembled around the mixing cylinder and over the bottom plate. At this point the sample preparation procedure differs from the one developed by Hill (1977), Mageau (1978) and Konrad (1980). These researchers used a rubber membrane around their samples to diminish wall friction, but during this experimental procedure the possibility of placing a 10 cm diameter rubber membrane was abandoned. The major reason for this decision is the friction that the membrane and the Plexiglass wall of the mixing cylinder develop. The friction impedes the mixing cylinder from moving vertically, hence restricting its retrieval. After the PVC jacket is assembled around the cylinder vacuum grease is used to cover the joints of the PVC jacket. The cell is now ready to receive the specimen with minimal possibility of leakage.

The rubber stopper which plugs the end of the sample is removed (Figure 04-06c). When this happens the vacuum is released, so the porous stone disk falls into its exact position in the inner part of the freezing cell pedestal (Plate 04-06). Excess slurry fines or water are withdrawn from within the sample mixing cylinder, and are weighted later when oven dried to determine the exact fines content in the sample. The mixing cylinder is then carefully and steadily withdrawn so the specimen is deposited within the freezing cell in a very loose, homogeneous, saturated state (Figure 04-06d). The sample is left for 30 minutes to settle and the new burette reading is recorded. During this period of time the transducer starts to show excess porepressure readings due to the new head of water. Due to the high permeability of the sample the head is quickly stabilized.

After the PVC jacket is positioned the Resistance Temperature Detectors outlets are connected to the data acquisition system. Until this moment, both temperature baths are in continuous circulation but only the bottom plate is receiving the coolant. This does not create any temperature gradient since both the bottom plate and the room are almost at the same temperature. Once the reading of the burette stabilizes, the top piston is positioned (Figure 04-06e) and the load guide bar with the aluminum support for the LVDT is installed and pressed between the spacers and the barrel clamp screws. The next step is the

installation of the LVDT rod with its core placed on top of the PVC jacket. The bearing ball is installed on top of the piston and then the hanger system assembled on top of the piston ram. The system is left for 30 minutes under the weight of the hanger system only. Once the burette indicates that the system has equalized a new burette reading is recorded.

The dead weight is placed on the hanger system and once more a new burette reading is recorded after 30 minutes. At the end of this period of time, the specimen is ready to have the temperature gradient applied to start the frost heave test (Plate 04-07). The total stress applied to the specimen creates excess porepressures and due to the high permeability of the specimen, water is expelled through the port placed in the top plate. The water accumulates and is removed from the top of the plate with the help of a 5 cc syringe. This operation is performed to avoid the freezing of this excess water once the low temperature coolant is circulated through the top plate.

Variations in the dial gauge, which is already in place, confirms if the sample is relatively loose. Three different readings of the dial gauge are recorded after the top plate is placed. The first one is recorded 30 minutes after the top plate and the hanger system are installed. The second one is recorded after another 30 minutes, and coincides with the equalization of the burette readings, and the last reading after the test is completed. These readings give the dry densities and therefore, the void ratios of the specimen at the start and at the end of the test.

Finally, a check of all the readings is carried out and, after the cold room temperature has equalized, the circulation of coolant through the top plate is started. The time and date of the start of the experiment is recorded on the output printed by the datalogger, which has been recording data since the porepressure transducer was set to zero. The door of the cabinet is closed and the initial reading of the burette is taken. The next readings of the burette are taken at 30 and 60 minutes and afterwards at 2, 4, and 8 hours. Subsequent time intervals are 6 to 9 hours, depending on the length of the test.

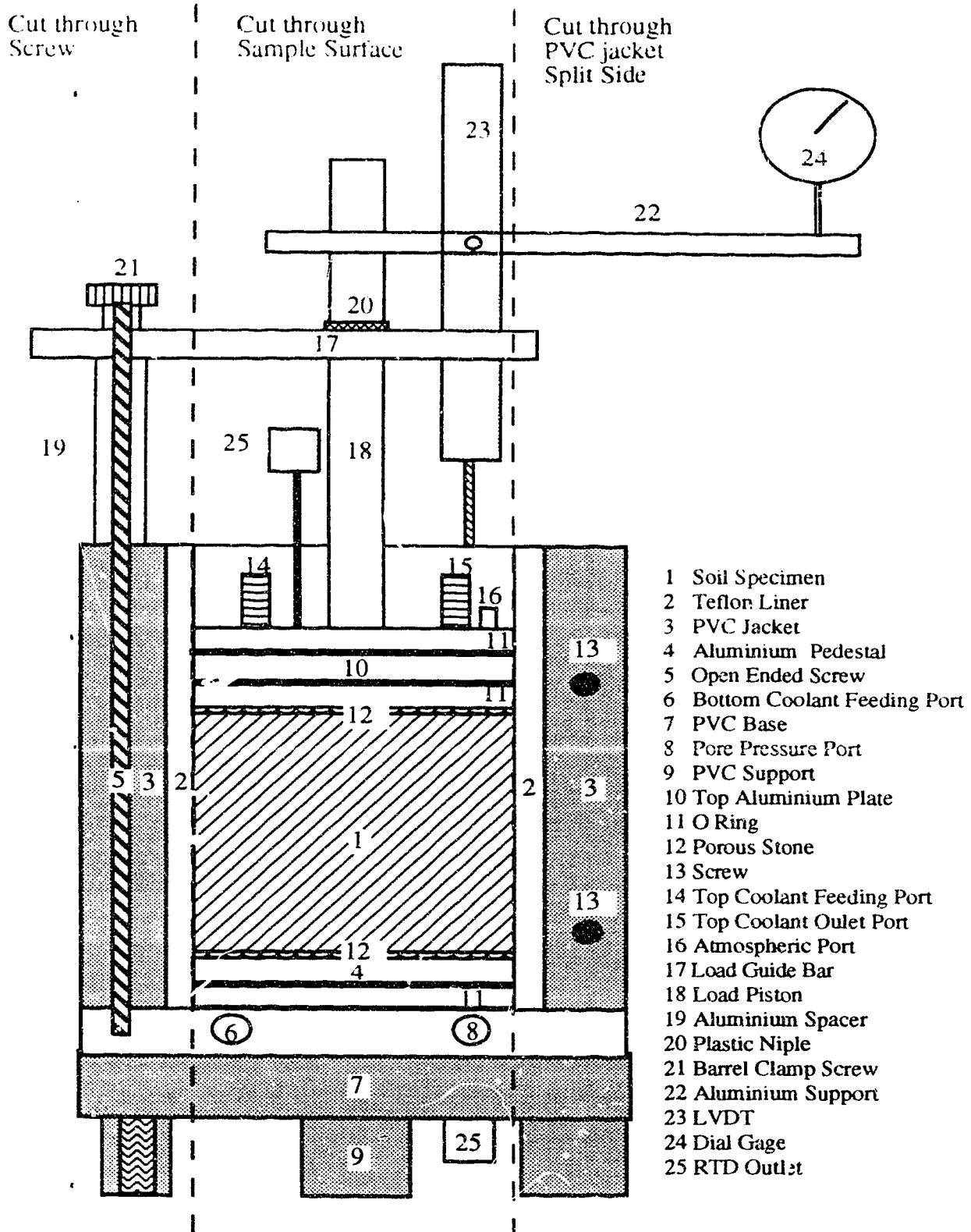
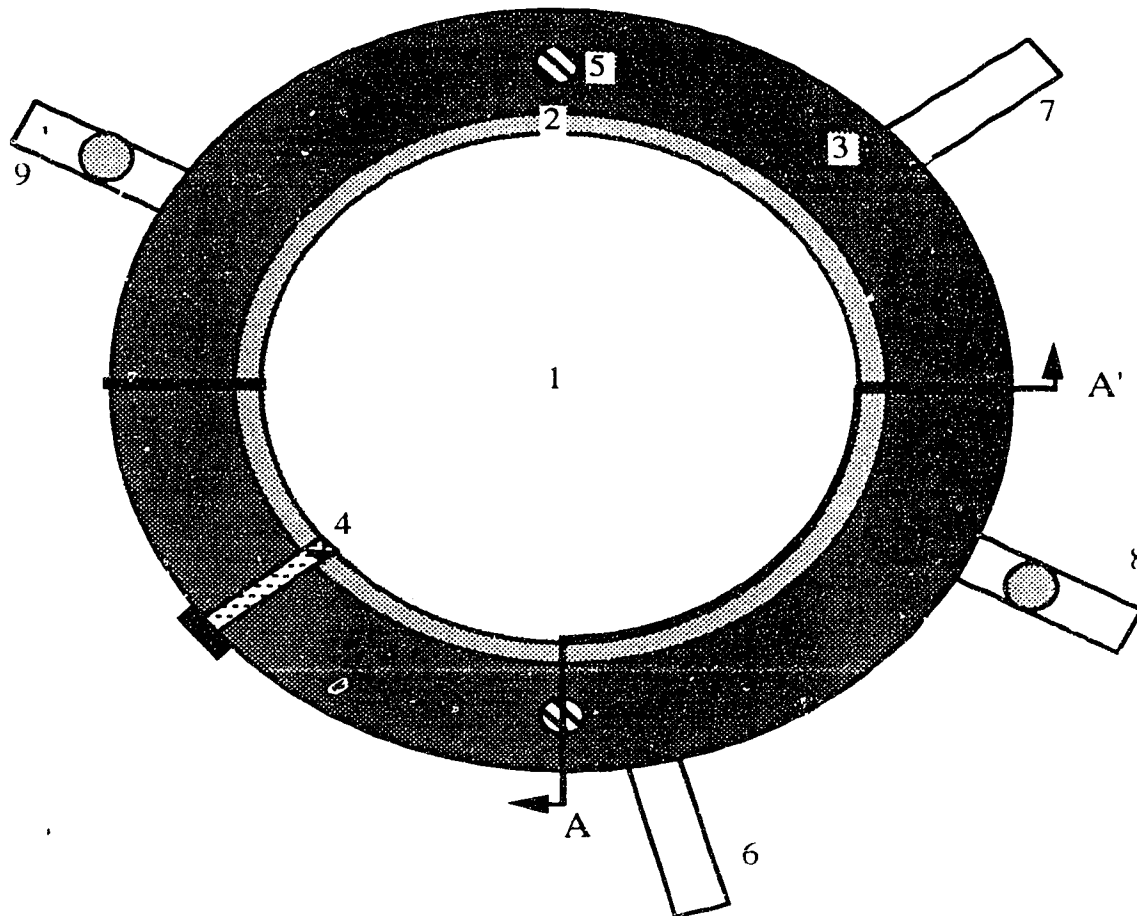


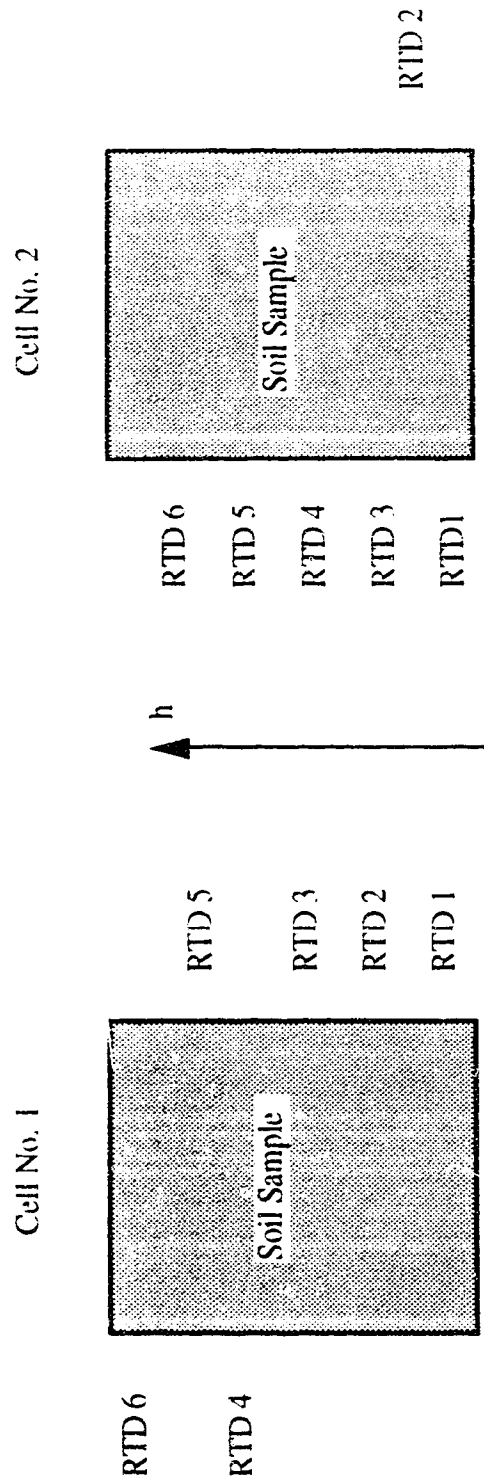
Figure 04-01.- Cutaway View (AA') of the Freezing Cell



- 1 Soil Specimen
- 2 Teflon Liner
- 3 PVC tube
- 4 Resistance Temperature Detector (RTD)
- 5 Open Ended Screw
- 6 Bottom Coolant Feeding Port
- 7 Bottom Coolant Outlet Port
- 8 Pore Pressure Transducer Port
- 9 Drainage Port

Figure 04-02.- Top Cutaway view of the Freezing Cell

Position of the Resistance Temperature Devices



RTD	1	2	3	4	5	6
Cell 1 h (cm)	1.2	2.4	3.1	5.4	7.3	9.4
Cell 2 h (cm)	1.0	2.0	3.1	4.5	5.0	7.3

Figure 04-03.- Position of the Resistance Temperature Devices on the Freezing Cells Walls

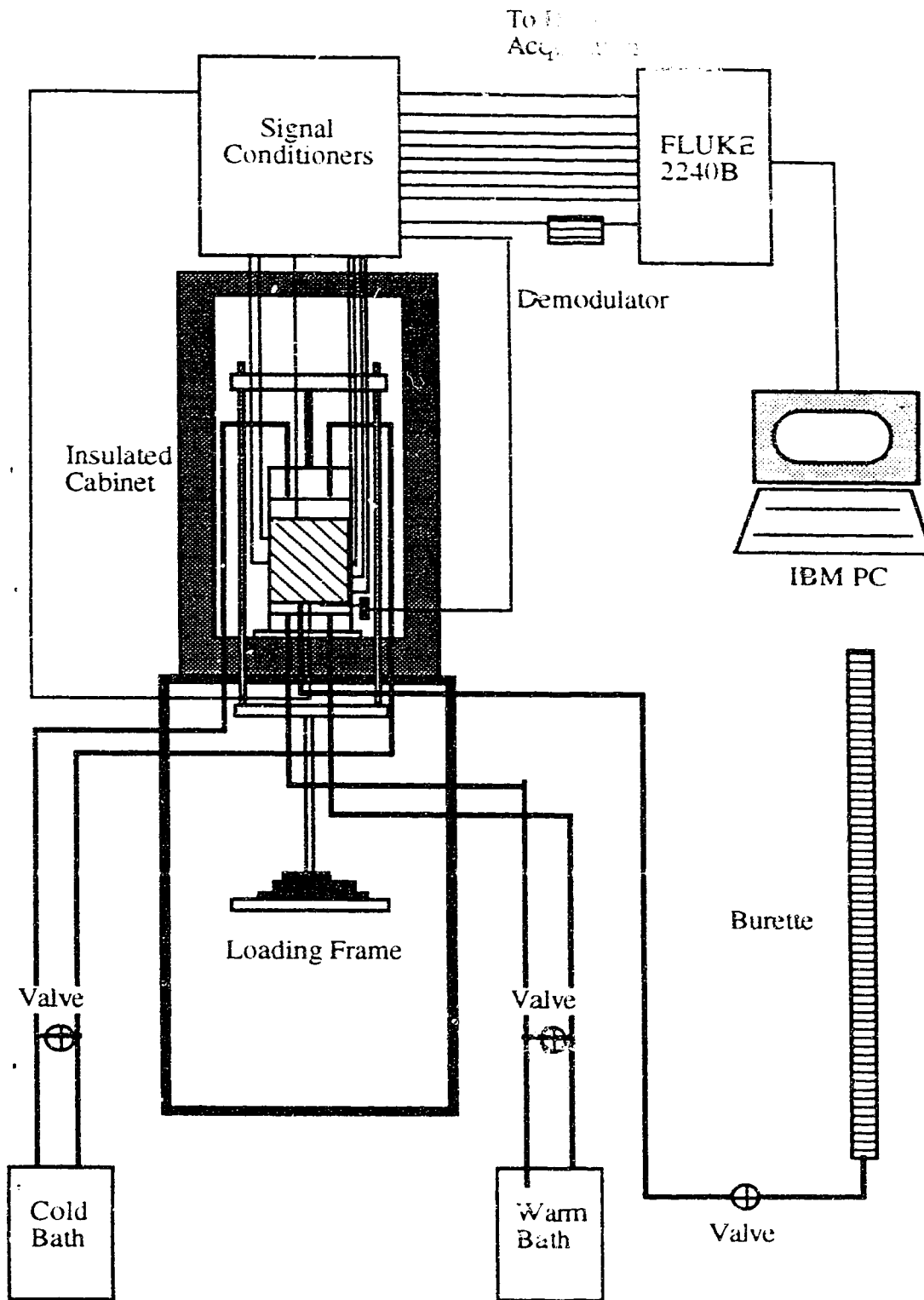


Figure 04-04.- Schematic Layout of the Freezing Cell and Data Logging Equipment Set-up

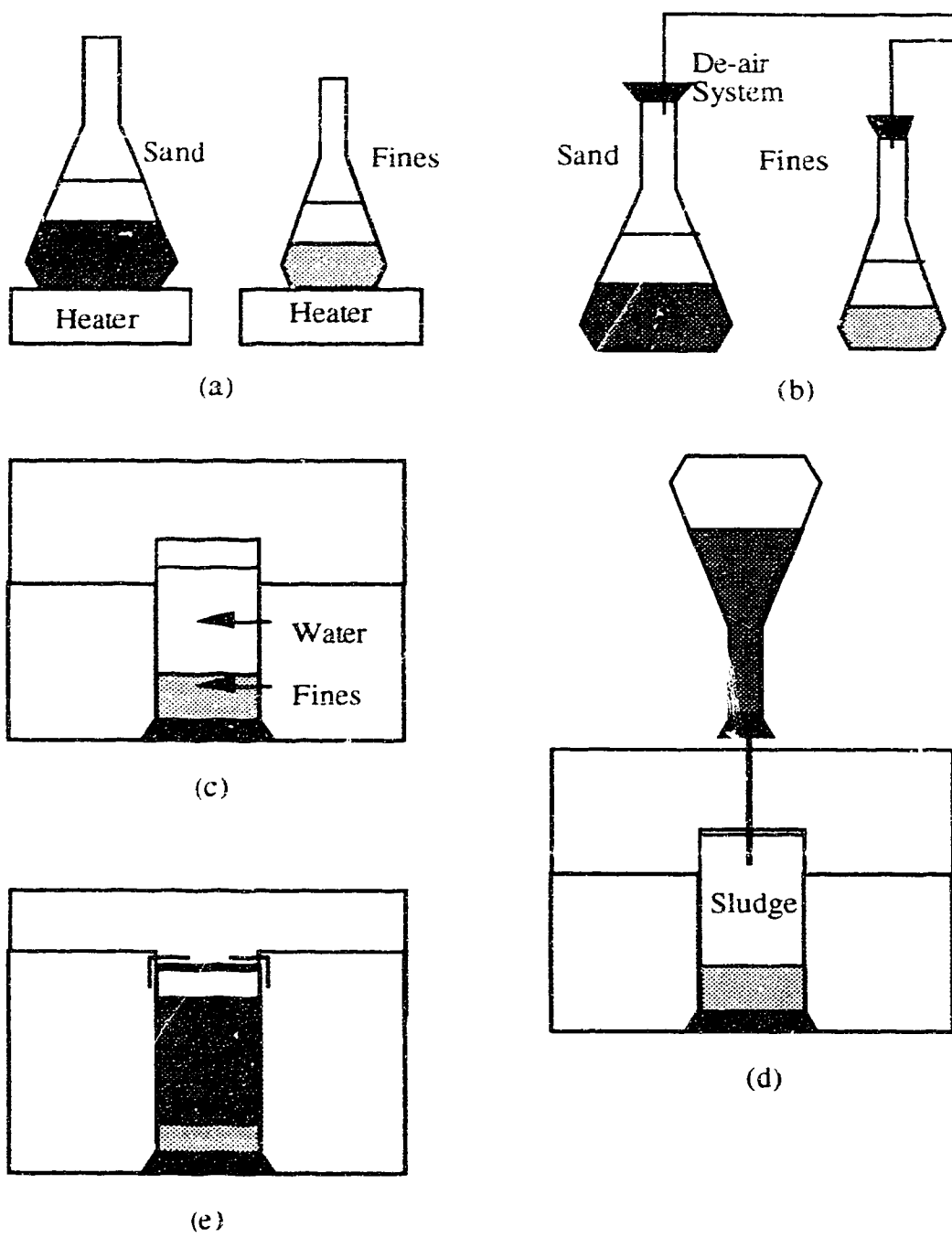


Figure 04-05.- Schematic Procedure of Sample Preparation. Part A

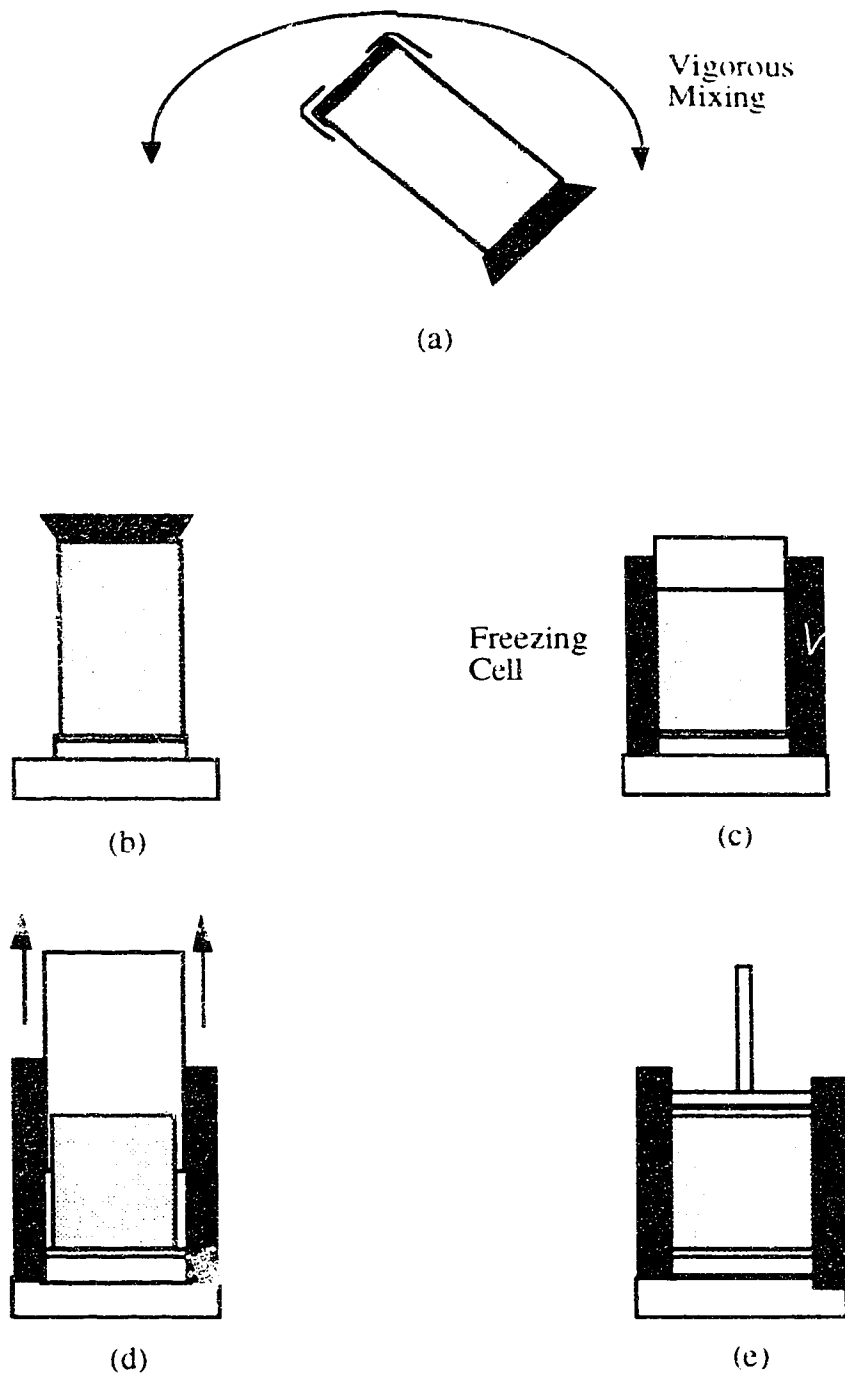
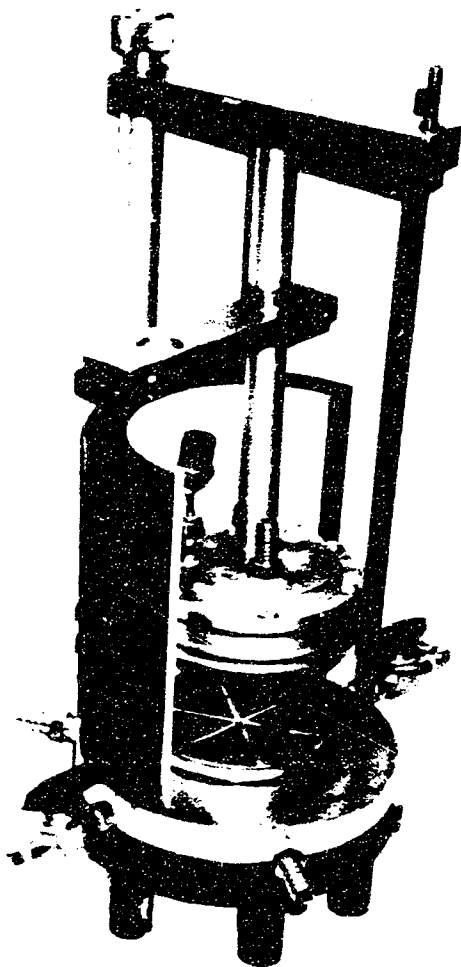
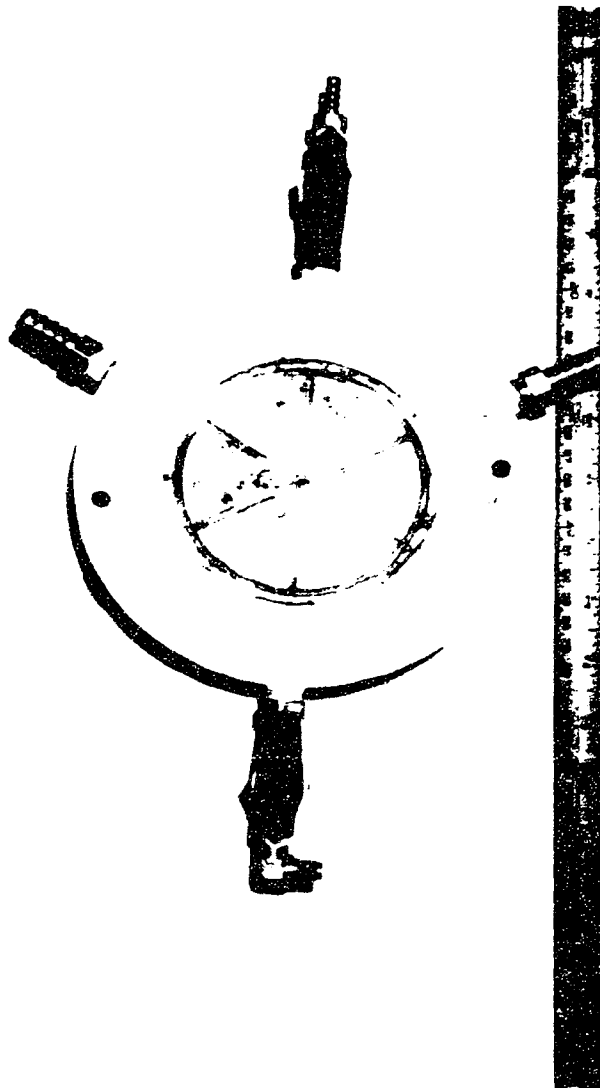


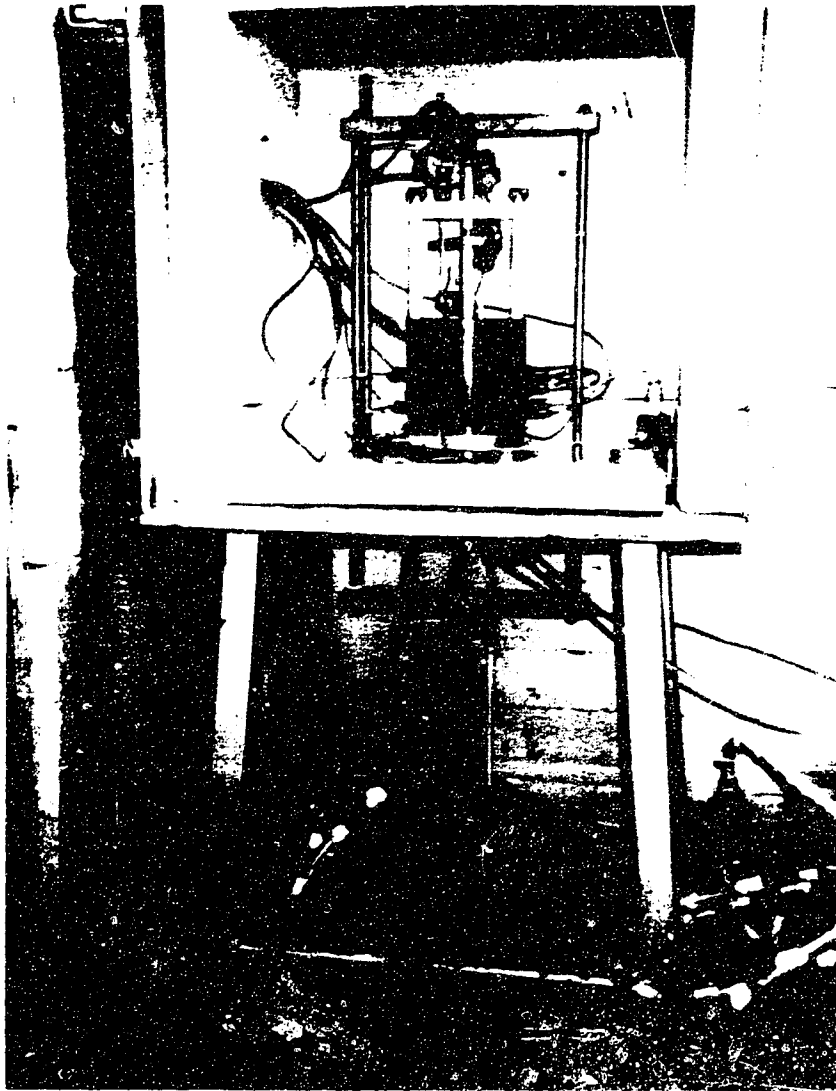
Figure 04-06.- Schematic Procedure of Sample Preparation. Part B



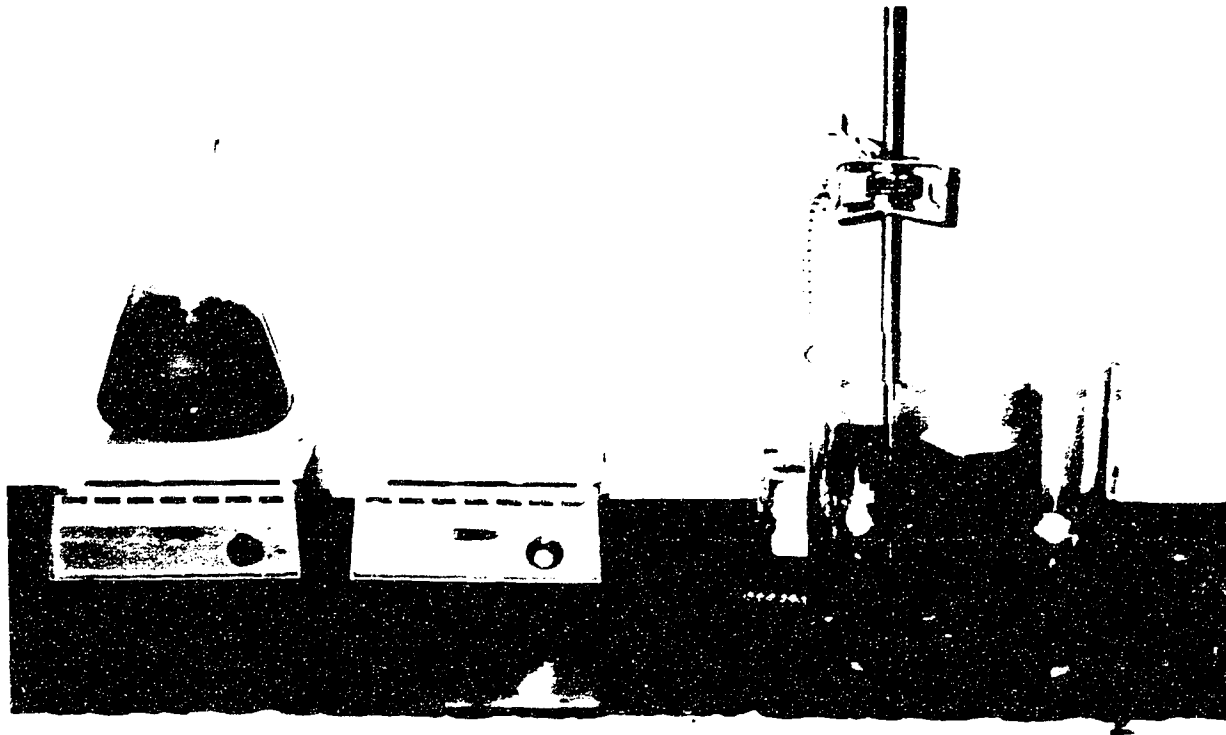
04-01.- Lateral view of the freezing cell without part of the PVC jacket.



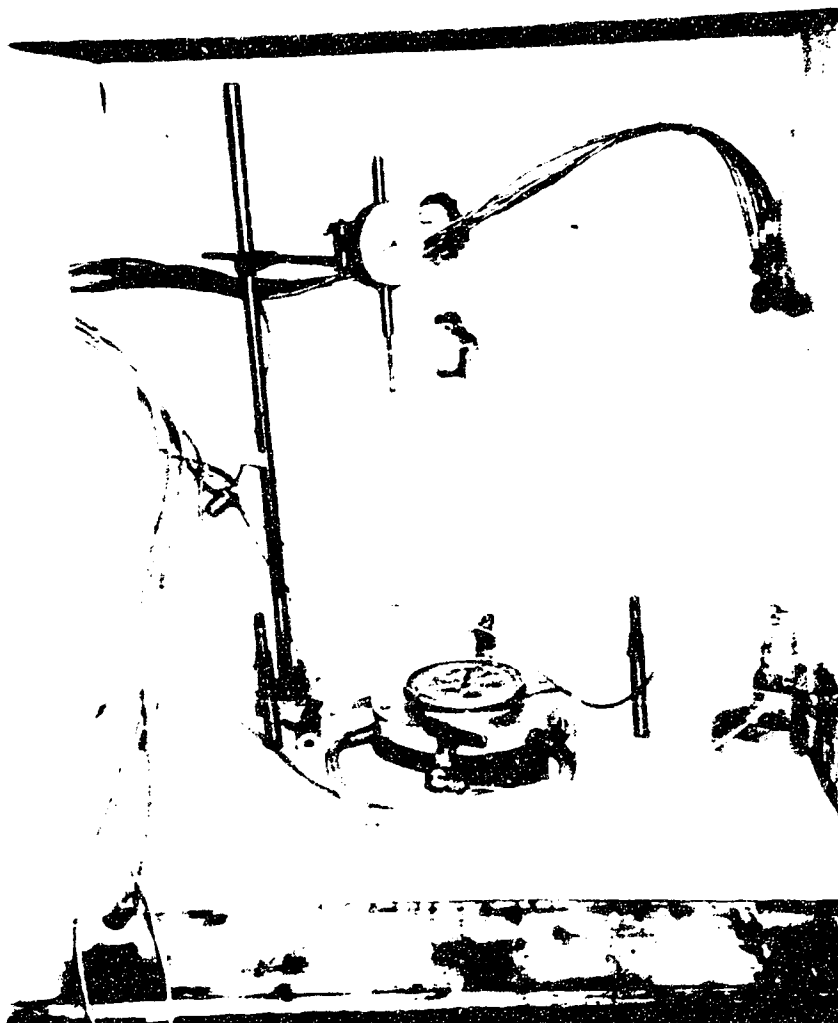
04-02.- Top view of the bottom of the freezing cell.



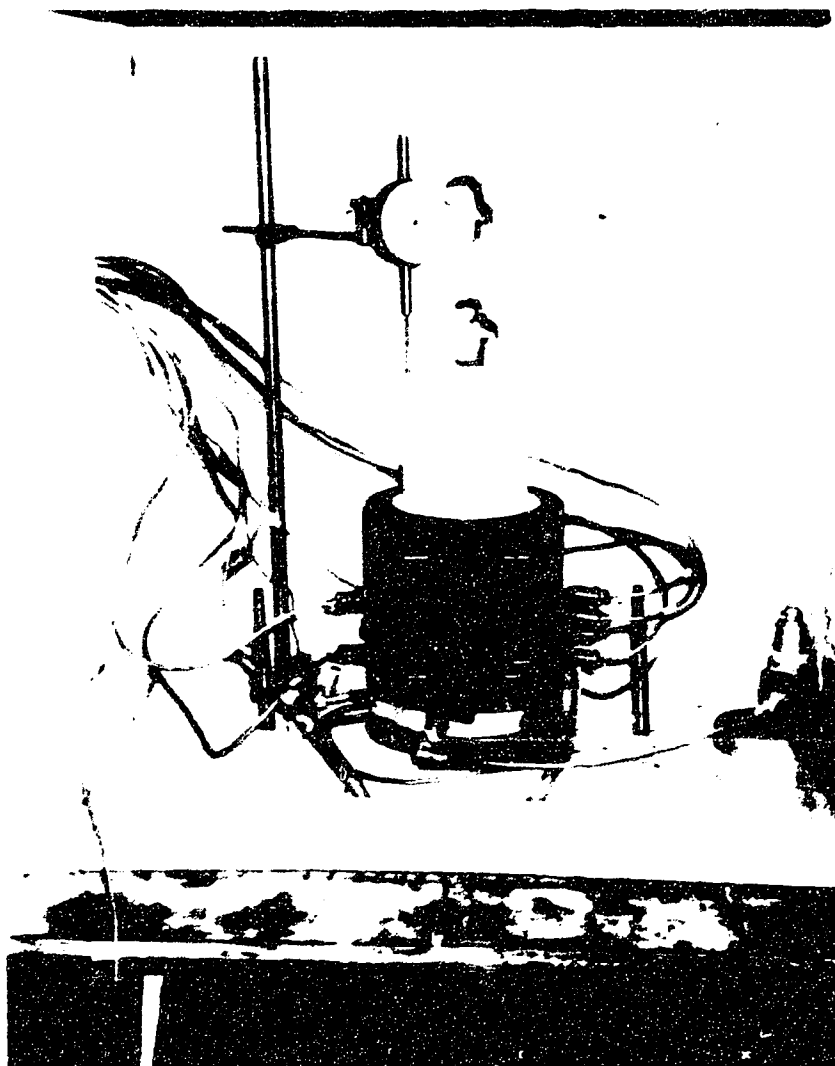
04-03.- View of the freezing cell and the hanger system.



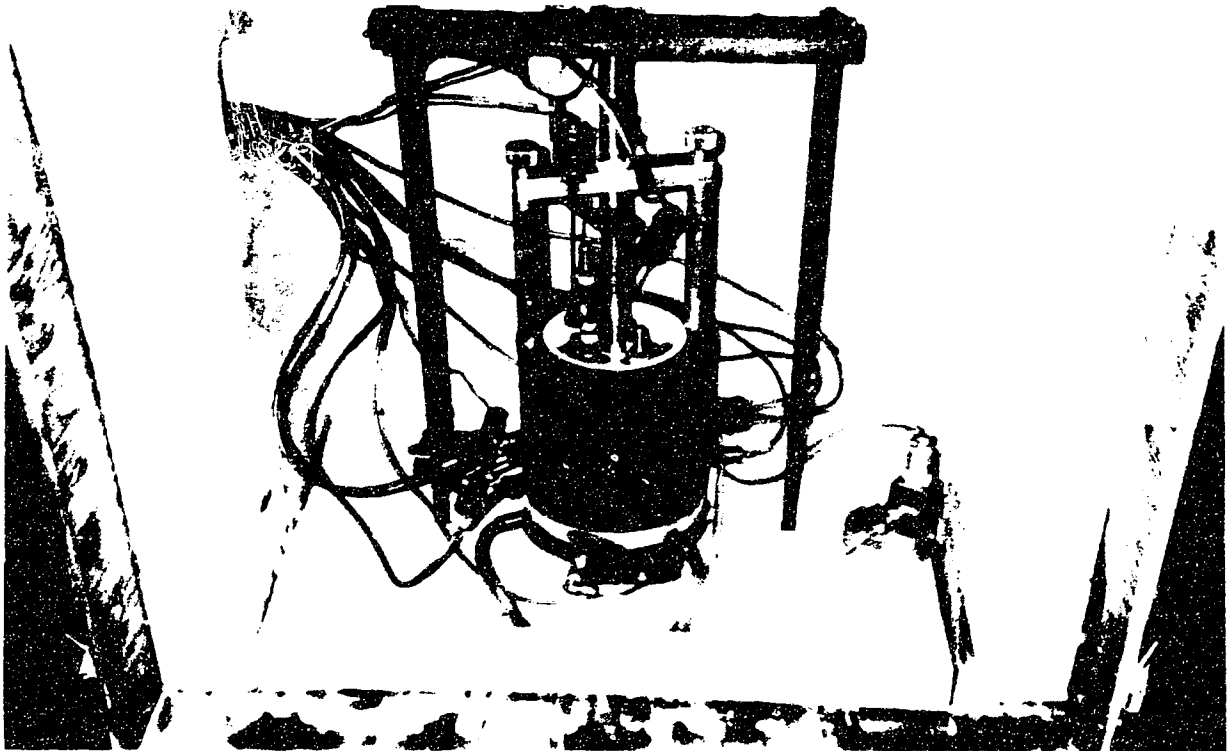
04-04.- Preparation of samples using the Modified Slurry Deposition Method.



04-05.- View of the freezing cell prepared to receive the sample.



04-06.- View of the mixing cylinder before retrieval.



04-07.- View of the freezing cell ready to receive the temperature gradient.

V. UNIAXIAL FREEZING TEST RESULTS AND ANALYSIS

5.1 Foreword

The objective of this study is to study and evaluate the performance of sandy soils such that ground freezing can be used to assist in the retrieval of undisturbed samples of cohesionless soils. The ground freezing method to be modelled is the same as used by Sego *et al.* (1990) at the Duncan Dam (section 2.3.3). During the freezing process, the soil's interstitial water changes phase; thus, the disturbance of the *in situ* void ratio by frost heave is a concern. In Chapter III the basic factors that control the frost heave phenomenon have been outlined. The soil remains undisturbed during freezing provided that the volume of the expelled water is equal to the volume of the ice expansion forming in the pores, which is the case in most of the clean sands retrieved by ground freezing methods (Table 02-03). However, in most natural sandy soils containing varying amounts of fines water may be adsorbed rather than expelled during freezing. Then the subsequent expansion of the soil due to the water adsorption is the main obstacle to obtaining an undisturbed sample by using the ground freezing technique.

The ability of a soil to undergo frost heave is dependent upon the fines fraction of the soil provided that water and freezing temperatures are readily available. In this chapter the laboratory results outlining the influence on frost heave behavior induced by the amount and type of fines contained within a cohesionless soil are presented and analyzed. Reviewing the literature presented in Chapter III, it appears that no correlation based on the fines fraction has been developed which can practically distinguish between non-frost-susceptible and frost susceptible soils. Also, there appears to be no parameter which can correlate the amount of fines to the magnitude of frost heave of frost susceptible soils subjected to a set of freezing soil conditions. In this chapter a criteria based on the specific surface area of the fines fraction and the clay mineral content of the soil is proposed in an effort to overcome these difficulties and to assist in evaluating the possibility of using the ground freezing technique for undisturbed sampling purposes.

5.2 Laboratory Testing Program

5.2.1 Description of Soils Used in this Study

To carry out this study different fine grained soils were mixed with one type of cohesionless soil, designated as the Duncan 2 Sand. This material was recovered from the field program carried out by the geotechnical group of the Civil Engineering Department of

the University of Alberta at the Duncan Dam during the summer of 1990 (section 2.3.3). The sand used to prepare the specimens was designated as the Duncan 2 Sand, since the 22% fines material from the original Duncan 0 Sand had been separated to form a cohesionless soil with no fines. The gradation curves of both sands are presented in Figure 05-01 and Figure 05-02. The maximum and minimum dry density as well as the maximum and minimum void ratio for the Duncan 0 and Duncan 2 sands are given in Table 05-01.

The gradation curves of the fine grained soils used in this study are presented from Figure 05-03 to Figure 05-08. The characterization of each fine grained soil used as the fines portion of the soil mixtures is presented in Tables 05-02a and 05-02b. The specific surface areas were determined using the Ethylene Glycol Monoethyl Ether method or EGME. Tables 05-02a and 05-02b also contain the characterization of two other fine grained soils that were not used in any of the laboratory test series. The Athabasca Clay and the Bentonite were characterized to illustrate a more representative range of specific surface area for soils. The distribution of the clay and non-clay minerals in each one of the fine grained soils is presented from Figure 05-09 to Figure 05-12, and are expressed as a percentage of the total fines content based on the area under the curve in the diffractogram. The mineralogy identification of each fine grained soil by X-ray diffraction is given in Appendix D, from Figure D-01 to Figure D-13.

5.2.2 Organization of the Laboratory Results

The procedure to obtain the sand-fines mixtures used during the uniaxial freezing tests was previously discussed in Chapter IV. In order to sufficiently appreciate the differences in the laboratory results caused by freezing, the laboratory program was divided into two parts. The first part of the laboratory program was devoted to observing the effect of freezing on specimens composed solely of non plastic sand-fines mixtures. The second and longer part of this research was devoted to observing the effect of freezing on mixtures with different types and amounts of plastic fines. Hence, the amount and type of dry fines material by weight of the total sand-fines mixtures was consistently varied during the laboratory program.

In the first part of the laboratory program only two different non-plastic fines were used, the fines from the original Duncan Dam sand and the Flume Silica fines. The details of the results obtained in the first part of the laboratory program are outlined in section 5.3.1. In the second part of the laboratory program the approach to prepare the soil mixtures was different than that from the first part since large variations in their behavior during freezing with small changes in the amount and type of the fines fraction were

expected. The specimens for each series were initially prepared with fines content of 5%, 10% and 20% of the total weight of sand-fines mixture. The maximum amount of fines was 20% since the skeletal void ratio could not be used for larger amounts of fines within a soil (section 4.2.2).

During both parts of the laboratory program the exact amount of fines and clay mineral contained in each test specimen were determined after the freezing experiment was terminated. The frozen and unfrozen portions of the specimens were collected for water content determination and from these samples the homogeneity and distribution of the fines within the specimen was checked by wet sieving and weighting the portions of soils above and below the 75 μm particle size. As discussed in section 3.2.3, the type of clay mineral plays a fundamental role in the ability of a soil to undergo frost heave. Therefore, different types of fines were used in this study to observe their effect on the frost heave behavior of each soil mixture. The second part of the laboratory program was separated into different series, each series corresponding to the different type of plastic fines added to the mixture. This part of the laboratory program is described in detail in section 5.3.2.

5.2.3 Boundary Conditions

For the evaluation of the frost susceptibility of soils, it is important to compare measured frost heave results with a frost heave parameter which has its origins in the theory of ice-lens formation and frost heave. Therefore, freezing tests must be conducted to determine whether or not a soil will undergo frost heave and to determine the relevant frost heave parameter that will control the initiation of frost heave. Chamberlain (1981) performed a survey of some of the major transportation departments in countries in which frost heave was a concern and realized that no standard technique was used to evaluate the frost susceptibility of a soil. He concluded that freezing tests employed until that time for this purpose were poorly designed and conducted. As a result he developed, at the CRREL laboratories, a new freezing test (Chamberlain, 1987) which includes two freeze-thaw cycles.

The freezing apparatus and test procedure used during the present study, as detailed in Chapter IV, emulates but does not reproduce the CRREL procedure. Extensive data is available from previous studies (Hill, 1977; Mageau, 1978 and Konrad, 1980) using the same test apparatus. The main purpose of the CRREL standard test is to simulate extreme natural freezing conditions. Therefore, the boundary conditions applied to the soil during the test procedure outlined by Chamberlain (1987) are set to obtain the most conservative parameters needed for design in a natural cold region environment. The test procedure as

proposed by Chamberlain (op. cit.) cannot be applied to evaluate artificial ground freezing since in this case the soil can be subjected to a rather unusual temperature boundary condition imposed by the use of liquid nitrogen at a uncommon freezing temperature of -196°C .

When a steep negative temperature of such magnitude is applied to an unfrozen soil, the temperature within the unfrozen soil decreases exponentially as the distance increases from the point of contact yielding high temperature gradients. Hence, modelling the behavior of the soil by the CRREL procedure near to the freezing pipe would not be practical because the apparatus (section 4.1.2) is not designed for such temperature gradient. Furthermore, it was determined on site (Figure 02-13) that the natural ground temperature varied with depth, this implying a different temperature gradient through all the finite region of the stratum in which the freezing pipe is confined (section 2.3.3). The situation to be simulated in this study is not that of the region adjacent to the freezing pipe but that of the region subjected to the advance of the freezing front in the area where the samples are obtained. The freezing process of interest for the uniaxial freezing tests performed for this study occurs in one step without the need for alternate freeze-thaw cycles.

As described in section 2.3.3, the coring of the frozen samples at the Duncan Dam was performed 0.5 m apart from the freezing pipe. It is assumed that the temperature gradient developed at that distance is about the same as the temperature gradient used in the CRREL freezing tests, that is $0.4^{\circ}\text{C}/\text{cm}$ (Chamberlain, 1987). This gradient is achieved in the laboratory by applying to the approximately 10 cm long specimens a constant boundary temperature of $+2^{\circ}\text{C}$ on the warm side and of -2°C on the cold side of the freezing apparatus. The use of this gradient was criticized by Svec (1989) since such high gradients do not occur frequently in nature and, if it happens to occur, it is of short duration. However, for the purposes of this research, this temperature gradient is acceptable and simulates artificial freezing near the advancing freezing front in the sampling region. The main advantage of this laboratory temperature gradient is that it does not allow the freezing front to advance beyond two thirds of the length of the test specimen. Furthermore, once the final freezing front ceases to advance and the steady state condition is established, it is also possible to observe the growth of an ice lens within the middle portion of the test specimen.

In the present study stress has been treated either as a constant boundary condition or as a variable. All the specimens, with the exception of the multistage (MS) series (Table 05-04) as explained elsewhere in this chapter, were subjected to a constant total stress during the test. Although Yoshimi *et al.* (1978) carried out their experimentation with a

total stress of 33 kPa, it was convenient to initially apply a lower total stress to the first round of tests, and then raise it for a second battery of tests. The total stress applied to the samples was chosen to be 24 kPa for the first battery of tests and 65 kPa for the second battery of tests. Based on the work of Yoshimi *et al.* (op. cit.), the expansive strain becomes less than 0.1% when the surcharge exceeds 33.3 kPa for tests on Tonegawa sand. This corresponds to an overburden pressure at a depth of 2.6 m if the ground water table is at 1 m below ground surface for the Tonegawa sand. In this study, the stress of 24 kPa is applicable to a sample which would be retrieved from about 1.4 m below the ground surface, and the stress of 65 kPa to a sample retrieved from a depth of 5.5 m, if a unit weight of 20 kN/ m³ is used for the soil with the water table located at 1 m depth.

5.3 Uniaxial Freezing Tests Results

The results to be presented herein are organized on the basis of laboratory similarity. Table 05-03 presents the chronological sequence in which the tests were carried out. Four uniaxial freezing tests using Devon Silt were performed in order to verify the freezing procedure and equipment calibration. The results of these tests were compared with similar test results obtained by Konrad (1980). The experiments yielded results which were comparable so the test equipment was deemed acceptable. Then tests using the modified Kuerbis and Vaid (1989) sample preparation method (section 4.2.3) were performed to evaluate the procedure to prepare loose sand samples (UFT No. 1 to UFT No.9, Table 05-03). These tests were used to verify that homogeneous coarse grained soil specimens could be prepared. These verification tests were carried out using a very uniform silica sand (S1) with gradation between the 212 μ m and 425 μ m particle size. Once the sample preparation procedure was established and the equipment calibrated to give reproducible results, the uniaxial freezing tests for the soil mixtures were started.

5.3.1 Freezing Test Results and Analysis of Soil Mixtures with Non-Plastic Fines

The procedure outlined in Chapter IV was used to conduct all tests in the first part of the laboratory program. A total of eight tests were performed using non-plastic material and for as long as 90 hours; the composition of these samples can be found in Table 05-04. The characterization of the sands used is presented in Table 05-01 and the characterization of the Duncan 1 and Silica Flume Fines is given in Tables 05-02a and 05-02b. The grain size distribution of these fines are shown in Figure 05-03 and Figure 05-04, and the fines

mineral composition is presented in Figure 05-09. The X-ray diffractograms of these soils from which the mineral compositions were derived can be found in Figure D-01 and D-02 for the Duncan 1 Fines and D-03 Silica Flume Fines (Appendix D). As outlined in section 5.2.3 the tests in this part of the laboratory program were all carried out under a total stress of 24 kPa. The conditions under which each test was performed is outlined in Table 05-03. The complete record of the laboratory freezing tests is shown in Appendix C.

Four of the tests, D005, D006, LT01D0 and LT02D0, (Figure C-01 to Figure C-04) were performed using the Duncan 0 Sand in order to establish a reference for the other tests carried out with either plastic or non-plastic fines. From these four, D006 (Figure C-02) and LT02D0 (Figure C-04) were tested for more than 80 hours in order to observe if any variation from the steady state conditions occurred with time. From the four remaining tests, D1100 (Figure C-05) was tested using the Duncan 1 Fines and D202 (Figure C-06) using the Duncan 2 Sand. The other two, D2CS20 and D2CS30 (Figure C-07 and Figure C-08 respectively) were a mixture of the Duncan 2 Sand with different amounts of the Silica Flume Fines. All eight specimens initially expelled water when submitted to the temperature gradient, and then stayed constant after achieving the maximum level of water expulsion.

Figure 05-13 and Figure 05-14 compare the water expulsion and Tables E-01 and E-03 (Appendix E) summarizes the void ratios for the individual specimens tested. It can be observed from Table E-03 that no appreciable variation in the void ratio was recorded during these uniaxial freezing tests. Table E-01 presents the maximum amount of the water expelled (WE), and the predicted total amount of water expelled (WE_p) for each of the samples tested in this part of the laboratory program. The outflow of water was able to be predicted using equation 3-25 in Chapter III. The volume of soil used to calculate the water expelled was obtained from the height of the frozen section of the soil specimen after each test was completed. Both, the predicted and the maximum recorded values are similar, reaffirming Tsytovich's (1973) and Khakimov's (1957) conclusions about moisture migration in coarse grained soils (section 3.2.1).

The D0 series specimens (Table 05-04) composed of the original Duncan 0 Sand are analyzed first (Figure 05-13). The behavior of three out of a total of four samples performed under the D0 series yielded no significant differences. Despite of presenting the same pattern of freezing behavior the specimen LT01D0 (Figure C-03) expelled a greater amount of water. Sample LT01D0 was tested under similar conditions as the other three Duncan 0 Sand specimens, but the water expulsion from this specimen was approximately 25% more than in the other three. This difference could be explained by the slight increment in the temperature gradient across the sample (Table E-03), allowing the freezing

front to advance further into the sample than in the other specimens. The four specimens in this series yielded similar freezing behavior with an average of 20 ml of water expelled.

The next step was to add non-plastic fines to the Duncan 2 Sand in order to observe if significant changes occurred by changing the type of non-plastic fines. In two experiments the Duncan 2 Sand was mixed with the non-plastic Silica Flume Fines. These tests were named D2CS20 (Figure C-07) and D2CS30 (Figure C-08) corresponding to the CS series (Table 05-04). Both specimens differed in the amount of Silica Flume Fines added to the mixture as shown in Table 05-04. The observed water expulsion behavior from these samples was similar to that of all the other specimens in this part of the laboratory program (Figure 05-14). Even the freezing front advance behavior (Figures C-07 and C-08) is comparable to the results obtained for the Duncan 0 Sand as shown by the results under the series D0 (Figure C-01 to Figure C-04).

Throughout each of the freezing tests the samples in the D0 and CS series expelled about 15 ml of water during the first 10 hours. After this 10 hour period, the amount and rate of water expulsion varied with the composition of the test specimen. Increasing the amount of Silica Flume Fines fines caused the amount and rate of expulsion to decrease, such that the sample with 20.7% content of Silica Flume Fines (D2CS20, Figure 05-14) expelled water in a similar manner to the Duncan 0 Sand which had 22% fines (Figure 05-13). When the amount of Silica Flume fines in the specimen was increased to 30% (D2CS30), the amount of expelled water diminished by 20%. Upon noticing this phenomenon, it was decided to perform a uniaxial freezing test on a specimen constituted totally of non-plastic fines (i.e. $100\% < 75 \mu\text{m}$).

A test (UFT 18, Table 05-03) constituted of 100% Silica Flume Fines (Figures 05-04 and 05-09) could not be tested due to the strong attraction that the particles developed with the Plexiglass mixing cylinder. The retrieval of the cylinder from the freezing cell (section 4.2.3.5) proved to be impossible; therefore, the sample could not be prepared. Since testing a specimen entirely composed of the Silica Flume Fines was impractical, this experiment was carried out with a sample prepared with 100% Duncan 1 Fines (Figures 05-03 and 05-09). This test, D1100 (Figure C-05), was carried out without difficulty; thus, this test represents a lower boundary for the condition of non-heave under the imposed boundary conditions (section 5.2.3). Since a specimen containing 100% non-plastic fines was used to establish the lower boundary, the upper boundary would be established using a sample containing no fines and only coarse grained soil. The upper boundary was determined by testing the Duncan 2 Sand, D202 (Figure C-06), which had no fines (i.e. $0\% < 75 \mu\text{m}$) (Figure 05-02). Both tests, the D1100 (Series D1, Table 05-04) and D202 (Series D2, Table 05-04) tests, exhibited expulsion of water as did the original

Duncan 0 Sand. The results of these tests are compared to the Duncan 0 Sand (Figure 05-13) and the soil mixtures containing the Flume Silica Fines (Figure 05-14).

In summary, the first part of the laboratory program showed that expulsion of water during controlled freezing tests does not depend on the soil gradation or on the amount of fines provided the fines are non-plastic. One may conclude from these experiments that a soil containing solely non-clay minerals will expel water during freezing and not experience frost heave if subjected to similar boundary conditions (section 5.2.3). The magnitude of water expulsion depends on the temperature boundary conditions and initial void ratio of the soil. Finally, based on the results of these experiments, it is reasonable to expect that the chances of retrieving undisturbed samples of saturated sand by using the ground freezing technique are very good if the soil is constituted of non-clay minerals and it is sampled at a depth greater than 1.5 m. The limits of the use of the ground freezing technique in soils with plastic fines depends on the amount and type of clay of the fines. These were examined in the second part of the laboratory program as outlined in the next section.

5.3.2 Freezing Test Results and Analysis of Soil Mixtures with Plastic Fines

The same test procedure used in the first part of the study was used to conduct the experiments with plastic fines. Three different fine grained soils were used to prepare the soil mixtures tested during this second part of the laboratory program, so the results are presented as three separate series. The fines used to make up the fines portion of the test specimens came from Devon Silt, Commercial Illite and Commercial Kaolinite. The characteristics of these soils are presented in Tables 05-02a and 05-02b. Their grain size distributions are presented in Figures 05-05, 05-06 and 05-08 respectively. The X-ray diffractograms of these soils can be found in Figures D-04, D-06 and D-10 (Appendix D). The X-ray diffraction curves from which the mineral composition diagrams were derived (Figures 05-10 and 05-11) are presented in Figures D-05, D-07 and D-11.

The presentation of the tests in this part of the laboratory program is, again, not based on the chronological order in which the specimens were tested but on their laboratory similarities. The conditions under which each of the specimens were tested can be found in Table 05-03. All the first sets of experiments of the three series were tested under a total stress of 24 kPa and the second set, if any, under a total stress of 65 kPa. Table 05-04 summarizes the composition of the sand-fines mixtures and Table E-03 summarizes the final steady state condition of the freezing tests. The complete results of each test under the

imposed temperature and stress boundary conditions are presented in Appendix C. The initial skeletal void ratio ($e_{sk,i}$) and final skeletal void ratio ($e_{sk,f}$) of each specimen calculated through equation 4.01 are reported in Tables E-02 and E-03 (Appendix E).

After observing the freezing behavior of the non-plastic fines (Figure C-25) it became evident that, if excess pore pressures were able to develop during the advance of the freezing front and no influx of water was recorded while establishing the steady state condition, the probability of a change in void ratio of the soil would likely not occur. In physical terms, the sample will not exhibit disturbance by having water migrating outwards during the advance of the freezing front provided that consolidation does not occur. In contrast, if water is attracted rather than expelled disturbance of the specimen occurs and the soil is said to exhibit frost susceptibility behavior. With this concept established, the second part of the laboratory program was started to distinguish between a frost susceptible and a non-frost susceptible soil. With the purpose of clearness and effectiveness in illustrating the pore water migration, the outflow of water is represented by the positive values and the intake of water by the negative values.

The first series to be analyzed involves specimens with different amounts of Devon Silt Fines as the fines component of the mixtures. Three specimens containing the fines of the Devon Silt were tested under a stress of 24 kPa. The components of these artificially mixed soils are presented in Table 05-04 under the DS series. The water expulsion and water intake for the DS series specimens are plotted in Figure 05-15. Sample D2DS20 (Figure C-11) attracted water and underwent frost heave while D2DS10 (Figure C-10) initially expelled water and remained constant for the first 50 hours of the test and then began to intake a small amount of water and heaved at the end of the test. Sample D2DS05 (Figure C-09) expelled water throughout the test and did not heave. Therefore, the boundary between frost susceptible and non frost susceptible soils with this type of plastic fines is between 4.9% and 10.3% fines content. The boundary can be expected to be closer to 10.3% based on the behavior of D2DS10 during the freezing experiment. D2DS10 showed a sharp drop in the water expelled (Figure C-10) and porepressure (Figure C-26b) after fifty hours. It is believed that the abrupt change was caused by the release of an air bubble during the process of water expulsion. Even though this was an unexpected radical change, this sudden decrease in pore pressure did not affect the already established steady state freezing conditions of the specimen. The pore pressure variation developed during the three tests using the Devon Silt Fines is shown in Figure C-26. It can be observed that sample D2DS20 (Figure C-26c) definitively developed suction pressures. Although D2DS05 and D2DS10 were in the non-heaving category, the pore pressure behavior of D2DS10 was very erratic (Figure C-26b).

The next test series used the Illite Fines as the fines fraction of the soil mixture. Three tests under a total stress of 24 kPa and two others under 65 kPa were performed during the IL series (Table 05-04). The water outflow and water influx for these specimens are plotted in Figure 05-16. D2IL20 (Figure C-14) was the only test in the first series which heaved. Samples D2IL05 (Figure C-12) and D2IL10 (Figure C-13) did not show any features of frost heave, even though the pore pressures during the D2IL05 test were erratic (Figure C-27a). Parts of the data from D2IL05 and D2IL20 were lost, but this did not affect the interpretation of the freezing test results. Sample D2IL20 behaved in a classic manner for frost heave samples, first expelling water and then after a short period of time attracting water, and undergoing frost heave. The tendency of the pore pressures recorded during the D2IL20 test (Figure C-27c) supports the observed frost heave behavior.

In the second battery of tests of the IL series (Table 05-04) the specimens were tested subjected to a total stress of 65 kPa. Sample D2IL102 (Figure C-15) did not show any signs of heaving whereas sample D2IL202 (Figure C-16) definitively heaved. Figure 05-29 shows how increasing the vertical stress reduces the ability of these specimens to undergo frost heave. The difference in water migration behavior becomes evident by comparing the specimens D2IL10 and D2IL102. The increase in total stress caused D2IL102 to expel approximately 60 % more water than D2IL10 in the first series. D2IL202 is another example of how specimens with this type of fines are affected by the increase in stress. D2IL202, tested under 65 kPa with 17.8% of fines content (Table 05-04) started to expel water after 75 hours, while D2IL20 tested under 24 kPa and with 12.8% of fines content developed a definite pattern of frost heave behavior. This confirms that external pressure strongly increases the water content in frozen soils (section 3.2.2).

The third series of tests used the Kaolinite Fines for the fines portion of the specimens. The water outflow and water influx for these specimens are plotted in Figure 05-17. The composition of these specimens can be found in Table 05-04 under the KL series. The specimens in the first battery of tests, such as D2KL10 (Figure C-18) and D2KL20 (Figure C-19), with a fines fraction greater than 9% attracted large amounts of water immediately after the tests were initiated and consequently heaved. The test D2KL05 (Figure C-17) expelled water during the first stage of the test until it peaked at about 20 hours, to then started to attract water and heave. The recorded rate of frost heave also exhibits a definite increasing trend after this period of time. An almost identical pattern is followed by the specimen D2KL052 (Figure C-20), except that this specimen was tested under a total stress of 65 kPa. The increase in total stress from 24 kPa to 65 kPa does not appear to affect the freezing behavior of samples with this type of fines. Several other tests

in the KL series (Table 05-04) were run with different amounts of fines and overburden stresses, and frost heave occurred during all of these tests. The pore pressures developed during the first battery of the KL series are shown in Figure C-28. The suction pressures are consistent with the behavior shown by the water intake readings (Figure 05-30).

Two other series of tests, those designated as MS and TS (Table 05-03) were run with different purposes. The MS series (Table 05-04) was set forth to establish if the behavior of a soil changes while being subjected to different load stages during the same uniaxial freezing test. Two specimens were tested under these conditions, MSKL20 (Figure C-21) and MSIL10 (Figure C-22). In both tests the change in overburden stress did not result in any significant change in the frost heave behavior and the rate of the water expulsion did not change as the stress was increased. Hence, it appears that once steady state conditions are established the rate of water expulsion will not be affected by an increase in stress, at least in the time frame in which these tests were carried out. Although this conclusion is based on the behavior of only two tests, it is recommended that this test procedure should not be used since no difference could be observed from samples tested in this way compared with samples tested without variation of the total stress. The TS series was set for the purpose of observing the behavior of a tailings sand from a gold mine. This soil was never characterized but it was useful in the sense that it proved that tailings sands are able to be tested by this experimental procedure. The results from two tests performed on this soil are presented in Figure C-23 and Figure C-24. Both of the samples started to intake water and therefore heave under the imposed temperature and stress boundary conditions.

5.4 Characterization of the Test Soils Based on the Specific Surface Area

5.4.1 Re-analysis of the Laboratory Data

Correlations between parameters based on the soil Atterberg limits and either its frost susceptibility or the magnitude of frost heave have proved to be inaccurate (section 3.3.2). Nevertheless, an attempt has been made to explain the observed response to freezing of the specimens tested in the second part of the laboratory program based on the Atterberg limits of the fines fraction and the amount of fines. Skempton (1953) defined Activity as follows;

$$A = PI / (\% \text{ by weight finer than } 2\mu\text{m}) \quad [5.01]$$

where **A** is the parameter called Activity and **PI** is the Plasticity Index of the soil. Skempton (op. cit.) noticed that the higher the Plasticity Index, the more pronounced the colloidal properties of a clay were. This is logical since the colloidal properties are due largely to the finest particles, and in particular to the clay minerals which constitute the majority of the clay sized soils. Hence, this definition is adequate to define the mineralogy of soils composed predominantly of fine grained particles. However, for the soils studied in this research the predominant particle size is that of sand, that is, particles with mean particle diameter larger than 75 μm . Hence, if the Plasticity Index would had been determined for the artificially mixed soils tested herein by strictly following the ASTM-D-3281 specifications, the specimen's Activity would had been close to zero and classified as non-plastic.

Skempton (op. cit.) developed the parameter Activity because it combines the amount of clay sized particles within the soil and the degree of plasticity into one parameter. In an effort to follow the same logic a modified Activity has been defined as the Fines Activity or **A_f**, and is expressed as

$$A_f = PI_{ff} / CS \quad [5.02]$$

where **PI_{ff}** is the Plasticity Index of the fines fraction and **CS** is the amount of clay sized particles within the soil, i.e. the percentage by weight of the particles with mean particle diameter smaller than 2 μm . The Plasticity Index of the fines fraction is a deviation from the specifications detailed in the ASTM-D-3281 since it is determined by performing the numerical difference between the liquid limit of the fines fraction and the plastic limit of the fines fraction, as follows;

$$PI_{ff} = LL_{ff} - PL_{ff} \quad [5.03]$$

The Fines Activity values determined for each specimen tested in the laboratory program are presented in Table 05-04. It is important to note that the Plasticity Index of the fines fraction, **PI_{ff}**, is constant for any particular type of fines, as shown in Table 05-02a. Hence, increasing the amount of clay size soil decreases the Fines Activity, **A_f**, with the result of increasing the frost susceptibility of the soil. Therefore, soils with a large value of **A_f** may not heave because of the small amount of clay mineral present.

The differences in frost heave behavior among the test samples containing different types of fines became evident after observing the results from the second part of the laboratory program (Figures 05-15, 05-16 and 05-17). By making use of the Fines

Activity parameter It can be observed from Table 05-04 that specimens with $A_f < 8$ heaved under a stress of 24 kPa. This value dropped to around 4 when the stress was increased to 65 kPa in the IL series, but still A_f is approximately 8 for the KL series. Hence, the Kaolinite Fines are not as susceptible to diminish their capacity of attracting water as in the case of the Illite Fines when increasing the stress. Nevertheless, this appreciation is based on limited data and more tests are necessary to prove these conclusions. The attempted relationships based on the Atterberg limits of the fines fraction and a parameter dependent on them are illustrated in Figures 05-18 and 05-19. Figure 05-18 presents a plot of A_f against the liquid limit of the fines fraction, LL_{ff} , (Rieke *et al.*, 1983). For the three soils chosen to compose the fines fraction of the specimens the range of LL_{ff} was not very large and varied from 39% to 50%. Figure 05-19 presents a plot of A_f against the Fines Factor, R_f , (Eq. 3.10, section 3.3.2) proposed by Rieke *et al.* (1983). Values of R_f for each specimen are presented in Table 05-04. It appears that specimens with R_f greater than about 25 heaved under an applied stress of 24 kPa. This value increases to about 120 under an applied stress of 65 kPa for the IL series, and as in the previous relationship the Kaolinite Fines, despite of the increase in total stress still heaves with an R_f of 25. Once more, this conclusions are based on limited data and more testing is required.

Although the Atterberg limits have given an indication in the exhibited frost heave behavior of the specimens, it is believed that the use in this study of the specific surface area for characterization purposes will offer advantages over the Atterberg limits, the principle being of accuracy. The inaccuracy of the Atterberg limits is more noticeable if specimens tested in this laboratory program are compared with respect to their exhibited behavior. The specimens D2DS10 (Figure C-10), D2IL10 (Figure C-13) and D2KL10 (Figure C-18) are used for illustration purposes. The Kaolinite Fines, the Devon Silt Fines and the Illite Fines have the nearly the same Plasticity Index (Table 05-02a), the tested specimens had almost the same amount of fines (Table 05-04) and if the hydrometer results would had been used (Figures 05-05, 05-06 and 05-08) to obtain the amount of clay size particles their A_f values would not be so dissimilar. All these samples were tested under the same boundary conditions (Table 05-03, section 5.2.2), but despite of these similarities the frost heave response of the specimens are significantly different. The sample with Devon Silt Fines expelled water and slightly heaved after 120 hours and the one with Illite Fines did not heave while the specimen with Kaolinite Fines started to heave after 10 hours. The only basic difference among them is that the fines fraction of the specimens have different mineralogy; therefore, the Atterberg limits do not have enough capability of showing these features.

The inaccuracy of the Atterberg limits may be attributed in part to the fact that the index tests used to determine the limits are unable to quantify the condition of non-clay mineralogy of soils. The Atterberg limits are determined following the specifications in the ASTM-D-3281; hence, it not only fails to describe the plasticity of sandy soils once the limits are determined in the material with mean particle size smaller than 425 μm , but their determination is subjected to laboratory errors and manipulation. Even more, the Atterberg limits are, as well pointed out by Lambe and Whitman (1968), *set arbitrarily, and thus it is unlikely that the limits per se can be completely interpreted fundamentally*. It could be argued that this condition can easily be corrected if the Atterberg limits are determined for the fines fraction. Such deviations were done by Rieke *et al.* (1983) in order to define the liquid limit, and in this study with the Plasticity Index but these deviations of the specifications do not solve the problem for fine grained soils constituted of non-clay minerals. In contrast, the specific surface area not only quantifies the mineralogy of any type of fines and can be linked quantitatively to the thickness of the adsorbed water layer (section 3.3.3), but also it is independent of the mechanical manipulation of the soil.

Based on the concepts explored in section 3.3.3 a correlation involving the specific surface area has been investigated. The specific surface area may be a more sensitive characteristic of the soil since it can be related quantitatively to the adsorbed water layer or the unfrozen water in a freezing soil. In order to obtain a relationship between the fines and the frost heave response, a more detailed analysis of the clay mineralogy in the fine grained soils was then necessary. A detailed mineralogical analysis was performed on all the fines used in the first and second part of the laboratory program. These results, shown in Table 05-02b and Figures 05-09 to 05-12, illustrate that the fines differ in mineral composition and in the amounts and type of clay mineral present in each soil. The most relevant aspect of the mineralogical analysis of the fines was the distribution and concentration of the clay and non-clay minerals in the soils. If a frost susceptibility parameter is proposed it must consider the amount of clay minerals present in a soil rather than just the clay size fraction of the soil.

The data from Rieke and Vinson (1982), later used by Rieke *et al.* (1983) as shown in Table 03-02, provides an opportunity to explain the importance of considering the amount of clay rather than the amount of clay sized particles (i.e. $< 2\mu\text{m}$). In their research four different soils were used for the fines portions of the soil mixtures. A total of 31 uniaxial freezing tests were performed on mixtures that consisted of 80 to 95% sand with varying amounts of silt, montmorillonite and poorly or well crystallized kaolinite (see Table 03-02 for details). They determined the Segregation Potential (section 3.1.2) of these artificially prepared soil mixtures and, although it was not necessarily determined under

conditions of steady state, it is useful to examine their findings. Three of their tests, catalogued as No. 2, No. 5 and No. 6, were run using only Hanover Silt to constitute the fines fraction. These tests were conducted using 5, 10 and 20% of the Hanover Silt by total sample weight, respectively. If the gradation curve for the Hanover Silt is analyzed, not more than 5% is of clay size. The tests with 10 and 20% fines heaved, and values for Segregation Potential are presented. Only the mixture with 5% of fines did not frost heave. This suggests that at a low amount of clay mineral in the soil, frost heave did not occur. Once the proportion of silt added was increased, the amount of clay mineral added to the soil was sufficient to initiate the process of water inflow to the sample and so its tendency to heave.

The difference in behavior of the KL series with respect to the other series became evident after the mineralogical analysis since the Kaolinite Fines proved to be entirely composed of pure clay minerals (Figure 05-11) with a high specific surface area (Table 05-02b), while the Devon Silt Fines (Figure 05-10) are dominated by non-clay minerals. The different behavior of the Illite mixtures in the IL series became obvious, as well, because of the amount and distribution of the illite in the fines mineral composition. In conclusion, it is reaffirmed (Horne, 1987) that the Atterberg limits are not the most appropriate characteristics of the soils for frost heave analysis and can only be affirmed that the modified Activity parameter decreases as the frost susceptibility increases, due only to the increase in its plasticity. In order to correlate the frost heave behavior to the various basic soil characteristics using a single parameter became clear to the author that the specific surface area (section 2.2.1) should be the quantitative measure that better describes the influence of the various constituent minerals and their relative proportions in the fines contained in the soil.

Because of the results on the mineralogical evaluation, it was determined that the amount of clay mineral to be used in a frost susceptibility criteria should be the clay mineral content of the soil with mean particle diameter smaller than $75\ \mu\text{m}$, rather than that contained below the artificial $2\ \mu\text{m}$ boundary. The $2\ \mu\text{m}$ clay size is just an approximate boundary, and does not significantly aid in the understanding of what influences the frost heave of a soil. This supports the discussion in section 3.3.2, where the amount of clay mineral was considered to be a more important measure than the clay size. It was not clear whether a weighted value for each type of clay mineral or for the whole clay mineral fraction should be associated with the specific surface area of the fines fraction. The second option was adopted since it was impractical to obtain a single value of specific surface area for each clay minerals. Delineating a boundary between the frost heave and the non-heave behavior of soils defined by parameters based on the specific surface area of its

fines became an obvious consideration. In order to achieve this objective, tests using plastic fines and following the same test procedures were reevaluated. Since it is proposed that the specific surface area is fundamental to the correct analysis and interpretation of the frost heave test results, the proposed parameters based on the specific surface area will be discussed in the following sections.

5.4.2 Background in the Surface Area Parameters

Hoshino (1977), discussing the quality of the undisturbed samples recovered by Yoshimi *et al.* (1977), states that the *in situ* density may be disturbed if the proportion of the fines content exceeds a certain limit value. Therefore, it is a matter of determining this limit value in order to define the region of confidence in which the ground freezing technique can be effectively used. The conclusions drawn in section 3.3.3 and supported by the concepts in the section 5.4.1, suggest that this limit value, which is based on the fines content, is rather variable and depends on the type of minerals contained in the fines portion of the soil. This is logical, since the more frost susceptible these minerals are the lower the fines content limit should be. Therefore, the lower becomes the probability of retrieving an undisturbed sample when using the ground freezing technique in a soil with different types of clay minerals.

This idea is not new and in fact has been considered since frost heave first became a concern, nevertheless accuracy in its determination has been a problem. Any new parameter used to define frost heave needs to include both, the physicochemical characteristics of the various constituent minerals and the relative proportions in which these minerals are present in the soil. The first and simplest approach to describe the frost susceptibility of soils was to incorporate the percentage of the clay size particles as the basic parameter. This parameter is still in use in present day frost susceptibility criteria throughout the world, and it is commonly associated with the physicochemical characteristics of the soil through simple tests such as the Atterberg limits. More recently, the Fines Factor parameter R_f (sections 3.3.2 and 5.4.1), first defined by Rieke *et al.* (1983) and later modified by Knutsson *et al.* (1985), was proposed to define the frost susceptibility of soils. Although, like earlier parameters (section 3.3.1), the Fines Factor is also based on the gradation curve and the Atterberg limits. The major break through in this traditional thinking was Home's (1987) Surface Area Factor which included the specific surface area of the soil as part of a parameter which could indicate differences in the water suctions at the frost front. Ideally, parameters used in frost susceptibility criteria must be obtained at low cost since the evaluation often occurs during ongoing construction

activities. In contrast, the ground freezing technique is expensive and requires more accurate assessment than is possible using the conventional frost susceptibility criteria.

Considering this background, it is reasonable to assume that the specific surface area could be a more sensitive parameter to explain the relationship between the basic soil characteristics and the response of soil to freezing (section 5.4.1). The available published data on frost heave (Table 03-02) only provides values of the specific surface area for the complete soil sample, and in rare cases, the specific surface area of the fraction under the 75 μm particle size is provided. The classic approach towards classification of soils with respect to its grain size and specific surface area does not properly quantify or qualify the clay mineralogy of the soil. Traditionally classification is represented by the percentage of all the soil with mean particle diameter smaller than the 2 μm particle size. Indeed, the specific surface area of this fraction of the soil has seldom been reported in any previous research work. This lack of information on the type of clay minerals present in the soil prevents a proper appreciation of the role of the clay and non-clay minerals in the soil fines fraction.

Based on the hypothesis that only the minerals contained in the fines fraction of a soil are able to develop suction, and considering that the frost heave behavior is dependent on the mineralogical differences in the fines fraction, one may conclude that only the fines fraction should be considered for frost heave analysis. Hence, it is reasonable to expect that the specific surface area is the quantitative measure that better describes the characteristics of the soil fines fraction, which in turn controls the frost heave process. In order to better understand the relevance that the clay mineral contained within the soil has in the frost heave behavior, it is proposed that two different values for the specific surface area should always be determined. One value should be obtained for the material with mean particle size smaller than the 2 μm , which is a more representative value of the clay minerals contained within the soil, and another for the fines portion of the soil, that is, the soil fraction with mean particle diameter smaller than 75 μm . This information will provide a better indication of the role played by the clay mineral fraction and its influence in the parent soil.

The first proposed parameter is based on results from measurements on the soil particles smaller than 75 μm and is solely related to this fraction of the soil. This parameter is the Fines Mineralogy Ratio or Z_v and is defined as

$$Z_v = \frac{CM_f}{I_{SSA}} \quad [5.04]$$

where CM_f is the clay mineral content as a percentage by weight of the fines fraction, that is, the soil under the 75 μm particle size. I_{SSA} is the Intensity of the Surface Area for the fines fraction, and is defined as the ratio of the two specific surface area values determined from the fines fraction of the soil. I_{SSA} is defined as:

$$I_{SSA} = \frac{S_c}{S_f} \quad [5.05]$$

where S_c is the specific surface area for the fraction of the soil with mean particle diameter smaller than 2 μm size and S_f is the specific surface area for the fraction of soil with mean particle diameter smaller than the 75 μm size. The reasons and implications of why these parameters are proposed are explored in section 5.4.3. The Fines Mineralogy Ratio and Intensity of the Surface Area of the soils used to compose the fines portion of the specimens tested in the laboratory program are given in Table 05-02b

The Fines Mineralogy Ratio is based on only one fraction of the soil, but the composition of the whole soil, especially in the case of the sandy soils, still has to be considered. Therefore, it is important to define another parameter, that considers the increasing influence of the fines as the clay content becomes predominant within the soil. For this purpose a parameter is proposed to be used in conjunction with the Fines Mineralogy Ratio. This parameter is also based on the specific surface area and is identified as the Surface Area Index or Ω_z . The Surface Area Index is defined as

$$\Omega_z = \sqrt{CM \times S_f} \quad [5.06]$$

where CM is the clay content of the soil expressed as a percentage by weight of the soil and S_f is the specific surface area of the fraction of soil with mean particle diameter smaller than 75 μm . The detailed derivation of this parameter is explored in section 5.4.4. The Surface Area Indexes of the specimens which participated of the laboratory program are given in Table 05-04.

5.4.3 The Fines Mineralogy Ratio

In order to define the Fines Mineralogy Ratio or the Z_v parameter it is important to clarify the term *clay*. When used as a particle size term, it refers to all constituents of a soil smaller than the 2 μm particle size. As a mineral term, it refers to specific minerals termed the *clay minerals*, which are primarily hydrous aluminum silicates, with magnesium or iron occupying all or part of the aluminum positions in these minerals, and with alkalis,

such as sodium or potassium or alkaline earth, such as calcium or magnesium, also present as essential constituents in some of them (Grim, 1968). Not all clay mineral particles are finer than the $2\mu\text{m}$ particle size, nor are all non-clay minerals coarser than $2\mu\text{m}$. Thus, the amounts of clay size and clay mineral in any soil are not necessarily the same. To avoid confusion, it is best to use *clay size* when referring to compositions in terms of particle size and *clay mineral* or simply *clay content* when speaking of the mineral composition (Mitchell, 1976).

The fines fraction is, in fact, a size fraction of soil considered to be under the $75\mu\text{m}$ particle size incorporating non-clay minerals, such as quartz, and colloidal clay minerals. The amount of each type of soil forming the material within this soil size range does not indicate neither the type or the amount of the clay or non-clay minerals present in it. Linnel and Kaplar (1959) considered the clay mineral content to be the main influence on frost susceptibility. Taking this into consideration, if a given soil is frost susceptible, its behavior is dependent on the proportion of clay minerals of various sizes present in this soil fraction. Thus, it is not the amount of material smaller than $75\mu\text{m}$ or the amount of material smaller than $2\mu\text{m}$, but the amount of clay mineral present in the soil fraction smaller than $75\mu\text{m}$ that is important as was suggested by the test results (section 5.3.2).

Using this logic, it can be concluded that the lower the clay mineral content in a soil, the lower the specific surface area of the fines portion of the soil. On the other hand, as discussed previously, the specific surface area which better describes the contribution of the clay minerals contained in the soil is the value which corresponds to the soil particles smaller than the $2\mu\text{m}$ size. As pointed out before, quartz mineral can be present in the clay size fraction, that is, the fraction of the soil with mean particle diameter smaller than $2\mu\text{m}$. Nevertheless, its quantity is normally so low that it does not influence the characteristics of the clay minerals when expressed in terms of their specific surface area. The ratio between the specific surface areas of these two fractions of the fines, the Intensity of the Surface Area or ISSA as defined in equation 5.05, quantifies both, the mineralogical uniformity of the fines and the influence of the clay mineral portion upon the fines fraction of soils containing clay minerals. In Table 05-02b this dimensionless parameter is determined for the fine grained soils used in the laboratory program. The more ISSA tends to unity the more uniform or the more similar are the minerals that compose the fines fraction of the soils. The Kaolinite Fines (Figure 05-11) and the Bentonite Fines (Figure 05-12) have different clay minerals but as can be observed in Table 05-02b, their values of ISSA are close to 1.0 and represent, as expected, a more uniform material. In contrast, the larger this ratio the lower the intensity in which the clay minerals exert their influence upon the fines fraction as illustrated for in the Duncan 1 Fines (Figure 05-09).

Two totally different materials such as a clay and a non-plastic soil can have the same ISSA without implying that both are composed of the same type of minerals. This position is better exemplified by the values yielded from the Athabasca Clay Fines (Figure 05-11) and the Silica Flume Fines (Figure 05-09). Both of these fines are referred in Table 05-02b and their specific surface areas are given; nevertheless, both of them possess virtually the same ISSA. The Silica Flume Fines have an S_c equal to fifteen while the Athabasca Clay possess a much higher S_c more than one order of magnitude larger. Hence, the difference between these two soils resides not in the magnitude of the Intensity of the Surface Area per se, but in the magnitude of the specific surface areas used to determine it. Due to the origin of the specific surface areas, the Intensity of the Surface Area is a value solely associated to the fines fraction of soils.

The Fines Mineralogy Ratio or Z_v , defined in equation 5.04, can yield the same result for two different soils depending on the type and amount of clay minerals present in their fines fraction. This fact is extremely beneficial when frost heave behavior of soils is being evaluated. For example, a soil with a small quantity of a very active clay mineral can yield the same Z_v value as a soil which has a larger quantity of less active clay mineral. The Kaolinite Fines (Figure 05-11) and the Bentonite Fines (Figure 05-12) are exemplified for demonstration purposes. The structure of the clay minerals composing the major part of these fines are significantly different (Mitchell, 1976), and so are their properties. Indeed, the difference among their specific surface areas (Table 05-02b) is so large that they could not be classified as the same type of soil. Nevertheless, when the Fines Mineralogy Ratio is determined for these fine grained soils (Table 05-02b), they yield approximately the same Z_v values.

From a review of previous studies, two groups have conducted work on frost heave and included the variation of clay minerals. The most recent study is the one by Rieke *et al.* in 1983 who concluded that the mineralogy of the sand-silt-clay mixtures affected the Segregation Potential (section 3.2.3). Their findings confirmed the observations of Lambe *et al.* (1958) (Figure 03-06), that kaolinite mixtures have a higher frost susceptibility than montmorillonite mixtures. The conclusions which Rieke *et al.* (op. cit.) formulated, with respect to the differences in the ability of clays to trigger frost heave, are similar to those published 14 years earlier by Lambe *et al.* (1969). Lambe *et al.* (op. cit) defined the order of the ability of clay minerals to produce frost heave, in an increasing order: muscovite, calcite, magnesite, iron montmorillonite, illite, kaolinite, nontronite and attapulgite. This order was defined based on results of frost heave tests carried out with soils composed of almost pure clay minerals.

These findings have little practical use; since, in nature, the composition and distribution of the soil minerals differs from one soil to the other and, clay and non-clay minerals in the fines fraction of soils are generally randomly combined. The Fines Mineralogy Ratio parameter can be used for all of the possible combinations of clay and non-clay minerals contained within the fines fraction since this parameter depends on the specific surface area, which in turn is a representative value for all the minerals in the fines fraction of the soil. The Athabasca Clay Fines (Figure 05-11) serves as an excellent example of how representative the specific surface area (Table 05-02b) can be, since in this fine grained soil several clay and non-clay minerals exist. In summary, the Fines Mineralogy Ratio defines the potential activity of the minerals encountered in the fines fraction of a given soil and, its tendency is to increase as the soils becomes more plastic (Table 05-02b). More data has to be collected on the specific surface area of natural soils in order to correctly evaluate the validity of these parameters.

5.4.4 The Surface Area Index

The Surface Area Index as proposed in equation 5.06 is easy to understand since it is based on the same qualitative approach adopted by Professor Skempton when he introduced in 1953 his paper: "The colloidal activity of clays". He defined a parameter called Activity (Eq. 5.01, section 5.4.1), which is based on the Plasticity Index of the soil and the percentage of the clay sized particles (i.e., $< 2\mu\text{m}$). Most of the studies considering the influence of the fines content upon the frost susceptibility of soils are based on the Plasticity Index, which in turn is obtained from the tests carried out on the soil which passes through the No. 40 sieve, that is, the soil fraction with mean particle diameter smaller than $425\mu\text{m}$ (ASTM-D-3281). Furthermore, these studies do not differentiate between the $75\mu\text{m}$ particle size and the $2\mu\text{m}$ particle size. In contrast, the line of thinking which is being followed in this study considers that the plasticity of soils is due solely to the soil particles smaller than $75\mu\text{m}$, that is, the fines fraction. The Surface Area Index, Ω_z (Eq. 5-04, section 5.4.2), and Activity incorporate both *the characteristics of the various constituent minerals and the relative proportions in which these minerals are present in the soil* (Skempton, 1953).

Skempton (op. cit.) concluded that the determination of the characteristics of the soil by means other than the Atterberg limits was a lengthy and a difficult process. He proposed the Plasticity Index to correlate with the behavior of soils, particularly that of more plastic soils. Finally, he suggested that the Atterberg limits were the best quantitative measures to combine the effects of all the basic characteristics of a clay. Today, techniques

such as the X-ray diffraction are no longer time consuming and difficult. Perhaps excessive importance has been attributed to the Atterberg limits while soil characterization could better be determined by other more advanced techniques. X-ray diffraction of the soil can characterize the type and amount of the minerals contained in the fines, and the specific surface area can be determined by methods such as the Ethyl Glycol Method. Skempton's original reason for using the Plasticity Index to characterize the clay is no longer justified since more detailed quantitative methods are now available.

The relationship between the Atterberg limits and the specific surface area can be explained as follows. The Atterberg limits are related to the amount of water attracted to the surfaces of the soil particles. The amount of attracted water will be largely influenced by the amount and type of clay mineral that is present in the soil. The specific surface area is a more sensitive measure of clay mineralogy than the Plasticity Index because of the great increase in surface area per mass which occurs with decreasing particle size and because the specific surface area is not determined using procedures which are sensitive to mechanical manipulation of the soil as in the case of the Atterberg limits tests (section 5.4.2). Therefore, the specific surface area allows for a better description of the mineralogical influence of the colloids than does the Plasticity Index.

The Surface Area Index is, therefore, an indication of the influence which the colloidal particles contained in the fines fraction have on the overall behavior of the soil. The properties of the clay minerals contained in the fines fraction are represented by the specific surface area of this portion of the soil (S_f) and the magnitude of their presence is represented by the percentage by weight of the clay minerals in the soil (CM). The square root of the product of both parameters is used as a mathematical mechanism to compress the range in values for the given soil. The reason to use the square root in this parameter will become clear when discussed in Chapter VI. By making use of the square root, the dimension of the Surface Area Index becomes $LM^{-1/2}$ or $m/g^{0.5}$ in SI units. The author considered relating the specific surface area of the fines with the clay content in different ways, but found this combination to be more suitable. It might be argued that this appreciation is too simplistic but it was considered that the Surface Area Index must represent the increasing influence of the the fines fraction as this fraction becomes predominant in a soil.

Let us consider for example the Surface Area Index of a fine grained soil with a given specific surface area. Suppose that the particles that compose this fine grained soil possess a mean diameter smaller than $75 \mu m$ size and it is totally composed by a clay mineral; hence the CM_f is equal to its CM , which is 100% and the Surface Area Index will quantify the maximum possible mineral influence to which this soil can be subjected. If

sand is added to the fines that once constituted the whole soil, the fines now becomes just a fraction of it. The **CM** of the soil can vary from 0.1% to 99.9%, but the **CM_f** will continue being 100%. Therefore, the **S_f** remains constant since the fines contain the same type of clay mineral and is uniquely related to the fines fraction. Hence, the behavior of these infinite number of cases could be quantified by the Surface Area Index since the specific surface area of the fines have remained constant for all of the possible alternatives.

Although the Activity parameter defined by Skempton in 1953 and the Surface Area Index parameter proposed herein were derived for different purposes and from different sources, they describe in essence the same phenomenon. Skempton considered that if a number of different samples are taken from a particular clay stratum, the Activity of these samples will be approximately the same. This may be the case as well for the Surface Area Index, but more data in natural soils must be collected to verify this statement. In this section a parallelism between the Activity and the Surface Area Index has been described, and in both parameters the Plasticity Index and the specific surface area of the fines fraction remain constant as long as the type of fines do not change. Qualitatively, the percentage of the clay mineral fraction of the soil is as well parallel to his definition of clay fraction, that is, the soil with mean particle diameter smaller than 2 μm . In conclusion, the magnitude of Activity and the Surface Area Index parameters is certainly different, not because of the sources but because of the directions that both studies followed, one directed to the study of clays and the other to the study of sandy soils.

5.5 Laboratory Results Analysis Based on the Surface Area Parameters

For clarification purposes, the term colloid is used to describe a particle whose behavior is controlled by the surface-derived forces rather than the mass-derived forces. A clay particle is a colloid because of its small size and irregular shape. The smaller a particle size the larger its specific surface area. The size range of colloids has been more or less arbitrarily set as from 1 nm to 1 μm , while atoms and molecules have diameters less than 1nm. Most particles larger than approximately 1 μm are predominantly influenced by forces of mass. A specific surface area of 25 m^2/g has been suggested as the lower limit of the range of colloidal particles (Lambe and Whitman, 1968), that is, the higher possible limit for a non-clay mineral. Therefore, this value is used to model the worst condition for a material at the boundary of the colloidal range. This hypothetical sample is composed entirely of a clay mineral (i.e. **CM** = 100%) with a particle size at the limit of colloid size (i.e. specific surface area of 25 m^2/g). Hence by using equation 5.03, the Surface Area

Index for this soil is $\Omega_z = 50 \text{ m/g}^{0.5}$. This value is assumed to be the boundary between frost heave and non-frost heave regions for the non-plastic soils.

With the proposed parameters (sections 5.4.2 and 5.4.3) a link between the soil characteristics and its frost heave behavior can be established in quantitative terms. The Fines Mineralogy Ratio of the Kaolinite Fines (Table 05-02b) is in the same range with the value presented for the Bentonite Fines. The Kaolinite presents a high specific surface area, unusual to this type of clay mineral, but is due to the large amount of amorphous material in its structure (see Mitchell, 1976: 45 for normal values); hence, it behaves like a very active plastic soil. Based on the results from the frost heave tests in the KL series (Figure 05-30), and since the value of the Fines Mineralogy Ratio of this soil is so similar to the Z_v of the Bentonite (Table 05-02b), this value is established as the limit for any plastic soil that undergoes frost heave. Hence, it is assumed that a plastic soil with $Z_v \cong 70$ will undergo a frost heave behavior even if the soil possess a small quantity (say 0.5%) of plastic fines.

For the soils in between these two points, that is, the non-plastic ($Z_v = 0.1$ and $\Omega_z = 50$) and the highly plastic soils ($Z_v = 70$ and $\Omega_z = 0$), the whole range of natural soils exist. Even though scarce amount of data is available, the boundaries established by the Devon Silt and the Illite series (section 5.3.2) will be helpful for the purpose of establishing the variance in the borderline between frost susceptible and non-frost susceptible regions. In the DS series the D2DS10 test (Figure C-10, Table 05-04) is considered to represent the response at or near the boundary. If the values for the Surface Area Index of the DS series in Table 05-04 are analyzed, the boundary between a frost heaving and non-heaving sample must be near $\Omega_z = 15$. Based on the results of the specimens with Illite Fines composing their fines fractions (Table 05-04) the established boundary for the first battery of the IL series is around $\Omega_z = 13$. Thus, the difference between the Devon Silt and the Illite fines is small in terms of their boundaries with respect to frost susceptibility.

The Fines Mineralogy Ratio of the specimens corresponds to the Fines Mineralogy Ratio of the type of fines which composed its fines portion in each series, that is, the value of Z_v given in Table 05-02b. The Fines Mineralogy Ratio is a parameter corresponding solely to the fines fraction; hence, the properties of the fines defined by this ratio will not be affected by the amount of sand added to the soil. This is very convenient since a relationship between the Fines Mineralogy Ratio and the Surface Area Index could be determined if sufficient amount of data is collected from natural soils. Although the Fines Mineralogy Ratio quantifies the activity of the fines fraction, it must be used in conjunction with the Surface Area Index in order to determine whether a given soil will or will not present frost heave behavior. By characterizing the fines and the soil with the surface area

parameters proposed in section 5.4.2 it is possible to define a boundary between the samples which underwent frost heave and those that did not heave. Although the established boundary between frost heave and non-heave behavior is represented for practical purposes in Figure 05-33 by a straight line, this may not be the case and more data is necessary to verify this trend.

In summary, the boundary between the frost heave and non-heave regions is extended and fixed at $\Omega z = 50$ for $Z_v = 0.1$, and at $\Omega z = 0$ for $Z_v = 70$. There is an area in this plot, between $Z_v = 0.2$ and $Z_v = 2$, that has not been properly confirmed by laboratory test data. Nevertheless, it is believed that this region corresponds to soils with low amounts of low active clay minerals. A region which must correspond to the behavior of silts is assumed to lie between $Z_v = 2$ and $Z_v = 15$. Since the values for Z_v are plotted using a logarithmic scale, the variability of the values occur in a more rapid manner, hence the region for most clays is assumed to begin when the Fines Mineralogy Ratio surpass the value of fifteen. These boundaries are subjected to review since more data must be compiled to certificate the validity of these regions.

In conclusion, a boundary has been established between areas of frost susceptible soil and non-frost susceptible soil using the data in the laboratory program and a criteria based on the amount of clay mineral present in the soil and the specific surface areas of different clay mineral sizes in the fines portion of the soil. Early in section 5.4.1 it was stated that the more frost susceptible the clay minerals are the lower the fines content limit should be; hence, the smaller the chances of retrieving an undisturbed sample when using the ground freezing technique in a soil with different types of clay minerals. By using the Surface Area Index it is possible to predict the development of frost heave under a constant temperature gradient since the behavior of the soil is dependent on the behavior of the fines fraction, which in turn is dependent on the specific surface area. The proposed criteria leaves enormous space for improvement and development.

Figure 05-01.- Grain Size Distribution of
Duncan 0 Sand

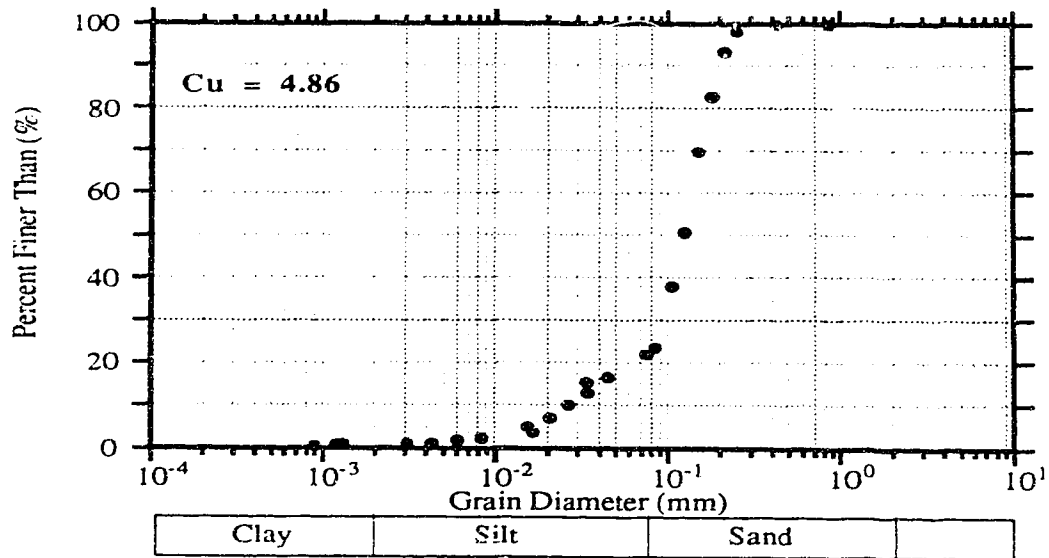


Figure 05-02.- Grain Size Distribution of
Duncan 2 Sand

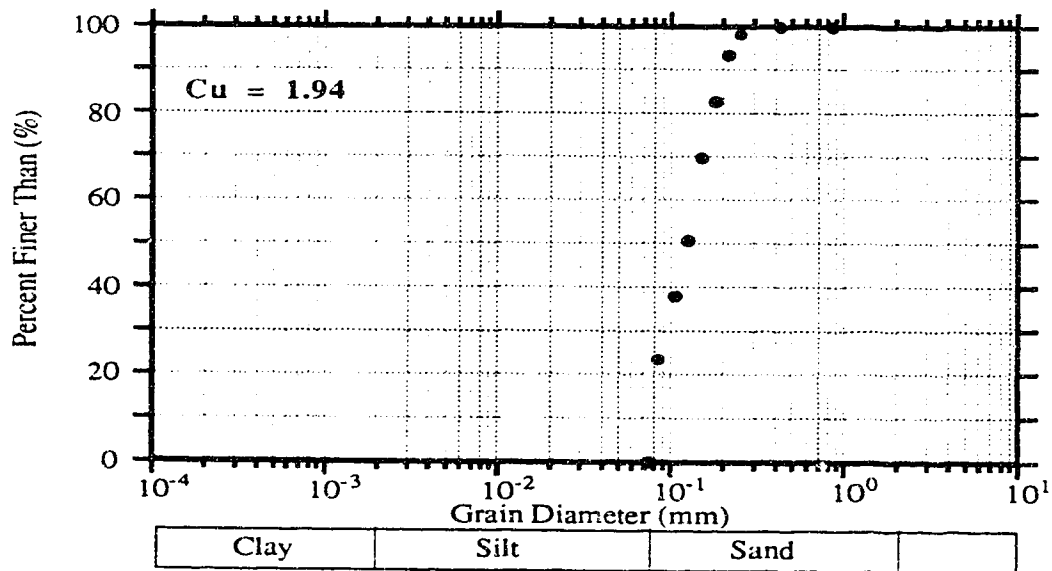


Figure 05.03.- Grain Size Distribution of
Duncan 1 Fines

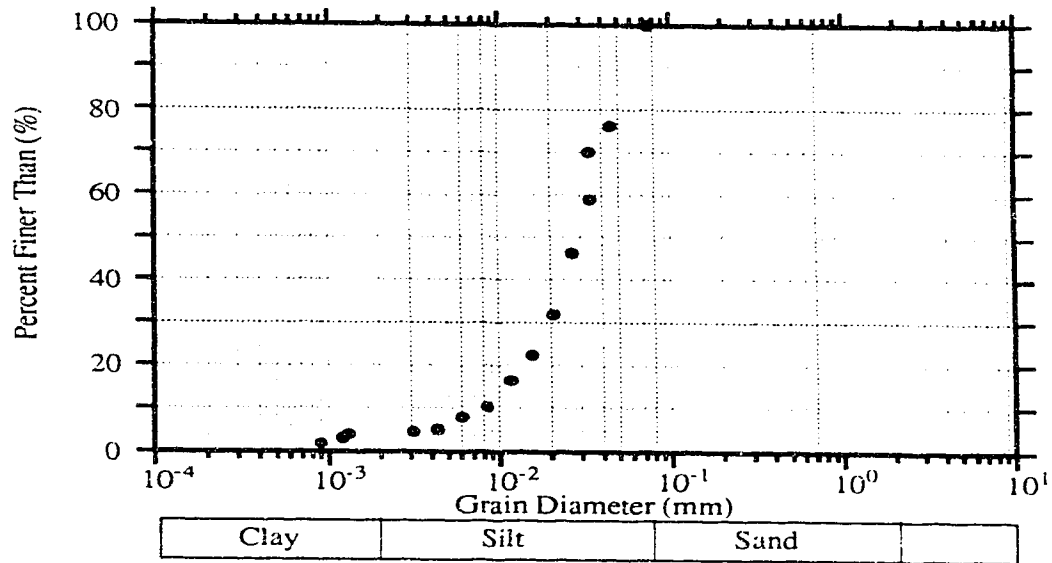


Figure 05-04.- Grain Size Distribution of
Silica Flume Fines

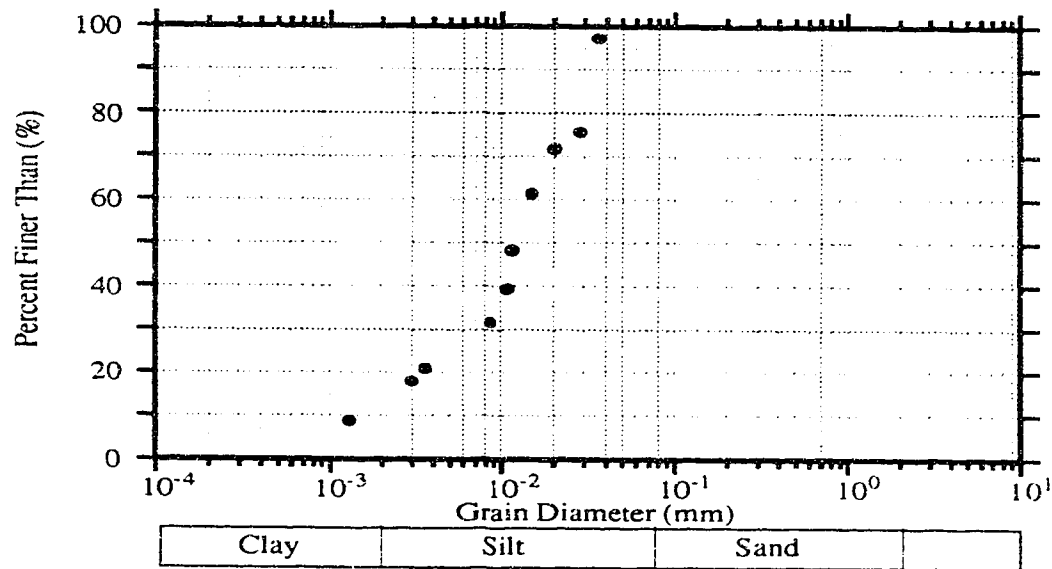


Figure 05-05.- Grain Size Distribution of
Devon Silt Fines

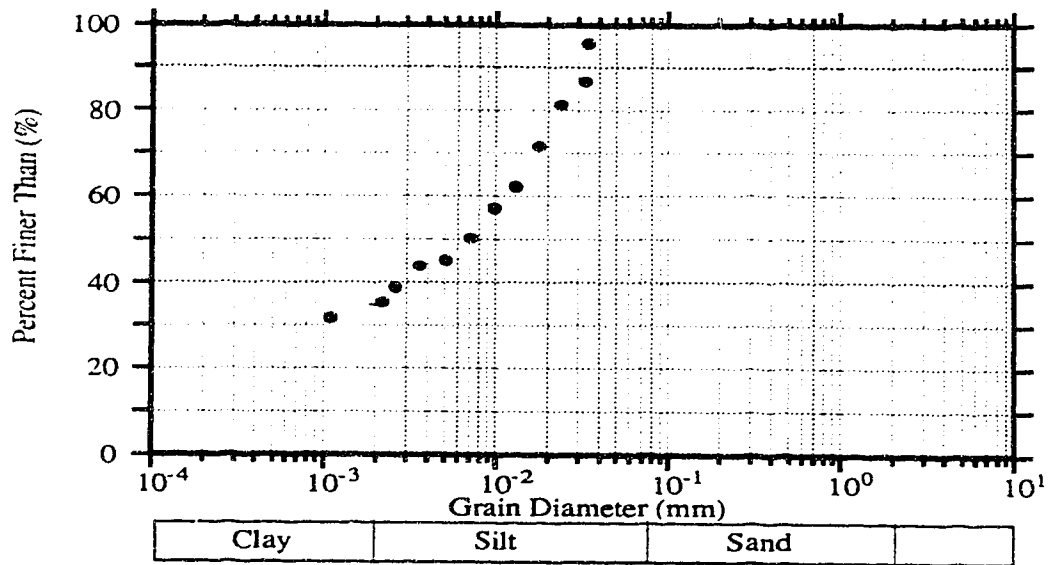


Figure 05-06.- Grain Size Distribution of
Illite Fines

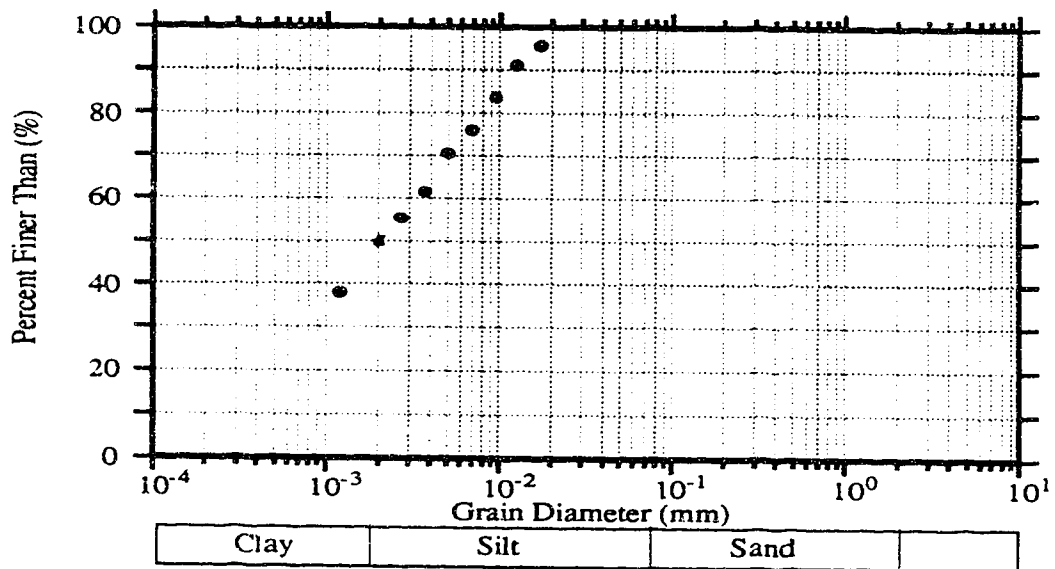


Figure 05-07.- Grain Size Distribution of
Athabasca Clay Fines

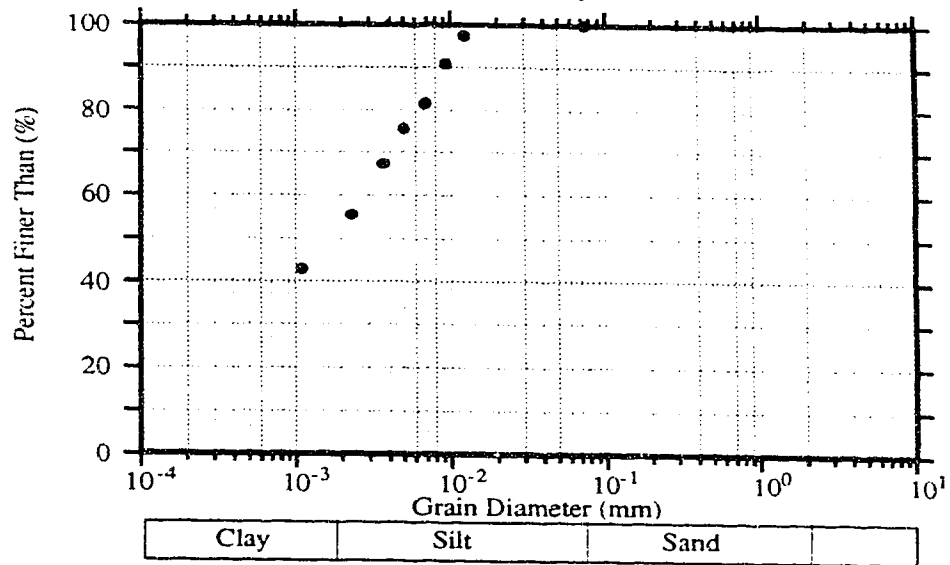


Figure 05-08.- Grain Size Distribution of
Kaolinite Fines

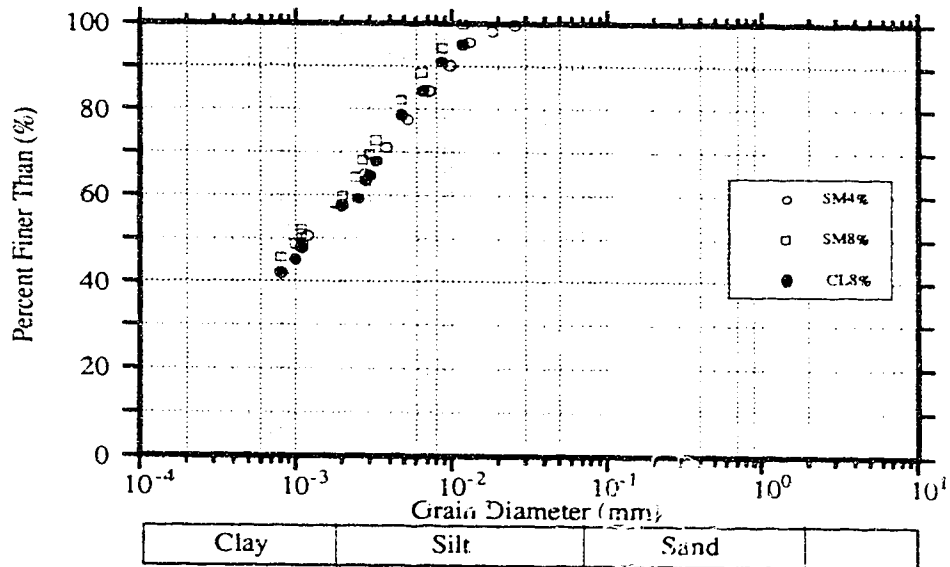


Table 05-01 Sands Characterization

Sand	Unit Weight Dry max (g/cm ³)	Unit Weight Dry min (g/cm ³)	Void Ratio max	Void Ratio min	Gs
Duncan 0	1.64	1.12	1.12	0.65	2.74
Duncan 2	1.56	1.31	1.15	0.79	2.82

Fines Characterization

Table 05-02a Atterberg Limits, Specific Gravity and Activity

Identification		Atterberg Limits			Gs	Clay Size (%)	A
Name	Abbreviation	PLlf (%)	LLlf (%)	PIlf (%)			
Duncan 1	D1	Non Plastic		0.0	2.85	1.1	0.0
Silica Flume	CS	Non Plastic		0.0	2.65	10.5	0.0
Devon Silt	DS	21.0	39.0	18.0	3.00	22.6	0.8
Illite	IL	31.9	41.3	9.4	2.75	16.0	0.6
Athabasca Clay	AC	21.3	41.8	20.5	2.68	40.9	0.5
Kaolinite	KL	32.0	50.0	18.0	2.60	56.5	0.3
Bentonite	BT	36.5	609.5	572.9		83.2	6.9

Table 05-02b Clay Mineralogy, Surface Area Characterization and Specific Surface Area Parameters

Identification		% Clay Mineral			Specific Surface Area (m ² /g)		Intensity I(SSA)	Z _v	Ω _z (m ² /g0.5)	ξ (g0.5/m)
Name	Abbreviation	CMc (<2 μm)	CMf (<75 μm)	NCMF (<75 μm)	Sf (<75 μm)	Sc (<2 μm)				
Duncan 1	D1	1.1	1.1	98.9	9	152	16.9	0.1	3.1	
Silica Flume	CS	0.0	0.0	100.0	7	15	2.1	0.0	0.0	
Devon Silt	DS	22.2	22.2	77.8	93	485	5.2	4.3	45.4	0.65
Illite	IL	16.0	24.4	75.6	67	164	2.4	10.0	40.4	0.79
Athabasca Clay	AC	37.2	45.5	54.5	12.5	275	2.2	20.7	75.4	0.58
Kaolinite	KL	56.5	100.0	0.0	64	94	1.5	65.1	80.0	0.88
Bentonite	BT	83.2	84.9	15.1	65.5	805	1.2	68.9	235.5	0.97

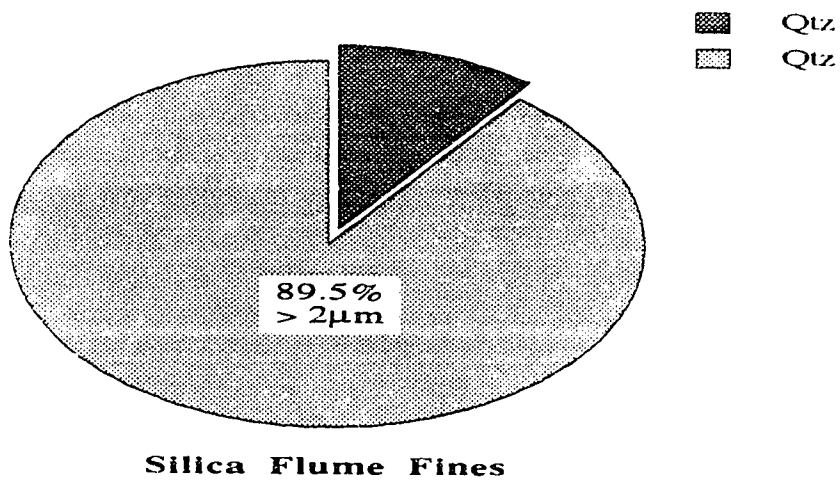
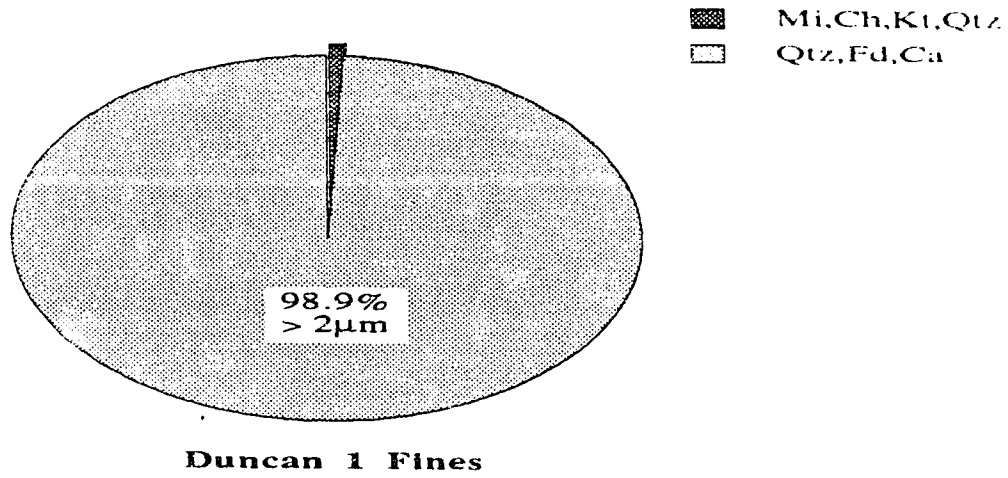


Figure 05-09.- Mineralogy of the Duncan 1 Fines and Silica Flume Fines by Percentage

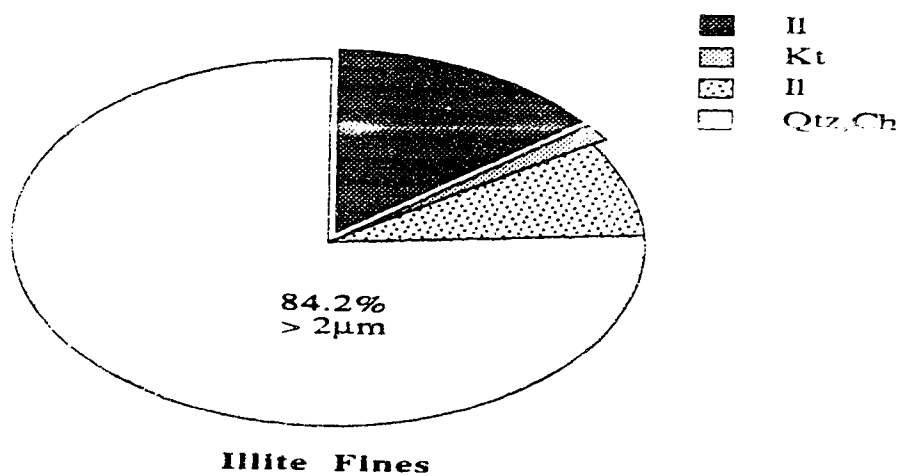
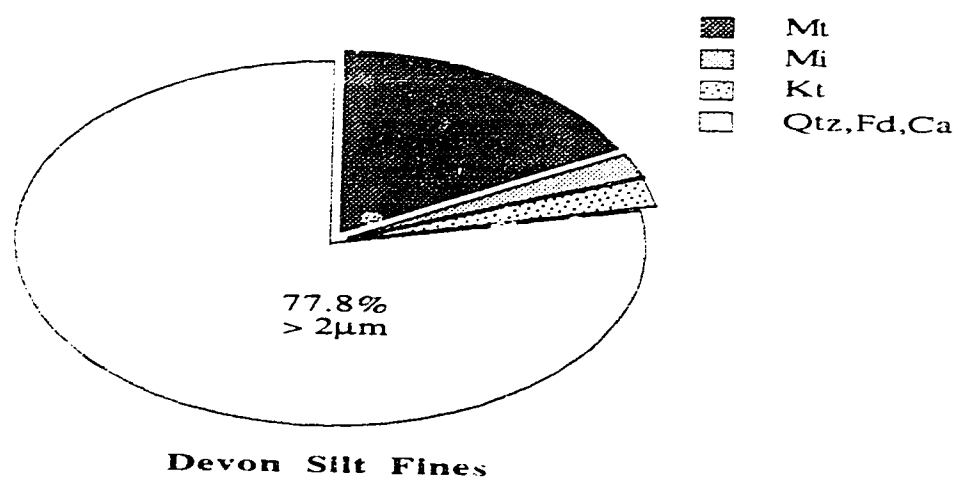


Figure 05-10.- Mineralogy of the Devon Silt Fines and Illite Fines by Percentage

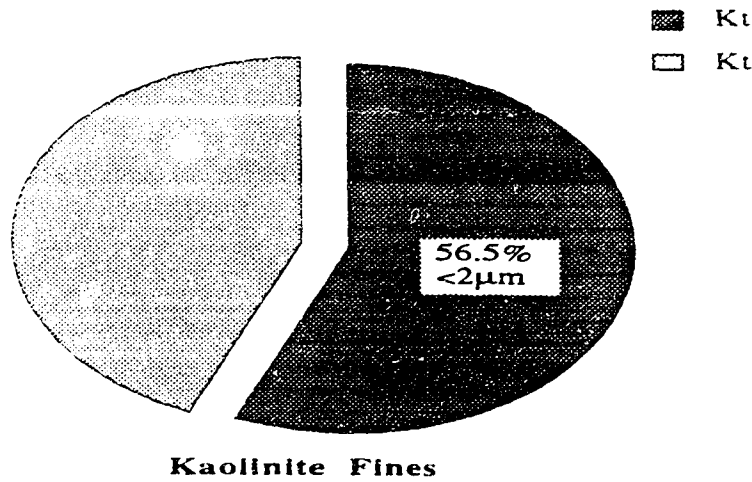
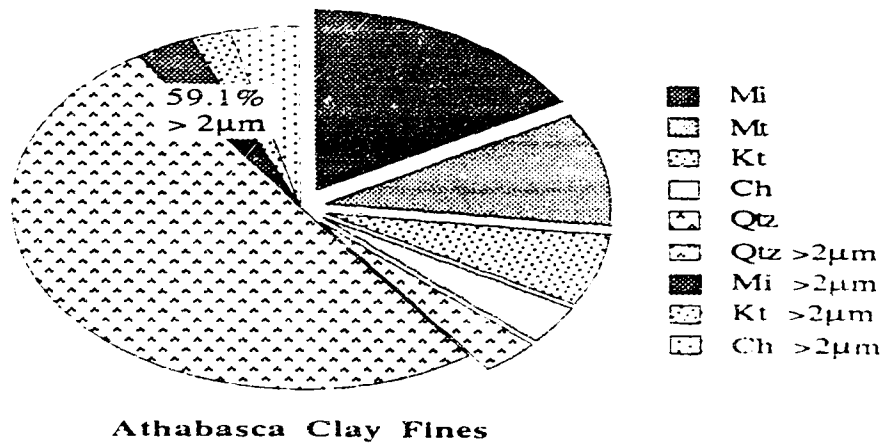


Figure 05-11.- Mineralogy of the Athabasca Clay Fines and Kaolinite Fines by Percentage

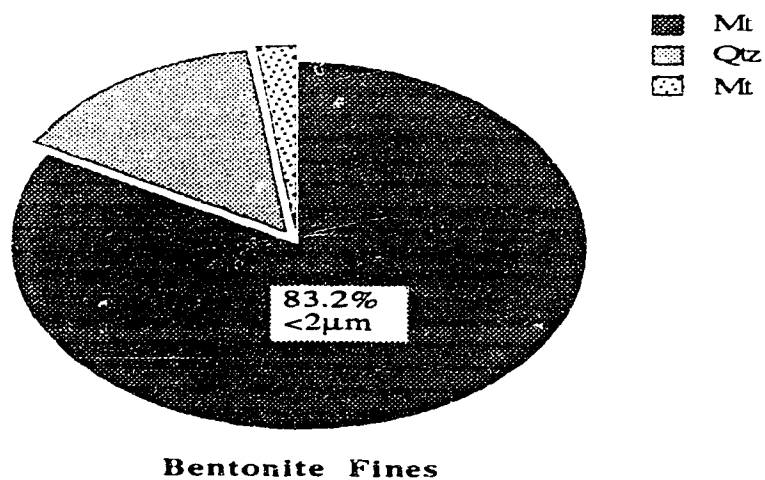


Figure 05-12.- Mineralogy of the Bentonite Fines by Percentage

Table 05-03 Table of Uniaxial Freezing Tests Performed During the Laboratory Program

UFT No	Series	Surcharge kPa	Test	Total	Heave	Void Ratio	Final Water If/ (ml)	Time (h)	Delta T (C)	Performance
01 - 05	DS	24		4	YES	Not Recorded	Not Recorded	25	10	Calibration
06 - 09	SI	24		5	NO	Not Recorded	Not Recorded	25	4 - 9	Calibration
10 - 13	SI	24		4	NO	Not Recorded	12 - 19	25	3 - 4	Calibration
14	D0	24	D001 - D004	4	NO	Not Recorded	Not Recorded	25	Problems	Incorrect
15	D0	24	D005	1	NO	Recorded	E: 16.6	45	4	Correct
16	CS	24	D2CS13	1	NO	Recorded	E: 6.8	45	12	Incorrect
17	D2	24	D201	1	NO	Recorded	E: 9.7	45	14	Incorrect
18	D2	24	D202	1	NO	Recorded	E: 25.0	45	4	Correct
19	CS	24	D2CS100	1	Not Analyzed	Not Recorded	Not Reliable	Not Analyzed	Not Analyzed	Incorrect
20	CS	24	D2CS20	1	NO	Recorded	E: 19.6	50	4	Correct
21	CS	24	D2CS30	1	NO	Recorded	E: 16.1	50	4	Correct
22	DS	24	D2DS01	1	YES	Not Recorded	Not Recorded	50	4	Correct
23	D0	24	L701D0	1	NO	Recorded	E: 23.0	200	4	Correct
24	TS	24	TS0101	1	YES	Recorded	E/I: 13.1	100	4	Correct
25	TS	24	TS0102	1	YES	Recorded	E/I: 6.3	140	4	Correct
26	D0	24	L702D0	1	NO	Recorded	E: 20.1	100	4	Correct
27	D0	24	D006	1	NO	Recorded	E: 17.6	100	4	Correct
28	KI	24	D2KL20	1	YES	Recorded	E: 159.9	100	4	Correct
29	KI	24	D2KL05	1	YES	Recorded	E: 14.7	90	4	Correct
30	L1	24	L703KL	1	Not Analyzed	Recorded	10.8	Not Analyzed	Not Analyzed	Incorrect
31	KI	24	D2KL10	1	YES	Recorded	E: 154.2	70	4	Correct
32	L1	24	L704KL	1	YES	Recorded	E: 127.0	360	4	Data Lost
33	DS	24	D2DS05	1	NO	Recorded	E: 8.9	90	4	Correct
34	DS	24	D2DS10	1	NO	Recorded	E: 2.4	160	4	Correct
35	MS	MS	MSKL20	1	YES	Recorded	E: 150.4	160	4	Correct
36	DS	24	D2DS20	1	YES	Recorded	E: 127.4	100	4	Correct
37	KI	65	D2KL05	1	Not Analyzed	Recorded	E: 199.0	Not Analyzed	4	Incorrect
38	II	24	D2KL05	1	YES	Recorded	E: 110.2	05	4	Correct
39	D1	24	D2KL05	1	NO	Recorded	E: 19.6	60	4	Correct
40	II	24	D2KL05	1	NO	Recorded	E/I: 18.7	135	4	Correct
41	MS	MS	MSKL05	1	NO	Recorded	E: 13.3	240	4	Correct
42	II	24	D2KL05	1	NO	Recorded	E: 8.9	140	4	Correct
43	II	65	D2KL05	1	NO	Recorded	E: 28.4	100	4	Correct
44	KI	65	D2KL05	1	YES	Recorded	E: 5.9	120	4	Correct
		65		1	YES	Recorded	E/I: 0.6	120	4	Correct

Table 05-04 Summary of the Soil Constituency of the Samples Tested by UFT

Series	Battery	Test	% Soil Fraction by Weight				AF Pliff/CS	Rf (%)	% Clay Mineral by Weight		Ω_L (mg/0.5)
			Clay Size <2 μ m	Silt (>2&<75 μ m)	Sand (>75 μ m)	Fines Fraction <75 μ m			NCM (%)	CM (%)	
D0		D005	0.2	21.6	78.2	21.8	0.0		21.6	0.2	1.47
D0		D006	0.2	21.6	78.2	21.8	0.0		21.6	0.2	1.47
D0		L701D0	0.2	21.6	78.2	21.8	0.0		21.6	0.2	1.47
D0		L702D0	0.2	21.6	78.2	21.8	0.0		21.6	0.2	1.47
D1		D1100	1.1	98.9	0.0	100.0	0.0		98.9	1.1	3.15
D2		D202	0.0	0.0	100.0	0.0	0.0		0.0	0.0	0.00
CS		D2CS20	2.2	18.5	79.3	20.7	0.0		20.7	0.0	0.00
CS		D2CS30	3.2	26.9	73.9	30.1	0.0		30.1	0.0	0.00
DS	1st	D2DS05	1.1	3.8	95.1	4.9	16.3	13.9	3.8	1.1	10.06
DS	1st	D2DS10	2.3	8.0	89.7	10.3	7.7	61.5	8.0	2.3	14.58
DS	1st	D2DS20	4.2	14.5	81.3	18.7	4.3	202.6	14.5	4.2	19.65
IL	1st	D2IL05	0.8	4.2	95.0	5.0	11.8	9.7	3.8	1.2	9.04
IL	1st	D2IL10	1.4	7.6	91.0	9.0	6.5	31.4	6.8	2.2	12.13
IL	1st	D2IL20	2.0	10.8	87.2	12.8	4.6	63.5	9.7	3.1	14.47
IL	2nd	D2IL102	1.3	6.8	91.9	8.1	7.3	25.4	6.1	2.0	11.51
IL	2nd	D2IL202	2.8	15.0	82.2	17.8	3.3	122.7	13.5	4.3	17.06
KL	1st	D2KL05	2.7	2.1	95.2	4.8	6.6	26.0	0.0	4.8	17.53
KL	1st	D2KL10	5.1	4.0	90.9	9.1	3.5	93.6	0.0	9.1	24.13
KL	1st	D2KL20	11.2	8.6	80.2	19.8	1.6	443.0	0.0	19.8	35.00
KL	2nd	D2KL052	2.1	1.6	96.3	3.7	8.6	15.5	0.0	3.7	15.49
KL		L704KL	2.8	2.2	95.0	5.0	6.4	28.3	0.0	5.0	17.89
MIS		MSKL20	10.8	8.4	80.8	19.2	1.7	416.6	0.0	19.2	35.05
MIS		MSIL10	1.3	6.8	91.9	8.1	7.3	25.4	6.1	2.0	11.51

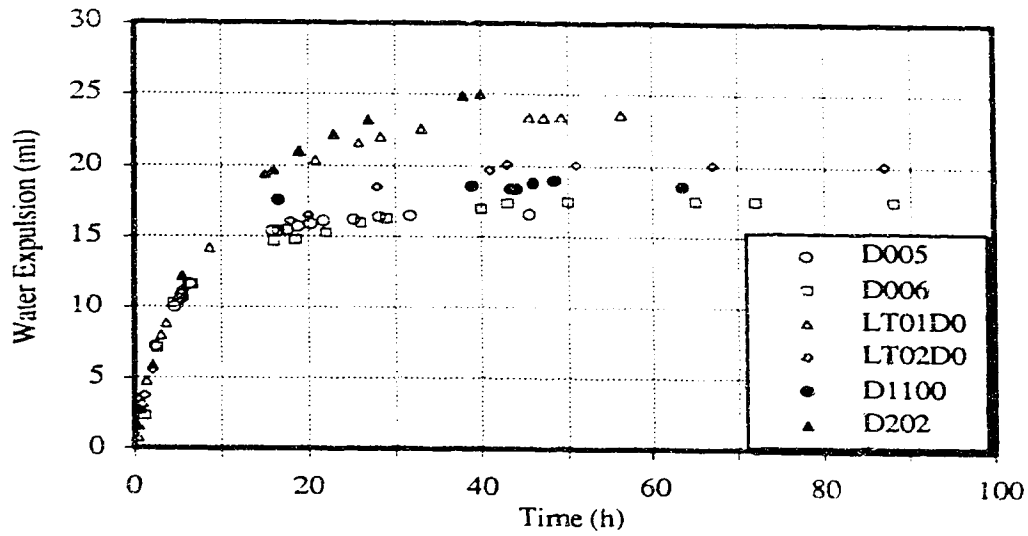


Figure 05-13.- Water Expulsion Duncan Sand Series

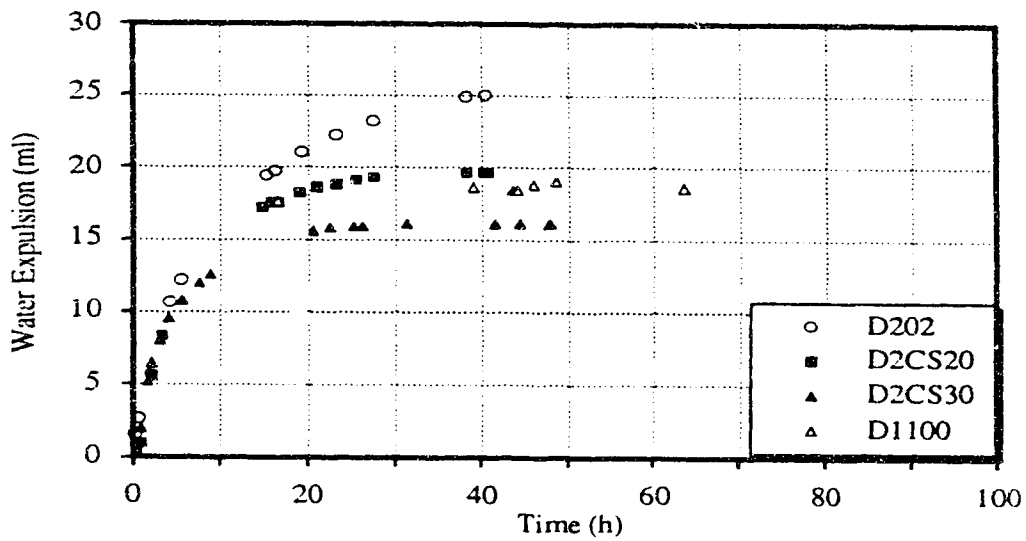


Figure 05-14.- Water Expulsion Silica Flume Series

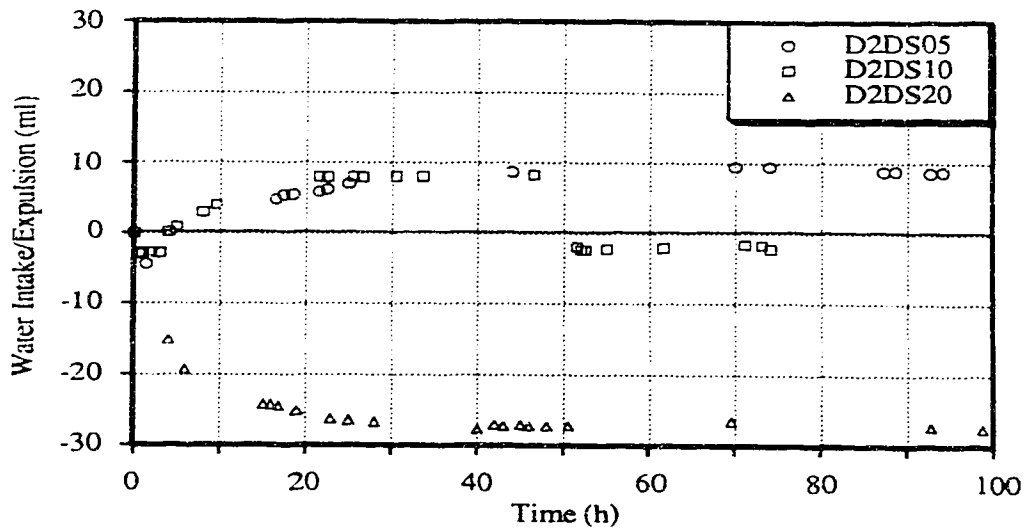


Figure 05-15.- Water Expulsion/Intake Devon Silt Series

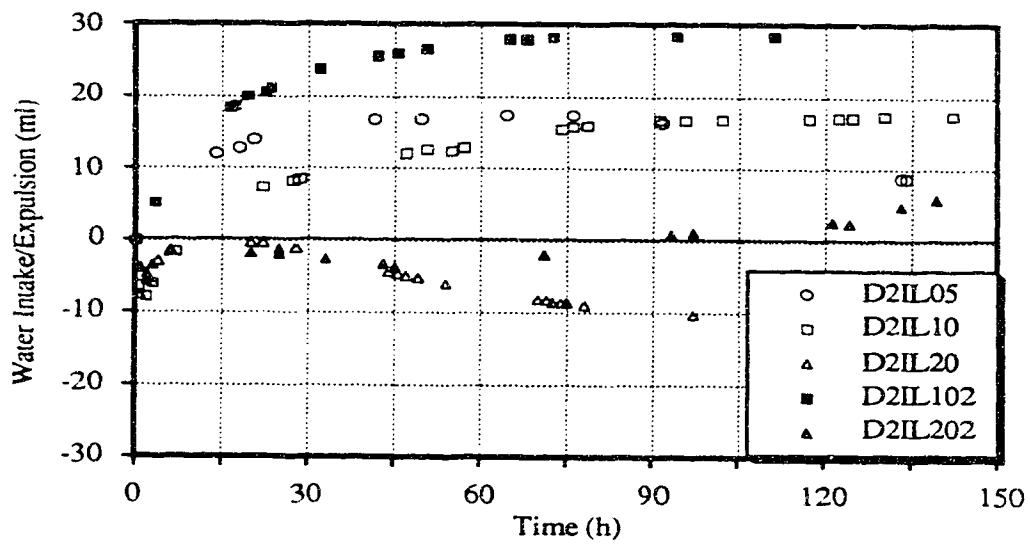


Figure 05-16.- Water Expulsion/Intake Illite Series

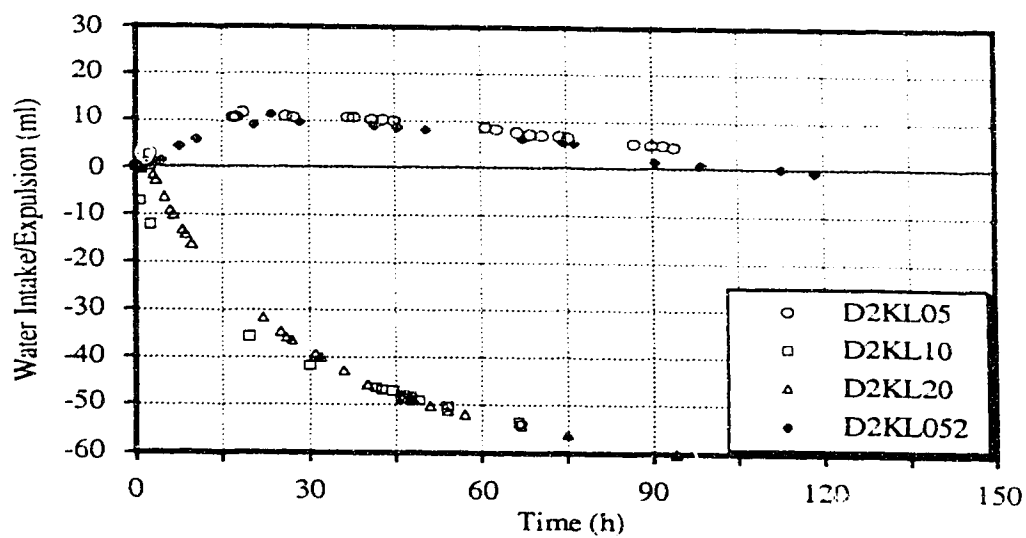


Figure 05-17.- Water Expulsion/Intake Kaolinite Series

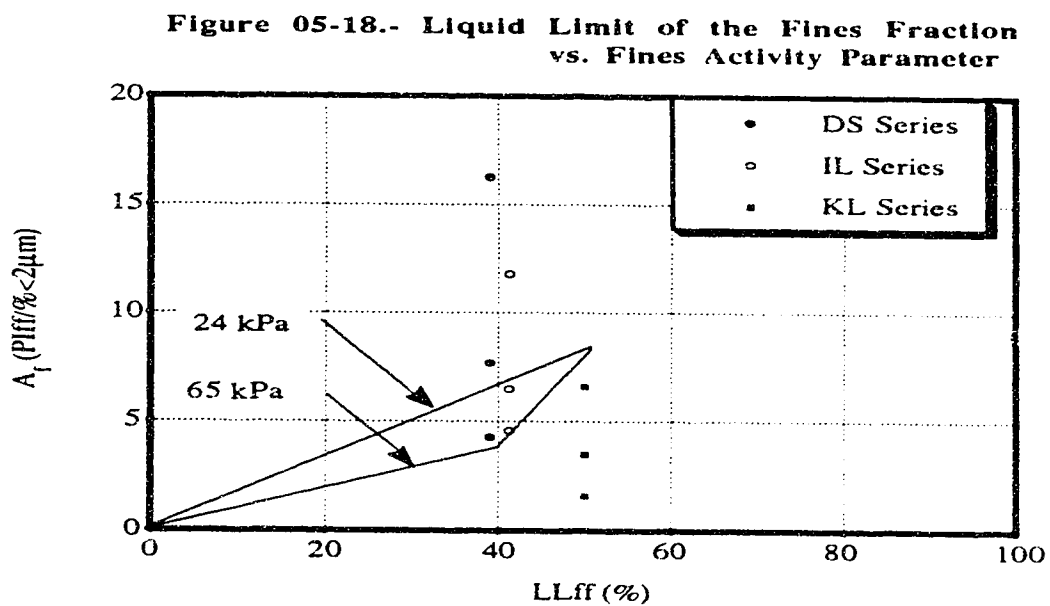
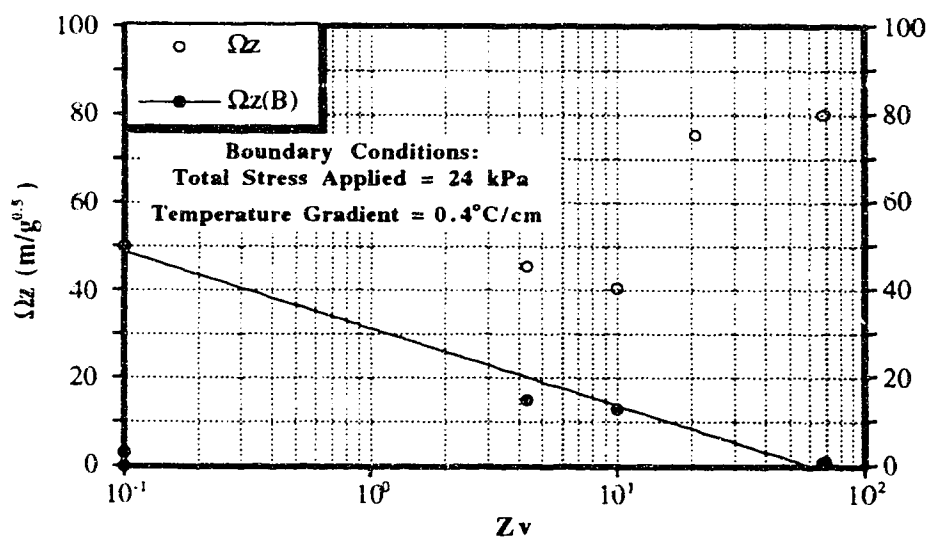
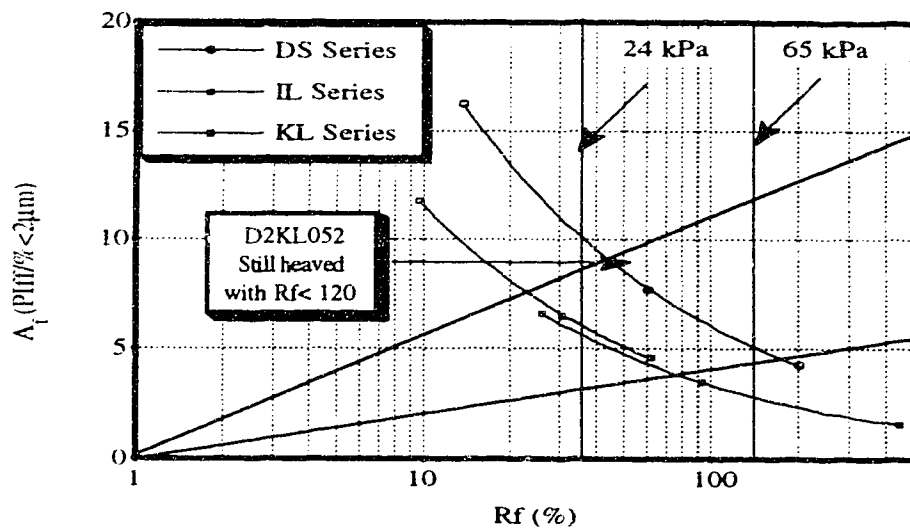


Figure 05-18.- Liquid Limit of the Fines Fraction vs. Fines Activity Parameter

Figure 05-19.- Fines Factor vs. Fines Activity Parameter

Figure 05-20.- Boundary for Frost Behavior
Based on the Surface Area Parameters

VI. SURFACE AREA CRITERIA APPLIED TO SEGREGATION POTENTIAL

6.1 Introduction

6.1.1 Foreword

As discussed in Chapter V, this research study was designed to establish a confidence region in which, based on the soil characteristics, the ground freezing technique can be efficiently applied to assist in the retrieval of undisturbed sandy soil samples. Although the boundary between frost susceptible and non-frost susceptible soils still has to be confirmed with more data, it seems that the trends obtained by the surface area criteria are logical and acceptable. Since a region of non-frost susceptibility has been successfully established by making use of the specific surface area of the fines fraction and its mineral content, it will be now examined if the proposed surface area parameters (section 5.4.2) can be used to evaluate a measure of the frost susceptibility of soil. Since data from the samples that experienced frost heave have been compiled, a correlation between the Segregation Potential, SP_o (section 3.1.2), and the surface area parameters may be developed. This correlation will be discussed in this chapter to establish whether or not the surface area criteria can be related to the Segregation Potential.

6.1.2 Background on Correlations to the Segregation Potential

Rieke *et al.* (1983) proposed the Fines Factor parameter (section 3.3.2) to characterize the soil for correlation with the Segregation Potential, SP_o (section 3.1.2). This Fines Factor, R_f parameter, is based on the Atterberg limits and gradation of the soil and does not accurately represent the differences among the various clay minerals (section 5.4.1). Nevertheless, Rieke *et al.* (op. cit.) recognized the influence that the specific surface area had on the frost heave behavior of soils. They published for each of their soil mixtures an *effective specific surface area*. This is a value determined by adjusting the specific surface areas of the components of the fines in proportion to their percentages by weight within the mixtures. Hence, their published values do not properly represent the characteristics of the fines contained within each soil mixture as the Fines Mineralogy Ratio proposed in this study (section 5.4.3).

Horne (1987) attempted a relationship between the specific surface area and the Segregation Potential by making use of the specific surface area in a parameter that he called the Specific Surface Factor or SSF , which he defined as

$$SSF = (LL/SSA) \times \% \text{ clay} \quad [6.01]$$

where **LL** is the liquid limit of the soil and **SSA** is the specific surface area of the soil. Two main discrepancies of the author with this relationship are with respect to the ambiguous term *clay* and the **LL/SSA** ratio. Although the clay size expressed as a percentage by weight of the soil is of general use, it is an artificial boundary and it is not as meaningful for frost heave behavior observation purposes as it is the clay mineral content (section 5.4.3). The ratio of the liquid limit to the specific surface area is said by Horne (op. cit) to be an estimate of the thickness of adsorbed water at the liquid limit. Nevertheless, although derived from soil properties parameters, it does not represent a soil property per se or even the fines fraction basic characteristics as proved elsewhere in this chapter.

This parameter, although not described in section 3.3.2, is the last in a short list of propositions in the attempts to correlate the basic characteristics of the soil with its behavior when submitted to freezing. Nevertheless, it has its own merit since it is the first one that uses the specific surface area as an index which could better model the observed cryogenic behavior of a soil. The Specific Surface Factor parameter per se is a break through in starting to understand a more accurate way of how the soil should be correctly characterized for frost heave purposes. The use of the specific surface area is appropriate, especially in linking the particularities of the soil mineralogy to its frost heave behavior. However, the use of the Surface Area Index (section 5.4.4), as given in equation 5.06, offers the advantage of representing the amount and the influence of the clay mineral involved in each test or any given soil. To support the statements and parameters proposed in Chapter V, the results from the laboratory program will be analyzed in order to obtain a relationship between the exhibited frost heave behavior of the specimens represented by the measured Segregation Potential and the proposed surface area parameters.

6.2 The Surface Area Related to Frost Heave Behavior

6.2.1 The Segregation Potential Determination

As explained in Chapter III (sections 3.1.2 and 3.2.2) the Konrad and Morgenstern model (1980) is the frost heave model used to analyze the frost heave behavior of the test specimens in this research. The Segregation Potential is the measured parameter in their model which relates the suction at the frost front, to the segregation temperature and the permeability within the frozen fringe (Appendix A). Since the calculation of the Segregation Potential for practical purposes is based on equation 3.02 (section 3.1.2), the

calculation of the water intake rate or water influx velocity and the temperature gradient in the active region of the freezing soil becomes quite important. The calculated values of the Segregation Potential are summarized in Table 06-01 for the samples that underwent frost heave. The temperature gradient or **Grad T_u** of each one of the specimens tested during the laboratory program are given in Table E-03 and the water influx velocity or v (Table 06-01) was obtained from the water expulsion curve of each specimen (Appendix C).

Concerns have been risen by different researchers about the Segregation Potential and its variability with respect to the temperature gradient (section 3.1.2). Considering these concerns, the test specimens were subjected to only one temperature gradient throughout the laboratory program (section 5.2.3) and the specifications set forth by Konrad (1987a) were closely followed in order to avoid confusion as to how the Segregation Potential was calculated in this study. Nevertheless, it was noticed that under the imposed boundary conditions (section 5.2.3), the Segregation Potential is highly dependent on the variation in the influx velocity during the process of water intake. This susceptibility decreases with time as the steady state conditions are established and a constant intake rate is recorded, at least this was the case with the specimens tested in this study (Figures 05-15, 05-16 and 05-17). Thus, it was necessary to determine not only the correct slope of the water intake curve, but also the time at which a constant value could had to be recorded.

As stated in section 5.3.2, the volume of water which the frost heave specimens adsorbed with time are represented by negative values of water intake (Figures 05-15, 05-16 and 05-17). All the samples presented in Table 06-01 behaved in a similar manner to that stated by the Konrad and Morgenstern model. An accurate evaluation of the velocity at which the water was being adsorbed was determined by obtaining the first derivative of the water intake curve with time, as shown in Figures 06-01 and 06-02. In order to calculate the Segregation Potential for the samples that heaved, it was decided to use the water influx velocity at $t = 50$ hours (Table 06-01). This standardized time was determined after observing that, for the majority of the specimens a steady state condition was only achieved after a period of 50 hours, even if the freezing front had stopped advancing several hours before. Good examples of this behavior can be observed in the laboratory measured curves for the D2KL10 (Figure C- 18) and the D2KL20 (Figure C-19) specimens, since their water intake rate stabilized after 50 hours.

Figure 06-01 for the Kaolinite series and Figure 06-02 for the Devon Silt and Illite specimens clearly show that if the Segregation Potential at $t = 25$ hours would be calculated, it would yield a higher Segregation Potential value, or in some cases not yielding any Segregation Potential at all because of terminating the test too early. D2KL05

(Figure 17) and D2KL052 (Figure 20) serve to support why a uniaxial freezing test should be conducted for a minimum of fifty hours. In this cases the samples were still expelling water at $t=25$ hours while at $t=50$ hours a definite pattern of water intake was observed. Furthermore, the calculation of the influx velocity at $t=25$ hours would lead to errors similar to those Rieke *et al.* (1983) committed when they considered that the steady state was reached, while in fact their tests were terminated too early. Probably because the tests were not continued longer and because the water influx velocity was calculated, especially for the higher clay content specimens, over the rapidly changing part of the water intake curve is that the Segregation Potential reported are larger than expected. Therefore, it is recommended that in the future a uniaxial freezing tests should be run for 75 hours to allow an accurate determination of the correct slope of the water intake curve.

The calculated Segregation Potential is also dependent on the length of the active zone within the freezing sample. The length of the active zone in each one of the specimens was measured manually, by dial gauge and by the RTD signal recording. These values are presented in Table E-03 with the skeletal void ratios for all the tested specimens. The length was measured manually after the test was terminated and calculated by recording the final position of the frost front using the RTD readings (section 4.1.2) (Appendix C). Even though no noticeable ice lenses were observed in any of the test specimens during the laboratory program, a difference between the manually and automatically recorded lengths was observed. Nevertheless, the RTD readings were assumed to be the more accurate, and it was from these measurements that the temperature gradient of the active system (unfrozen soil and frozen fringe) T_u was calculated. Table E-03 summarizes not only the manually measured length of the frozen and unfrozen parts of the specimen but also the final height determined using the dial gauge mounted on top of the freezing cell (section 4.2.3.5).

6.2.2 Relationship Between Specific Surface Area and the Liquid Limit

In Chapter V the specific surface area parameters were used to define a boundary between frost heaving and non-frost heaving behavior. The question left to be evaluated is whether these same parameters can be used to associate the rate of frost heave of a soil as is predicted by the Segregation Potential with the same soil characteristics. This cannot be proven directly, since the data from this study is insufficient to observe the total variation in the Segregation Potential for a wide enough range of soil types. Even the available published data (Table 03-02) have limitations since specific surface area associated with frost heave results is so scarce that this relationship cannot be established conclusively. Nevertheless, if the specific surface area is proportional to some other soil property or

index parameter more commonly found in frost heave published data, the relationship could be established indirectly.

From the literature (section 3.3.2), it is quite obvious that attempts to correlate the liquid limit and frost heave behavior have been carried out. Seed *et al.* (1964) shows that the liquid limit of a soil is linearly related to the amount of clay in the soil. More recently, Muhunthan (1991) developed a relationship between the specific surface area of a clay and its liquid limit and proved it using available published data (Table 06-02). Muhunthan (op. cit.) made use of Goodeve's (1939) plastic flow theory for colloidal particles. According to this theory

$$F = (f_c \times c \times z) / 2 \quad [6.02]$$

where F is the shearing force per unit area, f_c is the critical force required to break an interparticle bond or link, c is the number of bonds or links per unit volume and z is the distance between the moving plane and the reference plane (i.e. the distance between the particles that are moving relative to each other).

Clay particles become parallel as they shear past each other (Marshall, 1949; Dawson, 1975). The Casagrande apparatus and the fall-cone apparatus are presently the most widely used devices to determine the liquid limit, and are designed to perform the test mechanically, the principal action being one of shearing. Hence, it is reasonable to assume that during a test on a soft clay the particles will attain a near parallel orientation, although this alignment may not be perfect. Consequently, it is reasonable to identify z as the average interparticle distance for a parallel arrangement of the colloids. Consider two parallel platelets of plan area A and thickness t , separated by an average distance z . If all the water lies between the clay platelets (i.e. interlayer water) with ρ_s being the density of the clay particles, ρ_w the density of water and S the specific surface area of the clay particles (i.e. specific surface area per unit mass) then the volume of water V_w is

$$V_w = A \times z \quad [6.03]$$

and the volume of soil V_s is

$$V_s = A \times t \quad [6.04]$$

The water content can be expressed as

$$w = \frac{M_w}{M_s} = \frac{Az\rho_w}{At\rho_s} = \frac{z\rho_w}{t\rho_s} \quad [6.05]$$

Neglecting the contribution from the edges of the platelet, the specific surface area S is

$$S = \frac{2A}{M_s} = \frac{2}{t\rho_s} \quad [6.06]$$

Hence

$$\rho_s = \frac{2}{tS} \quad [6.07]$$

Substitution of this value for ρ_s in equation 6.05, and rearrangement yields

$$z = \frac{2w}{S\rho_w} \quad [6.08]$$

Substitution of this value for z in equation 6.02, and rearrangement yields

$$w = \left(\frac{F\rho_w}{f_{cc}} \right) S \quad [6.09]$$

Equation 6.09 holds for all water contents. If the water content value corresponding to the liquid limit is denoted by LL , equation 6.09 can be rewritten as

$$LL = \left(\frac{F\rho_w}{f_{cc}} \right)_{LL} S \quad [6.10]$$

Since f_{cc} is the force required to break *all* of the bonds or links in a unit volume of this soil system, this force must depend linearly on the specific surface area. (Muhunthan, 1991) cites a study of Margheim and Low (1978), they presented results of f_{cc} against S for different clays which plotted on a straight line with an intercept. Accordingly, it is assumed that the following linear relationship between f_{cc} and S holds, as

$$f_{cc} = \alpha S + \gamma \quad [6.11]$$

where α and γ are material constants.

At the liquid limit, F has a common value for all clay-water systems. Hence at the liquid limit equation 6.11 can be rewritten as

$$\left(\frac{f_{cc}}{F\rho_w}\right)_{LL} = \beta S + \lambda \quad [6.12]$$

where β and λ are constants to be determined and are related to α and γ through a division by $F\rho_w$. Substitution of this equation in equation 6.10 yields

$$LL = \left(\frac{1}{\beta S + \lambda}\right) S \quad [6.13]$$

Muhunthan (1991) rearranged equation 6.13 as

$$\frac{1}{LL} = \lambda\left(\frac{1}{S}\right) + \beta \quad [6.14]$$

Muhunthan (op. cit.) validated the above derivation by collecting data from De Bruyn *et al.* (1957), Farrar and Coleman (1967) and Sridharan *et al.* (1988) (Table 06-02). The specific surface area was linearly related to the liquid limit with a good correlation factor.

Based on the frost heave literature and on the review of the specific surface area use for frost heave correlations (sections 3.3.3 and 5.4.2), the author believes that this relationship could be better expressed if equation 6.13 is rearranged and modified to relate the respective fines fraction values as follows:

$$LL_{ff} = \left(\frac{1}{\beta S_f + \lambda}\right) S_f \quad [6.15]$$

where LL_{ff} is the liquid limit of the fines fraction (Rieke *et al.*, 1983) and S_f is the specific surface area of the fines fraction (section 5.4.2). With the help of an algebraic mechanism in which the denominator of the first part in the second hand of the equation is multiplied and divided by itself equation 6.15 is transformed into

$$LL_{ff} = \left(\frac{\beta S_f + \lambda}{(\beta S_f + \lambda)^2}\right) S_f \quad [6.16]$$

By square rooting

$$\sqrt{LL_{ff}} = \left(\sqrt{\frac{\beta S_f + \lambda}{(\beta S_f + \lambda)^2}}\right) \sqrt{S_f} \quad [6.17]$$

Or

$$\sqrt{LL_{ff}} = \left(\frac{\sqrt{\beta S_f + \lambda}}{\beta S_f + \lambda} \right) \sqrt{S_f} \quad [6.18]$$

Simplifying equation 6.18, it can be expressed as

$$\sqrt{LL_{ff}} = \xi \sqrt{S_f} \quad [6.19]$$

where

$$\xi = \frac{\sqrt{\beta S_f + \lambda}}{\beta S_f + \lambda} = \sqrt{\frac{LL_{ff}}{S_f}} \quad [6.20]$$

Then

$$S_f = \frac{LL_{ff}}{\xi^2} \quad [6.21]$$

Muhunthan (1991) proposed values for β between 0.006 and 0.0085 and values for λ between 0.752 and 1.127. Most of the natural soils possess a specific surface area for their fines fraction between 25 (section 5.5) and 100 (Table 05-02b), yielding values for ξ between 0.90 to 1.02 for $S_f = 25$, and between 0.76 to 0.79 for $S_f = 100$. These values are used to determine approximate values of the ξ coefficient for a wide range of specific surface areas as shown in Figure 06-03. The higher the specific surface area the lower the value for the ξ coefficient, but this is not necessarily true for the portion of soils with S_f between 30 and 100. It was found, by determining the ξ coefficient for the lean plastic soils in Table 05-02b, that an approximate estimate of the specific surface area of the fines fraction value could be determined through the liquid limit of the fines fraction by preliminary adopting $\xi = 0.75$ in equation 6.21. It is then concluded that the square root of the liquid limit of the fines fraction is not only directly proportional to the square root of the specific surface area of the fines fraction, but it does have the same order of magnitude provided that an accurate value for ξ coefficient is given. The ξ coefficient has dimension and can be expressed as $M^{1/2}L^{-1}$ or $g^{0.5}/m$ in SI units. Table 05-02b provides data for these values from the fine grained soils used in the laboratory program which agrees well with this relationship as shown in Figure 06-03. Therefore, the relationship between the surface area parameters and the Segregation Potential parameter can be developed indirectly by the use of the liquid limit of the fines fraction, since its square root is directly proportional to the square root of the specific surface area of the fines fraction (Equation

6.18). Furthermore, if the product of LL_{ff} and S_f with the same constant is square rooted, both results must have to continue behaving linearly.

The derivation above proved that the parameter used by Horne (1987) (section 6.1.2) based on the ratio LL/SSA , that is, ξ^2 (equation 6.21) is nothing more than a proportional coefficient and not a proper characteristic of the soil as it was intended to be. The surface area parameter, Surface Area Index as proposed in equation 5.06 in section 5.4.2, is based on the specific surface area of the fines fraction and the clay content; nevertheless, the available data (Table 03-02) offers only values of the clay size. For the purposes of this study, it can be assumed that in most natural soils the clay size fraction of the soil and the clay mineral content of the soil are similar. Hence, the clay size fraction of the soil, that is, the percentage of soil under the $2\ \mu\text{m}$ particle size will be used assumed equal to the clay mineral content (CM) (Lambe and Martin, 1956). It must be remembered that this is an assumption which must be evaluated by future research. The clay size fraction enters into the definition of Surface Area Index as:

$$\Omega_z = \sqrt{CM \times S_f} \equiv \sqrt{CS \times S_f} \quad [6.22]$$

where CS is the clay size fraction of the soil expressed as a percentage of the soil by weight. The clay size fraction will be used as a constant for correlation purposes with the liquid limit of the fines fraction.

6.2.3 Frost Heave Behavior with Respect to the Liquid Limit

The Surface Area Index to be used from hereon will be based on the clay size rather than the clay content (equation 5.03) according to the relationship defined by equation 6.22. In order to evaluate the relationship between this parameter and the liquid limit, the same data Muhunthan (1991) used is applied in this study (Table 05-02b). To complement it, other data from Rieke and Vinson (1982), Xiaozu *et al.* (1985) and Kozlowski (1989) (Table 06-02) is used as well. With respect to the data used from Rieke and Vinson (1982) some points have to be clarified. Table 03-02 presents the data from Rieke and Vinson (1982) modified for the purposes of this study, once in it are specified the probable specific surface area of the fines fraction in each mixture rather than its effective specific surface area (section 5.4.1). Of the 31 tests carried out (Table 03-02), 14 were selected for comparison purposes based on the two considerations.

During the laboratory program carried out in this study (section 5.3.2) it was noticed that the lower the clay content in the soil, the shorter the time to reach the steady

state condition during a test. Based on this experience, the first consideration for the selection of Rieke and Vinson (1982) data was that the fines fraction should not exceed more than 10% by weight of the sample. The second is that the maximum clay size fraction should not exceed more than 5% by weight of the sample. The main reason for this selection is the author's concern with measured Segregation Potential values obtained during their research project. Specifically, the tests were run for less than 24 hours making the reported SP_o values larger than expected, since the specimens could not have reached a steady state condition during the length of the test (section 6.1.2). In order to better observe the trend of Ω_z with respect to the liquid limit of the fines fraction, the data is plotted in Figure 06-04. There is a strong relationship between these parameters showing that as Ω_z increases the LL_{ff} also increases. A regression analysis (Figure 06-05) of the data presented in Figure 06-04 is performed with the best fit linear relationship given by:

$$\Omega_z = -2.5 + (0.98 \times LL_{ff}) \quad [6.23]$$

Seems reasonable that this linear relationship passes through the origin representing all the non-plastic soils. Hence, the Fines Mineralogy Ratio is proportional to the liquid limit of the fines fraction.

In section 6.2.2 was proved that the square root of the specific surface area of the fines fraction (S_f) may be proportional to the square root of the liquid limit of the fines fraction (LL_{ff}) if an accurate value of ξ is given. It was also mentioned that the square roots of these parameters when multiplied by the same constant should continue behaving proportionally. Then, it is logical for the Surface Area Index (Eq. 6.22) to be proportional to a similar index in which the liquid limit of the fines fraction (LL_{ff}) replaces the specific surface area of the fines fraction (S_f). The resultant dimensionless parameter is defined as the Liquid Limit Factor or Ω_z^* . The Liquid Limit Factor is obtained when the square root of the liquid limit of the fines fraction times the amount of clay size fraction of the soil is taken. The Liquid Limit Factor is expressed as:

$$\Omega_z^* = \sqrt{CS \times LL_{ff}} \quad [6.24]$$

where CS is the clay size fraction expressed as a percentage by weight of the soil and LL_{ff} is the liquid limit of the fines fraction of the soil as defined by Rieke *et al.* (1983). Not all the Liquid Limit Factors were calculated using the liquid limit of its fines fraction, but those soils without the liquid limit of its fines fraction where mostly composed by fine grained

soils, so still the relationship is valid. The correlation can be observed in Figure 06-06 and the regression analysis (Figure 06-07) is best defined by the relationship

$$\Omega z^* = 7.8 + (0.7 \times \Omega z) \quad [6.25]$$

Observe that the adopted value for the ζ coefficient in section 6.2.2 as a preliminary assessment of the specific surface area of the fines fraction in natural soils is very similar to the value defining the slope inclination in equation 6.25. Rieke and Vinson's (1982) data is plotted again in Figure 06-08 with the intention to show that distinct relationships may exist between the more active from the less active clays when the Surface Area Index and the Liquid Limit Factor are correlated. More data are needed in order to establish possible boundaries between different types of soils

Although the liquid limit of the fines fraction LL_f is seldom measured, the liquid limit values are generally provided with all sets of frost heave data; hence, a correlation between frost heave parameters such as SP_o and the specific surface area is valid through the use of Ωz^* . The Surface Area Index (Ωz) will consequently be validated as a reliable parameter for frost heave prediction because of the interrelationship between Ωz^* (Eq. 6-24) and Ωz (Eq. 5-06), with the advantage of the last one being more accurate. Making use of the data presented in Table 03-02, three different plots are presented in Figures 06-09, 06-10 and 06-11 with respect to the Liquid Limit Factor. In Figure 06-09 the Liquid Limit Factor Ωz^* is plotted against the heave using data from Haley and Kaplar's (1952), and Moroto and Sakaruda's (1989). In Figure 06-10 the Liquid Limit Factor Ωz^* is plotted against the heave rate obtained from Lambe *et al.* (1969) and part of the data from Penner and Ueda (1977). Finally, in Figure 06-11 the Liquid Limit Factor Ωz^* is plotted against the Segregation Potential SP_o , using data obtained from Aitken (1974), Loch and Kay (1978), Konrad (1980), Rieke and Vinson (1982), Konrad and Morgenstern (1983), Knutsson *et al.* (1985) and Jessberger and Jagow (1989).

Careful examination reveals that, although obtained from different sources, the data tends to follow the same pattern. For example, in Figure 06-11 it can be shown with greater accuracy that the tendency is to increase the Segregation Potential as Ωz^* increases to a certain point ($20 < \Omega z < 40$), and then decrease as the soil starts to behave more as a clay. The decreasing rate of heave as Ωz^* increases is also observed in the data included in Figure 06-10. This, once again provides support to Lambe's (1958) statement that the more dominant the colloidal particles are in the soils, the lower the frost susceptibility of the soil, at least for short term frost heave tests as explained elsewhere in the next section. This plot is remarkably similar to the one presented by Jessberger and Jagow (1989) and

also somewhat similar to the plot presented in Figure 03-11 where SP_o is plotted against the Fines Factor or R_f .

6.3 Consequences

The data plotted in Figure 06-11 was compiled taking into consideration that it was obtained from tests conducted under similar boundary conditions as those conducted during this study (section 5.2.2). Therefore, the data in Figure 06-11 can be seen to demonstrate the behavior of a wide range of different soils with plastic fines, to which a temperature gradient of approximately $0.4\text{ }^{\circ}\text{C}/\text{cm}$ was applied during a uniaxial freezing test, and which was tested for at least 50 hours (section 6.2.1). Furthermore, the liquid limit with which the Liquid Limit Factor was calculated was obtained from the fines portion of the soil, or in the worst situation, from a liquid limit test carried out on soil with a maximum of 5% sand content. This plot (Figure 06-11) and the one released by Jessberger and Jagow (1989) are based on data which significantly rely on the SP_o values obtained by Rieke *et al.* (1983) for soils containing low amounts of fines. The comparison of their specific surface areas with data from this study (Tables 03-02, 05-02b and 06-01) was a difficult task. Hence, the Ω_z values published by Rieke *et al.* (1983) (see Rieke and Vinson, 1982 in Table 03-02) were recalculated using equation 6-24 and correspond to the modifications made to their published values of effective specific surface areas by using the Surface Area Index concept (section 6.2.3). Thereby, the reader must keep in mind that the Surface Area Index values from Rieke and Vinson (op. cit.) research presented in Figure 06-11 are approximate.

Figure 06-12 illustrates a curve fit to the data presented in Figure 06-11. Hence, the curve used to define a relationship between the Liquid Limit Factor and the Segregation Potential, is defined by the following relationship

$$SP_o = a\Omega_z^{*4} e(b\Omega_z^{*}) \quad [6.26]$$

where a and b are coefficients dependent on the time at which the Segregation Potential was determined in a particular frost heave test. In order to determine these coefficients several approaches can be used. For the purpose of this study the coefficients a and b were determined by both the graphical and the least squares methods. By the graphical method (Figure 06-13), a is the intercept with the vertical coordinate axis and b is the slope of the relationship between natural logarithm of SP_o/Ω_z^{*4} plotted against Ω_z^{*} . Figure 06-13 illustrates that the fit to the data is very good with the use of these parameters. The

least-squares method was used to produce the curve presented in Figure 06-12 after several iterations which yielded values for $a = 0.004$ and $b = -0.167$. The curve fit presented in Figure 06-12 is considered to be a phenomenological model. That is, it is based on the ability to accurately curve fit the data points rather than determining all the pertinent parameters via physical principles. The main weakness of a phenomenological model is its inability to be extrapolated with confidence. Therefore in order to use the curve fitted in Figure 06-11 any differences in samples or test equipment must be evaluated to ensure that the test results are within the limitations used to produce the curve.

The Surface Area Index (Ω_z) as well as the Liquid Limit Factor (Ω_z^*) and the Segregation Potential (SP_o) were calculated for the specimens that underwent frost heave during the present laboratory program. The respective values of each one of these tested specimens are summarized in Table 06-01. For sake of simplicity and comparison purposes the data from this study are also plotted in Figures 06-11 and 06-12. The values of the Liquid Limit Factor and the Segregation Potential when compare favourably with the other published data. The laboratory data obtained from this study also compares well with the empirical curve (Figure 06-12) defined by equation 6.26 from previous published data. This supports the use of the Surface Area Index, Ω_z (Eq. 5-06), as a reasonable parameter to model the behavior of soils for frost susceptibility criteria based on the Segregation Potential, since it is directly proportional to the Liquid Limit Factor, Ω_z^* (Eq. 6.24).

Once the Segregation Potential of soils are characterized using the proposed relationship (Eq. 6.26) it should be possible to define not only the frost heave and non-heave regions, but also to define regions of high and low frost susceptibility for a given set of test boundary conditions. Based on the results from the laboratory program carried out in this study (section 5.3.2), the boundary between frost heave and non-heave regions for the Illite series occurred when the Liquid Limit Factor reaches a value of $\Omega_z^* = 8$ (Table 06-01) compared to $\Omega_z = 13$ (Table 05-04). The interface for the Devon Silt series is approximately around the Liquid Limit Factor value of $\Omega_z^* = 10$ (Table 06-01) compared to $\Omega_z = 13$ (Table 05-04). If the curve in Figure 06-12 is examined in detail, its initial part corresponds to a large variation of Segregation Potential with a small increments in the fines content. The region of high frost susceptibility is assumed to start at about $\Omega_z^* = 7$ and finishing at about $\Omega_z^* = 50$. The boundary between high and low frost susceptibility is assumed to be at $SP_o = 5 \times 10^{-4}$ mm/s°C. Regions of low frost susceptibility for the imposed boundary conditions, that is low Segregation Potential, are established for soils in which the Liquid Limit Factors are lower than seven and higher than fifty.

The Segregation Potential is a parameter which depends on the suction and the permeability at the frozen fringe when a given constant gradient of temperature is applied to the soil (Appendix A). Suctions develop at the frost front, but in the case of the more plastic soils it takes a longer time for water to flow due to its low permeability. Therefore, it is a matter of time for soils dominated by clay mineral particles to start attracting water to the frost front and to establish a constant influx velocity. Thus, the end of the curve defined in Figure 06-12 will have a different shape beyond Ωz^* of 30 or 40. The curve will start to rise, which means that if a test is conducted for a longer period of time a higher Segregation Potential will be measured. The author has not been able to find any data for a medium to highly plastic fine grained soil subjected to a uniaxial freezing test for long periods of time to confirm this observation. The only study known to the author in which a long term frost heave test was carried out is the one conducted by Carlson and Nixon (1987) at a facility in Calgary, Alberta for a chilled pipeline studies. This soil is not valid for demonstrating the above statement since it is a silt and not a highly plastic soil. Concluding, it could be argued that this statement lacks laboratory or field confirmation, so it is strongly recommended that highly plastic clays should be tested for longer periods of time in order to determine the validity of this argument.

This behavior leads one to a recognition that frost heave of the more colloidal material is a time dependent phenomenon. In order to define time dependency in soils due to its freezing characteristics it is necessary to use a term called the Influx Potential. The ISSMFE Technical Committee on Frost (ISSMFE, 1989) defined adsorbed water as *the water retained in a soil mass by physicochemical forces. Its physical properties may differ from chemically combined water or mechanically held water at the same pressure and temperature*. Thus, the Influx Potential is the capacity of the clay minerals contained in a soil to stimulate the water migration from an external source into the soil and then become adsorbed water. The fact is that fine grained soils possess a high suction but a low hydraulic conductivity, and coarse grained soils a higher hydraulic conductivity but a lower suction. Therefore, even though a sandy soil contains the same clay minerals as a clayey soil, it will take less time to the sandy soil to adsorb water because of its higher permeability. This does not mean that the clayey soil will not adsorb water, but that it will take more time for it to occur because of its lower permeability.

The shape of the initial part of the curve, that is for $\Omega z < 20$ (Figure 06-12) will not change with time as is the case of the middle and the final part of the curve. This is because in sandy soils, even though suctions can develop rapidly, the clay minerals lose their ability to stimulate more adsorption of water since the amount of clay minerals is not large. This is likely to occur, especially in soils with the Liquid Limit Factor lower than ten, with

the result that frost heave decreases or does not occur. In contrast, for higher values of Liquid Limit Factor (Ωz^*), such as for sandy soils richer in clay minerals or silty soils, there is a tendency to have larger Influx Potentials. Since these soils are partly dominated by colloidal particles, the suction phenomenon will be partly time dependent. Soils with higher concentrations of colloidal particles, such as most clays, will display a low Influx Potential. In fact, since the suctions developed at the freezing front are not able to be measured as for silts or silty sands, it is definitely a time dependent process for water to migrate. The values used to produce the curve in Figure 06-12 were derived predominantly from samples with a minimum testing period of time of 50 hours; hence, the coefficient a in equation 6.26 do not vary and only the coefficient b will change for tests carried out for longer periods of time.

In summary, in this chapter the possibility of implementing the use of the specific surface area to aid the present classification of soils for frost susceptibility purposes has been proposed. This study has also identified a way to model the water influx; which achieves its maximum expression in the form of the proposed curve plotted in Figure 06-12, and is defined by equation 6.26. Although the data which was used to propose the behavior of suction is based on the liquid limit of the fines fraction of the soil, ideally the comparison would have been with the Surface Area Index as defined in section 5.4.4. Consequently, more data needs to be collected and researchers are encouraged to advance the proposed model. This phenomenological model is restricted with respect to the temperature gradient applied to the soil; therefore, it is also limited with respect to the Segregation Potential. The Segregation Potential with which the curve was fitted was calculated at a standardized time of 50 hours and the author encourages other researchers to consider this time period for short term frost heave tests and calculations due to the reasons discussed in section 6.2.1. Finally the water migration to the frost front is presented as a time dependant process and varies with the increasing amount and activity of the clay mineral present in the soil.

Table 06-01 Summary of the Characteristics and Segregation Potential of the Uniaxial Freezing Tests

Series	Test	Battery	L.H.f	Zv	Ω_z (m/g(0.5))	Ω_z^*	ensk1	eesk1	Influx Velocity (mm/s)	SPo (mm ² /s ²)
DS	D2DS05	1st	39.0	4.3	10.06	6.57	1.12	1.09		
DS	D2DS10	1st	39.0	4.3	14.58	9.53	1.20	1.15		
DS	D2DS20	1st	39.0	4.3	19.65	12.84	1.34	1.29	1.00E-05	2.25E-04
IL	D2IL05	1st	41.3	10.0	9.04	5.75	1.16	1.11		
IL	D2IL10	1st	41.3	10.0	12.13	7.71	1.08	1.07		
IL	D2IL20	1st	41.3	10.0	14.47	9.20	1.18	1.15	5.00E-05	1.00E-03
IL	D2IL102	2nd	41.3	10.0	11.51	7.32	1.09	1.04		
IL	D2IL202	2nd	41.3	10.0	17.06	10.85	1.27	1.17		
KL	D2KL05	1st	50.0	68.1	17.53	11.64	1.14	1.12	3.00E-05	6.75E-04
KL	D2KL10	1st	50.0	68.1	24.13	16.03	1.25	1.14	9.00E-05	2.03E-03
KL	D2KL20	1st	50.0	68.1	35.60	23.65	1.47	1.30	1.10E-04	2.48E-03
KL	D2KL052	2nd	50.0	68.1	15.39	10.22	1.07	1.01	2.70E-05	6.08E-04
KL	L704KL		50.0	68.1	17.89	11.88				
MS	MSK1.20		50.0	68.1	35.05	23.29				
MS	MSIL10		41.3	10.0	11.51	7.32	1.24	1.23		

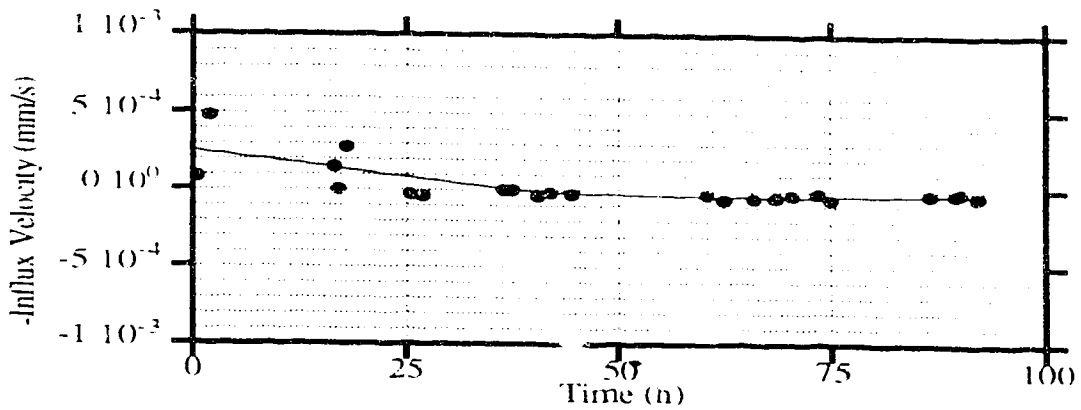


Fig 06-01a Kaolinite 1st Battery D2KL05

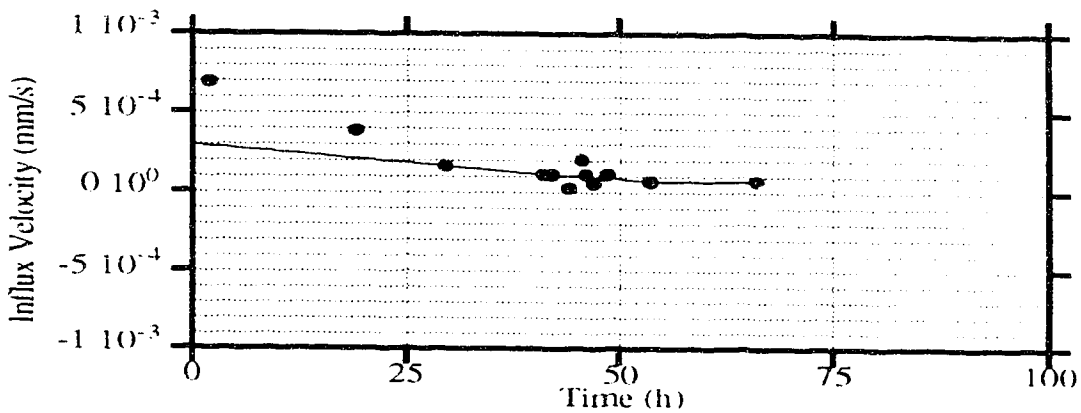


Figure 06-01b Kaolinite 1st Battery D2KL10

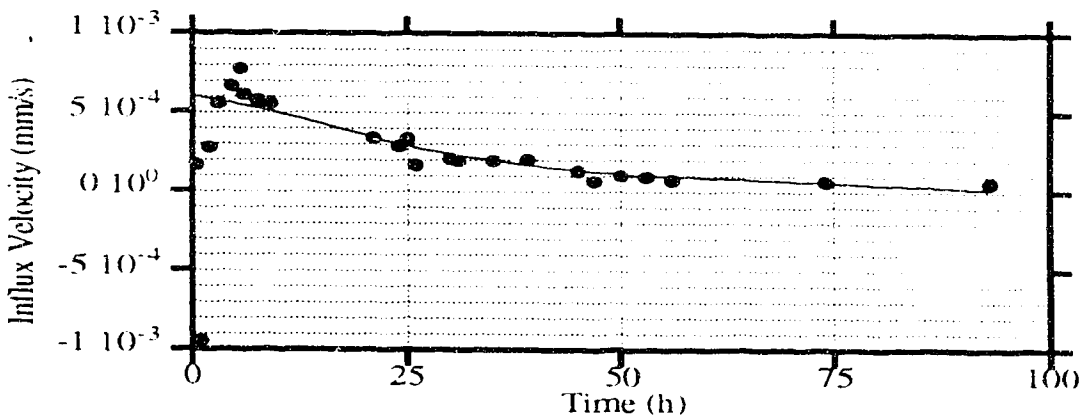


Figure 06-01c Kaolinite 1st Battery D2KL20

Figure 06-01.- Derivative Curve for the Water Intake Velocity from the Kaolinite 1st Battery

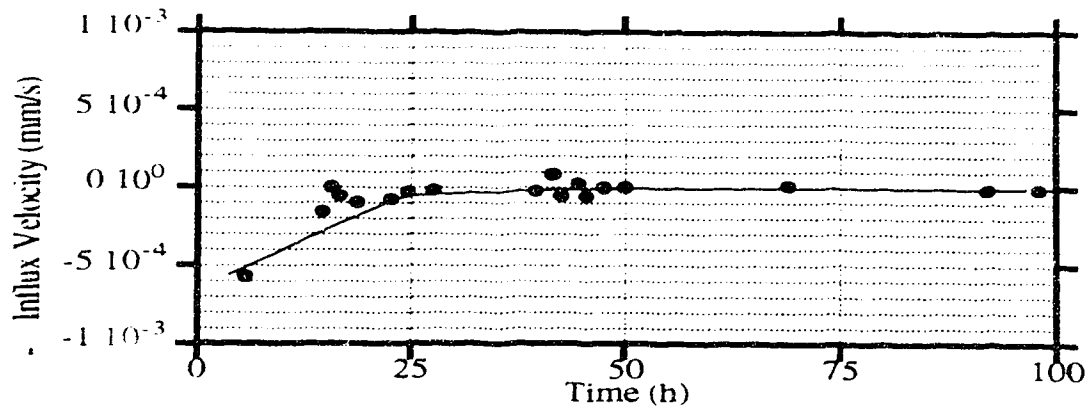


Fig 06-02a Devon Silt 1st Battery D2DS05

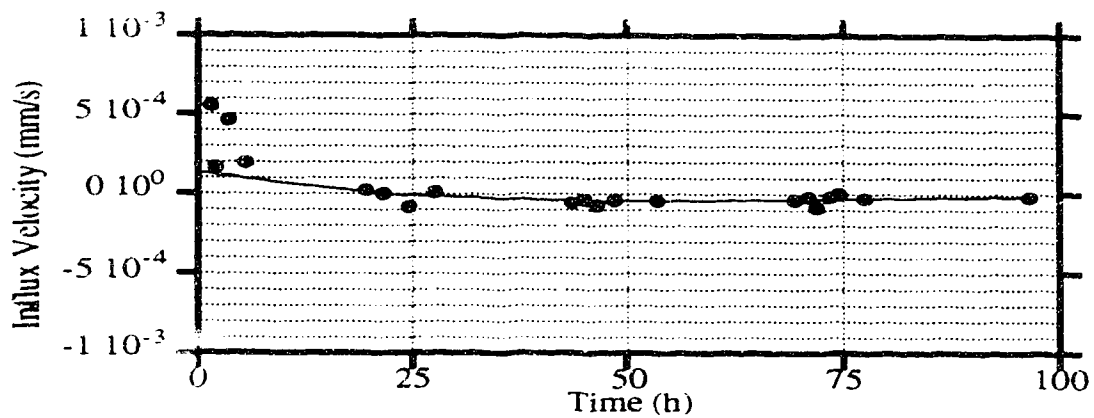


Fig 06-02b Illite 1st Battery D2IL20

Figure 06-02.- Derivative Curve for the Water Intake Velocity from the Devon Silt and Illite 1st Battery

Table 06-02 Compilation of Available Data including Specific Surface Area and Liquid Limit

Soil Specimen	Liquid Limit %	Plastic Index	Fines %	Clay Size %	Surface Area m ² /g	Δz m ² /g	Ωz^*
De Bruyn et al. (1957)							
Soil No.1	122.0				433.0	0.0	0.0
Soil No.2	105.0			56.0	326.0	137.5	78.0
Soil No.3	80.0			41.0	324.0	115.3	57.3
Soil No.4	82.0			47.0	225.0	102.8	62.1
Soil No.5	61.0			26.0	180.0	68.4	39.8
Soil No.6	85.0			23.0	169.0	62.3	44.2
Soil No.7	55.0			18.0	89.0	40.0	31.5
Soil No.8	52.0			7.0	69.0	22.0	19.1
Soil No.9	41.0			4.0	48.0	13.9	12.8
Soil No.10	36.0			21.0	38.0	28.2	27.5
Farrar and Coleman (1967)							
London clay	81.0	55.0		69.0	91.0	79.2	74.8
Lower London Tertiary clay							
Gault clay	79.0	52.0		64.0	96.0	78.4	71.1
Lower London Tertiary clay	71.0	39.0		43.0	97.0	64.6	55.3
Gault clay	76.0	49.0		58.0	80.0	68.1	66.4
Gault clay	70.0	45.0		56.0	98.0	74.1	62.6
Gault clay	102.0	68.0		69.0	133.0	95.8	83.9
Gault clay	121.0	89.0		60.0	186.0	105.6	85.2
Wexley clay	47.0	24.0		35.0	45.0	39.7	40.6
Wexley clay	68.0	43.0		62.0	94.0	76.3	64.9
Kimmeridge clay	72.0	50.0		64.0	79.0	71.1	67.9
Kimmeridge clay	77.0	53.0		67.0	126.0	91.9	71.8
Oxford clay	50.0	31.0		45.0	41.0	43.0	47.4
Oxford clay	72.0	48.0		56.0	88.0	70.2	63.5
Oxford clay	69.0	42.0		62.0	71.0	66.3	65.4
Lower Lias clay	48.0	25.0		43.0	65.0	52.9	45.4
Lower Lias clay	60.0	36.0		39.0	75.0	54.1	48.4
Keuper Marl	28.0	7.0		10.0	61.0	24.7	16.7
Marl in Keuper Sandstone							
Upper Coal Measures	36.0	17.0		25.0	34.0	29.2	30.0
WC Kaolinite	37.0	18.0		30.0	38.0	33.8	33.3
WC Kaolinite	43.0	17.0		100.0	10.0	31.6	65.6
PC Kaolinite	75.0	39.0		100.0	23.4	48.4	86.6
Na-Montmorillonite	135.0	79.0		100.0	97.4	98.7	116.2
Mura Clay							
Soil No.1	38.3	15.5	100.0	30.0	60.0	42.4	33.9
Soil No.2	25.0	11.2	64.0	25.0	40.2	31.7	25.0
Soil No.3	38.0	22.7	66.0	27.0	42.5	33.9	32.0
Soil No.4	47.0	25.5	41.0	25.0	77.6	42.9	34.3
Soil No.5	47.0	21.6	60.0	24.0	84.3	45.0	33.6
Soil No.6	73.0	32.6	87.0	21.0	172.6	60.2	39.2
Soil No.7	74.0	49.0	88.0	30.0	224.0	82.0	47.1
Soil No.8	75.0	41.2	89.0	30.0	225.8	67.3	52.0
Soil No.9	75.0	35.7	78.0	40.0	147.4	82.3	53.7
Soil No.10	100.0	77.2	90.0	51.0	157.2	92.3	71.4
Devon Silt							
Soil No.1	39.0	18.6	100.0	22.6	93.0	45.8	29.7
New York Shale							
Soil No.1	41.3	9.4	100.0	16.0	67.0	32.7	25.7
Athabasca Clay							
Soil No.1	41.8	20.5	100.0	40.0	125.0	77.5	47.3
Kaolinite							
Soil No.1	50.0	28.0	100.0	36.5	64.0	40.1	33.2
Bentonite							
Soil No.1	66.5	52.9	100.0	83.2	633.0	252.1	152.1

Figure 06-03.- Calculated and Theoretical Values for

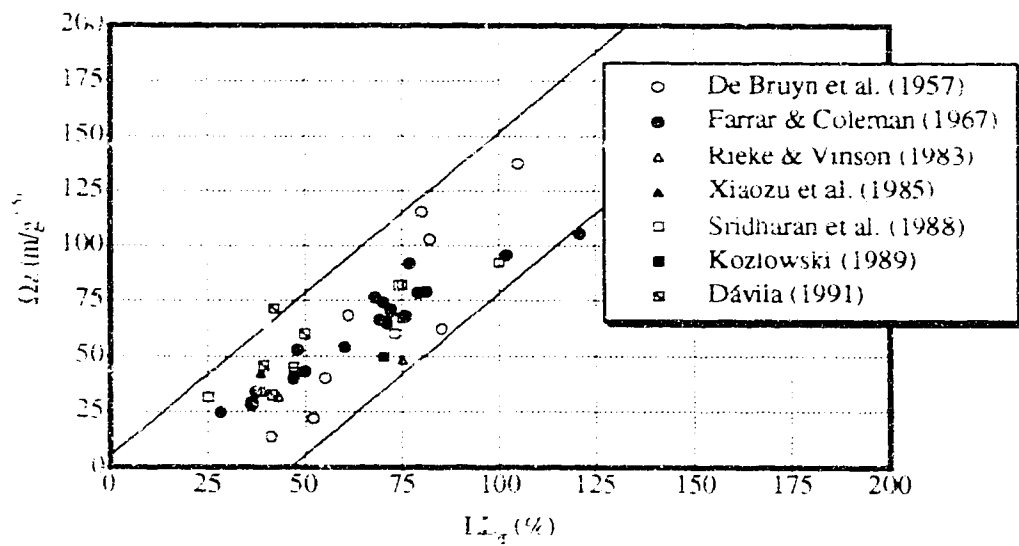
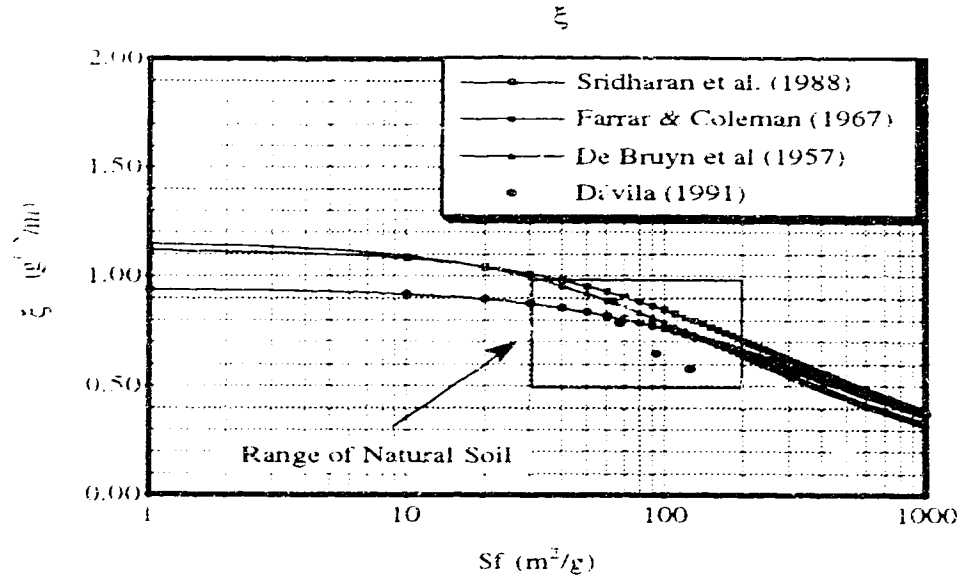


Figure 06-04.- Surface Area Index vs. Liquid Limit Comparison from Different Sources

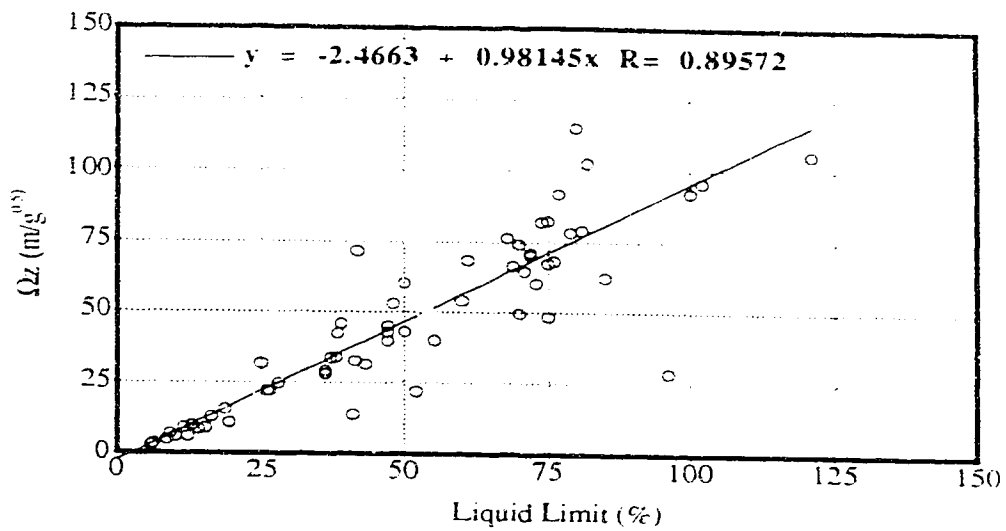


Figure 06-05.- Regression Analysis for Data in Figure 06-04

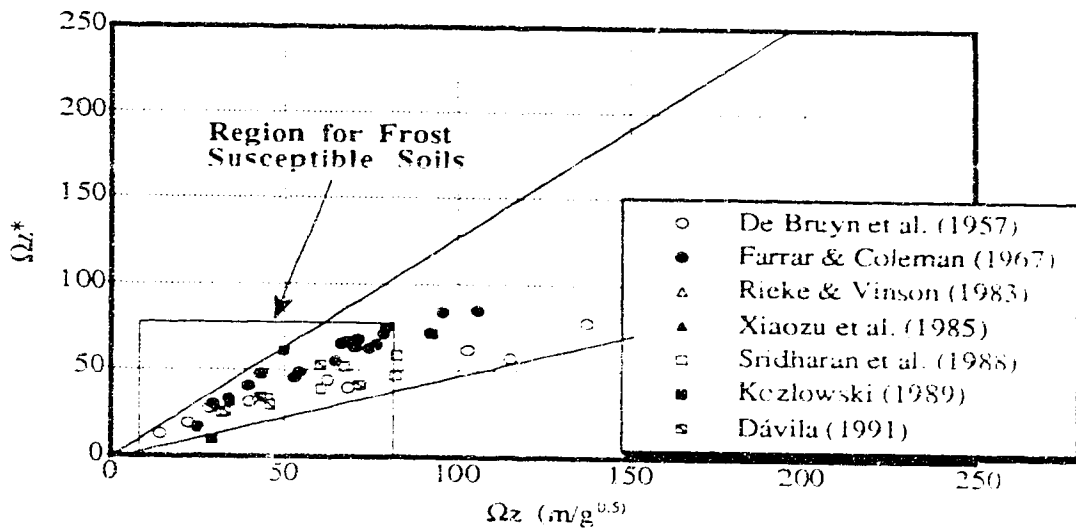


Figure 06-06.- Surface Area Index vs. Liquid Limit Factor Comparison from Different Sources

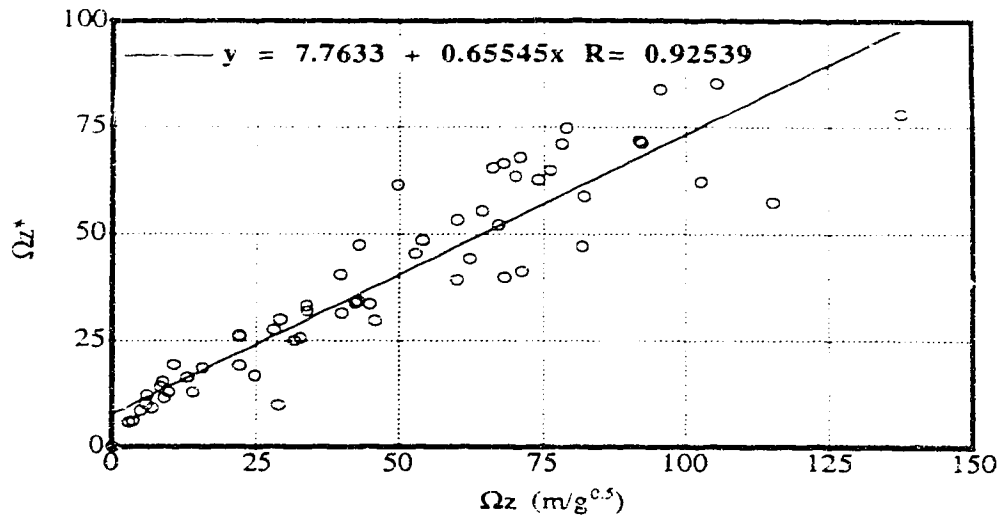


Figure 06-07.- Regression Analysis for Data in Figure 06-06

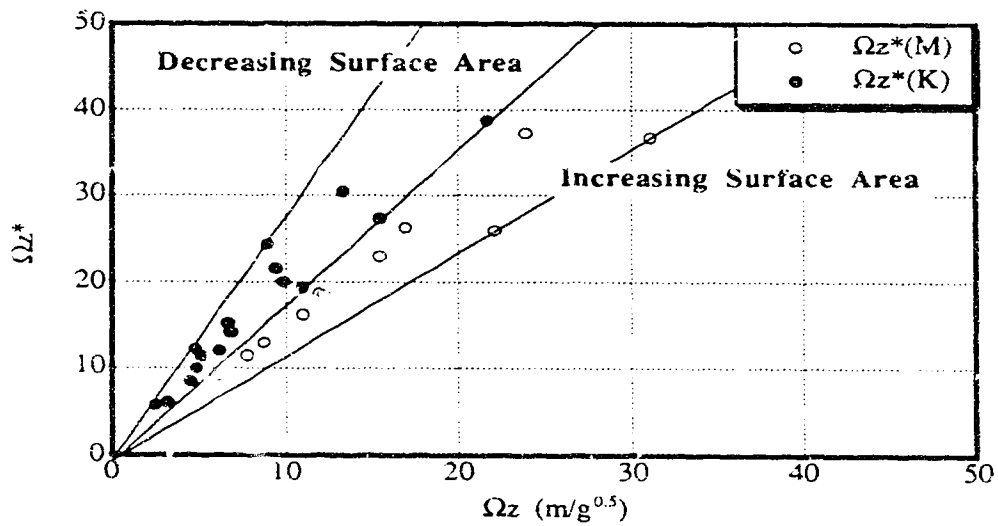


Figure 06-08.- Surface Area Index vs. Liquid Limit Factor
Modified Data after Rieke and Vinson (1982)

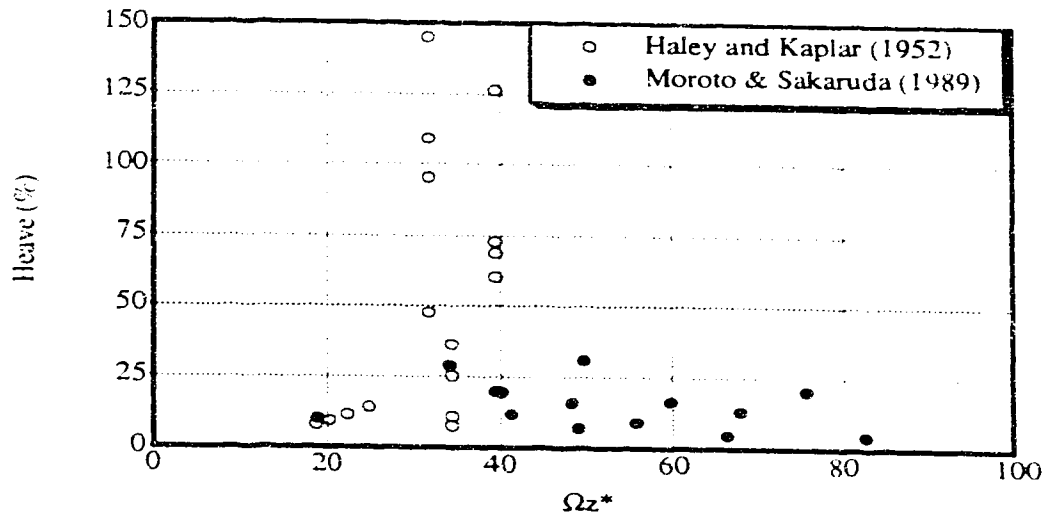


Figure 06-09.- The Liquid Limit Factor vs. Percent Heave
Data Compiled from Different Sources

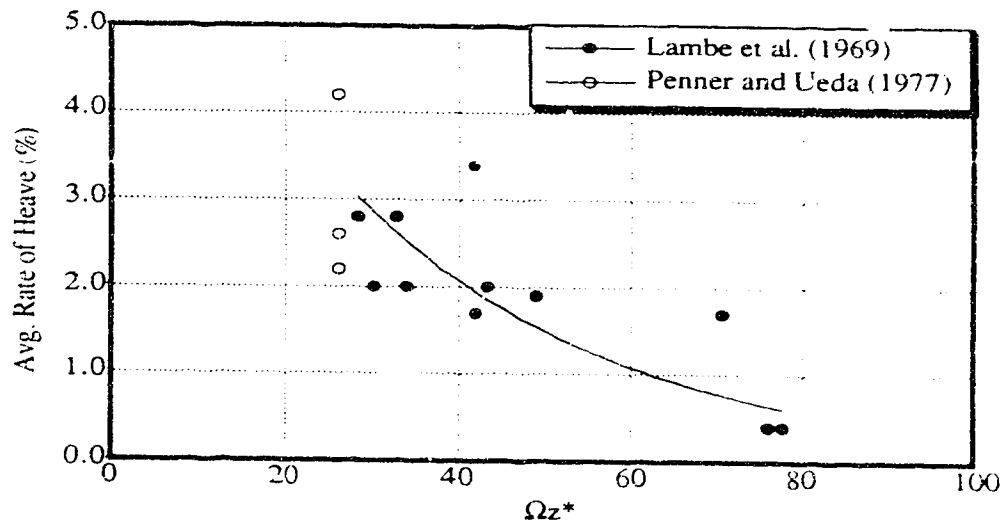


Figure 06-10.- The Liquid Limit Factor vs. Avg. Heave Rate
Data Compiled from Different Sources

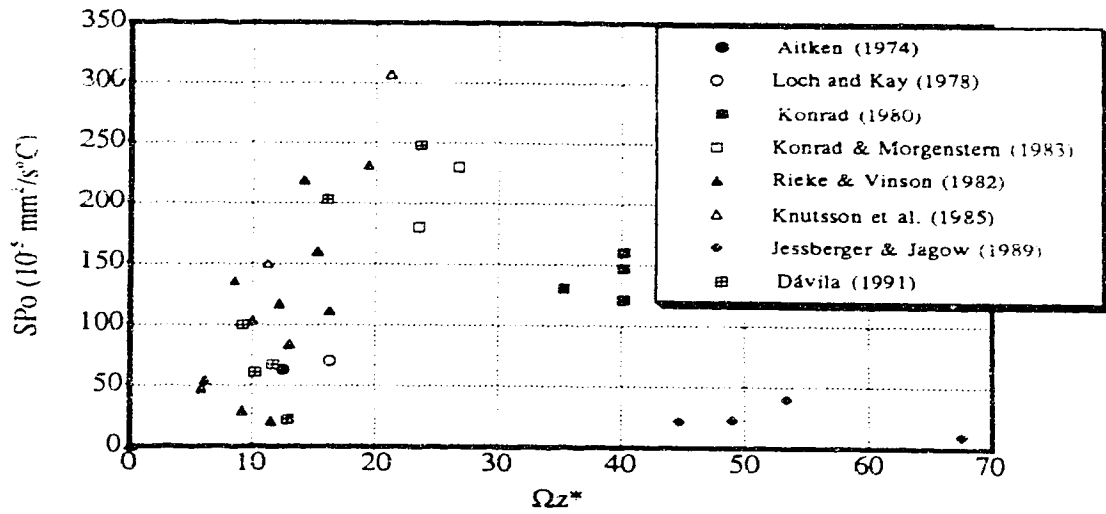


Figure 06-11.- The Liquid Limit Factor vs. Segregation Potential
Compiled Data from Different Sources

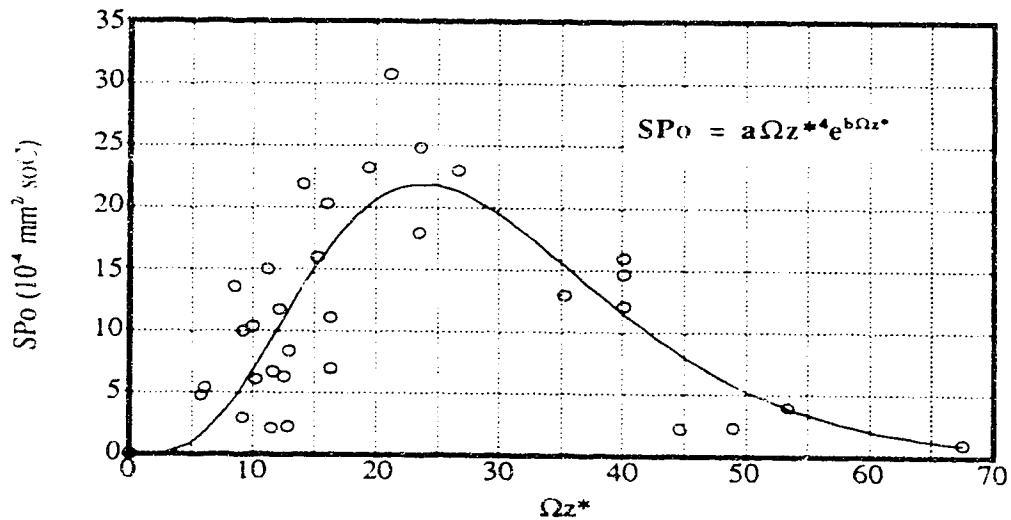


Figure 06-12.- Proposed Curve Fitting for Data in Figure 06-11

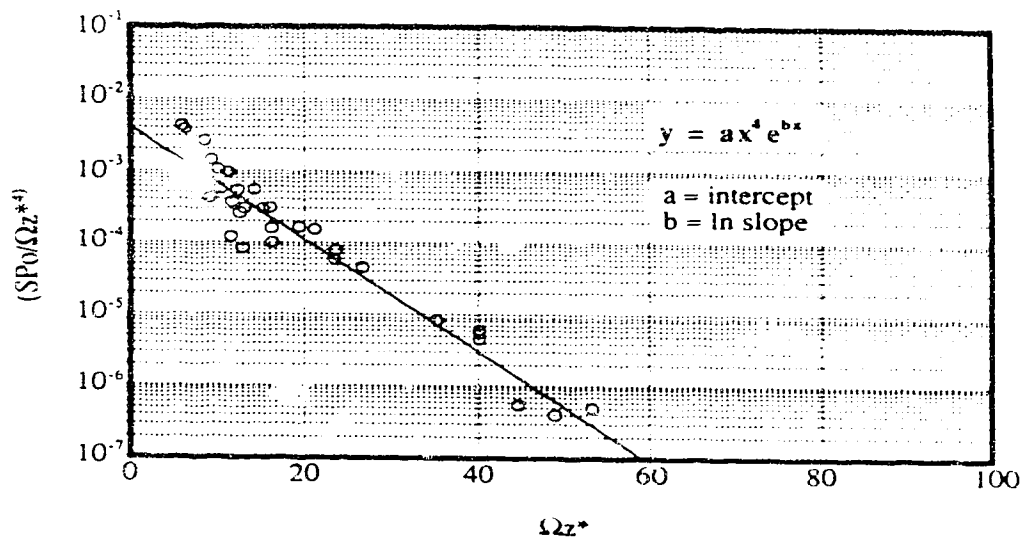


Figure 06-13.- Graphical Determination of Coefficients a and b

VII. CLOSURE

7.1 Summary

This research was undertaken to investigate in what loose sandy soils the ground freezing technique can efficiently be used to obtain undisturbed samples and, if possible, to provide guide-lines to explain the frost heave behavior of soils with varying amounts of fines. The most important factors affecting the frost heave of soils have been considered in order to establish which dominates the frost heave behavior of sandy soils. Among all the factors studied herein, it was determined that the type and quantity of the fines fraction of the soil are the main ones controlling the frost heave process in sandy soils. Since the behavior of a soil varies depending on the nature of the colloidal particles that it contains when subjected to a negative temperature change, it is assumed that the response to freezing varies with the activity of the fines. In order to quantify in a logic manner the effect of freezing, artificially prepared loose saturated sand specimens were submitted to uniaxial freezing tests. A parametric study was conducted by varying the type of clay constituting the fines fraction and varying the amount of clay minerals. The response of non-plastic fine grained soils was also studied to evaluate if the non-plasticity of the fines had an important effect. Characterization of the soils based on the specific surface area was found useful to assist in interpreting the frost heave data and to define the boundary between frost heave and non frost heave behavior.

7.2 Conclusions

The following conclusions are drawn from the work performed both in the field at the Duncan Dam and in the laboratory program presented in this thesis. The conclusions are detailed in that order.

- 1) At the present moment, the ground freezing technique as used at the Duncan Dam appears to be the best known way among other available techniques to obtain undisturbed samples of saturated cohesionless soil from depths up to 20 m for use in laboratory studies needed for seismic assessment purposes .
- 2) The amount of clay minerals and mineralogy of the fines contained in a sandy soil proved to be the most relevant aspect in the ability to obtain undisturbed sandy soil samples when using the ground freezing technique. Soils with different gradations and even large amounts of fine grained particles but constituted solely of non-plastic fines may be sampled undisturbed as if they were constituted solely by granular soil.
- 3) The surface area criteria successfully established a boundary between frost heave and

non-frost heave behavior with the use of the specific surface area and the mineral characteristics of the fines; hence, it is possible to establish a region of confidence for the use of the ground freezing technique. Two parameters are proposed to characterize the soil: the Fines Mineralogy Ratio and the Surface Area Index. The Fines Mineralogy Ratio (Z_v) defines the mineralogy of the soil fines fraction, and the Specific Surface Index (Ω_z) indicates the influence which the colloidal particles contained in the fines fraction have on the overall behavior of the soil.

4) It is proposed that frost heave tests should be conducted for at least 50 hours. However, a duration of 75 hours would be preferable as this would allow to accurately determine the correct slope of the water intake curve. The water influx velocity is best considered at 50 hours, since the water intake response and therefore the establishment of steady state conditions for the soils tested in this study required this amount of time to establish constant rate of water intake.

5) Soils can be classified according to their surface area characteristics with respect to their Segregation Potential. Sandy soils with less than 20% of moderately to highly active plastic fines, are able to develop rapid and high suction rates. Once the steady state condition has been reached it will tend to saturate its Influx Potential. Silts tend to have higher Influx Potentials and since these soils are partly dominated by colloidal particles, the suction phenomenon will be partly time dependent. Soils with higher concentrations of colloidal particles, such as most of highly plastic clays, will display a low Influx Potential and it is said to be highly time dependent for water migration.

6) The Segregation Potential has been correlated with the soil characteristics with the use of the Liquid Limit Factor. In the future, when correlating the mineralogy of soils with the Segregation Potential, the surface area criteria might be of better use. Even though it is not proved in this study, it is believed that this phenomenological model is defined by the shape of a surface if plotted in three dimensions considering time as the third axis.

7.3 Recommendations

1) More data has to be collected in natural soils in order to obtain a better boundary based on the surface area parameters. The trend stated by the surface area criteria has to be improved, especially in the region of low amounts of fines and low plasticity, that is, with Fines Mineralogy Ratio lower than four

2) In this study, it has been demonstrated that the parameters based on the specific surface area may correlate well with frost heave parameters. Implementing the use of the specific surface area to aid the present status of the soil classification system based on the proposed

surface area parameters is strongly recommended in order to accurately determine the correct boundaries between the characteristics of soils with plastic fines.

3) Based on the surface area criteria proposed in this study a chart should be developed in which the practicing engineer is shown how given a patterned soil region he could adapt for the field conditions the most suitable sampling technique for the better preservation of the natural structure of soils .

4) A testing program of long term uniaxial freezing tests should be carried out with the objective of determining the behavior of medium to highly plastic clays with constant temperature and stress boundary conditions.

5) Presently, a similar study to this one is being carried at the University of Alberta using the shear wave velocity concentrating its effort in sandy soils. The increment of the Fines Mineralogy Ratio value is dependent on the concentration of the plastic portion of the soils and it is believed that the higher the clay content of the soils the higher its Shear Wave Velocity. Therefore, linking the surface area parameters with this the shear wave velocity would result in a better and a more accurate characterization of lean to fat plastic soils.

BIBLIOGRAPHY

- AITKEN, G., 1974. Reduction of frost heave by surcharge stress. U.S. Army Cold Regions Research and Engineering Laboratory, CRREL Technical Report No. 184, 24 p.
- AKAGAWA, S., 1988. Experimental study of frozen fringe characteristics. Cold Regions Science and Technology, Vol. 15, pp. 209 - 223.
- ANDERSON, D.M., 1963. The latent heat of freezing soil water. Proc., 1st. Permafrost International Conference, Lafayette, Indiana, NRC-NAS. Publication No. 1287, pp. 238 - 239.
- ANDERSON, D.M. AND HOEKSTRA, P., 1965. Crystallization of clay-adsorbed water. Science, Vol. 149, pp. 318 - 319.
- ANDERSON, D.M. AND MORGENSTERN, N.R., 1973. Physics, chemistry and mechanics of frozen ground: a review. Proc., 2nd International Conference on Permafrost, Yakut, U.S.S.R., North American Contribution, U.S. National Academy of Sciences, pp. 257 - 288.
- ANDERSON, D.M. AND TICE, A.R., 1971. Low temperature phases of interfacial water in clay-water systems. Proc., Soils Science Society of America, Vol. 35, No. 1, pp. 47 - 54.
- ANDERSON, D.M. AND TICE, A.R., 1972. Predicting unfrozen water contents in frozen soils from surface area measurements. Frost Action in Soils, Highway Research Record No. 393, Highway Research Board, National Research Council, U.S. National Academy of Sciences, pp. 12 - 16.
- ANDERSON, D.M. AND TICE, A.R. 1973, The unfrozen interfacial phase in frozen soil water systems. Physics of Soil Water and Salts. Ecological Studies, Analysis and Synthesis, Vol. 4, pp. 107 - 125.
- ANDERSON, D.M., PUSCH, R. AND PENNER, E., 1978. Physical and thermal properties of frozen ground. **Geotechnical Engineering for Cold Regions** (Andersland, O.B. and Anderson, D.M., ed.) McGraw-Hill Book Co. Ch. 2. 450 p.
- ARVIDSON, W.D., 1973. Water flow induced by soil freezing. M.Sc. Thesis, The University of Alberta, Edmonton, Alta.
- ARVIDSON, W.D. AND MORGENSTERN, N.R., 1974. Water flow induced by soil freezing. Proc., 27th Canadian Geotechnical Conference, Edmonton, pp. 137 - 143.
- BALLA, T., MAKKAJ, B. AND BERGA, M., 1971. *Verfahren zur entnahme ungerstorter droben aur kornigen esdstoffen unter wasser*. Proc., 4th Budapest Conference on Soil Mechanics and Soil Eng., pp. 511 - 521.
- BESKOW, G., 1935. Soil freezing and frost heaving with special application to roads and railroads. The Swedish Geological Society, Series C No. 375, 26th Year Book, No. 3, Series C, No. 375. Translation by Osterberg, J.O., 1947. Northwestern University Technological Institute, Evanston, Illinois, 145 p.
- BOUYOUCOS, G.J., 1916. The freezing point method as a new means of measuring the concentration of soil solution directly in the soil. Michigan Agricultural Coll. Exp. Sta.

Technical Bulletin 24, 1 - 44.

BOZHENOVA, A.P., 1940. *Nekotoroe razvitie opytov Tabera po pucheniye gruntov s vertikal'noi sloistost'yu* (Developing Taber's experiments on the swelling of soils with vertical stratification). Trudy Instituta geologicheskikh nauk, No. 22, Inzhenerno-geologicheskaya seriya, No.1.

CARLSON, L.E. AND NIXON, J.F., 1988. Subsoil investigation of ice lensing at the Calgary, Canada, Frost heave test facility. Canadian Geotechnical Journal, Vol. 25, pp. 307 - 319.

CARY, J.W. AND MAYLAND, H.F., 1972. Salt and water movements in unsaturated frozen soil. Proc., Soils and Science Society of America, Vol. 36, No. 4, pp. 549 - 555.

CASAGRANDE, A., 1932. Discussion of Frost Heaving. Highway Research Board Proc., Vol 11, Pt. 1, pp 169 - 172.

CHAMBERLAIN, E.J., 1981. Frost susceptibility of soil, review of index tests. CRREL Monogr., 81 - 2.

CHAMBERLAIN, E.J., 1987. A freeze-thaw test to determine the frost susceptibility of soils. CRREL, Special Report 87 - 1.

COLLINS, P.M., 1986. Deformations around Arctic Pipelines. M.Sc. Thesis. The University of Alberta, Edmonton, Alta.

DA ROIT, R., LOYELO, L., MUZZI, F. AND SPAT G., 1981a. Effects of freezing on undisturbed sand sampling. Proc., 10th ICSMFE, Session 7, Stockholm.

DA ROIT, R., LOYELO, L., MUZZI, F. AND SPAT G., 1981b. In-situ undisturbed sand sampling by radial freezing for liquefaction analysis. Proc., International Conference on Recent Advances in Geotechnical Earthquake Eng. and Soil Dynamics Vol. 3, pp. 961 - 964.

DAWSON, R., 1975. An activated state model for clay suspension rheology. Transactions of the Society of Rheology. Vol. 19, pp. 229 - 244.

DE LOVERDO, 1910. *La congelation du sols dans le travaux du Metropolitain de Paris. Monographie sur l'etat actuel de l'industrie du Froid en France*, published by Association Francaise du Froid, II. Intern. Kaltekongress, Vienna.

DE BRUYN, C.M.A., COLLINS, L.E. AND WILLIAMS, A.A.B., 1957. The specific surface, water affinity, and exponential expansiveness of clays. Clay Mineralogy, Bulletin No. 3, 120 - 128.

DÜCKER, A., 1956. Is there a dividing line between non-frost-susceptible and frost-susceptible soils? *Gibt es iene Grenze zwischen frostsicheren und frostempfindlichen Lockergesteinen?* National Reseach Council of Canada, Technical Translation 722 (1958).

DUCROS, P. AND DUPONT, M., 1962. A nuclear magnetic resonance study of water in clays. In: Magnetic and electrical resonance and relaxation. Eindhoven: Compte. Rendu du XI Colloque Ampere.

FAHLQUIST, F.E., 1941. Undisturbed sampling of sediments. Geology Section Report,

- Providence District, Corps of Engineers. Providence, R.I., Nov.
- FARRAR, D.M. AND COLEMAN, J.D., 1967. The correlation of surface area with other properties of nineteen British clay soils. *Journal of Science*, Vol. 18, No. 1, pp. 118 - 124.
- GILPIN, R.R., A model for the prediction of ice lensing and frost heave in soils. *Water Resources*, Vol. 16, No. 5, pp. 918 - 930.
- GOODEVE, C.F., 1939. A general theory of thixotropy and viscosity. *Transactions of The Faraday Society*, Vol. 35, pp. 342 - 358.
- GOTO, S., SHAMOTO, Y. AND TAMAOKI, K., 1987. Dynamic properties of undisturbed gravel samples by in-situ frozen. *Proc., 8th Asian Regional Conference of SMFE*, Vol. 1, pp. 233 - 236.
- GRAHAM, J., WALKER, G.F. AND WEST, G.W., 1964. Nuclear magnetic resonance study of interlayer water in hydrated layer silicates. *Journal of Chemistry and Physics*, Vol. 40, pp. 540 - 550.
- GRIM, R.E., 1951. Relation of frost action to the clay mineral composition of soil materials. *Symposium on frost heave and frost action in soils*, Highway Research Board Special Publication No. 2, pp. 167 - 172.
- GRIM, R.E., 1968. **Applied Clay Mineralogy**, 2nd edition, McGraw-Hill, New York.
- HALEY, J.F. AND KAPLAR, C.W., 1952. Cold-room studies of frost action in soils. *Symposium on frost heave and frost action in soils*, Highway Research Board Special Publication No. 2, pp. 246 - 266.
- HARRIS, S.A. 1986. **The Permafrost Environment**. Barnes and Noble Books Co.
- HATANAKA, M., OGIMOTO, M. AND SUZUKI, Y., 1985. Liquefaction resistance of two alluvial volcanic soils sampled by in situ freezing. *Soils and Foundations*, Vol. 25, No. 3, pp. 49 - 63.
- HATANAKA, M., SUZUKI, Y., KAWASAKI, T. AND ENDO, M., 1988. Cyclic undrained shear properties of high quality undisturbed Tokyo gravel. *Soils and Foundations*, Vol. 28, No. 4, pp. 233 - 236.
- HECHT, A.M., DUPONT, M. AND DUCROS, P., 1966. *Etude des phenomenes de transport de l'eau adsorbée dans certains minéraux argileux par la resonance magnetique nucleaire*. *Bull. de la Soc. Francaise de Mineralogie et Cristallographie*, Vol 89, pp. 6 - 13.
- HEISE, F. AND HERBST, F., 1923. *Lehrbuch der Bergbaukunde*, Julius Springer, Berlin 2, 245 p.
- HILL, D.W., 1977. The influence of temperature and load on moisture transfer in freezing soil. M.Sc. Thesis, The University of Alberta, Edmonton, Alta.
- HILL, D.W. AND MORGENSTERN, N.R., 1977 Influence of load and heat extraction on moisture transfer in freezing soils. *Proc., Symposium on Frost Action on Soils*, University of Lulea, Sweden, Vol. 1, pp. 76 - 91.

- HOEKSTRA, P., 1965. Conductance of frozen bentonite suspensions. *Proc., Soil Science Society of America*, Vol. 29, pp. 519 - 522.
- HOEKSTRA, P. AND CHAMBERLAIN, E., 1964. Electroosmosis in frozen soil. *Nature* Vol. 203, pp. 1404 - 1407.
- HORIGUSHI, K., 1987. A model for prediction of ice lensing and frost heave in soils. *Water Resources*, Vol. 16, No. 5, pp. 918 - 930.
- HORIGUSHI, K. AND MILLER, R.D., 1983. Hydraulic conductivity of frozen earth materials. *Proc., 4th International Permafrost Conference*, Fairbanks, pp. 504 - 509.
- HORNE, W.T., 1987. Prediction of Frost Heave Using the Segregational Potential Theory. M.Sc. Thesis, The University of Alberta, Edmonton, Alta.
- HOSHINO, K., 1977. Soil Sampling. *Proc., 9th ICSMFE, Specialty Session 2*, Vol. 3 Tokyo, Japan, pp. 469 - 478.
- HVORSLEV, M.J., 1949. Subsurface exploration and sampling of soils for civil eng. purpose. Report of Committee on Sampling and Testing, Soil Mechanics and Foundations Div., ASCE, 521 p.
- ISHIHARA, K. AND SILVER, M.L., 1977. Large diameter sand sampling to provide specimens for liquefaction testing. *Proc., 9th ICSMFE, Specialty Session 2*, Tokyo, Japan, pp. 1 - 6.
- ISSMFE, 1989. Technical Committee on Frost, TC - 8, Appendix F. Frost in Geotechnical Engineering, VTT Symposium 95, Technical Research Centre of Finland, Vol. 1, pp. 46 - 70.
- JESSBERGER, H.L. AND EBEL, W., 1984. Influence of temperature and overburden pressure on frost heave. *Proc., 3rd International Offshore Mechanics and Arctic Engineering Symposium*, pp. 105 - 110.
- JESSBERGER, H.L. AND JAGOW, R., 1989. Determination of frost susceptibility of soils. Frost in Geotechnical Engineering, VTT Symposium 95, Technical Research Centre of Finland, Vol. 2, pp. 449 - 467.
- JOHNSTON, G.H., LADANYI, B., MORGENSTERN, N.R. AND PENNER, E., 1981. Engineering Characteristics of Frozen Soils. **Permafrost Engineering Design and Construction** (Johnston, G.H., ed.), Ch. 3. John Wiley and Sons. 540 p.
- JONES, R.H., 1981. Developments and applications of frost susceptibility testing. *Engineering Geology*, Vol. 18, pp. 269-280.
- JUMIKIS, A.R., 1966. **Thermal Soil Mechanics**, 2nd Ed. Rutgers University Press. 267 p.
- KHAKIMOV, K.H.R. 1957. **Artificial Freezing of Soils, Theory and Practice** (In Russian) (Zhukov, V.F. ed.). Israel Program for Scientific Translations (trans. Barouch, A., Heimann, H. ed.) 1965. IPST Cat. No. 1632
- KNUTSSON, S., DOMASCHUK, L. AND CHANDLER, N., 1985. Analysis of large scale laboratory and in situ frost heave tests. *Proc. 4th International Symposium on Ground*

Freezing, Sapporo, pp. 65 - 70.

KOLLBRUNNER, C.F. AND LANGER, C., 1939. *Probebelastungen und probebohrungen, Entnahme von ungestorten Bodenproben*. Loading tests and test borings, The obtaining of undisturbed samples. Privat-Gesellschaft fur Bodenforschung und Erdbaumechanik, Bericht No. 2, Zurich, Switzerland.

KONRAD, J.-M., 1980. Frost Heave Mechanisms. Ph.D. Thesis, The University of Alberta, Edmonton, Alta.

KONRAD, J.-M., 1987. Procedure for determining the segregation potential of freezing soil. *Geotechnical Testing Journal*, Vol. 10, No. 2, pp. 51 - 58.

KONRAD, J.-M., 1988. Influence of freezing mode on frost heave characteristics. *Cold Regions Science and Technology*, Vol. 15, pp. 161 - 175.

KONRAD, J.-M., 1989. Influence of cooling rate on the temperature of ice lens formation in clayey silts. *Cold Regions Science and Technology*, Vol 16, pp. 25 - 36.

KONRAD, J.-M. AND MORGENSTERN, N.R., 1980. A mechanistic theory of ice lens formation in fine-grained soils. *Canadian Geotechnical Journal*, Vol. 17, pp. 473 - 486.

KONRAD, J.-M. AND MORGENSTERN, N.R., 1981. The segregation potential of a freezing soil. *Canadian Geotechnical Journal*, Vol 18, pp. 482 - 491.

KONRAD, J.-M. AND MORGENSTERN, N.R., 1982a. Prediction of frost heave in the laboratory during transient freezing. *Canadian Geotechnical Journal*, Vol 19, pp. 250 - 259.

KONRAD, J.-M. AND MORGENSTERN, N.R., 1982b. Effects of applied pressure on freezing soils. *Canadian Geotechnical Journal*, Vol 19, pp. 494 - 505.

KONRAD, J.-M. AND MORGENSTERN, N.R., 1983. Frost susceptibility of soils in terms of their segregation potential. Proc., 4th International Conference on Permafrost, Fairbanks, National Academy of Science, Washington, D.C., pp. 660 - 665.

KONRAD J.-M. AND MORGENSTERN, N.R., 1984. Frost heave prediction of chilled pipelines buried in unfrozen soils. *Canadian Geotechnical Journal*, Vol. 21, pp. 100 - 115.

KOZLOWSKI, T., 1989. Investigation of the supercooling in clayey soils. VTT Symposium 95, Technical Research Centre of Finland, Vol. 1, pp. 293 - 299.

KUERBIS, R.H., 1989. M.A.Sc. Thesis, The University of British Columbia, Vancouver, British Columbia.

KUERBIS, R.H. AND VAID, Y.P., 1989a. Undrained behavior of clean and silty sands. Proc., Discussion Session on Influence of Local Conditions on Seismic response, XII ICSMFE, Rio de Janeiro, pp. 91 - 100.

KUERBIS, R.H. AND VAID, Y.P., 1989b. Sand sample preparation. The slurry deposition method. *Soils and Foundations*, Vol. 28, No. 4, pp. 107 - 118.

LADANYI, B. AND SAYLES, F.H., 1979. General Report. Session II: Mechanical Properties. Proc., 1st International Symposium on Ground Freezing, Bochum, Germany.

pp. 7-18.

LANGER, C., 1939. Report on undisturbed sampling of fine sand and silt by means of freezing, Paris, France.

LAMBE, T.W., 1958. Cold room studies, 3rd Interim Report. Appendix C: Mineral and Chemical Studies, Contract Report. Arctic Construction and Frost Effects Laboratory, Technical Report 43, Vol. 2. U.S. Army Engineer Div., New England, Waltham, Mass.

LAMBE, T.W. AND MARTIN, R.T., 1956. Composition and Engineering properties of Soil (IV). Proc., 35th Annual Meeting, Department of Soils, Geology and foundations, Highway Research Board, NRC

LAMBE, T.W. AND WHITMAN, R.V., 1968. **Soil Mechanics**. John Wiley and Sons Inc., 553 p.

LAMBE, T.W., KAPLAR, C.W. AND LAMBIE, T.J., 1969. Effect of mineralogical composition of fines on frost susceptibility of soils. US Army Cold Regions Research and Engineering Laboratory, CRREL Technical Report 207, 30 p.

LEBEDEV, A.F., 1936. *Pochvennye i gruntovye vody* (Ground Water). Izd. AN SSSR.

LEE, K.L. AND SEED, H.B., 1967. Cyclic stress conditions causing liquefaction of sand. ASCEJ, Vol. 93, No. SM1, pp. 47 - 70.

LIAO, S., 1985. Statistical analysis of liquefaction data. Ph.D. Thesis, Massachusetts Institute of Technology, Cambridge, Massachusetts.

LINELL, K.A. AND KAPLAR, C.W. 1959. The factor of soil and material type in frost action. U.S. Highway Research Board, Bulletin No. 225 pp. 81-126

LIGHTFOOT, T.B., 1886. Proc., Inst. of Mechanical Engineering (London), May, p. 238.

LOCH, J.P.G. AND KAY, B.D., 1978. Water redistribution in partially frozen, saturated silt under several temperature gradients and overburden loads. Soil Science Society of America Journal, 42, pp. 400 - 406.

LOVELL, C.W., 1958. Temperature effects on phase composition and strength of partially frozen soil. Highway Research Board, Bulletin No. 168, pp. 74 - 95.

MAGEAU, D.W., 1978. Moisture Migration in Frozen Soil. M.Sc. Thesis, The University of Alberta, Edmonton, Alta.

MAGEAU, D.W. AND MORGENSTERN, N.R., 1980. Observations on migration in frozen soils. Canadian geotechnical Journal, Vol. 17, pp. 54 - 60.

MARSHALL, C.E., 1949. The colloid chemistry of the silicate minerals. New York: Academic Press, pp. 85 - 90.

MARTYNOV, G.A., 1959. Principles of geocryology. Part I: General Geocryology, Chapter VI: Heat and moisture transfer in freezing and thawing soils. Akad. Nauk SSSR, p. 153 - 192. Translated by E. R. Hope, National Research Council of Canada Technical Translation No. 1065.

- MCROBERTS, E.C. AND MORGENSTERN, N.R., 1975. Pore water expulsion during freezing. Canadian Geotechnical Journal. Vol. 12, pp. 130 - 141.
- MCROBERTS, E.C. AND NIXON, J.F., 1975. Some geotechnical observations on the role of surcharge in soil freezing. Proc. Conference on Soil Water Problems in Cold Regions, Calgary, 1975, pp. 42 - 57.
- MILLER, R.D., 1963. Discussion of "Saturation, phase composition and freezing point depression in a rigid soil model" by Lange and McKim. Proc., 1st Permafrost International Conference, Lafayette, Indiana. NAS-NRC Publ. Na 1287, pp. 191 -192.
- MILLER, R.D., 1972. Freezing and heaving of saturated and unsaturated soils. Highway Research Record No. 393, National Academy of Sciences, Washington, D.C., 1972, pp. 1 - 11.
- MILLER, R.D., 1978. Frost heaving in non-colloidal soils. Proc., 3rd International Conference on Permafrost, National Research Council of Canada, Vol 1, pp. 707 - 709.
- MITCHELL, J.K., 1976. **Fundamentals of Soil Behavior**. Ed. by Lambe, T.W. and Whitman R.V. John Wiley & Sons, Inc., 422 p.
- MOROIO, N. AND SAKARUDA, T., 1989. Frost susceptibility of soils in Aomori province, Japan. Frost in Geotechnical Engineering, VTT Symposium 95, Technical Research Centre of Finland, Vol. 2, pp. 547 - 556.
- MUHUNTHAN, B., 1991. Liquid Limit and surface area of clays. Géotechnique, Vol 19, No.1, pp. 135 -138.
- MYRICK, J.E., ISAACS, R.M., LIU, C.Y. AND LUCE, R.G., 1982. The frost heave program of the Alaskan natural gas transportation system. ASCE Conference, Phoenix, Arizona, U.S.A.
- NERSESOVA, Z.A., 1950. *Izmenenie l'distosti gruntov v zavisimosti ot temperatury* (Variation of soil iciness as a function of temperature). DAN, SSSR, Vol 75, No. 6
- NERSESOVA, Z.A., 1951. *Otchet po teme Fiziko-khimicheskie protsessy v zameryayushchikh, merzlykh i ottaivayushchikh gruntakh* (Report on the Subject "Phisico-chemical processes in freezing, frozen and thawing soils). Arkhiv tsentral'noi merzlotnoi laboratorii Instituta Merzlotovedeniya AN SSSR.
- NERSESOVA, Z.A. AND TSYTOVICH, N.A., 1963. Unfrozen water in frozen soils. Proc., 1st Permafrost International Conference, Lafayette, Indiana. National Academy of Sciences - National Research Council Publication No. 1287, pp. 230 - 234.
- NIXON, J.F., 1982. Field Frost heave predictions using the segregation potential concept. Canadian Geotechnical Journal, Vol 19, pp. 526 - 529.
- NIXON, J.F., 1987. Ground freezing and frost heave, A review. The Northern Engineer, Vol. 19, No. 3 and 4, Fall/Winter, pp. 8 - 18.
- ODA, M., 1972. Initial fabrics and their relations to mechanical properties of granular material. Soils and Foundations, Vol. 12, No. 1, 17 - 36.
- ODA, M., KOISHIKAWA, I. AND HIGUCHI, T., 1978. Experimental study of anisotropic

- shear strength of sand by plane strain test. *Soils and Foundations*, Vol. 18, No. 1, pp. 25 - 38.
- OH-OKA, H., 1991, Unpublished. Up-to-date sampling techniques on sand and gravel by in situ freezing in Japan.
- O'NEILL, K. AND MILLER R.D., 1985. Numerical solutions for a rigid ice model of secondary frost heave. U.S. Army Cold Regions Research and Engineering Laboratory, CRREL Report 82 - 13.
- PARAMESWARAN AND MCKAY, 1983. Field measurements of electrical freezing potentials in permafrost areas. *Proc., 4th International Conference in Permafrost*, Fairbanks, National Academy Press, Washington. pp. 962 - 967.
- PENNER, E. 1959. The mechanism of frost heaving in soils. U.S. Highway Research Board, Bull. 225 pp. 1 - 22.
- PENNER, E. AND ELDRED, D., 1985. Equipment and methods for soil frost action studies. *Natl. Res. Counc. Canada, Div. Building Res. Intern. Rep.* 503.
- PENNER, E. AND UEDA, T., 1977. The dependence of frost heave on load applications, Preliminary results. *Proc., Symposium on Frost Action on Soils*, University of Luiea, Sweden, Vol. 1, pp 92 - 101.
- R. E. (Refrigeration Engineering), 1955. February, No. 2, p. 34.
- RADD, F.J. AND WOLFE, L.H., 1978. Ice lens structures, compression strenghts and creep behaviour of some synthetic frozen silty soils. *Proc., 1st International Symposium on Ground Freezing*, Bochum, Germany. pp. 115 - 130.
- RIEKE, R.D. AND VINSON, T.S., 1982. Correlative analysis of specific surface area and the frost heave susceptibility of soils. *Transportation Research Report 82 - 17*. Transportation Research Institute, Oregon State University, 107 p.
- RIEKE, R.D., VINSON, T.S. AND MAGEAU, D.W., 1983. The role of specific surface area and related index properties in the frost heave susceptibility of soils. *Proc., 4th International Permafrost Conference.*, Fairbanks, pp. 1066 - 1071.
- ROBERTSON, P.K., SEGO, D.C., DAVILA, R.S. AND SASSITHARAN, S., 1991. Development of ground freezing technology for procurement of undisturbed sediment samples. Report to the Dept. of Energy, Mines and Resources, Canada. DSS File No. OSC90 - 00335 -(009). 50 p.
- SANGER, F.J. AND SAYLES, F.H., 1978. Thermal and rheological computations for artificially frozen ground contraction. *International Symposium on Ground Freezing*, Bochum, pp. 1 - 23.
- SAYLES, F.H., 1988. State of the Art: Mechanical properties of frozen soil. *Proc., 5th International Symposium on Ground Freezing*, Nottingham, England. (Jones, R.H. and Holden, J.T, ed.). pp.143 - 165
- SCHMERTMANN, J.H., 1978. Guidelines for Cone Penetration Test, Performance and Design. Federal Highway Administration Report FHWA-TS-78-209. Washington D.C.

- SCOTT, R.F., 1959. The freezing process and mechanics of frozen ground. U.S. Army CRREL, Monograph MII-D1, 65 p.
- SEED, H.B., TOKIMATSU, K., HARDER, L.F. AND CHUNG, R.M., 1984. Report No. UCB/EERC-84/15, College of Engineering, University of Berkeley, Berkeley, California.
- SEED, H.B., WOODWARD, R.J. AND LUNDGREN, R., 1964. Fundamental aspects of the Atterberg limits. ASCE Journal of the Soil Mechanics and Foundation Division, Vol. SM3, pp. 75-105.
- SEGO, D.C., ROBERTSON, P.K. AND CYRE, G., 1990. Personal Communication.
- SINGH, S., SEED, H.B. AND CHAN, C.K., 1982. Undisturbed sampling of saturated sands by freezing ASCEJ, Vol. 108, No. GT2, pp. 247 - 264.
- SILVER, M.L., 1982. Undisturbed sampling of saturated sands by freezing. ASCE Journal, Geotechnical Div., GT2, pp. 247 - 264.
- SILVER, M.L., ISHIHARA, K. AND KITAGAWA, H., 1976. Undisturbed versus remolded cyclic strength of Niigata sand. ASCE Convention and Exposition, Chicago, 111. (Preprint 79).
- SMITH, G.R., 1962. Freezing solidifies tunnel shaft site. Construction Methods and Equipment, 44, No. 10, pp. 104 - 108.
- SMITH, M. AND TICE, A.R., 1988. Measurement of unfrozen water content of soils. Proc., 5th International Permafrost Conference, Trondheim, pp. 473 - 477.
- SKEMPTON, A.W., 1953. The colloidal "activity" of clays. Proc., 3rd ICSMFE, Switzerland, Vol 1, pp. 57 - 61.
- SRIDHARAN, A., RAO, S.M. AND MURTHY, N.S., 1988. Liquid Limit of kaolinitic soils. Géotechnique Vol. 38, No. 2, pp. 191 - 198.
- SUMGIN, M.I., 1929. Physico-mechanical processes in moist and frozen soils in connection with the bulging roads. Transpechat, Moskva.
- SVEC, O.J., 1989. A new concept of frost-heave characteristics of soils. Cold Regions Science and Technology, Vol. 16, pp. 271 - 279.
- TABER, S., 1929. Frost Heaving. Journal of Geology, Vol. 37, Vol 37, No. 5, pp. 428 - 461.
- TABER, S., 1930. The mechanics of frost heaving. Journal of Geology, Vol. 38, No. 4, pp. 303-317.
- TAIPING, Q., CHENCHUN, W., LUMIAN, W. AND HOISHAN, L., 1984. Liquefaction risk evaluation during earthquakes. Proc., International Conference on Case Histories in Geotechnical Engineering, St. Louis, Vol. 1, pp. 445 - 454.
- TAKAGI, S., 1980. The adsorption force theory of frost heaving. Cold Regions Science and Technology, Vol. 3, No. 1, pp. 57 - 81.
- TAKASHI, T., MATSUDA, M. AND YAMAMOTO, H., 1974. Experimental study on the

influence of freezing speed upon frost heave of soil under constant effective stress. Journal of the Japanese Society of Snow and Ice, 36, pp. 49 - 67.

TING, J.M., MARTIN, T. AND LADD, C.C., 1983. Mechanics of strenght for frozen sand. Journal of Geotechnical Engineering ASCE, 109(10). pp. 1286-1302.

TSYTOVICH, N.A., 1973. **Mechanics of Frozen Soil** (In Russian). Vysshaya Skhola Press Moskow. Translated by Scripta Technica Inc. (Swingzow, G.K. and Tschebotarioff, G.P., ed.) Scripta Book Co./McGraw-Hill Book Co. 1975. 426 p.

TSYTOVICH, N.A. AND SUMGIN, M.I., 1937. *Osnovaniya mekhaniki merzlykh gruntov*. (Fundamentals of frozen soil mechanics). Izd. AN SSSR, Moskva - Leningrad.

VAN GASSEN, W. AND SEGO, D.C., 1989. Problems with the segregation potential theory. Cold Regions Science and Technology, Vol. 17, pp. 95 - 97.

VINSON, T.S., AHMAD, F. AND RIEKE R.D., 1985. Factors important to the development of frost heave susceptibility criteria for coarse-grained soils. Transportation Research Record 1089, pp. 124 - 131.

WISSA, A.E. AND MARTIN, R.T. 1968. Behaviour of soils under flexible pavement: Development of rapid frost susceptibility tests. Massachusetts Institute of Technology, Dept. of Civil Eng. RR68-77 Soils Publication No. 224.

WILLIAMS, P.J., 1964. Unfrozen water content of frozen soils and soil moisture suction. Géotechnique 14, 231 - 246.

WILLIAMS, P.J., 1976. Volume change in frozen soils. Laurits Bjerrum Memorial Volume, Norwegian Geotechnical Institute, Oslo, pp. 233 - 246.

WINTERKORN, H.F., 1943. The condition of water in porous systems. Soil Science, Vol 56, No.4.

YOSHIMI, Y., HATANAKA, M. AND OH-OKA, H., 1977. A simple method for undisturbed sand sampling by freezing. Specialty Session 2 on Soil Sampling. Proc., 9th ICSMFE, Tokyo, Japan, pp. 23 - 28.

YOSHIMI, Y., HATANAKA M. AND OH-OKA, H., 1978. Undisturbed sampling of saturated sands by freezing. Soils and Foundations Vol. 18, No. 3, pp. 59 - 71.

YOSHIMI, Y., TOKIMATSU, K., KANEKO, O. AND MAKIHARA, Y., 1984. Undrained cyclic shear strength of a dense Niigata sand. Soils and Foundations, Vol. 24, No. 4, pp 131 - 145.

YOSHIMI, Y., HATANAKA, M., OH-OKA, H. AND MAKIHARA, Y. 1985. Liquefaction of sands sampled by in-situ freezing. Proc., 11th ICSMFE, San Francisco, Vol. 4, pp 1927 - 1930

YOSHIMI, Y., TOKIMATSU, K. AND HOSAKA, Y., 1989. Evaluation of liquefaction resistance of clean sands based on high-quality undisturbed samples. Soils and Foundations, Vol. 29, No.1, pp. 93 - 104.

APPENDIX A

Derivation of the Segregation Potential (After Konrad and Morgenstern, 1980)

The secondary heave model recognizes the existence of a zone between the frost heave where free porewater freezes and the base of the forming ice lens (Miller, 1972, 1978). A suction gradient develops due to the existence of unfrozen adsorbed water behind the frost front. The suction at the top of the ice lens can be shown to be related linearly to the segregational freezing temperature using the Clausius-Clapeyron equation. This can be derived by assuming that the ice lens is under zero external pressure. By virtue of the Clausius-Clapeyron equation the water pressure at the base of the ice lens is:

$$P_w = (L/V_w) \ln(T_s^*/T_0^*) \quad [A.01]$$

where P_w is the suction in the liquid film; L is the latent heat of fusion of water; V_w is the specific volume of water; T_0^* is the temperature of the freezing point of pure water (K); and T_s^* is the segregation freezing temperature (K). Dissolved salts are not considered in this equation. For T_s^* very close to T_0^* , equation A.01 reduces to:

$$P_w = (L/V_w T_0^*) T_s = M T_s \quad [A.02]$$

where $T_s = T_s^* - T_0^*$ is the segregation-freezing temperature in degrees Celsius; and M is a constant.

In terms of total head, equation A.02 becomes:

$$H_w = (P_w/\gamma_w) + h_e \quad [A.03]$$

where γ_w is the unit weight of water; and h_e is the elevation head. Neglecting the elevation head, equation A.03, reduces to:

$$H_w \cong (P_w/\gamma_w) = (M/\gamma_w) T_s = M' T_s \quad [A.04]$$

hence,

$$M' = \frac{H_w}{T_s} \quad [A.05]$$

Assuming that there is no accumulation within the frozen fringe and that Darcy's law holds, the mean velocity can be expressed as:

$$v = -K(z)\partial h/\partial z \quad [A.06]$$

Considering a two layered system, that is the unfrozen soil and the frozen fringe, the velocity of water through the frozen fringe can be approximated by equation A.05, using

$$v = K_{ff} \frac{\Delta H}{d} \quad [A.07]$$

where K_{ff} is the average permeability of the frozen fringe; ΔH is the head difference between the base of the ice lens and the frost front; and d is the frozen fringe thickness.

The head difference between the base of the ice lens and the frost front is:

$$\Delta H = H_w - h_u \quad [A.08]$$

where h_u is the suction at the frost front. The suction at the frost front can be determined by Darcy's equation applied through the unfrozen soil assuming that steady state flow exists through the unfrozen soil. The thickness of the frozen fringe d can be determined from the temperature gradient in the frozen fringe and the segregational freezing temperature, assuming that the temperature profile through the frozen fringe is linear.

$$d = \frac{T_s}{\text{grad } T_{ff}} \quad [A.09]$$

where $\text{grad } T_{ff}$ is the temperature gradient through the frozen fringe.

Combining equations A.07, A.08 and A.09 yields the following expression

$$v = K_{ff} \left(\frac{H_w - h_u}{T_s} \right) \text{grad } T_{ff} \quad [A.10]$$

or

$$v = SP_o \text{ grad } T_{ff} \quad [A.11]$$

where

$$SPo = K_{ff} \left(\frac{H_w - h_u}{T_s} \right) \quad [A.12]$$

Combining equation A.05 and A.12, yields

$$SPo = K_{ff} M' \quad [A.13]$$

Finally the integration of segregational heave rate over the duration of freezing gives the segregational heave $h_s(t)$:

$$h_s(t) = \int_0^t \frac{dh_s}{dt} dt = 1.09 \int_0^t v(t) dt \quad [A.14]$$

Hence, the total segregational heave will be determined by the semiempirical equation:

$$h_s = 1.09 SPo \text{ grad } T_{ff} \quad [A.15]$$

APPENDIX B

Khakimov's Method

The method proposed by Khakimov (1957) makes possible to conduct studies and solve very complex and practically important problems in the field of soil freezing. The method is based on the following assumptions:

a) The unsteady motion of heat is considered as a succession of stationary states, i.e., it is assumed that the temperature distribution in the soil in the course of a certain time interval is stationary and a function of the radius (r) only.

b) It is assumed that a linear relationship exists between the freezing radius (ξ), defined as the distance from the freezing pipe to the freezing front, and the heat source radius (R) defined as the distance from the freezing pipe to the point in the soil where the temperature has remained the same as before freezing. Therefore:

$$\xi = aR \quad [B.01]$$

where a is the proportionality factor. If the beginning of the freezing process is excluded R increases with the increase of ξ , and their ratio remains constant. The accuracy of the determination of R (just as of ξ) is a function of the accuracy of temperature measurements.

c) The soil iciness at a certain mean value of the subzero temperature is considered as a constant magnitude.

Due to the motives mentioned in section 3.2.1, Khakimov (op. cit.) was lead to the problem of disturbance of the natural structure of the saturated sand. Khakimov solves this problem for an axisymetrical geometry case where a sand deposit lies between layers of clayey soil and emerges to the surface at a considerable distance if compared with the distance of the sand layer. The rate of freezing and the amount of water squeezed out are uniform over the entire height of the sand layer. The amount of water squeezed out (m^3) during the growth of the freezing radius (R) by dR (in the course of time dt) is

$$\pi * [(\xi + d\xi)^2 - R^2] \cdot 1 \cdot n \cdot \alpha = KI 2\pi R \cdot 1 \cdot dt \quad [B.02]$$

Neglecting 2nd order infinitesimals, is obtained

$$\frac{d\xi}{dt} = \frac{KI}{n\alpha} \quad [B.03]$$

where α is the coefficient of water expansion during its transformation into ice ($\alpha =$

0.091); n is the sand porosity; k is the sand permeability (m/h); I is the hydraulic gradient.

This problem will be solved by the following equation

$$t = A \left(\xi^2 \ln \frac{\xi}{r_0} - \frac{\xi^2 - r_0^2}{r_0} \right) + B \frac{\xi^2 - r_0^2}{2} \quad [\text{B.04}]$$

where

$$A = \frac{1}{2\lambda(U_0 - U_m)} \left[(1 - n)W\gamma_i\delta + c_1\gamma_1 U_m + c_2\gamma_2 U_m \left(\frac{a^2 - 1}{2 \ln a} - 1 \right) \right] \text{ and } B = \frac{c_1\gamma_1}{2\lambda_1}$$

The differentiation of equation B.04 gives then

$$\frac{d\xi}{dt} = \frac{1}{\left(2A \ln \frac{\xi}{r_0} + B \right) \xi} \quad [\text{B.05}]$$

The substitution of equation B.05 in equation B.04 yields

$$K = \frac{na}{I \left(2A \ln \frac{\xi}{r_0} + B \right) \xi} \quad [\text{B.06}]$$

Equation B.06 connects the permeability to the rate of freezing of saturated sand at given temperature, thermophysical and other sand characteristics. It follows then:

a) at

$$K \geq \frac{na}{I \left(2A \ln \frac{\xi}{r_0} + B \right) \xi} \quad [\text{B.07}]$$

water will be squeezed out at the freezing boundary and will move into the second zone without disturbing the natural structure of the sand;

b) at

$$K < \frac{na}{I \left(2A \ln \frac{\xi}{r_0} + B \right) \xi} \quad [\text{B.08}]$$

the squeezing out of water, reflects Khakimov, may be accompanied by the drawing apart of the particles, i.e., by a disturbance of the natural sand structure.

If the permeability and the thermophysical properties of the sand are known, it is possible by means of inequation B.07 to select temperature conditions of freezing such that equation B.06 will be satisfied. According to Khakimov the set of formulas B.04, B.05 and B.06 solves the controversial question of the disturbance or preservation of the natural structure of saturated sand during freezing. In order to use equation B.06, it is necessary to know the hydraulic gradient I . The value of I depends on the conditions of bedding of the saturated layer and can be determined by solving the hydromechanical problem (either graphically or analytically). Khakimov (op. cit.) finds useful to simplify this question by considering the conditions imposed to the axisymmetrical problem and assuming that

$$I = \frac{H}{L + H} \quad [B.09]$$

where H is the depth of the saturated sand layer emerging at a distance L from the freezing zone. The substitution of this value of the gradient in equation B.09 yields

$$K = \frac{n\alpha\left(\frac{L}{H} + 1\right)}{\left(2A\ln\frac{\xi}{r_0} + B\right)\xi} \quad [B.10]$$

It follows from here that if condition in equation B.10 is satisfied at the start of the freezing, it will subsequently be even satisfied even for lesser values of k . In general k must be maximum at $\xi = r_0$; however, taking into account that the natural sand structure in the immediate vicinity of the freezing pipe may be disturbed as a result of the drilling operation, is assumed for practical purposes that $\xi = 2r_0$.

APPENDIX C

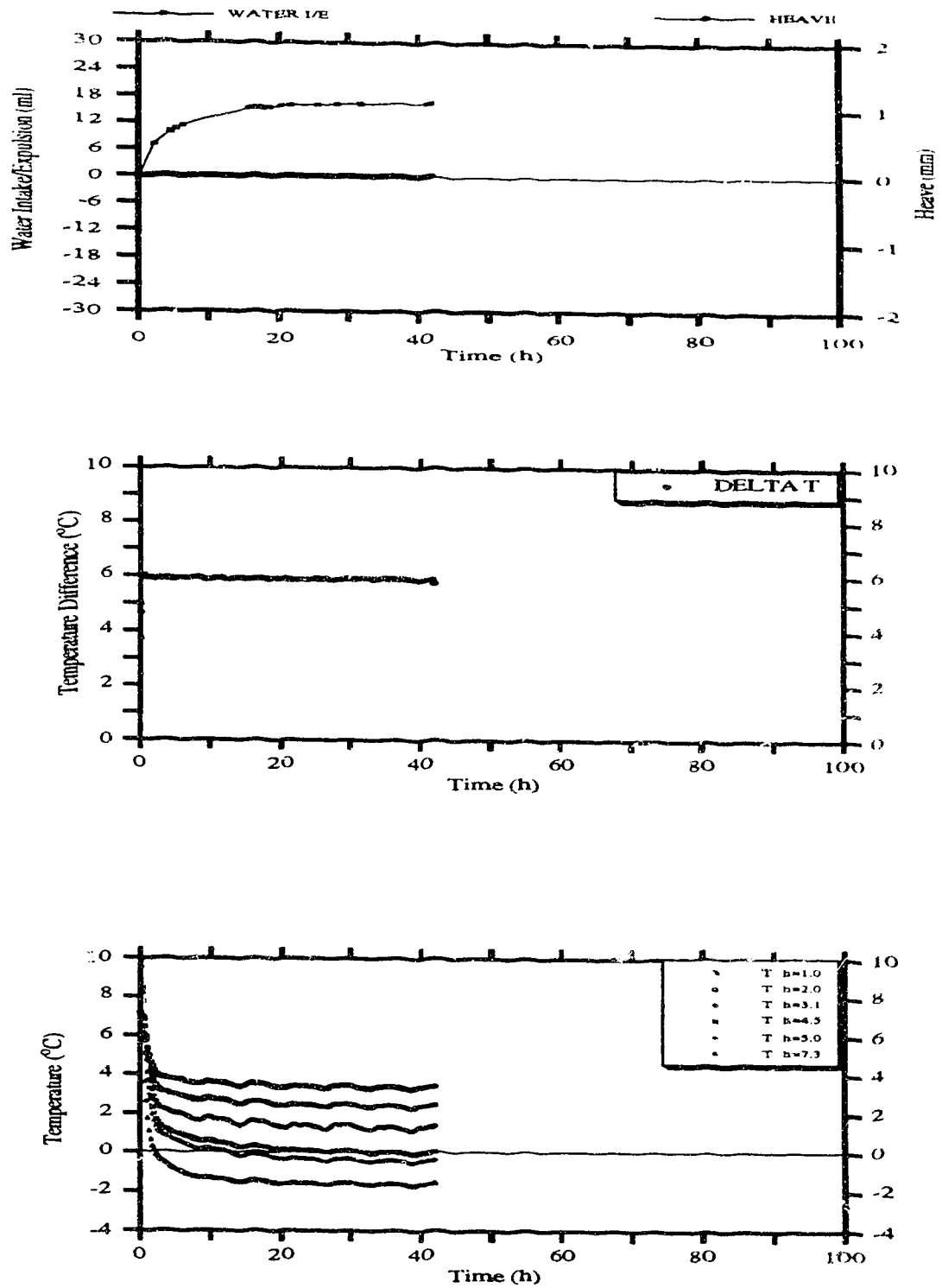


Figure C-01.- UFT 14. Specimen D005

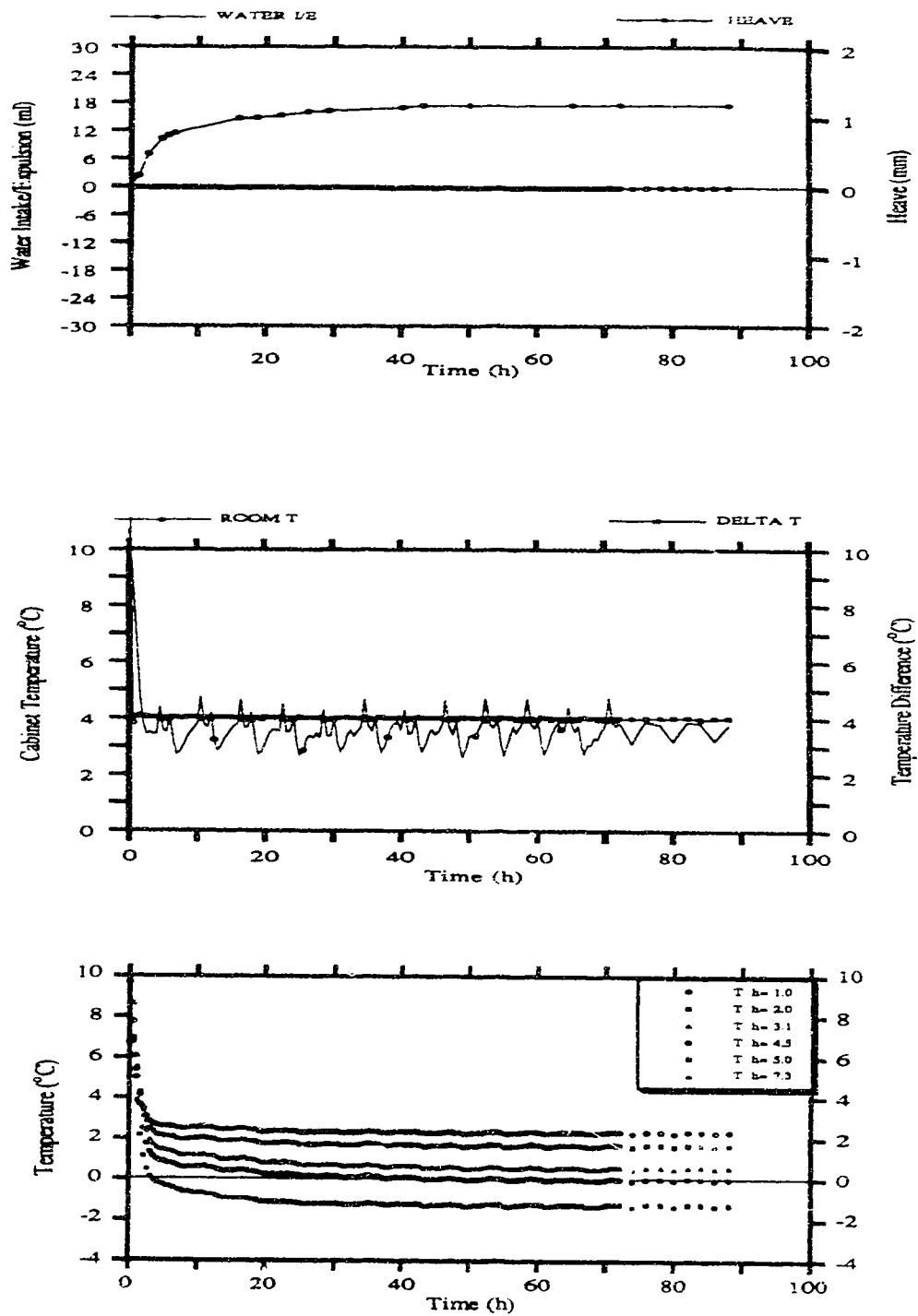


Figure C-02.- UFT 26. Specimen D006

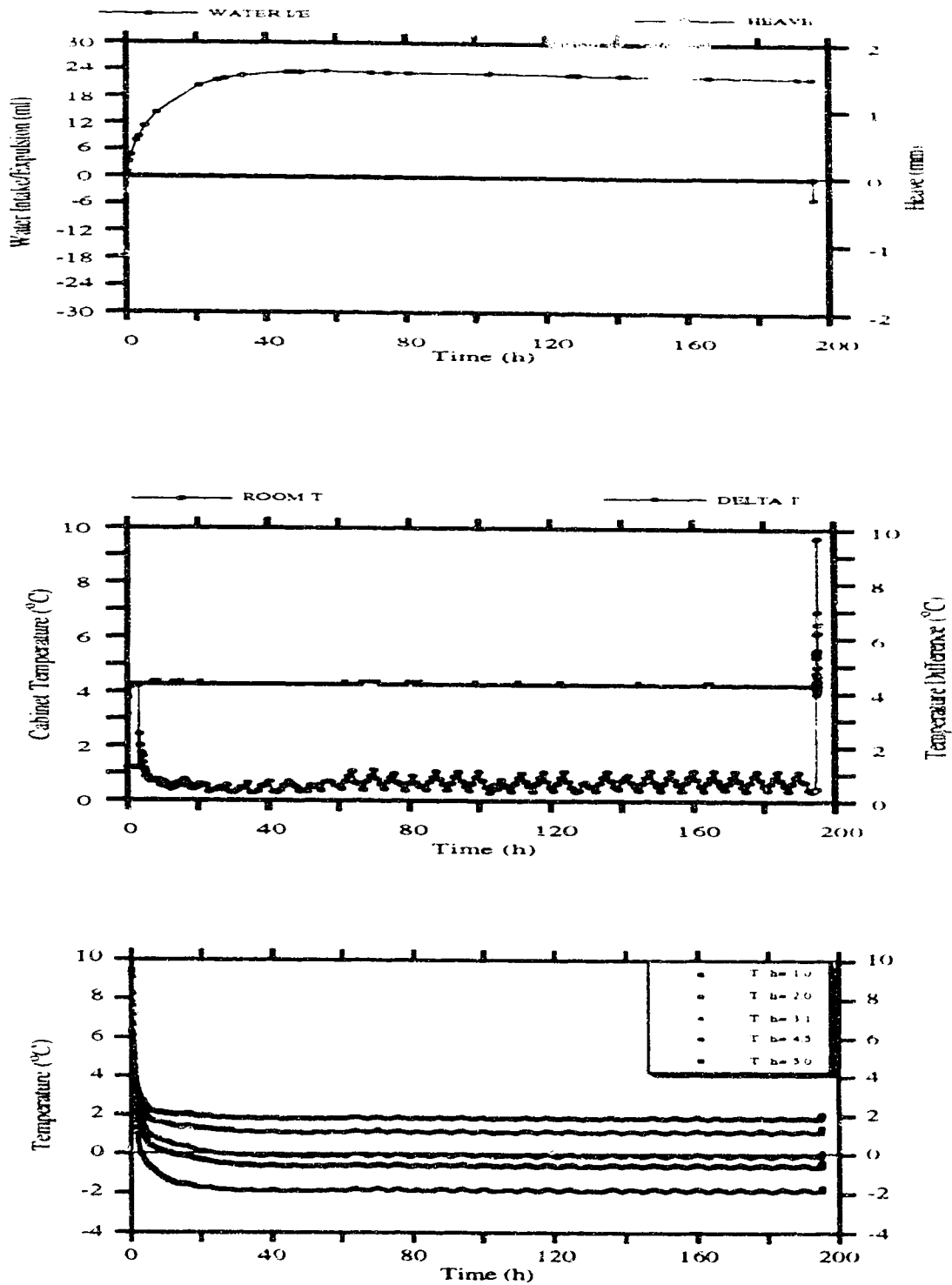


Figure C-03.- UFT 22. Specimen LT01DO

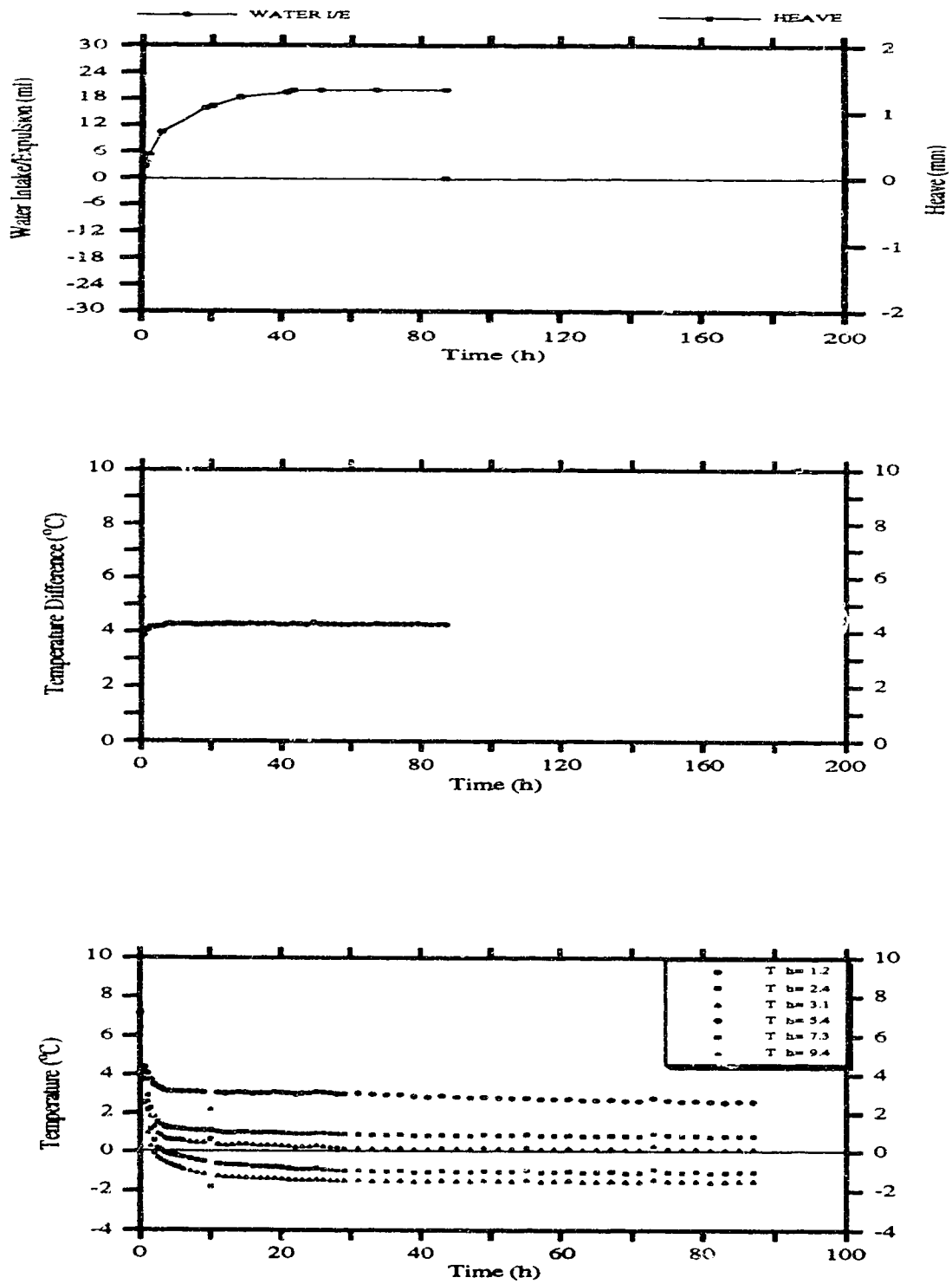


Figure C-04.- UFT 25. Specimen LT02D0

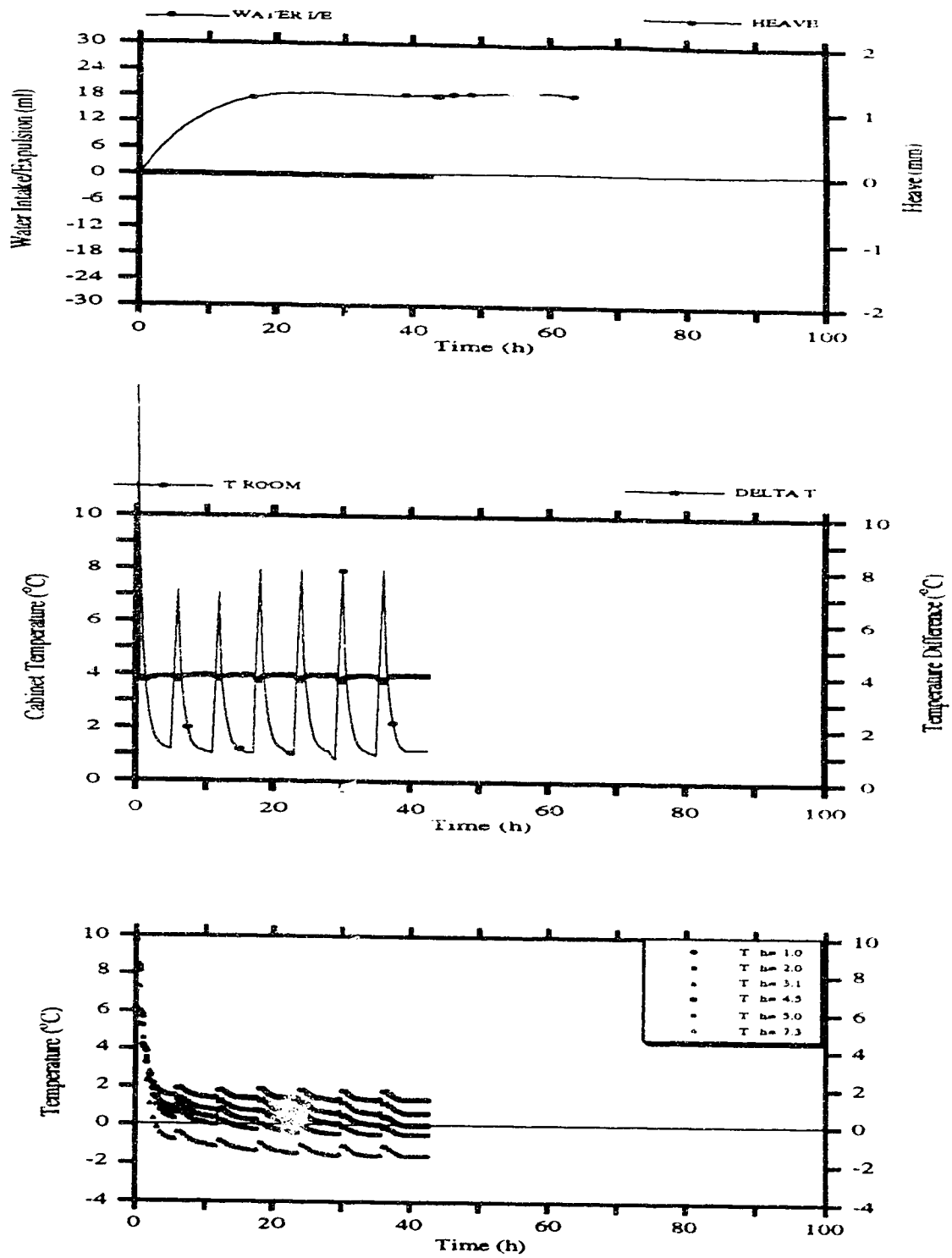


Figure C-05. UFT 38. Specimen D1100

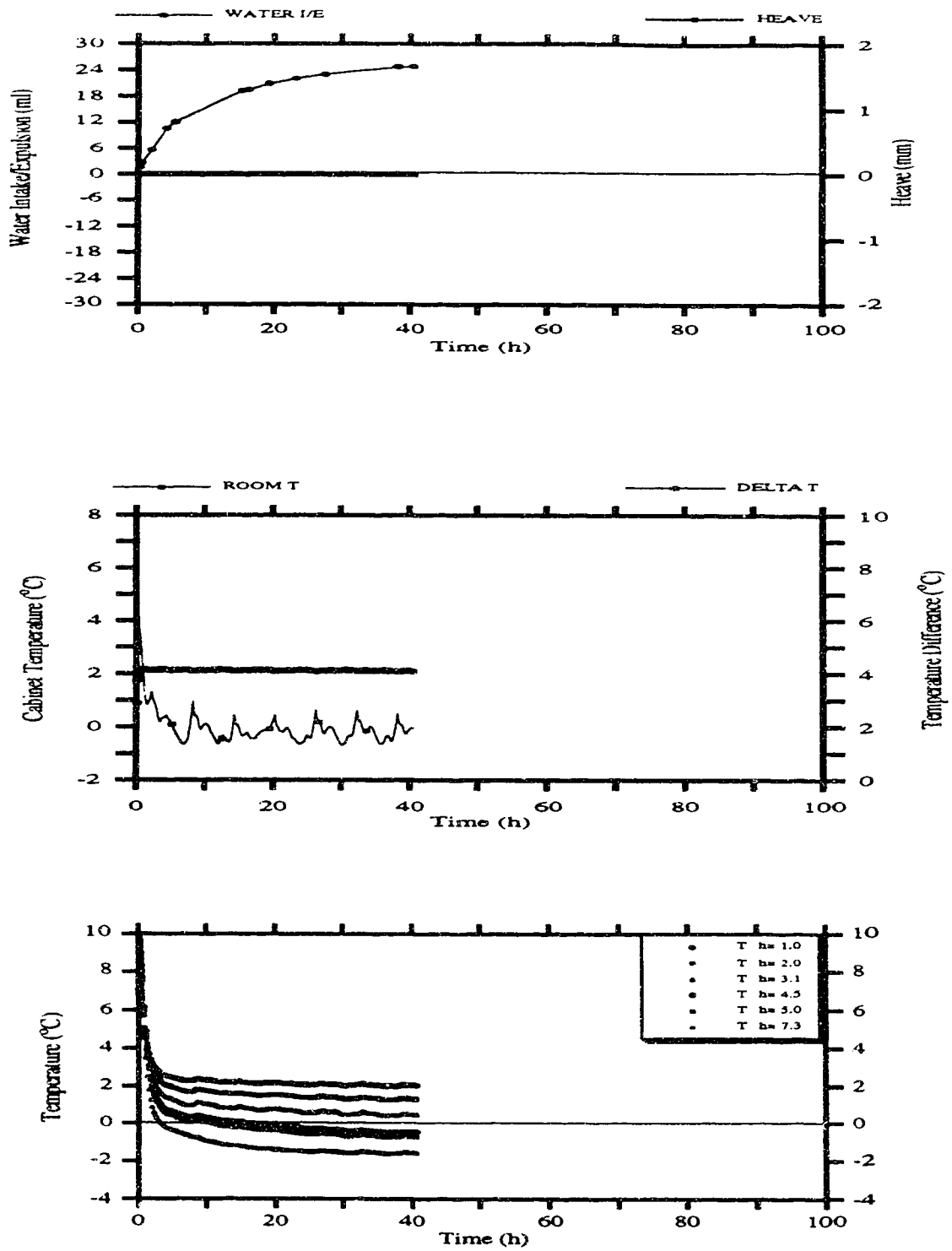


Figure C-06. UFT 17. Specimen D202

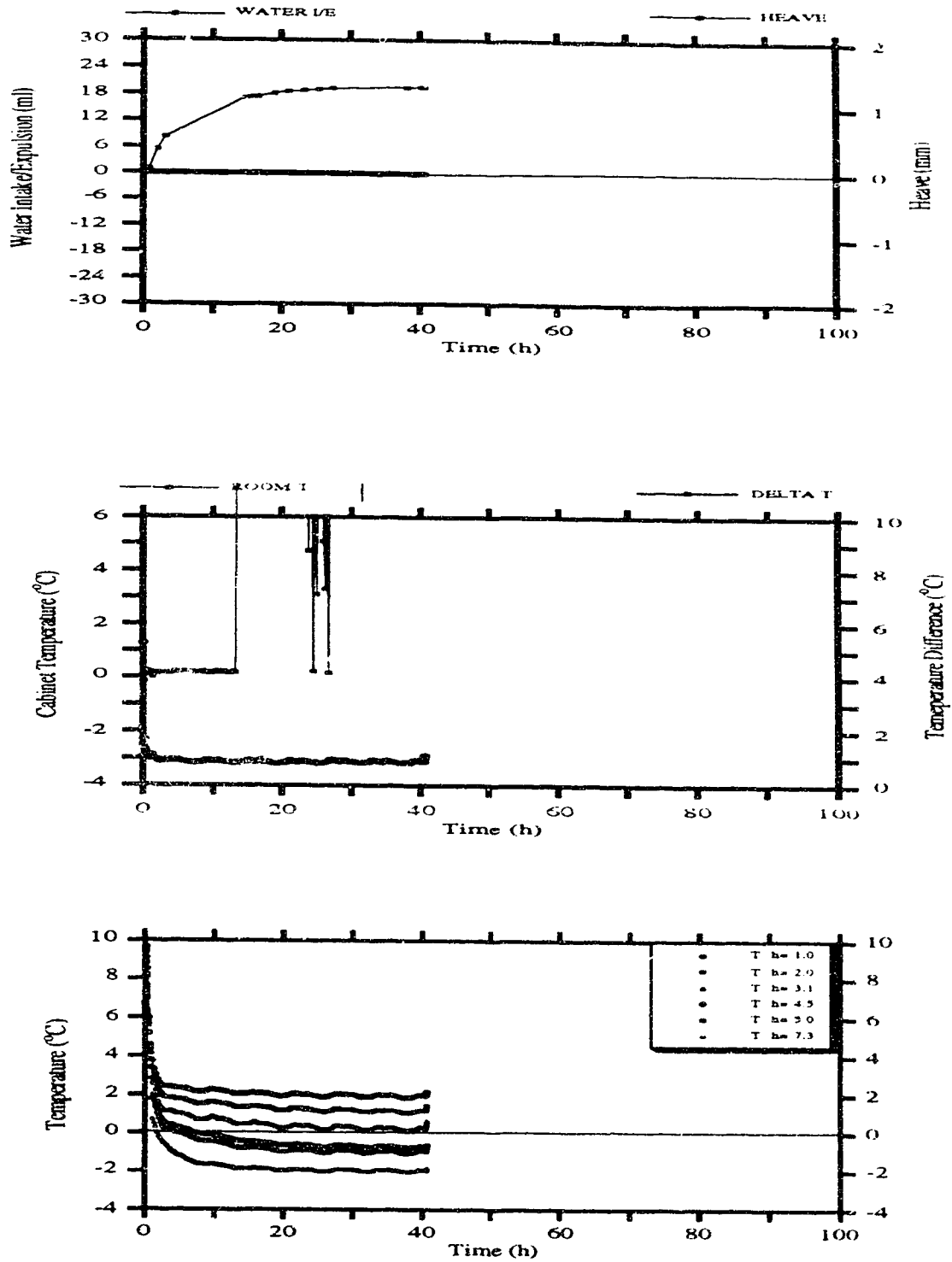


Figure C-07.- UFT 19. Specimen D2CS20

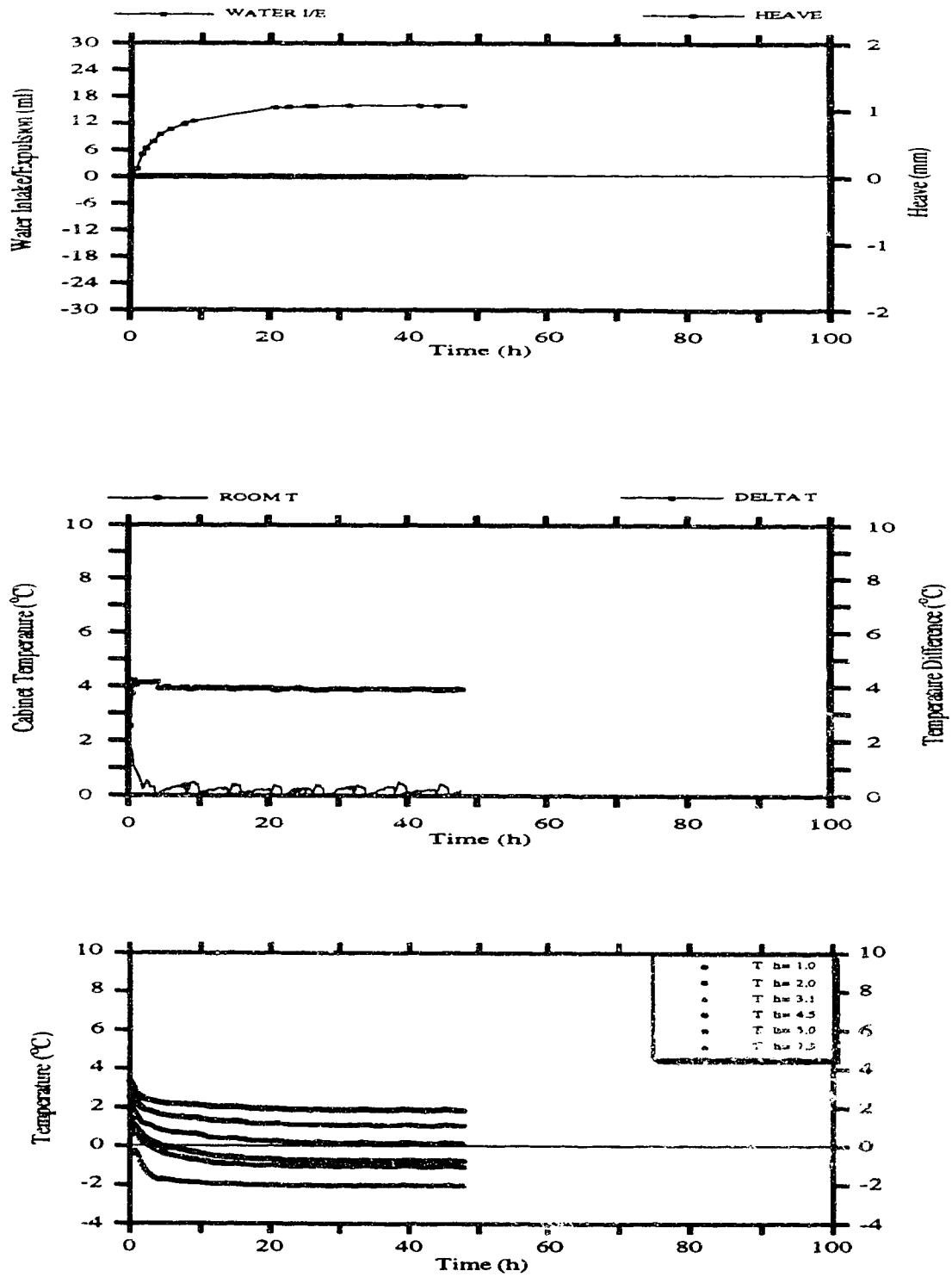


Figure C-08.- UFT 20. Specimen D2CS30

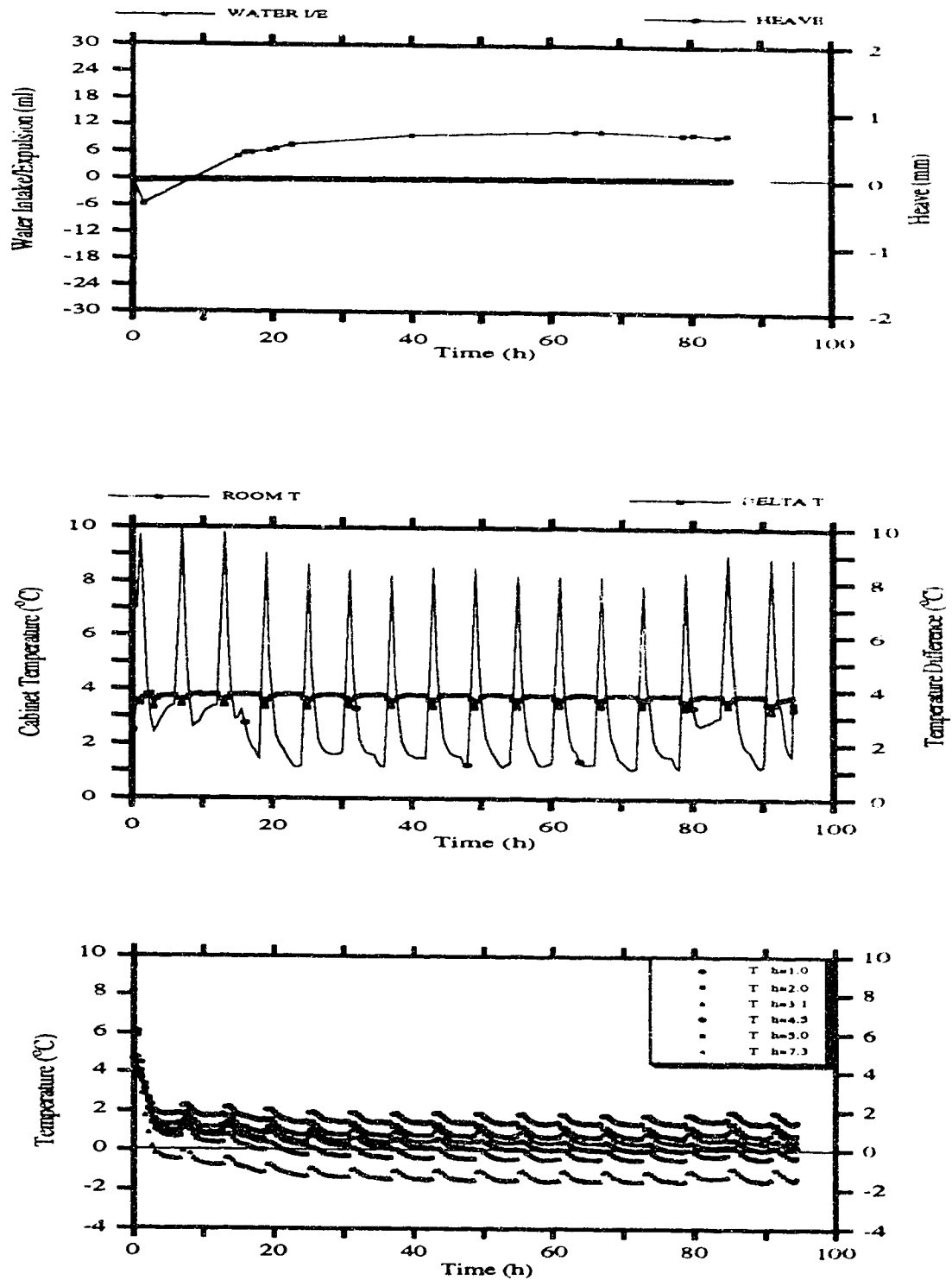


Figure C-09. UFT 32. Specimen D2DS05

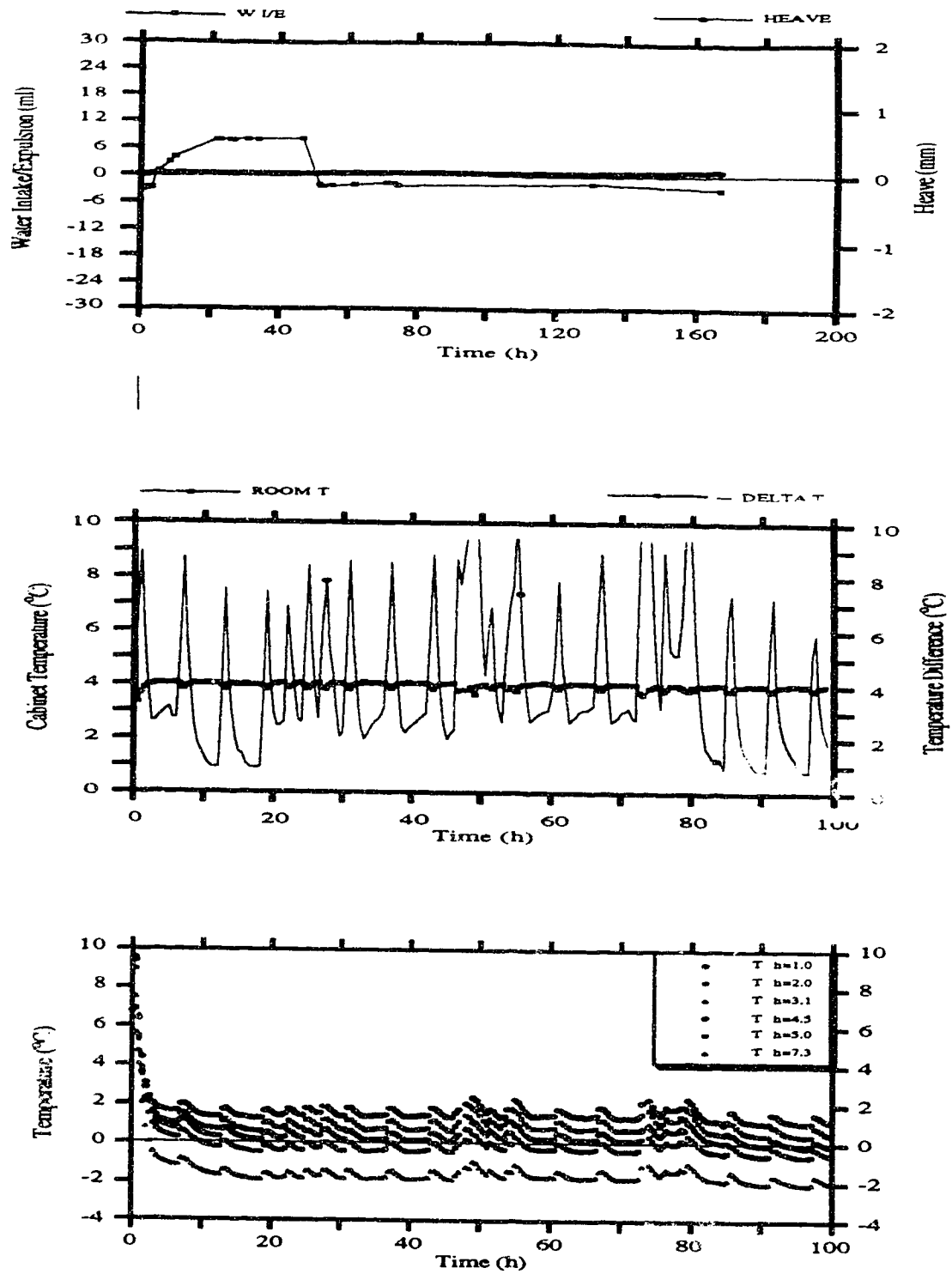


Figure C-10.- UFT 33. Specimen D2DS10

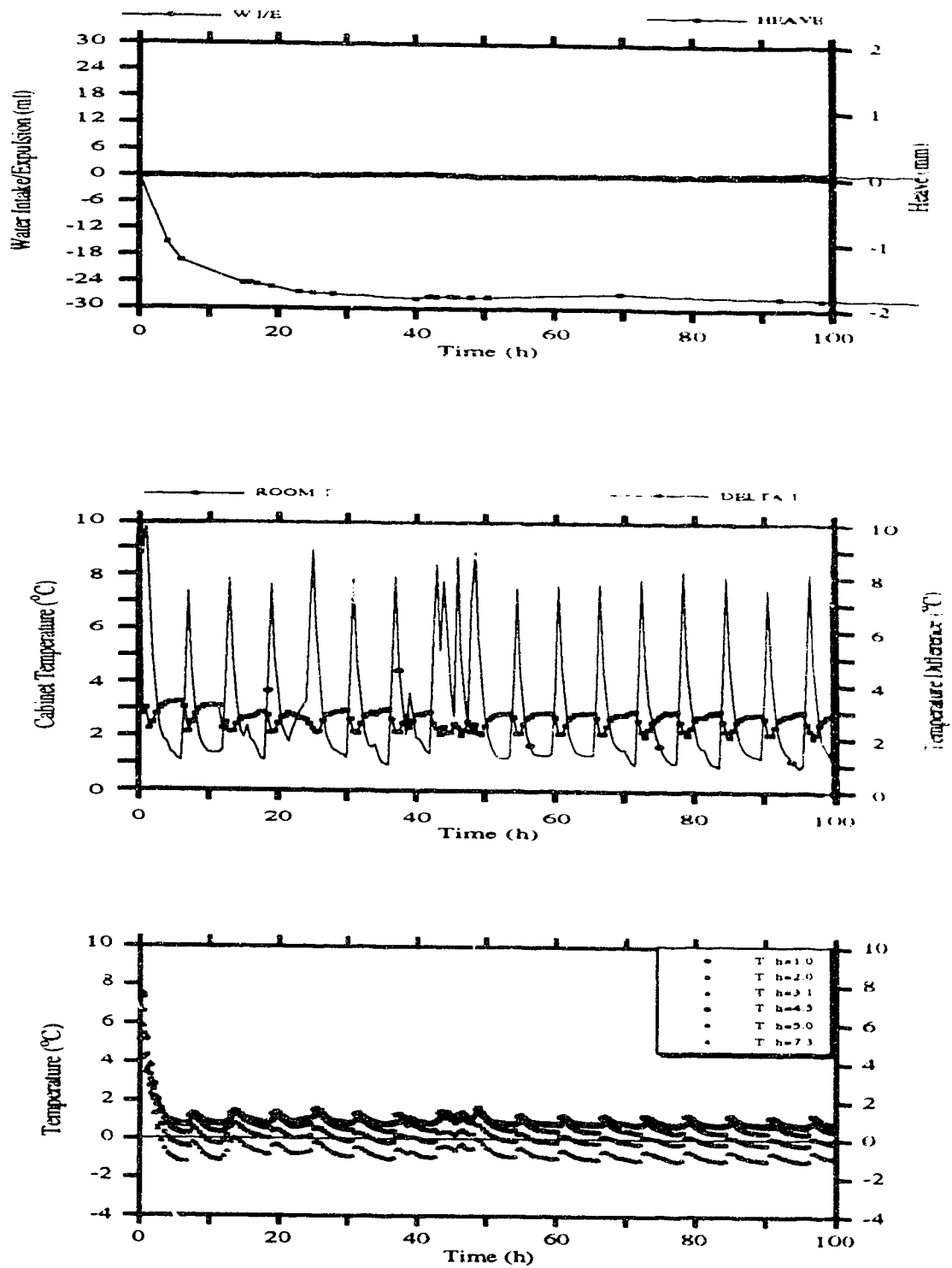


Figure C-11.- UFT 35. Specimen D2DS20

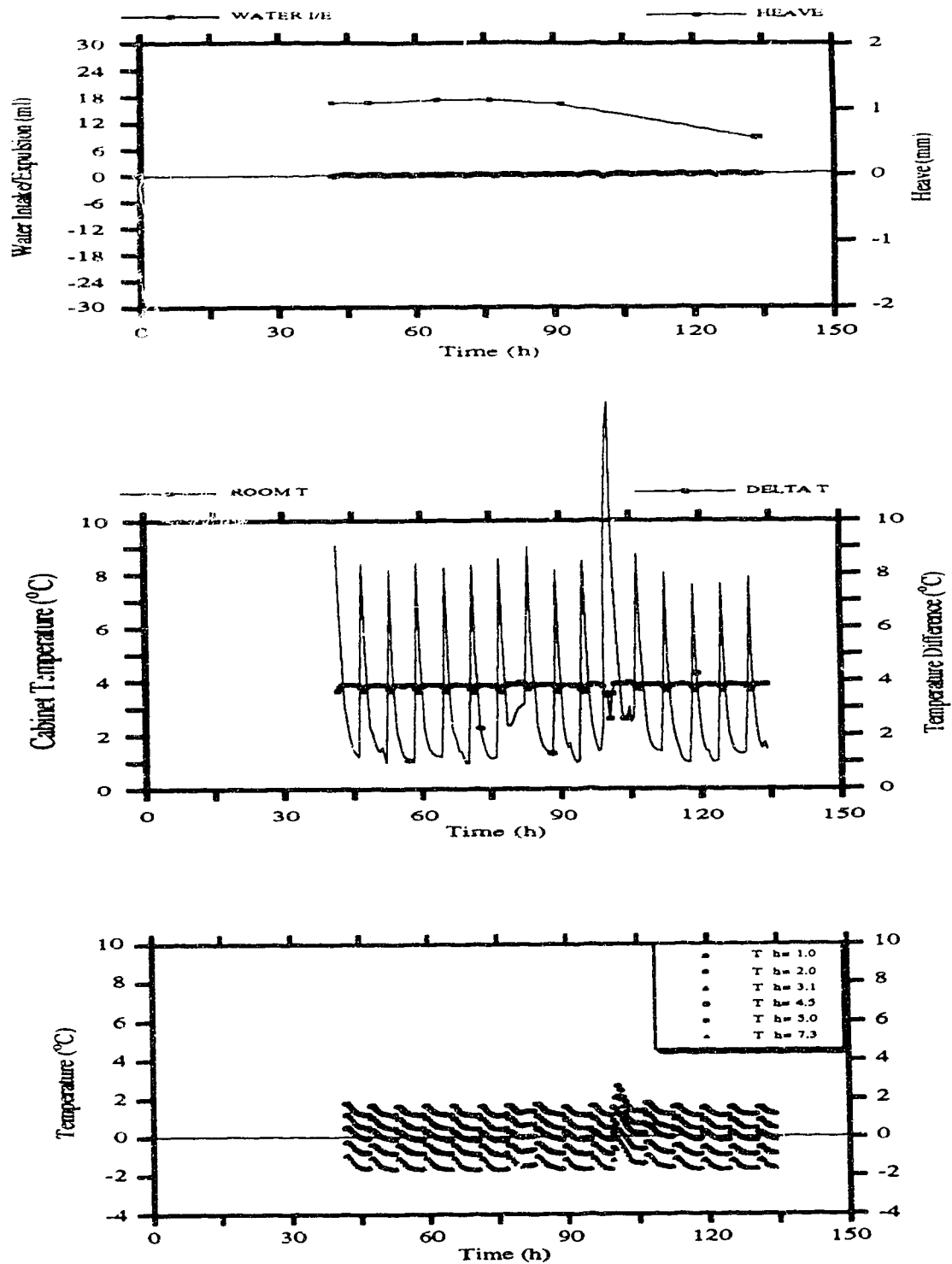


Figure C-12.- UFT 41. Specimen D2IL05

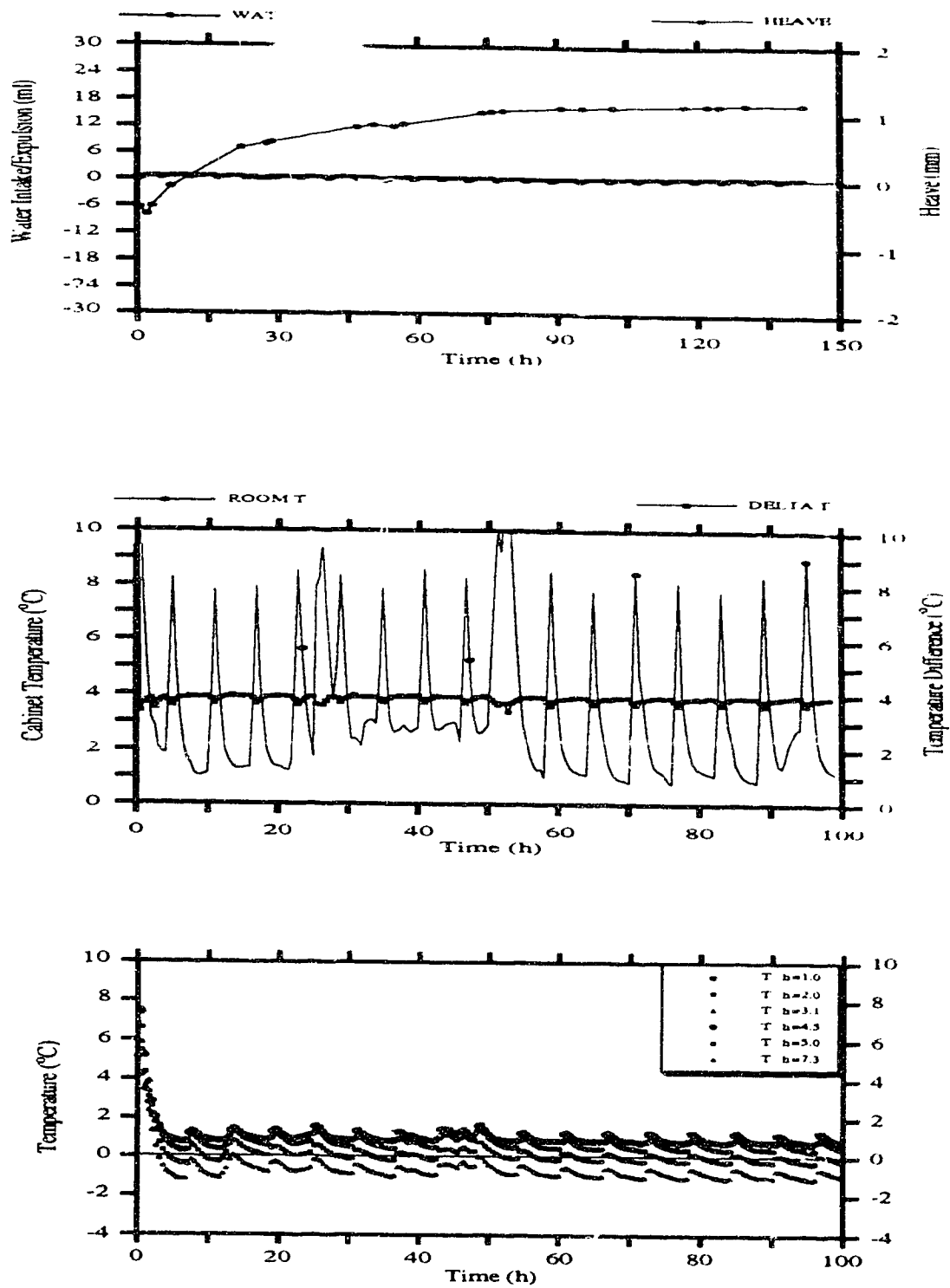


Figure C-13.- UFT 39. Specimen D2IL10

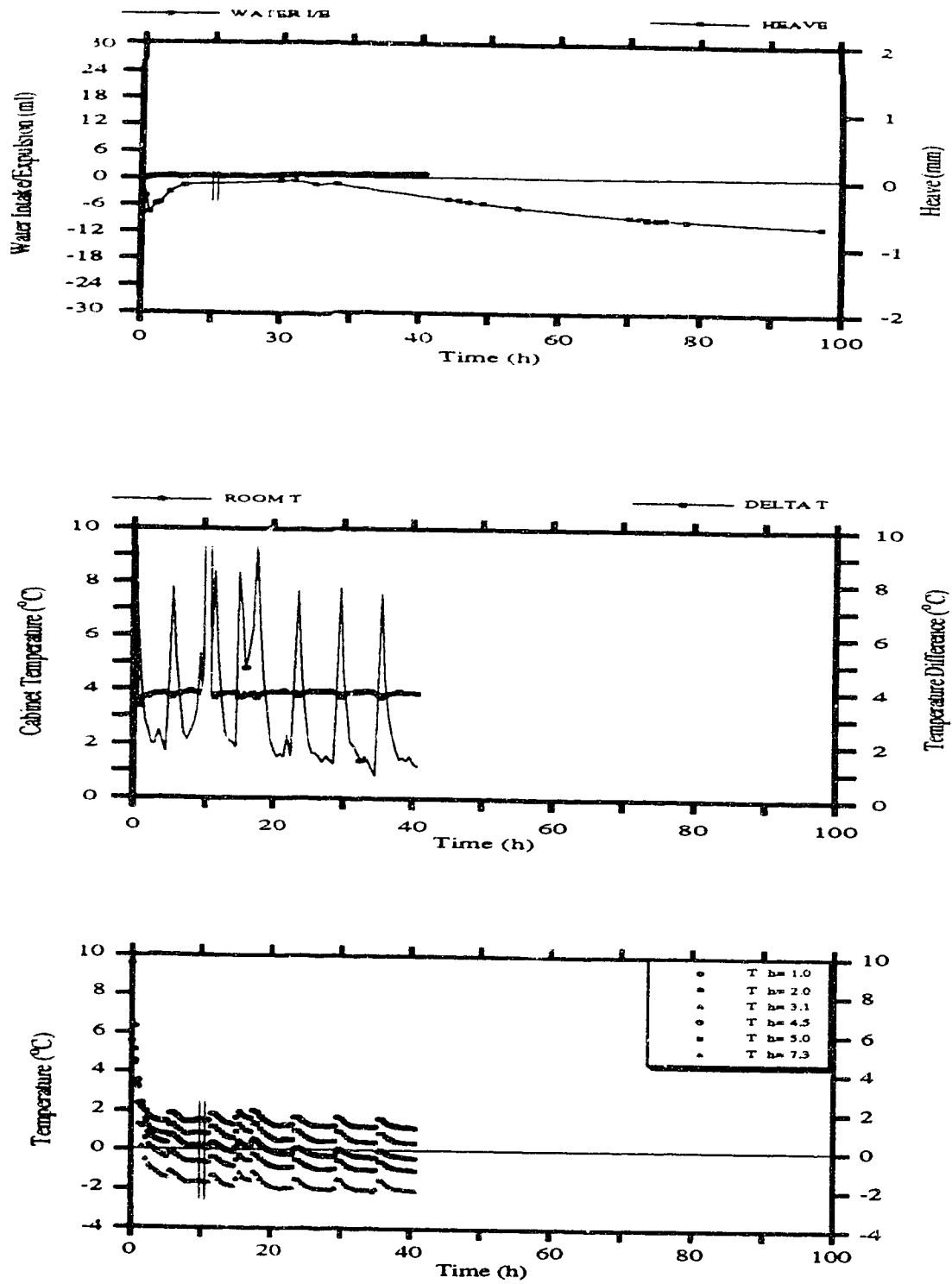


Figure C-14.- UFT 37. Specimen D2IL20

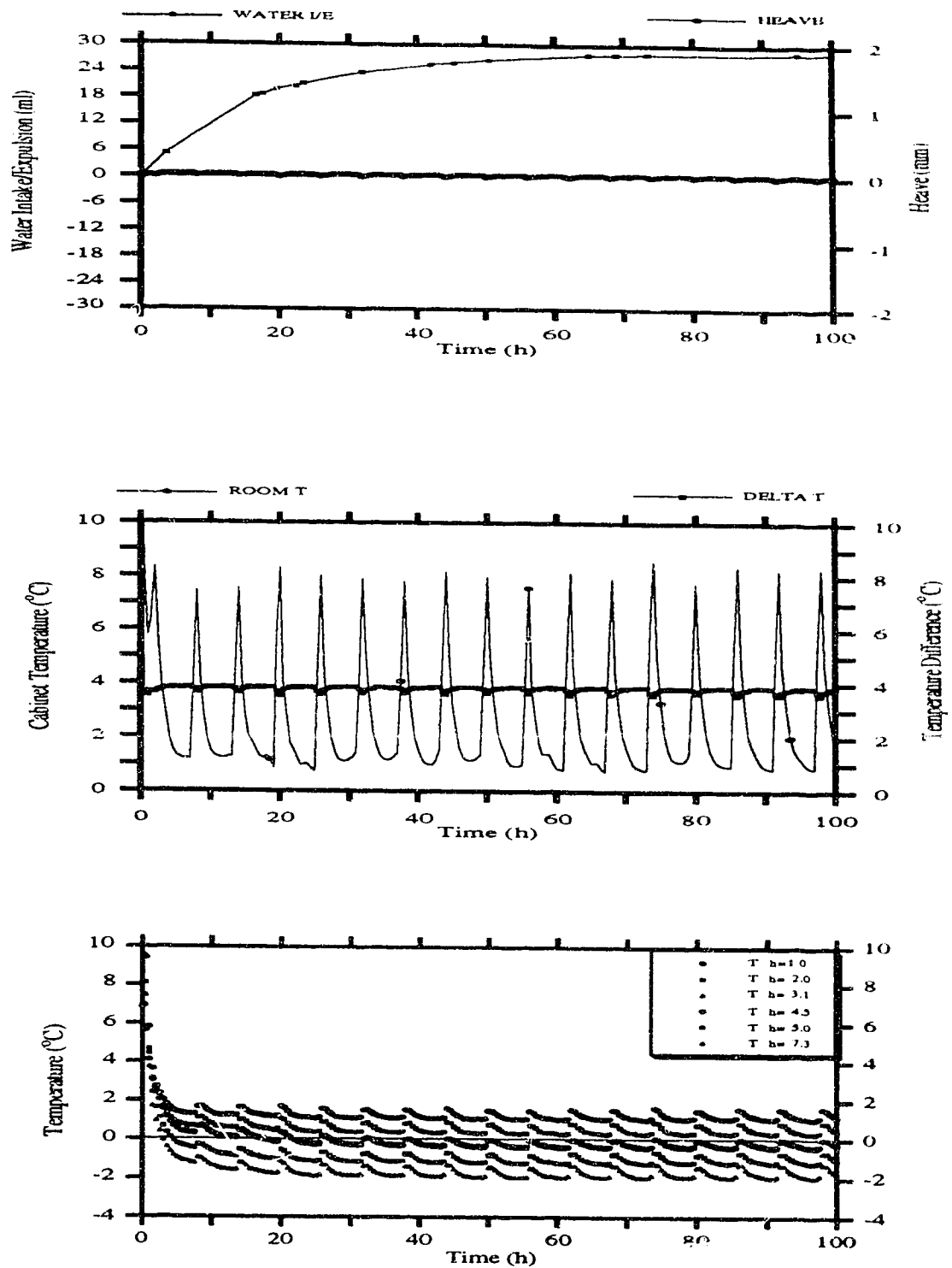


Figure C-15.- UFT 42. SpecimenD2IL102

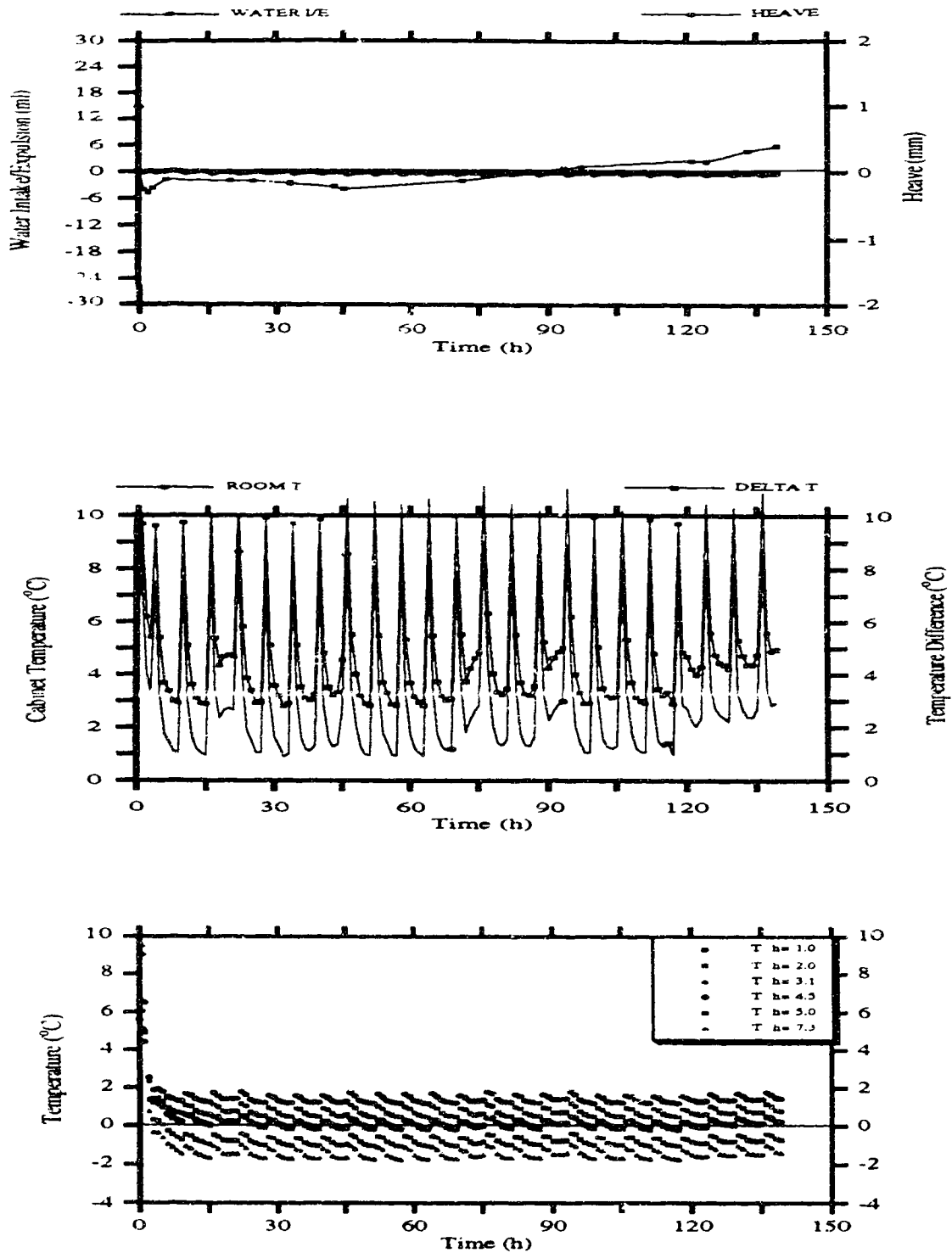


Figure C-16.- UFT 43. Specimen D2IL202

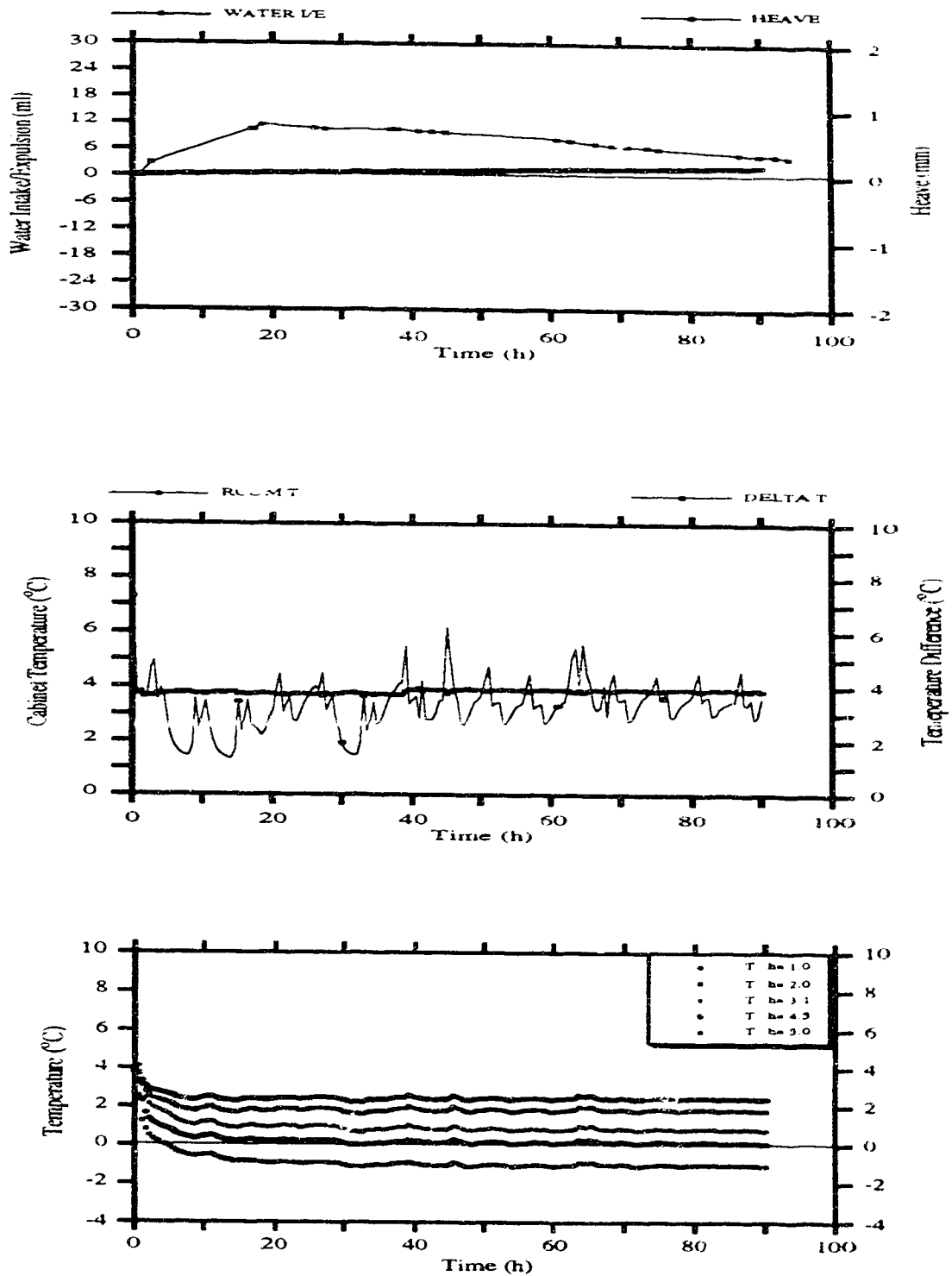


Figure C-17.- UFT 28. Specimen D2KL05

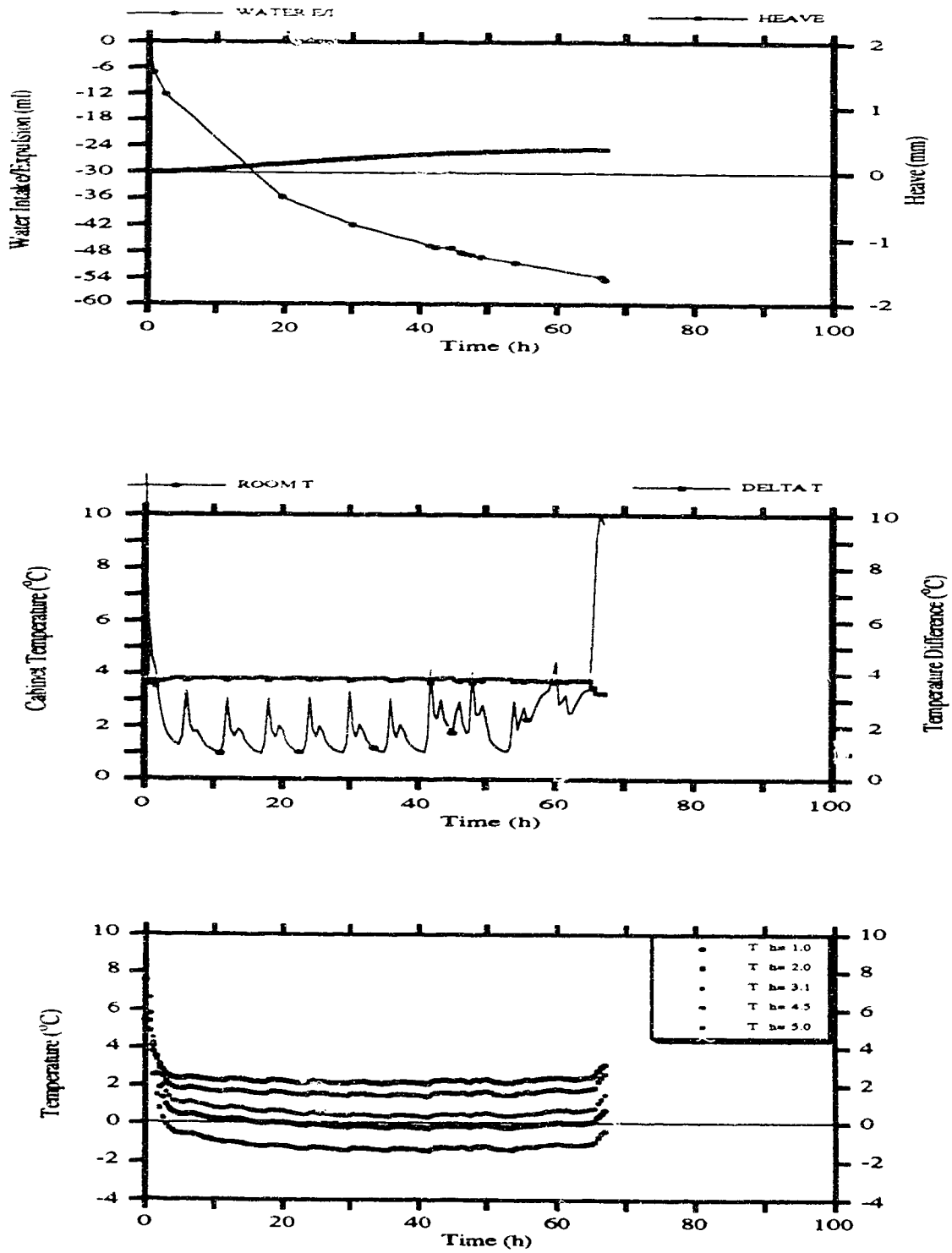


Figure C-18 - UFT 30. Specimen D2KL10

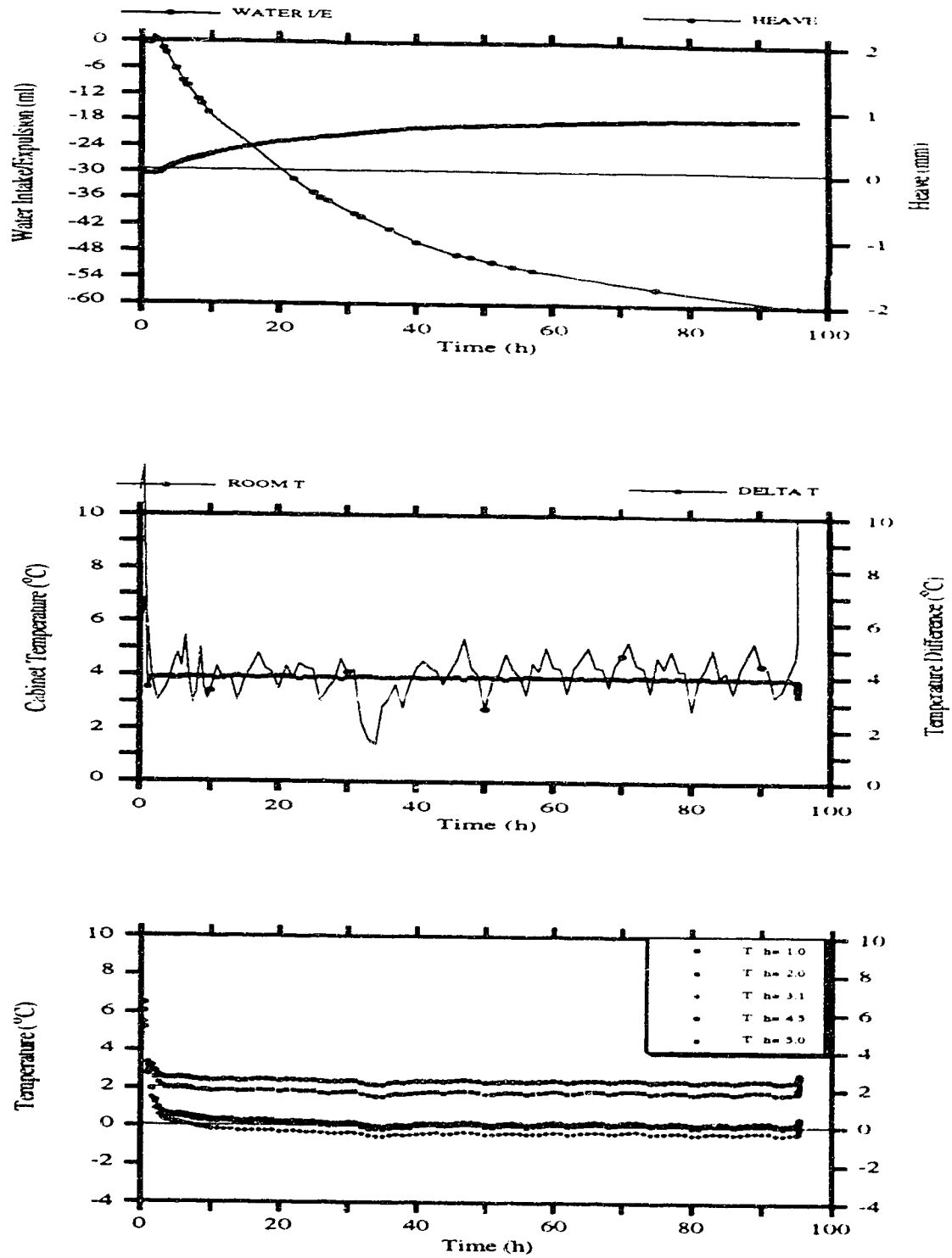


Figure C-19.- UFT 27. Specimen D2KL20

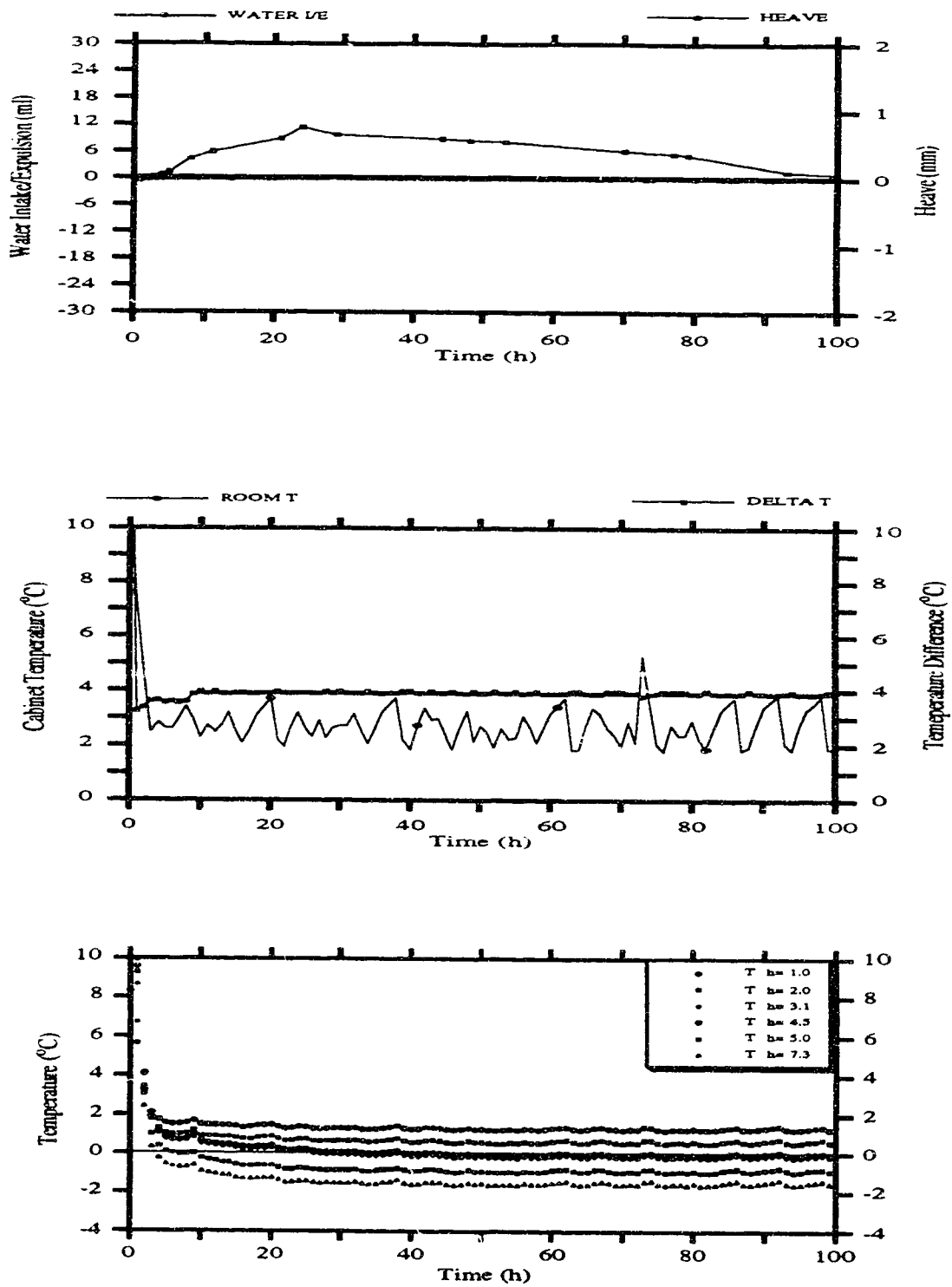


Figure C-20.- UFT 44. Specimen D2KL052

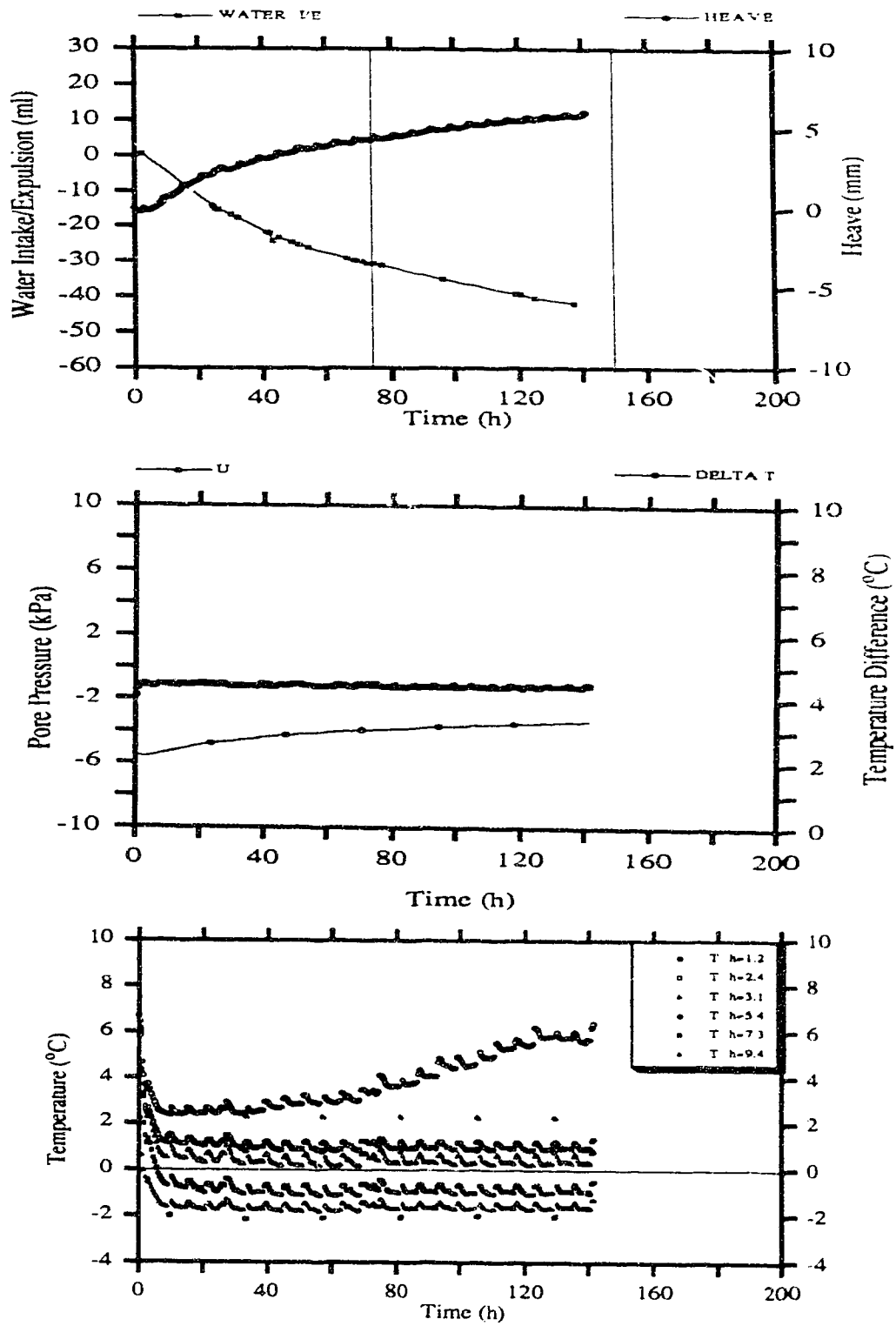


Figure C-21.- UFT 34. Specimen MSKL20

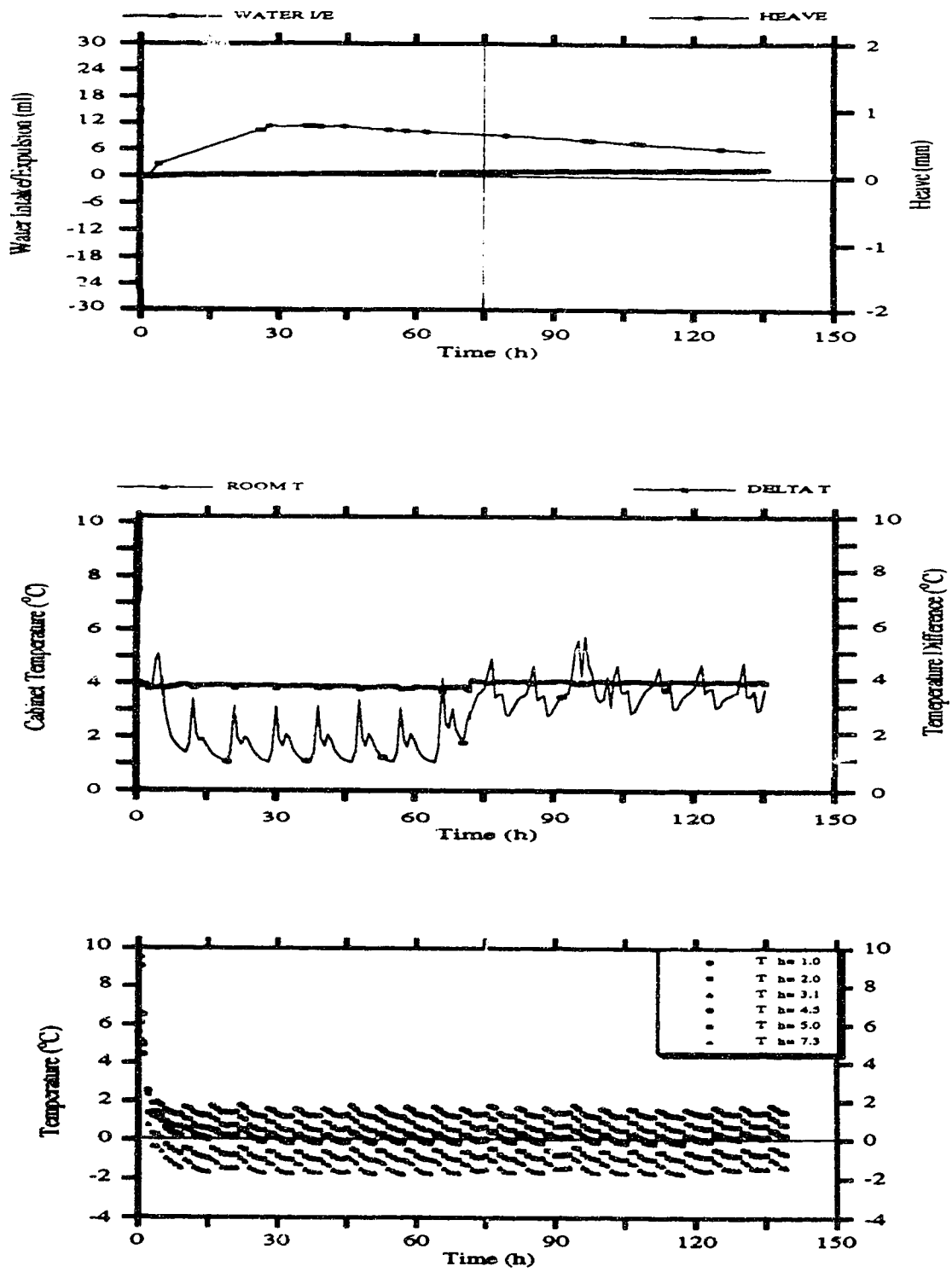


Figure C-22. UFT 40. Specimen MSIL10

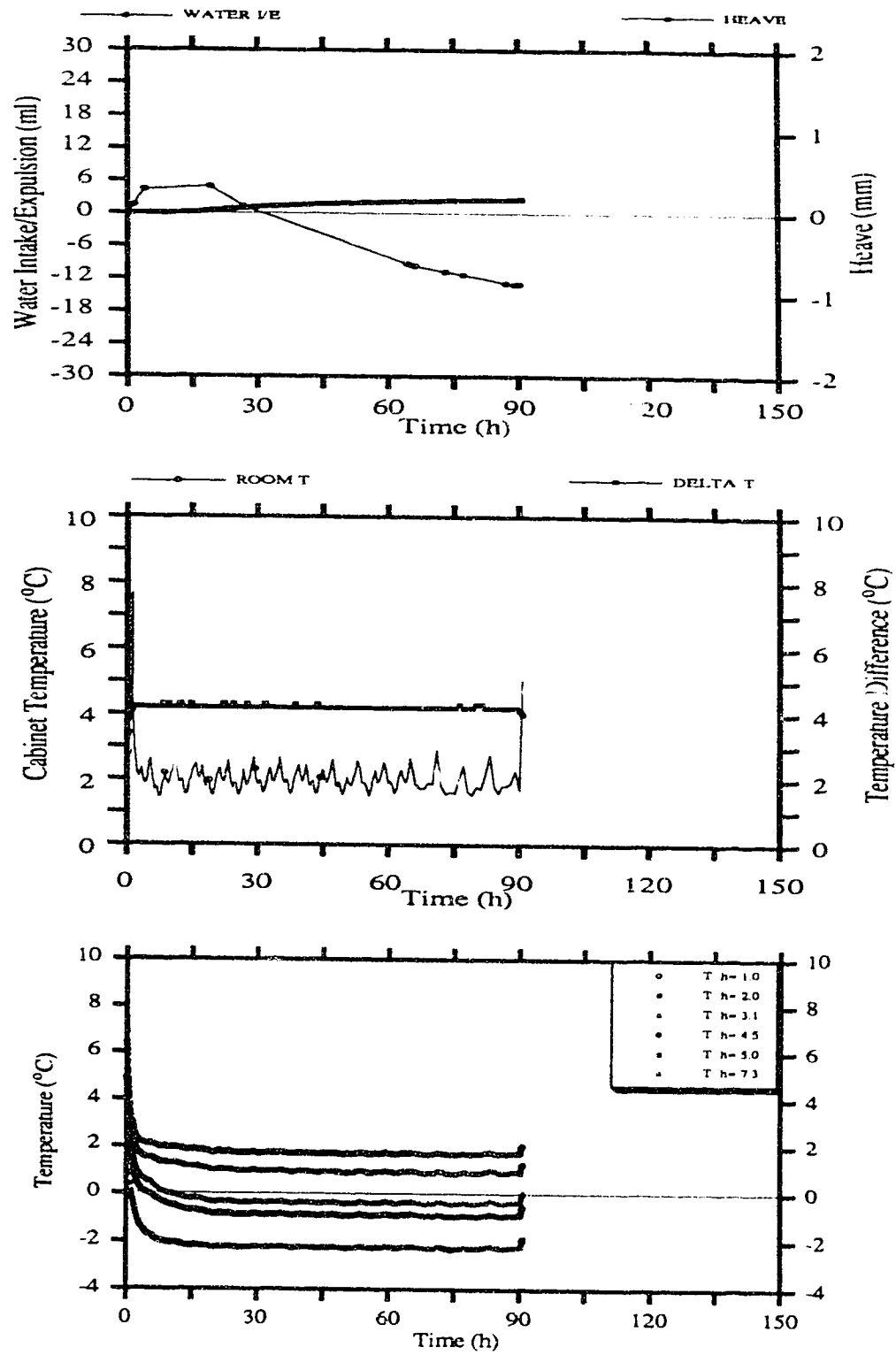


Figure C-23.- UFT 23. Specimen TS0101

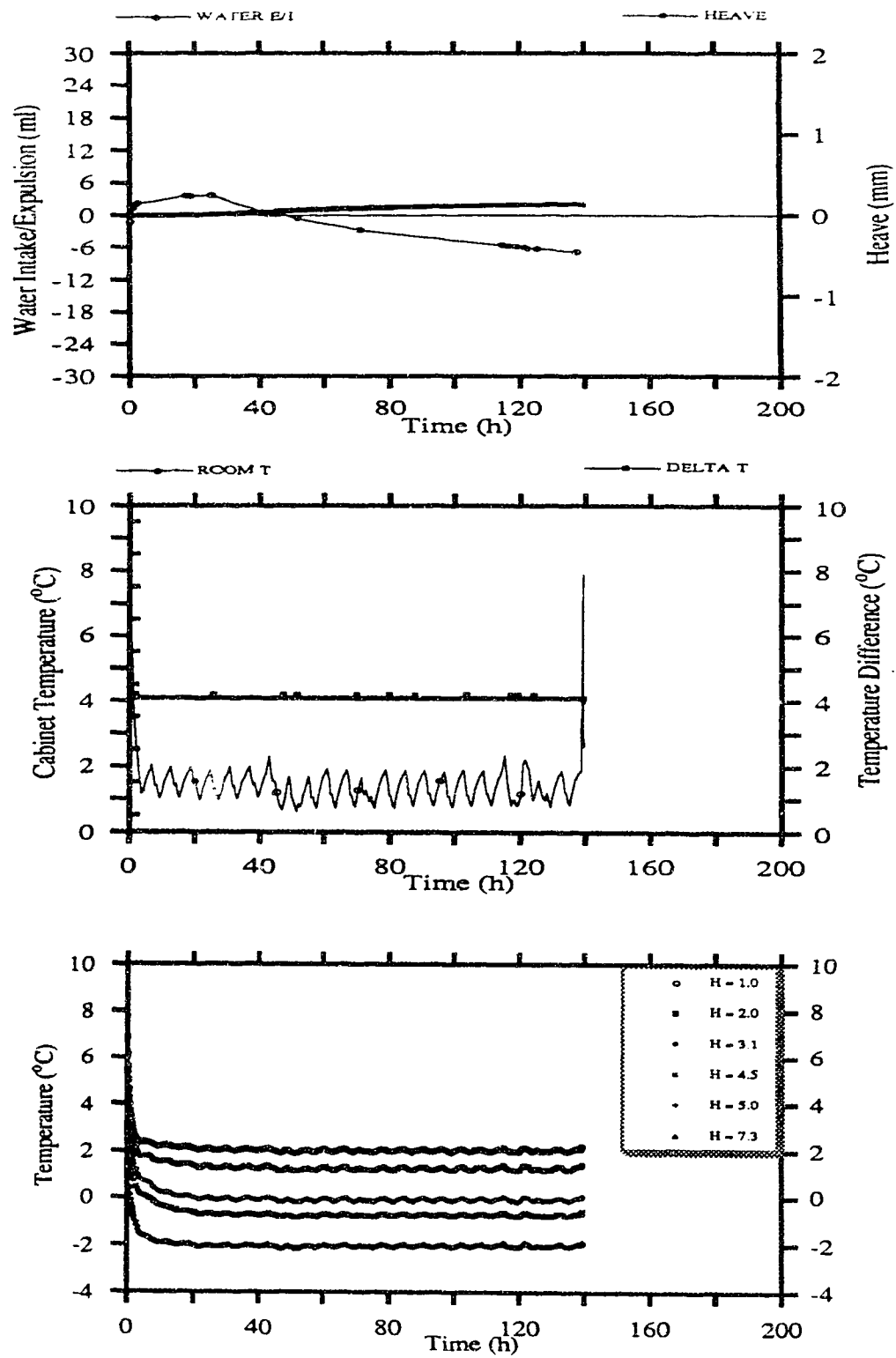


Figure C-24.- UFT 24. Specimen TS0102

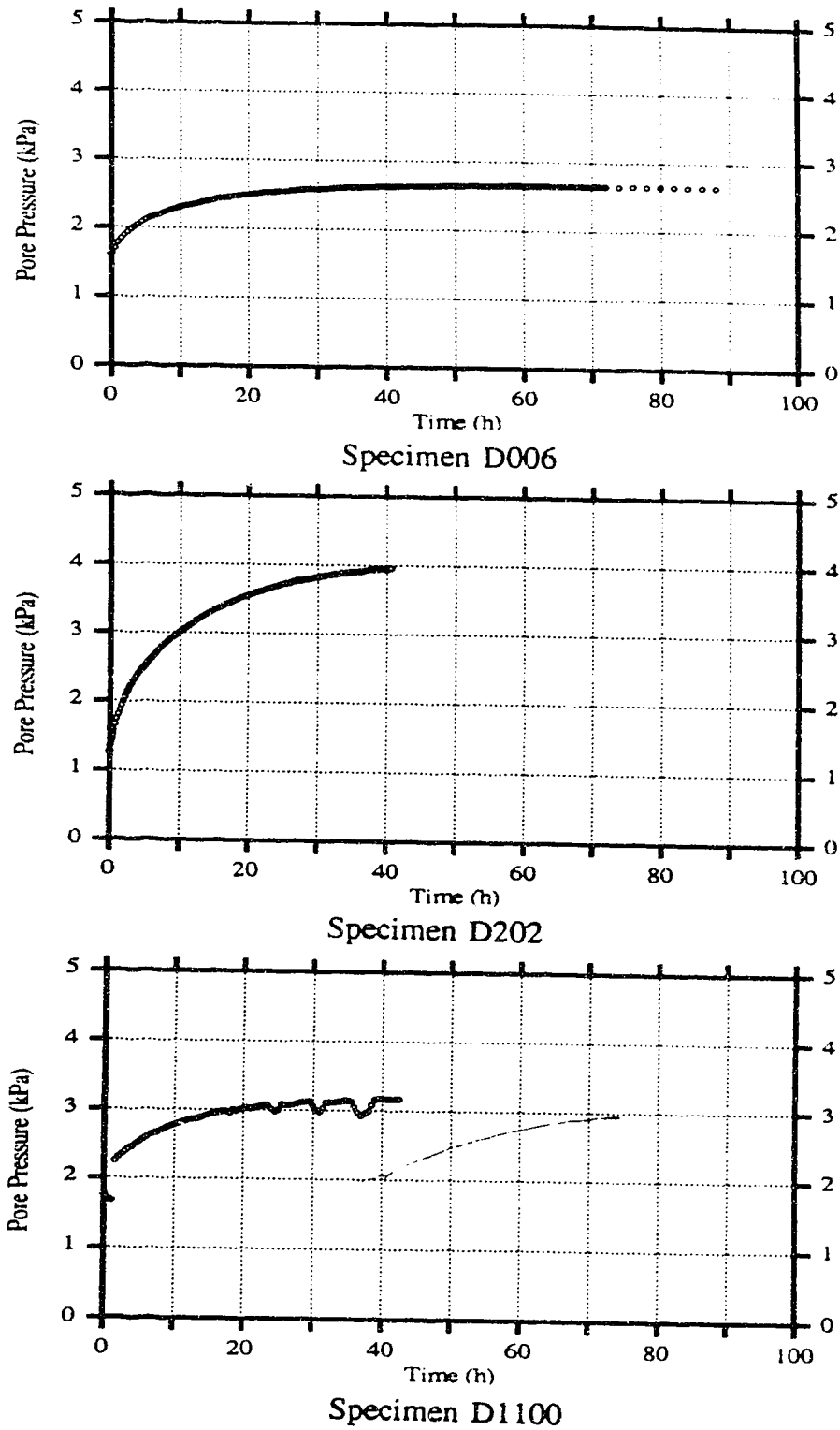


Figure C-25.- Porepressures Series D0, D1 and D2

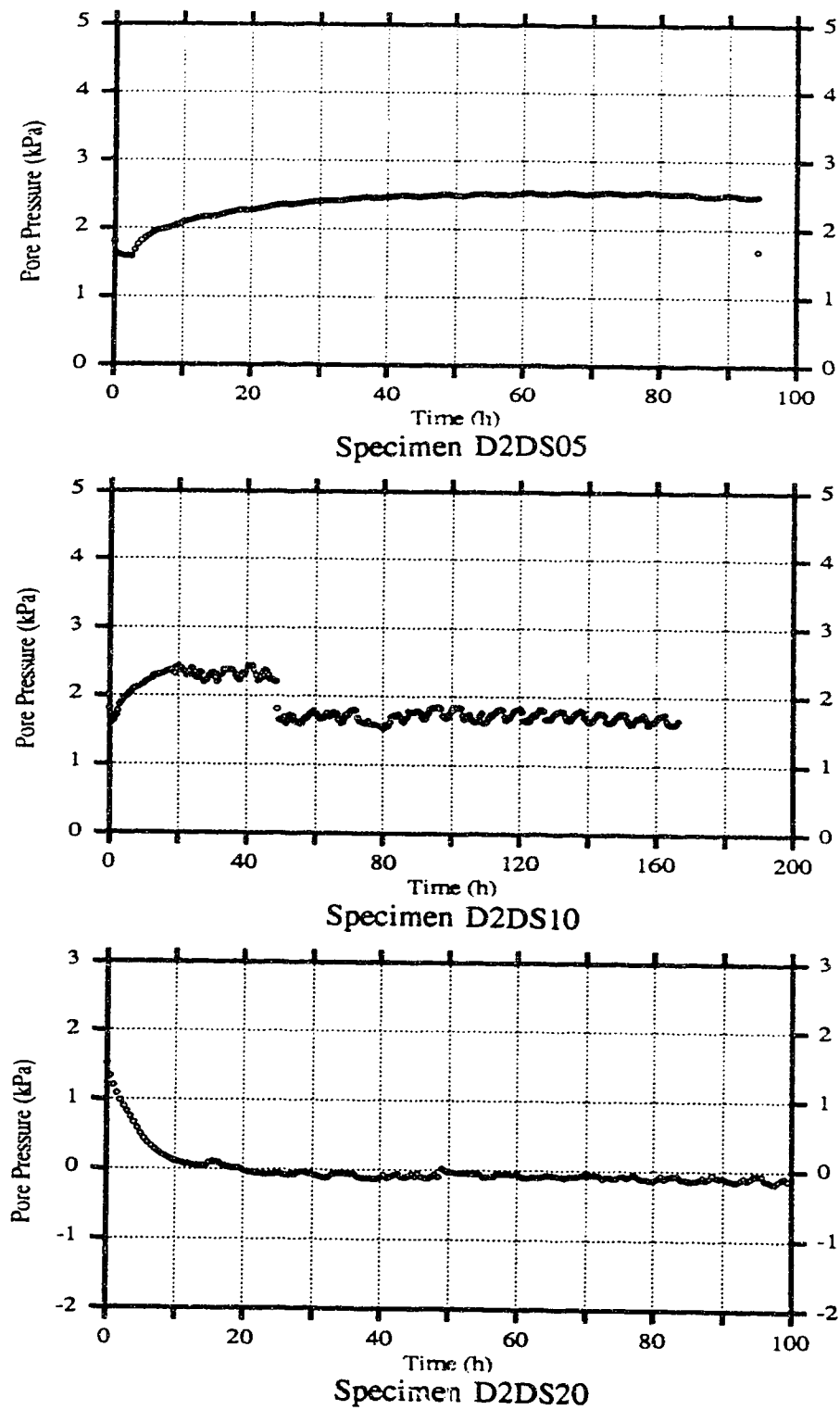


Figure C-26.- Porepressure Series DS

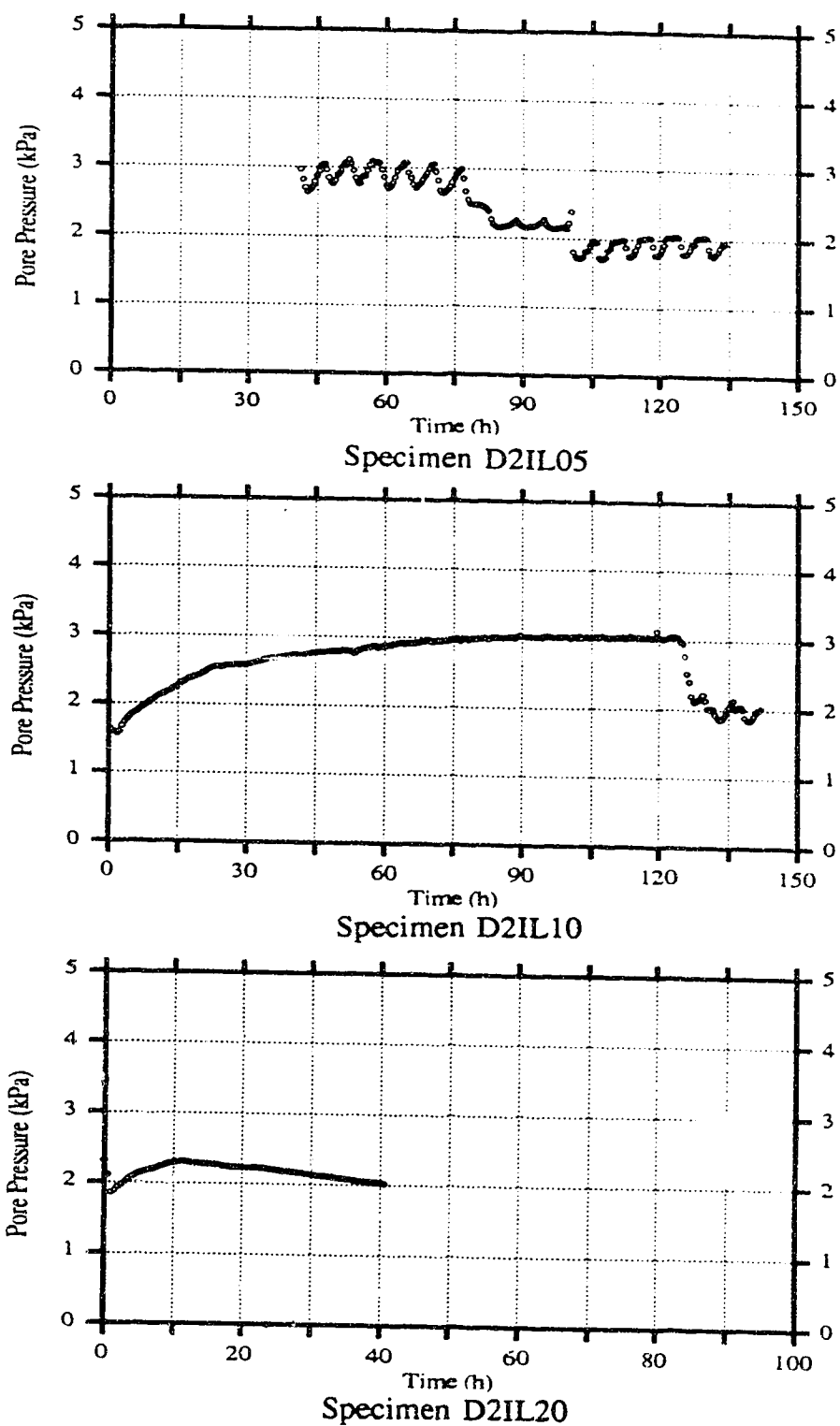


Figure C-27.- Porepressure Series IL

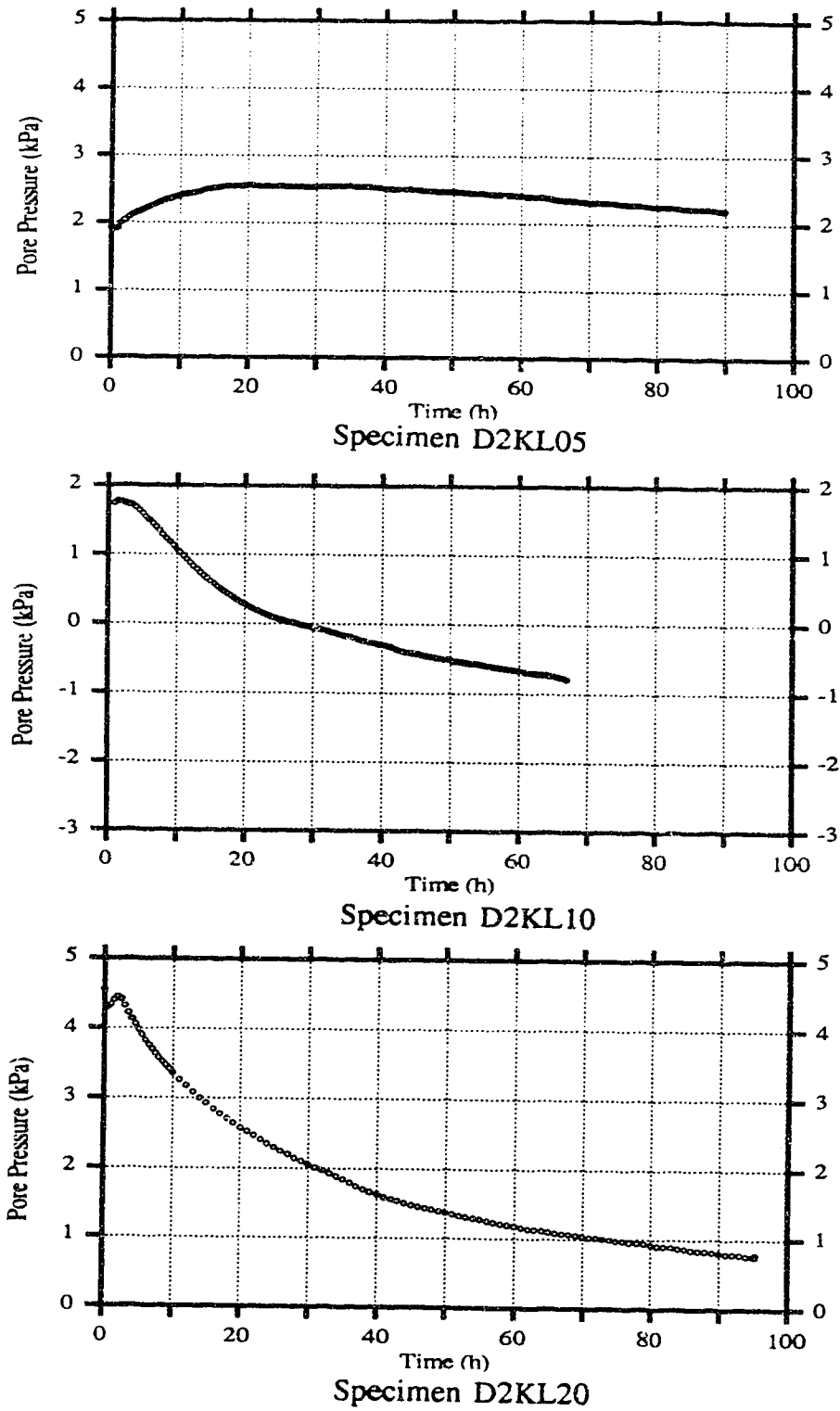


Figure C-28.- Porepressure Series KL

APPENDIX D

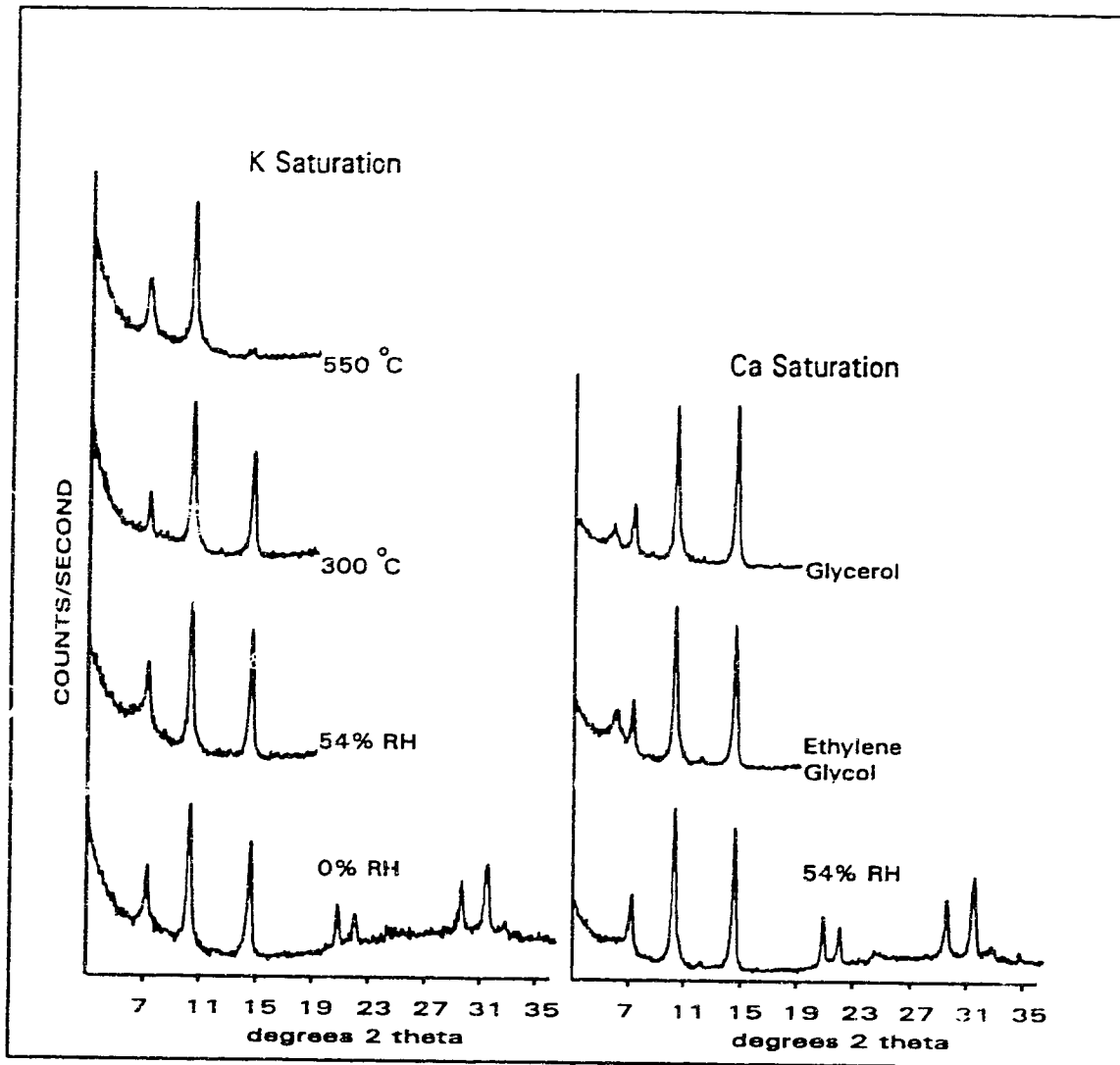


Figure D-01.- X-ray Diffractogram of the Duncan 1 Fines

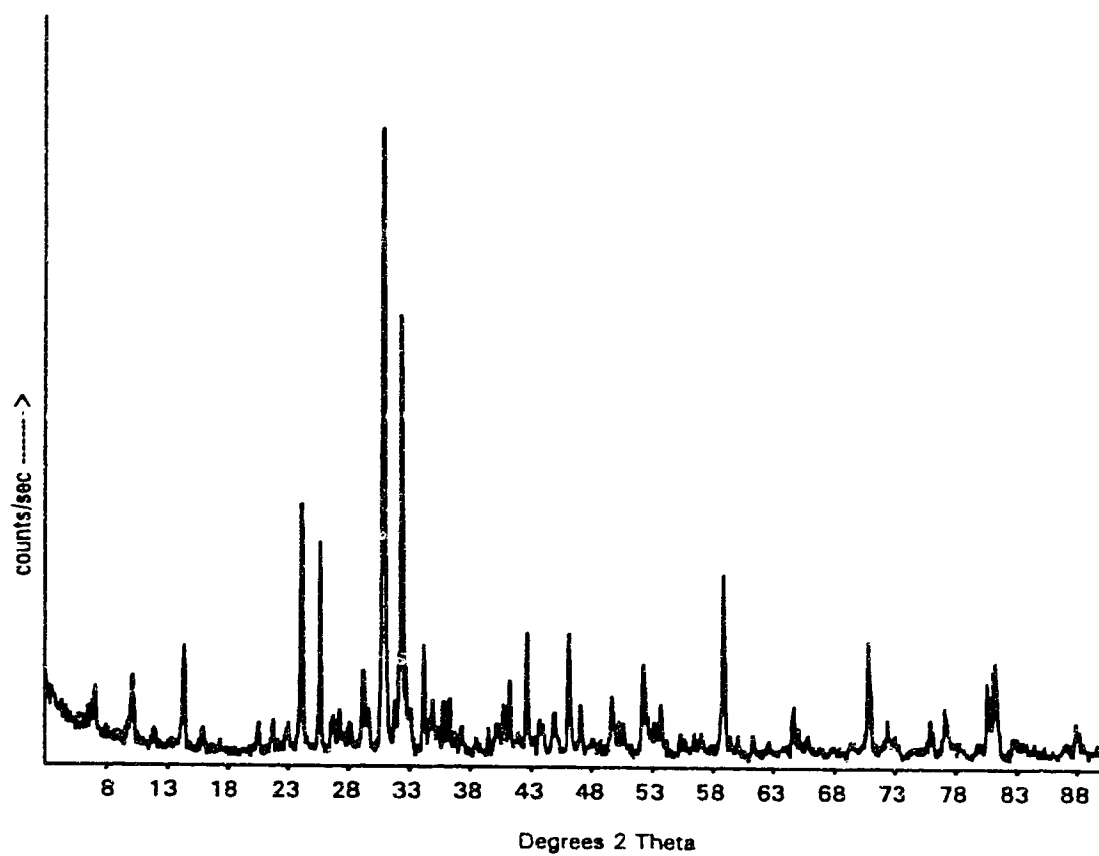


Figure D-02.- X-ray Diffractogram Curve. Duncan 1 Fines Mineral Distribution

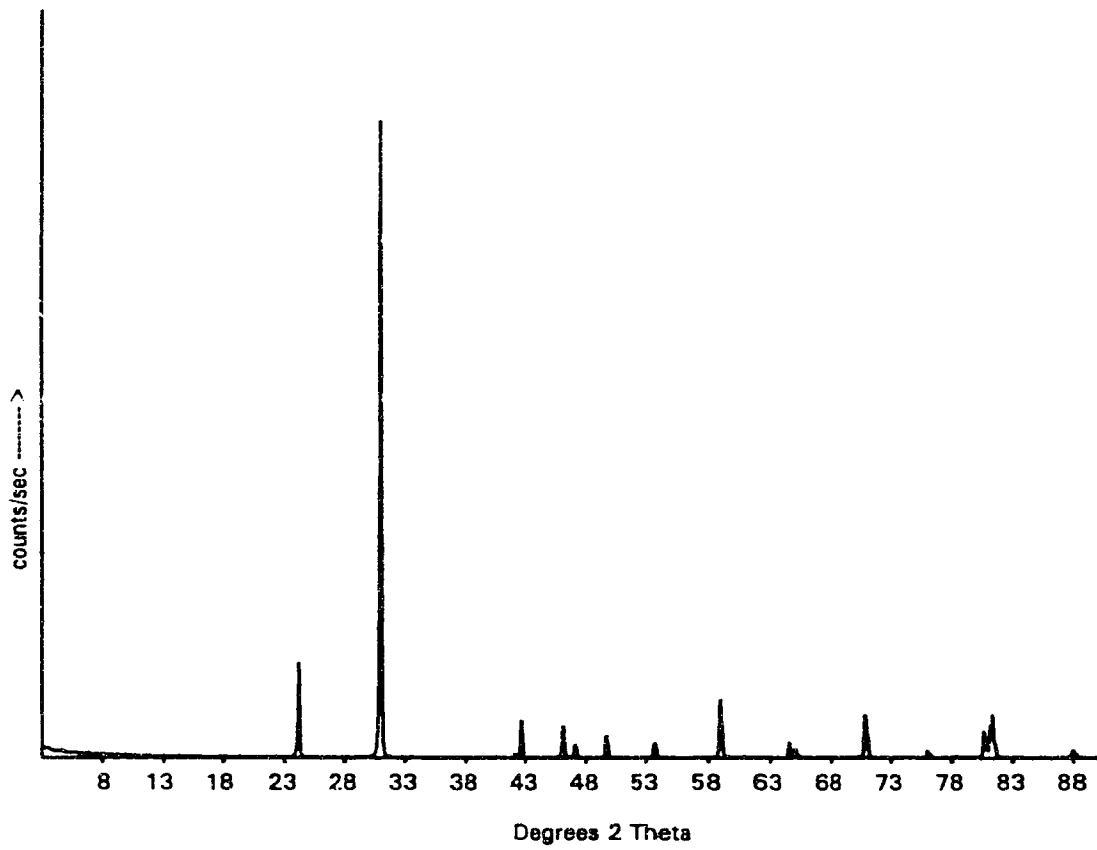


Figure D-03.- X-ray Diffractogram Curve. Silica Flume Fines
Mineral Distribution

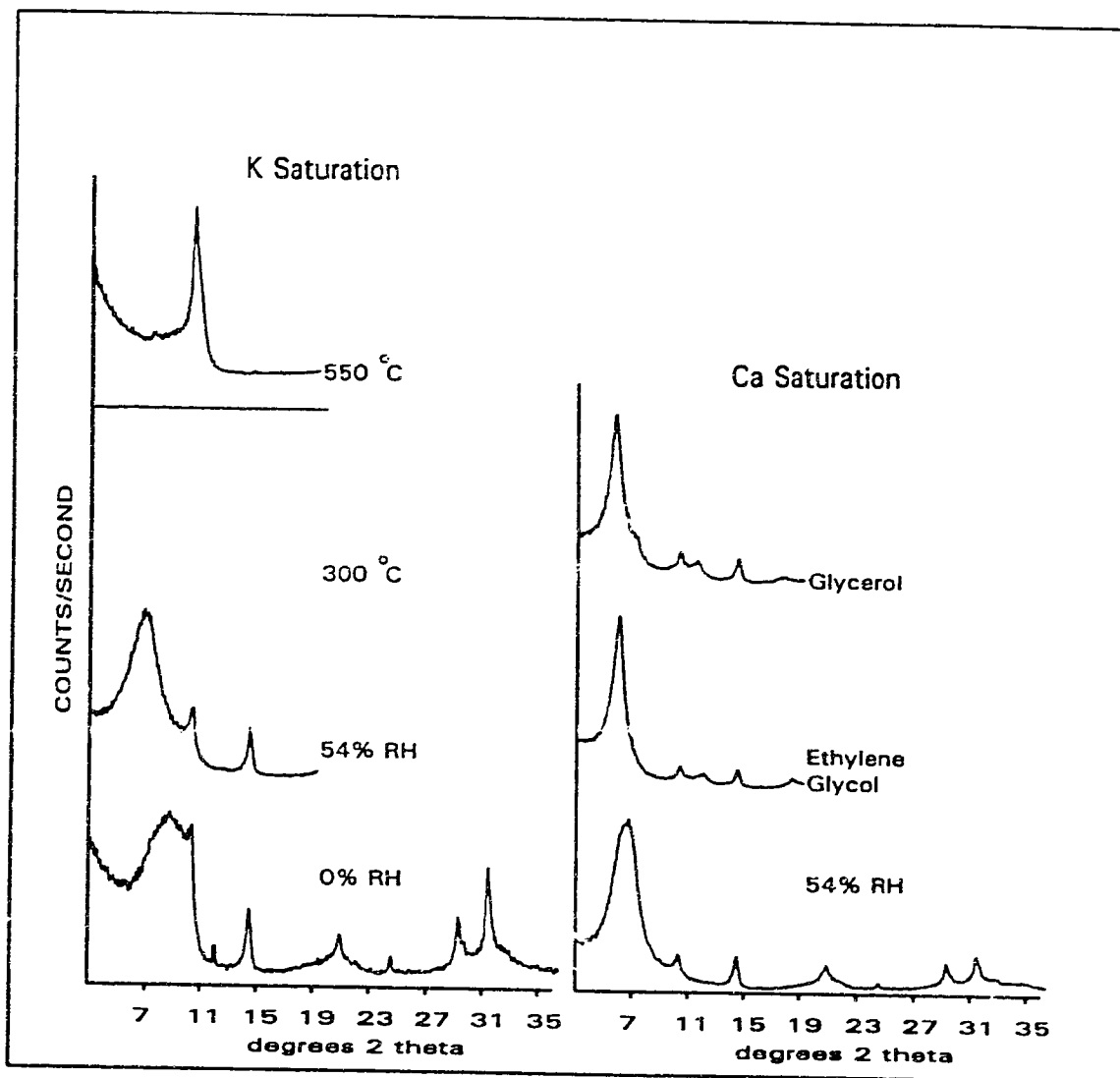


Figure D-04.- X-ray Diffractogram of the Devon Silt Fines

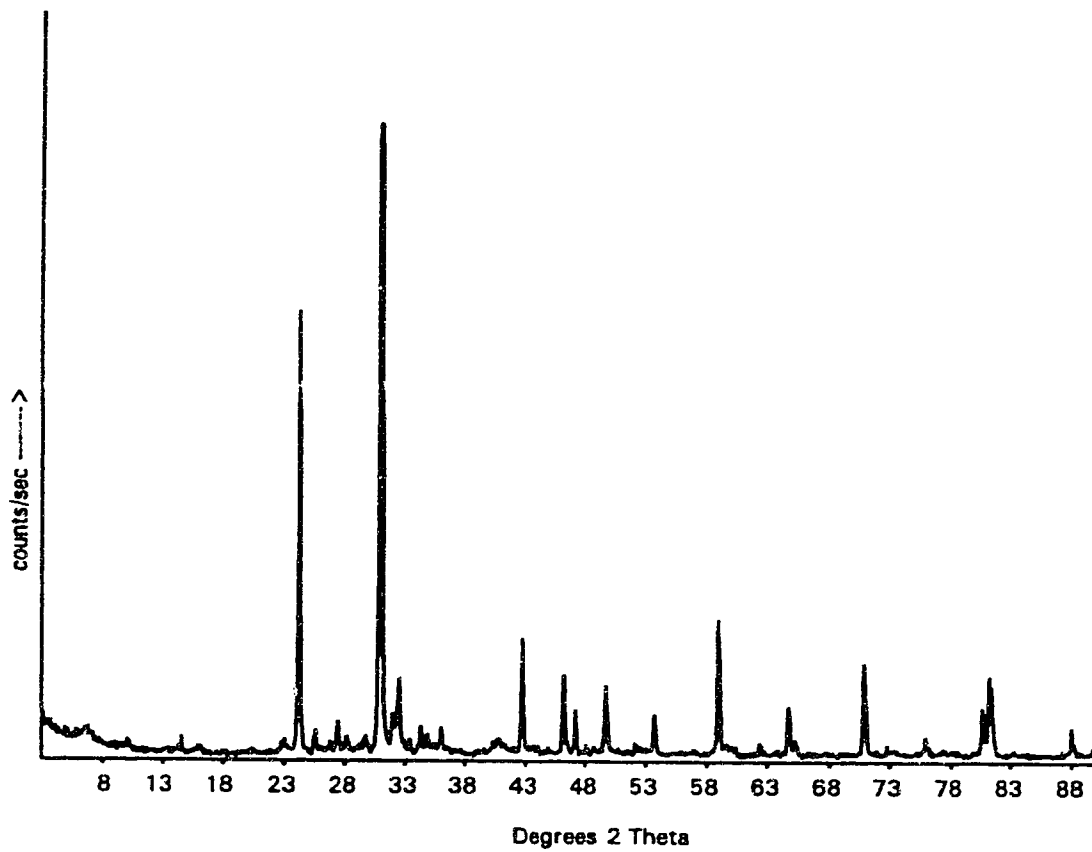


Figure D-05.- X-ray Diffractogram Curve. Devon Silt Fines Mineral Distribution

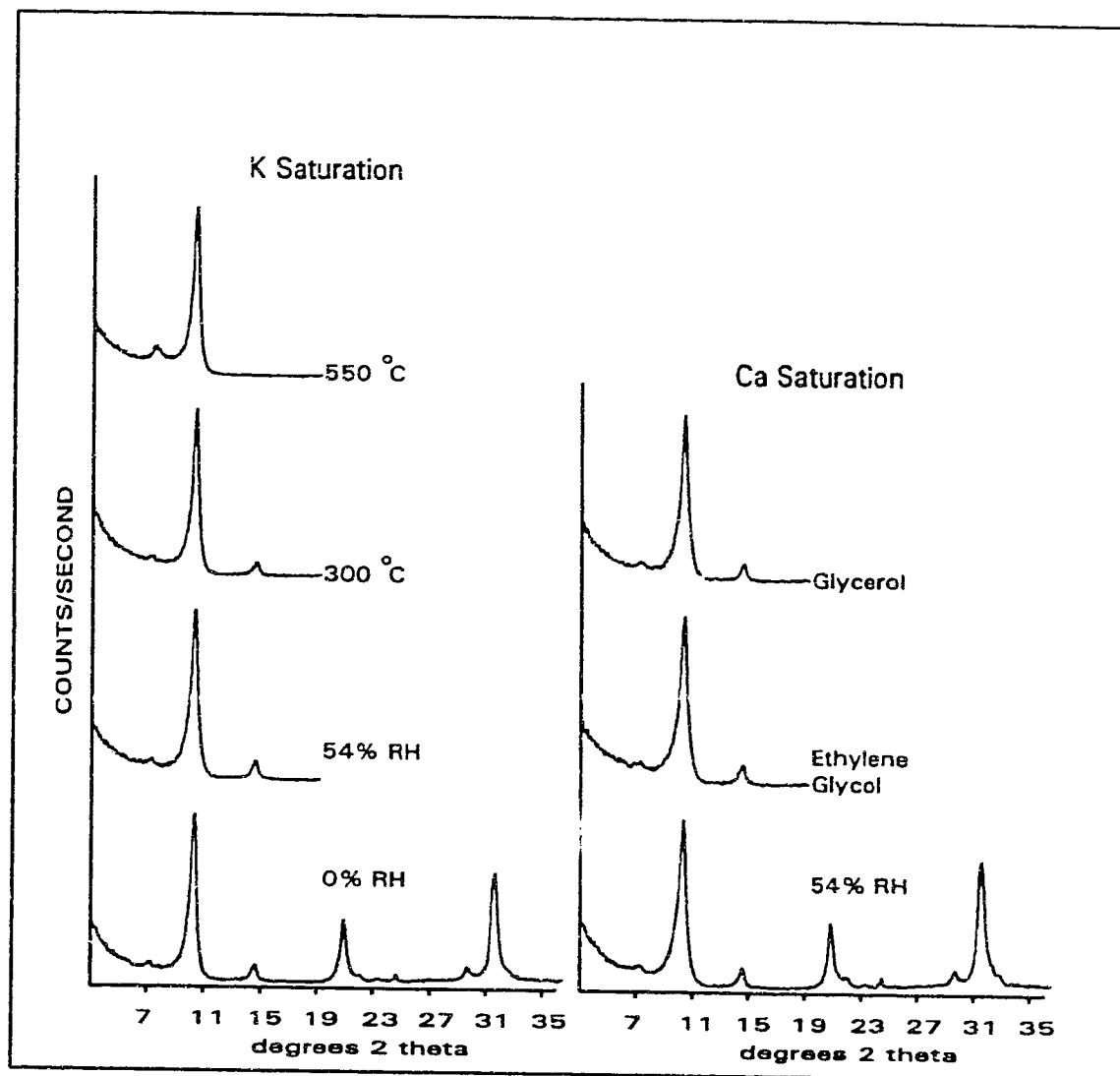


Figure D-06.- X-ray Diffractogram of the Illite Fines

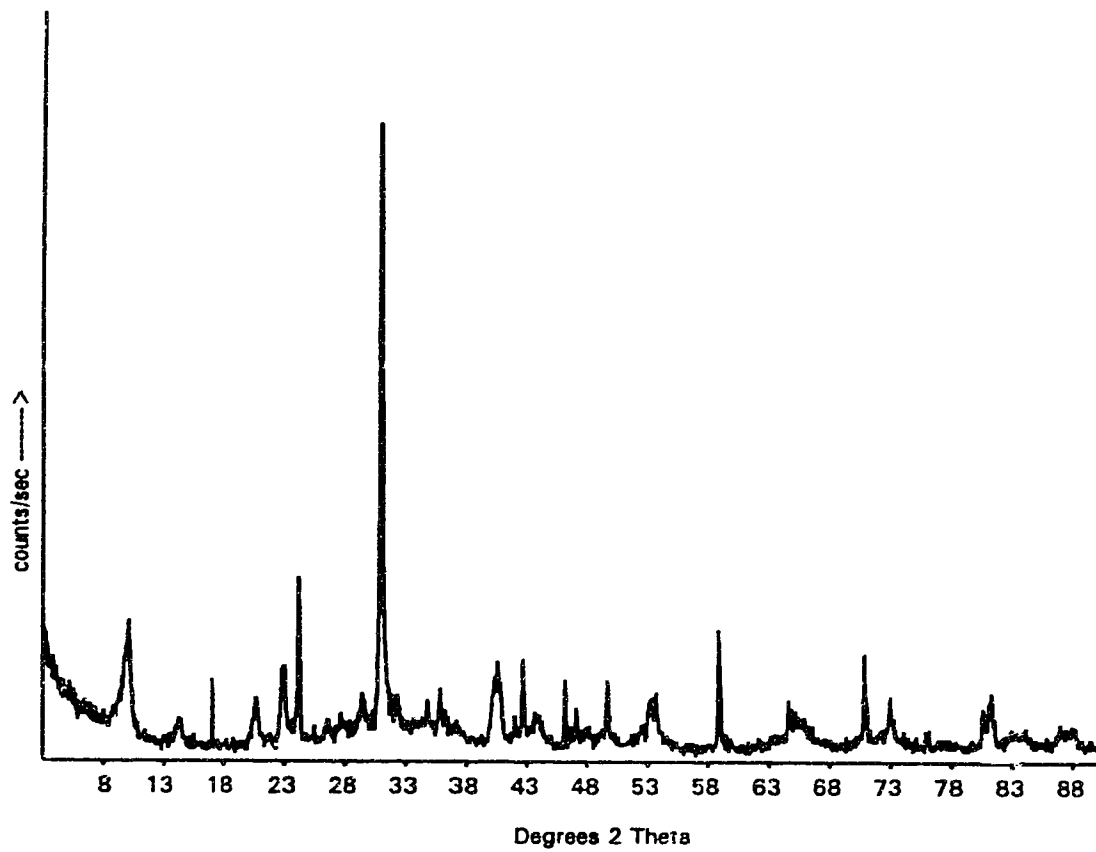


Figure D-07.- X-ray Diffractogram Curve. Illite Fines Mineral Distribution

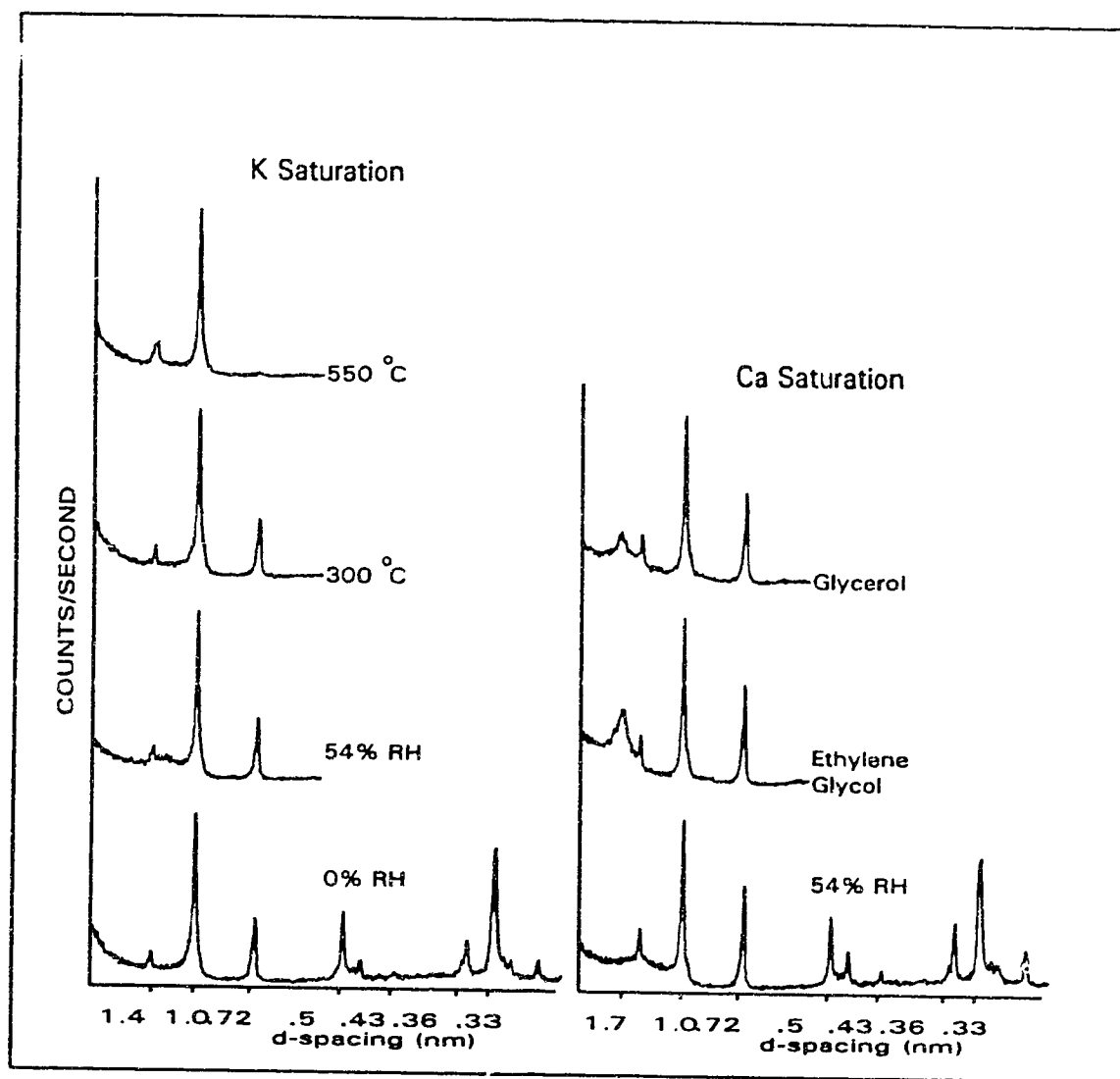


Figure D-08.- X-ray Diffractogram of the Athabasca Clay Fines

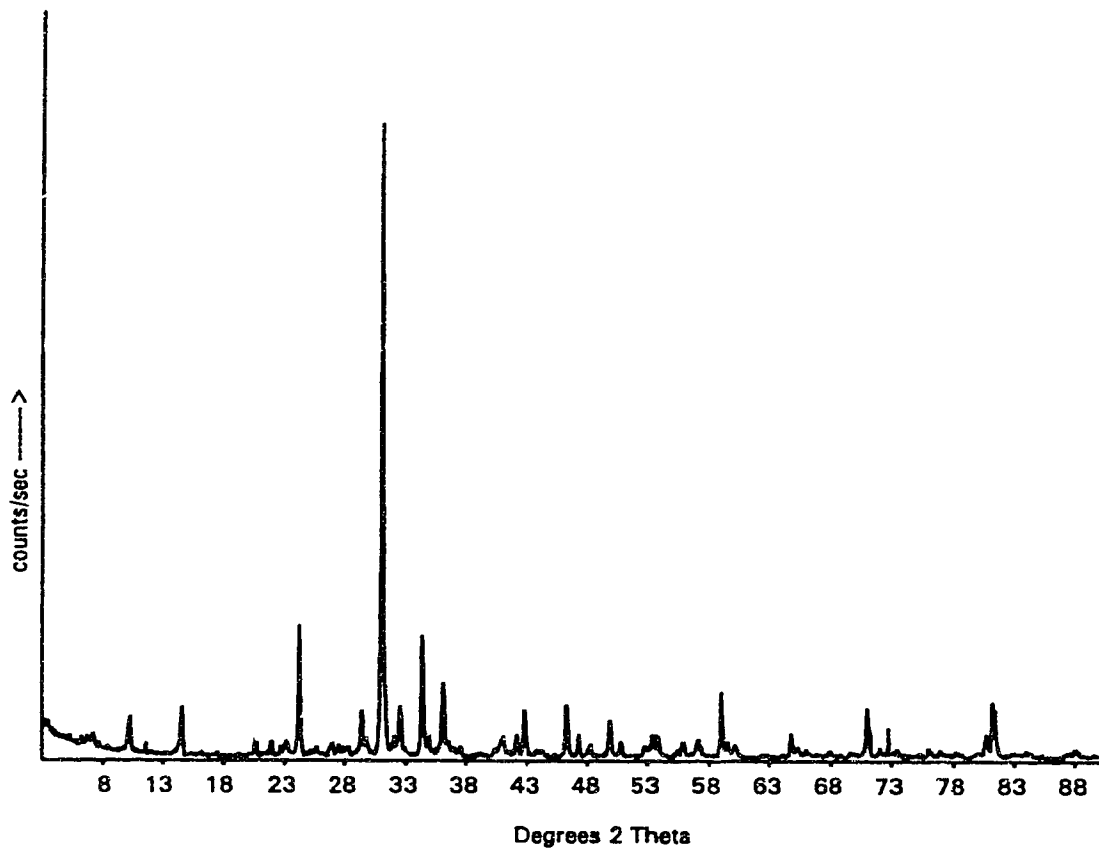


Figure D-09.- X-ray Diffractogram Curve. Athabasca Clay Fines Mineral Distribution

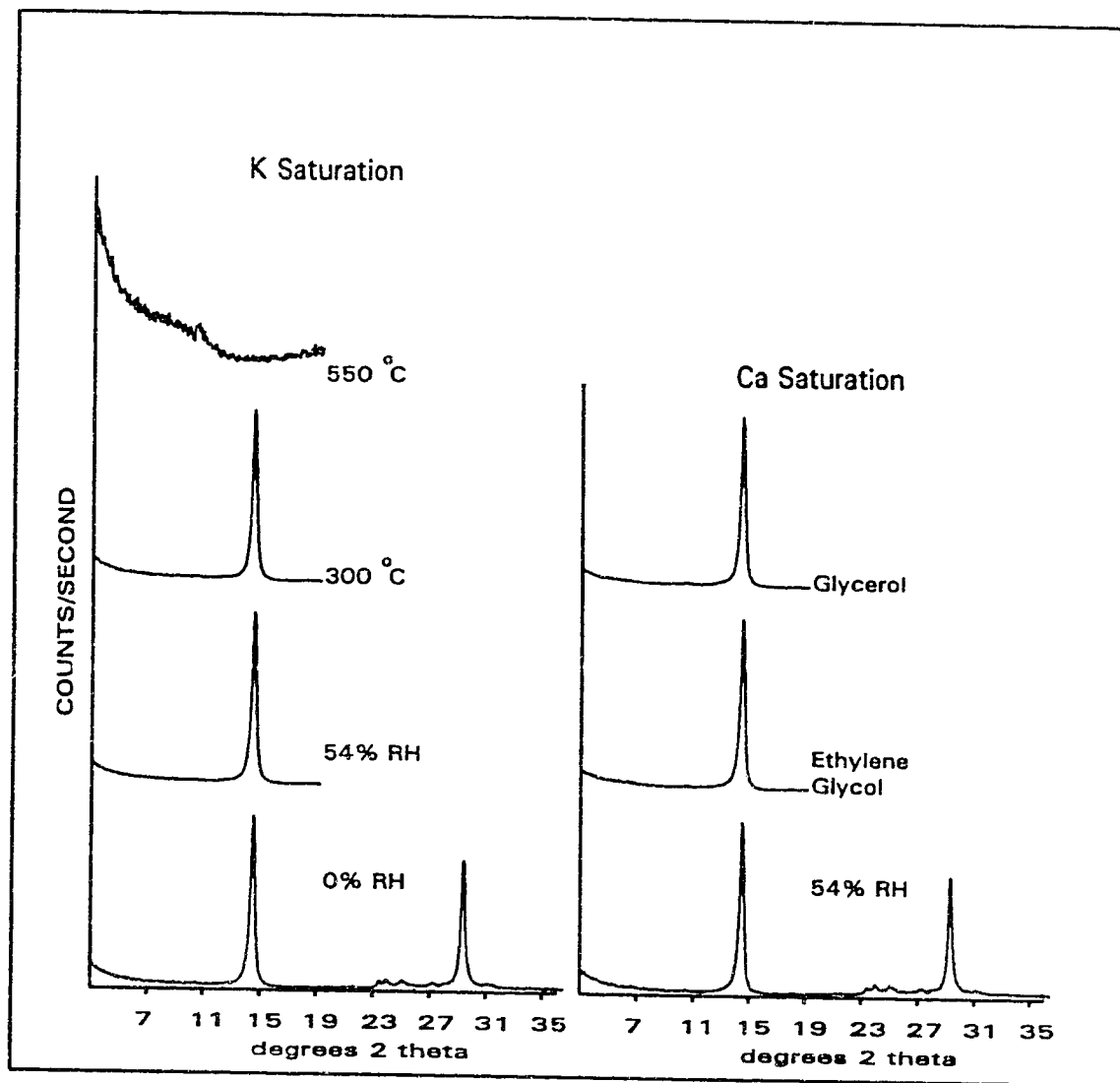


Figure D-10.- X-ray Diffractogram of the Kaolinite Fines

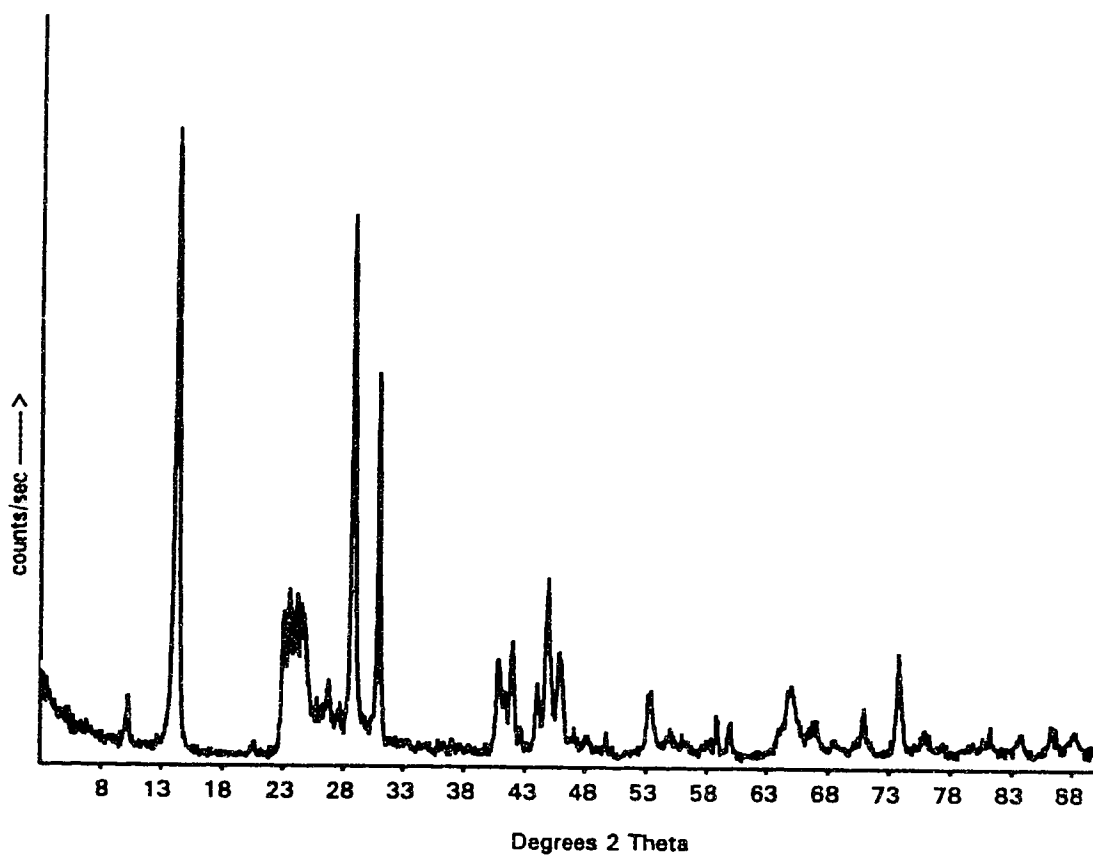


Figure D-11.- X-ray Diffractogram Curve. Kaolinite Fines Mineral Distribution

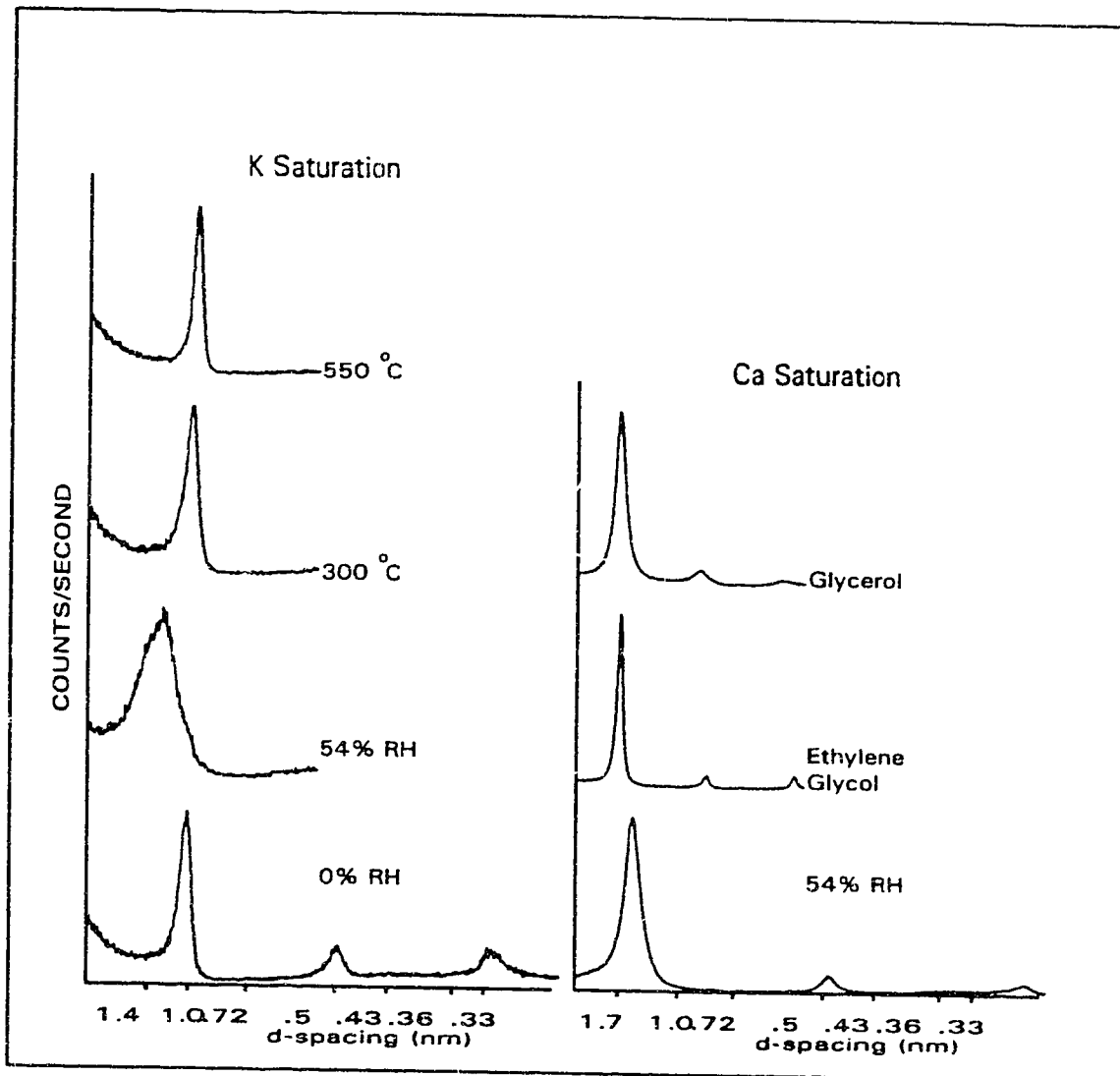


Figure D-12.- X-ray Diffractogram of the Bentonite Fines

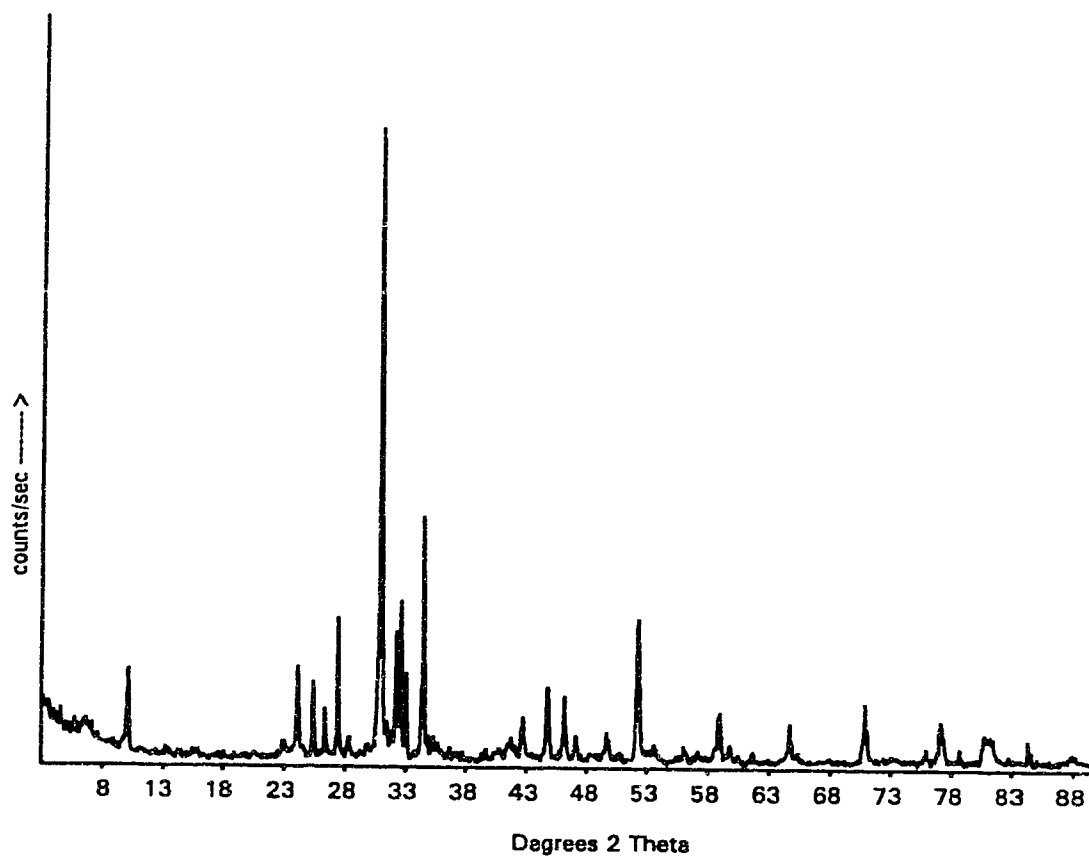


Figure D-13. X-ray Diffractogram Curve. Bentonite Fines Mineral Distribution

APPENDIX E

Table E-41
Void Ratio Determination for Non-clay Mineral Mixtures

UPT No.	Series	Test	G _s	Weight (g)	h _i (cm)	h _c (cm)	M (cm)	V _i	V _c	V _f	Density _i	Density _c	a _i	a _c	Grad T	W _{1,p} (m ³)	W ₂ (m ³)
14	D0	D005	2.74	1114.1	9.92	9.92	9.92	779.1	779.1	779.1	1.4	1.4	0.9	0.9	0.38	16.16	18.77
26	D0	D006	2.74	1297.5	11.41	11.41	11.41	896.1	896.1	896.1	1.4	1.4	0.9	0.9	0.36	21.11	17.60
22	L7	L701D0	2.74	1298.4	11.44	11.27	11.27	898.5	885.1	885.1	1.4	1.5	0.9	0.9	0.36	25.62	23.60
25	L7	L702D0	2.74	1300.0	11.31	11.36	11.12	904.0	884.4	873.4	1.4	1.5	0.9	0.9	0.37	22.52	20.10
38	D1	D101	2.85	1297.1	11.74	11.61	11.58	922.1	911.6	909.5	1.4	1.4	1.0	1.0	0.34	26.22	25.00
17	D2	D202	2.82	1269.9	11.43	11.35	11.35	897.7	891.4	889.9	1.4	1.4	1.0	1.0	0.36	26.22	25.00
19	CS	DXS30	2.74	1250.1	10.27	10.11	10.11	806.6	794.0	794.0	1.5	1.5	0.8	0.8	0.40	21.19	19.60
20	CS	DXS30	2.74	1116.3	9.39	9.22	9.22	717.5	724.1	724.1	1.5	1.5	0.8	0.8	0.43	18.87	16.10
23	TS	TS0101	2.70	1248.2	9.50	9.25	9.42	746.1	726.5	739.8	1.7	1.8	0.6	0.5	0.45	20.14	13.10
24	TS	TS0102	2.70	1244.5	9.22	9.06	9.18	724.1	711.6	711.0	1.7	1.7	0.6	0.5	0.44	18.10	6.10

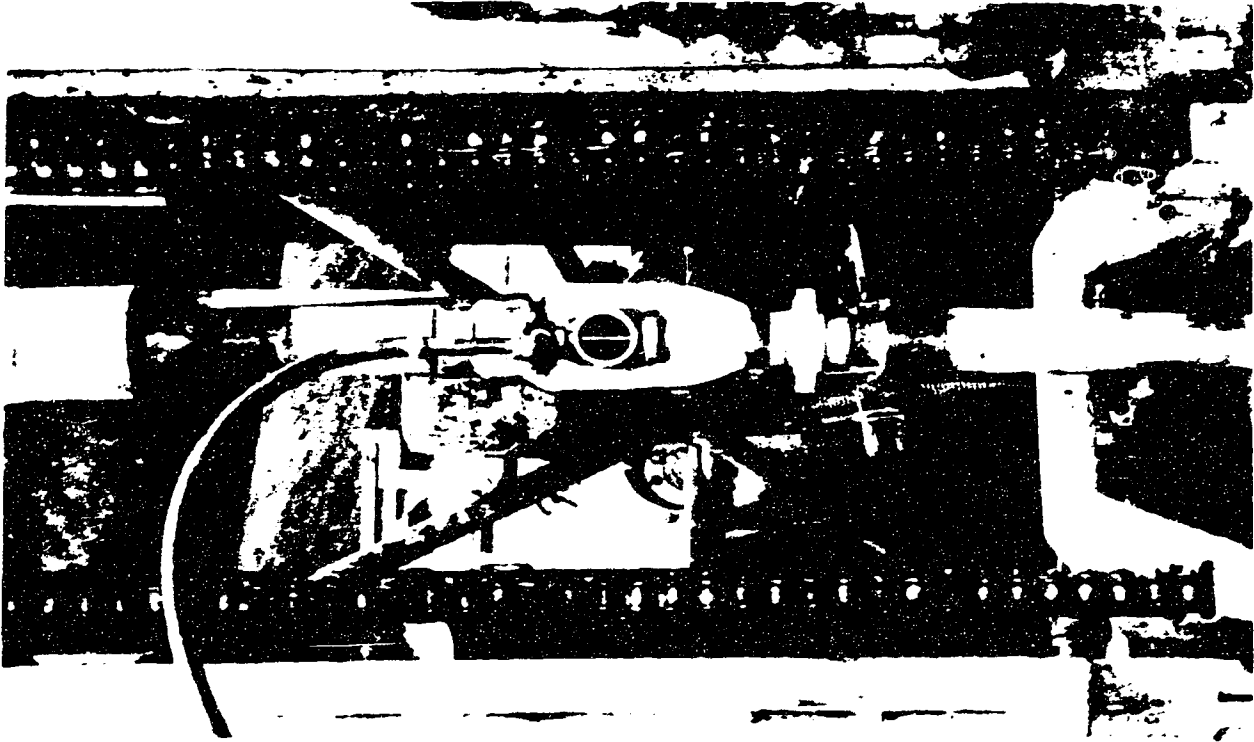
Table E-02

Void Ratio and Final Freezing Front Determination

Series	Test	e_i $e_{i(1)}^*$	e_f $e_{f(1)}^*$	Manual Measurement			Dial Gauge		R ₁₁₁ (cm)	Grain Tu (α C/mm)	
				Unfrozen (cm)	Frozen (cm)	Σ (U.F) (cm)	h _f (cm)	Manual		R ₁₁₁	
D0	D005	0.90	0.90	5.25	4.85	10.10	9.92	4.50	4.50	0.04	0.04
	D006	0.90	0.90	5.30	6.25	11.55	11.41	4.50	4.50	0.04	0.04
	L701D0	0.90	0.90	3.79	7.75	11.54	11.27	3.50	3.50	0.05	0.06
	L702D0	0.90	0.90	5.50	6.37	11.87	11.12	3.50	3.50	0.04	0.06
D1 D2	D101	1.00	1.00	5.45	6.46	11.91	11.58	4.50	4.50	0.04	0.04
	D202	1.00	1.00	3.96	7.44	11.40	11.33	3.80	3.80	0.05	0.05
CS CS	D2CS20	0.80	0.80	3.63	6.63	10.26	10.11	3.50	3.50	0.06	0.06
	D2CS30	0.80	0.80	3.58	5.93	9.51	9.22	3.50	3.50	0.06	0.06
DS DS DS	D2DS05	1.12*	1.09*	5.78	6.07	11.85	11.67	3.00	3.00	0.03	0.07
	D2DS10	1.2*	1.15*	5.02	6.14	11.16	11.33	4.50	4.50	0.04	0.04
	D2DS20	1.34*	1.29*	7.79	3.00	10.79	10.76	4.50	4.50	0.03	0.04
IL IL IL IL IL	D2IL05	1.16*	1.11*	5.30	6.57	11.87	11.80	4.50	4.50	0.04	0.04
	D2IL10	1.08*	1.07*	4.39	6.62	11.01	11.12	4.00	4.00	0.05	0.05
	D2IL20	1.18*	1.15*	5.38	4.38	9.76	9.83	4.00	4.00	0.04	0.05
	D2IL102	1.09*	1.04*	4.75	6.06	10.81	10.86	3.80	3.80	0.04	0.05
	D2IL202	1.27*	1.17*	5.11	6.39	11.50	10.66			0.04	
KL KL KL KL	D2KL05	1.14*	1.12*	5.82	6.30	12.12	12.00	4.50	4.50	0.03	0.04
	D2KL10	1.25*	1.14*	6.45	5.33	11.78	11.64	4.50	4.50	0.03	0.04
	D2KL20	1.47*	1.3*	6.08	5.70	11.78	11.73	4.50	4.50	0.03	0.04
	D2KL032	1.07*	1.01*	5.11	6.39	11.50	11.42	4.50	4.50	0.04	0.04
MS MS	MSKL20			4.43	6.89	11.32	Not Recorded	4.50	4.50	0.05	0.04
	MSIL10	1.24*	1.23*	7.15	4.95	12.10	11.85			0.03	
TS TS	TS01	0.60	0.50	3.32	6.45	9.77	9.42	2.80	2.80	0.06	0.07
	TS02	0.60	0.50	3.95	5.79	9.74	9.18	3.10	3.10	0.05	0.06

APPENDIX F

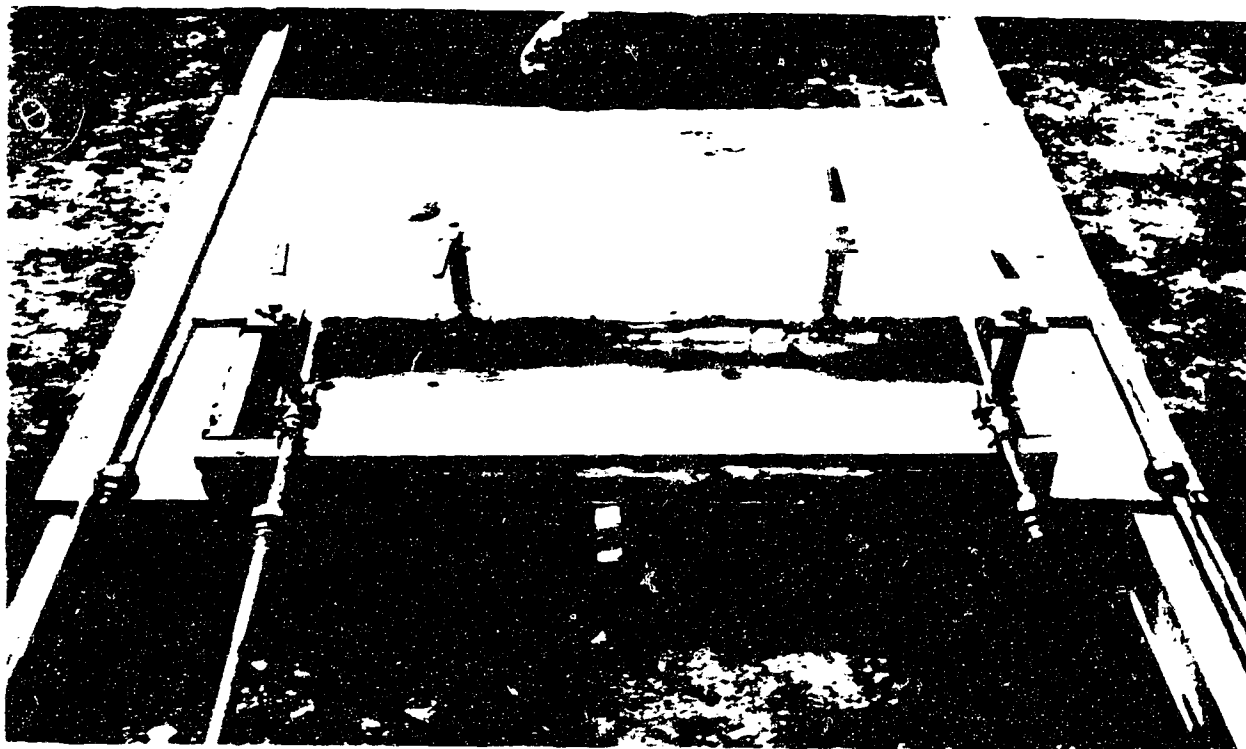
APPENDIX F



F-01.- Placement of the jetting pipe and pushing of the first section in FP1.

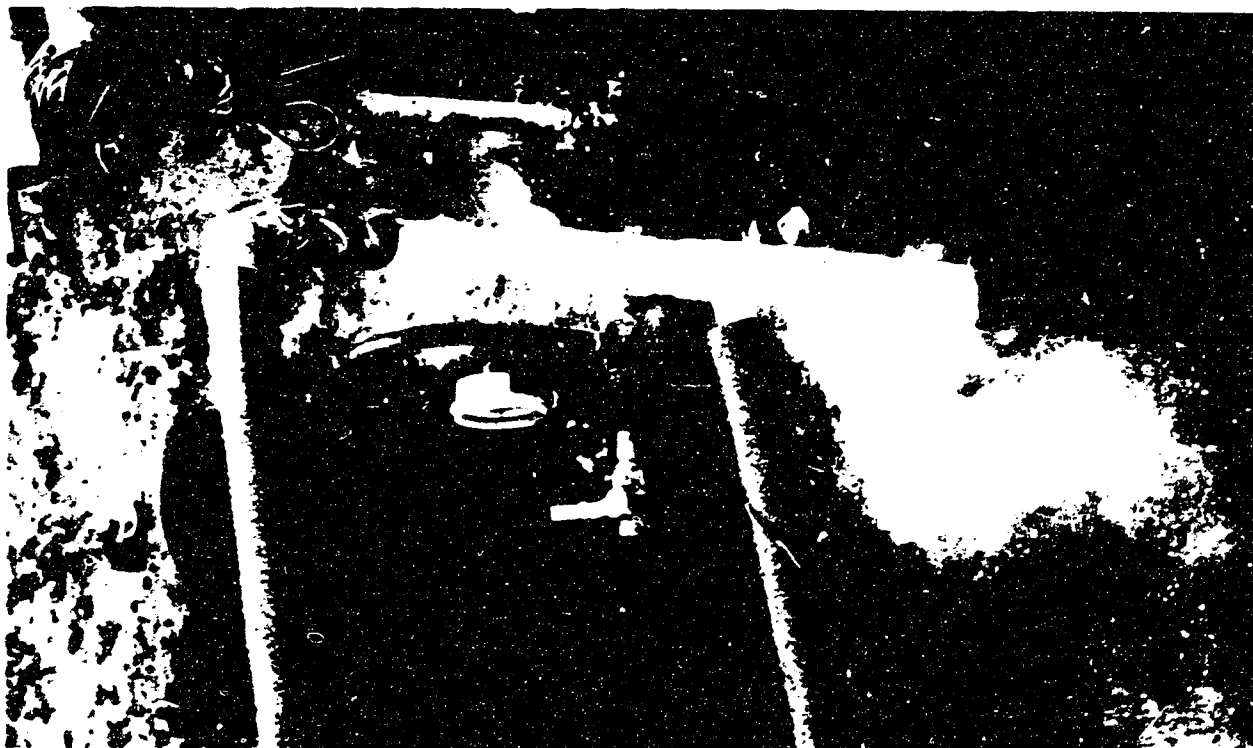
F-02.- Soldering the 2" copper tubes of the Second Section of the freezing system.

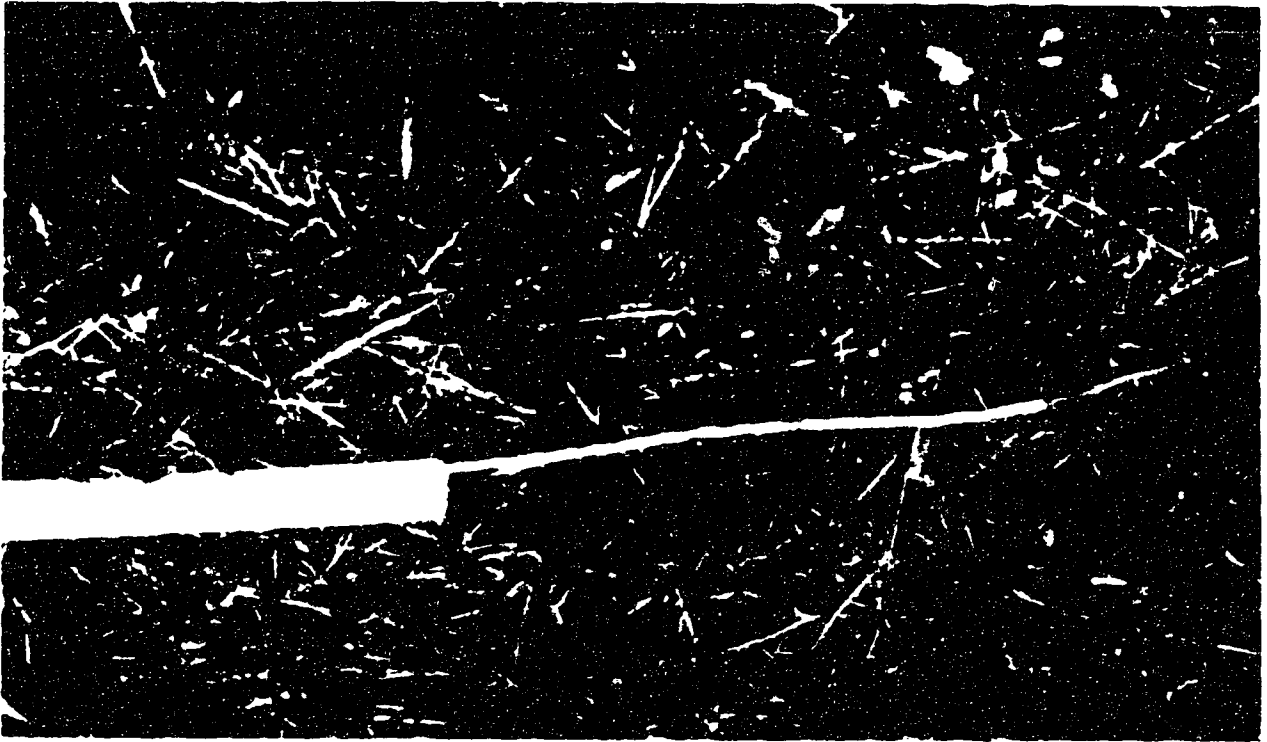




F-03.- Close-up of the valves distribution.

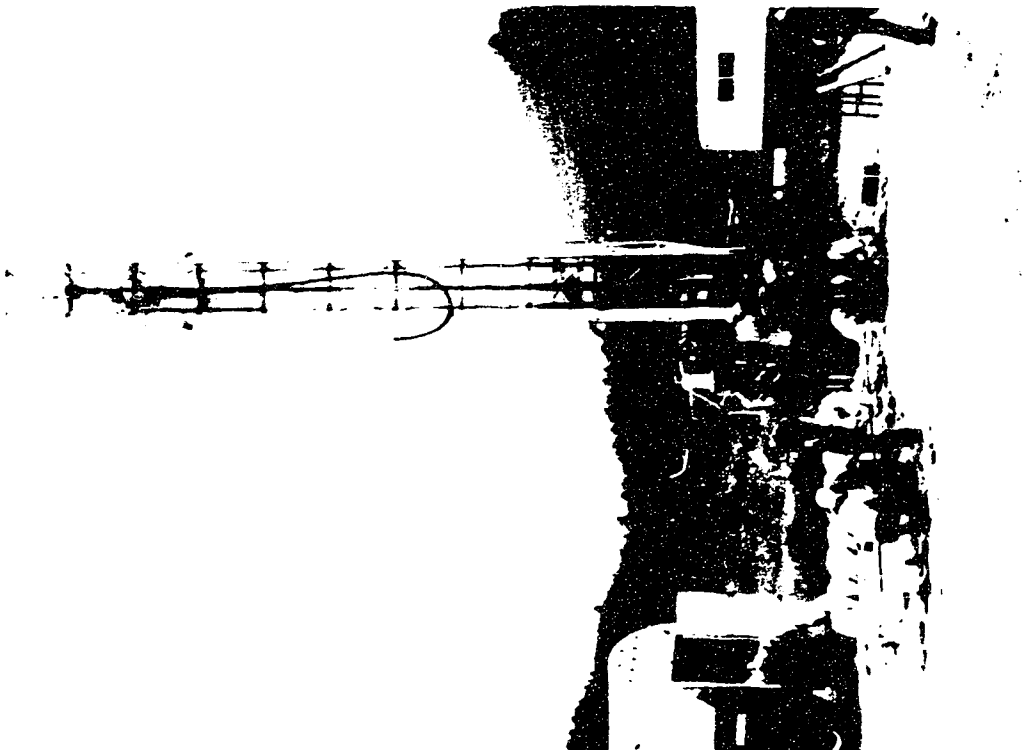
F-04.- Close-up of FP1 submitted to liquid nitrogen distribution.

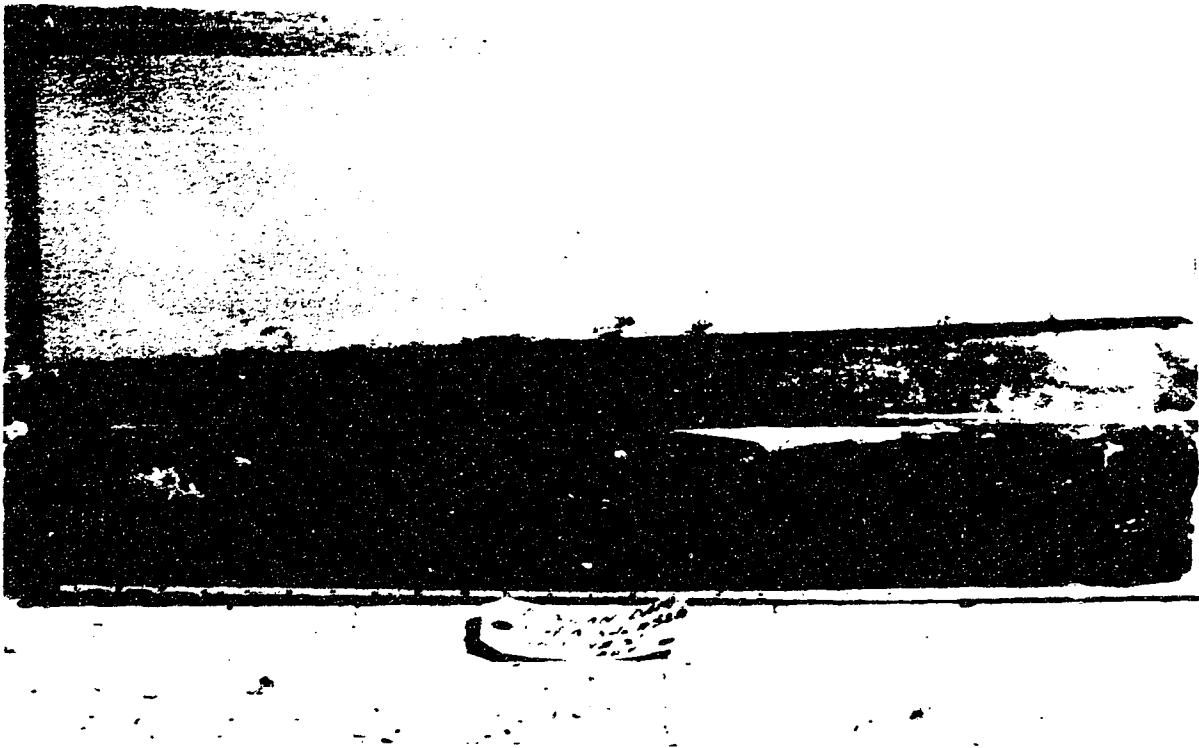




F-05.- RTD with attached cable inside the 0.5" PVC tube.

F-06.- Preparation of S1 for sampling and view of surface piping of the freezing system.

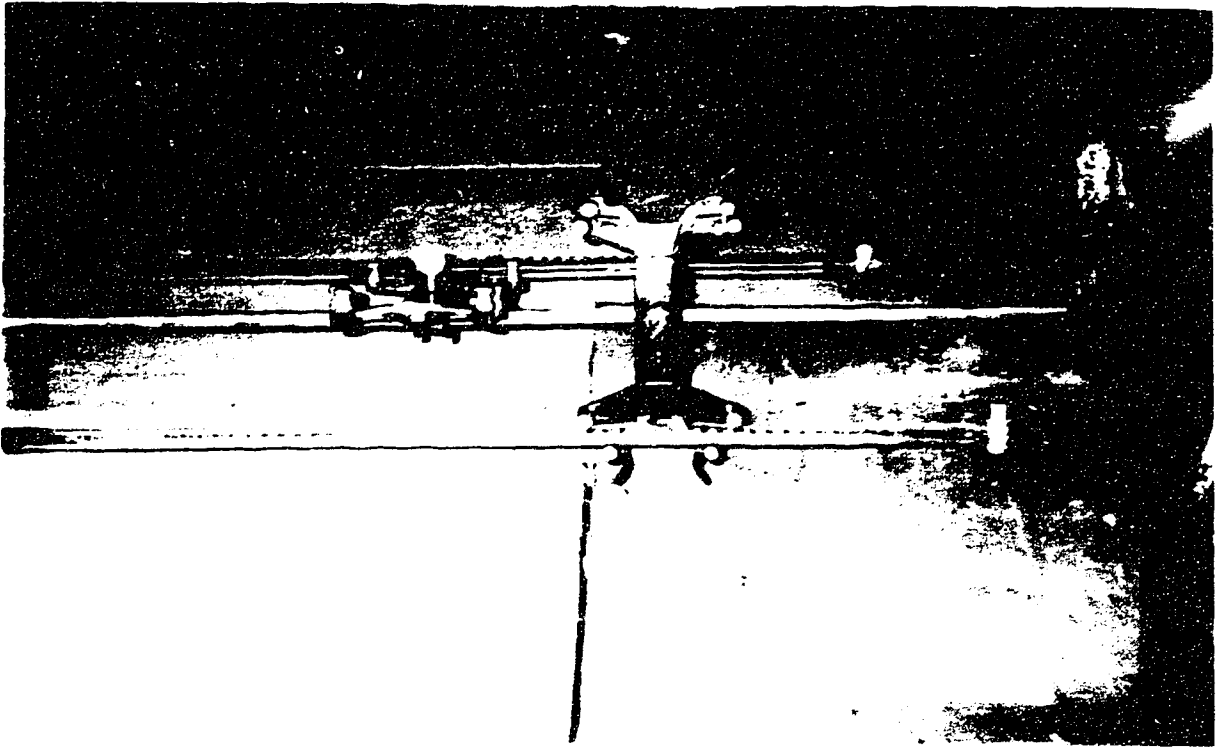




F-07.- Retrieved sample of undisturbed Duncan Sand.

F-08.- View of the demodular for System 01 and System 02 with their RTD signal conditioner boxes.





F-09.- View of the burettes to measure the water expulsion or water intake.

F-10.- View of the data acquisition system.

